TREATMENT OF ORGANIC CONTAMINANTS FROM WATER USING AN INTEGRATED SORPTION-OXIDATION SYSTEM

By
S M Ghausul Hossain

Submitted in fulfilment for the degree of

Doctor of Philosophy

Faculty of Engineering

University of Technology, Sydney (UTS)

Australia

2012

Certificate

I certify that the work in this thesis has not previously been submitted for a degree, nor has it been submitted as part of requirements for a degree. I also certify that this thesis is my own work and it does not contain any material previously published or written by another person except where due acknowledgement is made in the text.

Signature of Candidate

Abstract

In-situ treatment of chlorophenols using a permeable reactive barrier is still an emerging research area. A novel integrated sorption-oxidation barrier is proposed and systematically investigated in a neutral pH, very poorly buffered water. Intermittent injections of permanganate oxidise dissolved and sorbed chlorophenol as well as the woody sorbent with manganese dioxide formed as a by-product.

Common woody biomass (pine/hardwood) were evaluated as a cost effective sorbent. Chlorophenol uptake on these was relatively low (3–8 mg g^{-1}) with evidence of sorption hysteresis. Increased sorbent particle size and reactions with the oxidant did not significantly affect sorption. Under dynamic conditions non-equilibrium sorption occurred with higher flow rates.

Oxidation within the porous media was complex with multiple oxidation processes occurring simultaneously. An analytical method was developed to allow the quantification of chlorophenol in the presence of a quenching agent. This allowed the collection of kinetic data for the permanganate oxidation reaction. Oxidation of dissolved chlorophenol by manganese dioxide was found to be minimal. Early time data showed that the oxidation rate of pine (0.06 min^{-1}) was less than for chlorophenol sorbed on pine (0.07–0.12 min^{-1}) which was much less than for dissolved chlorophenols (0.4–1.48 min^{-1}). This suggests that the reaction between permanganate and pine materials is kinetically controlled and will dominate only after the oxidation reaction with chlorophenol. The rate of sorbed chlorophenol oxidation decreased with increasing contaminant hydrophobicity. In column studies the oxidation of the pine sorbent was

found to be both pH and residence time dependent. Some evidence of sorbent/column plugging and reduced sorbent oxidant demand due to manganese dioxide precipitation was found at pH 6.15 but not at pH 2.

The research has shown that a novel sorbent-oxidation barrier system that can treat chlorophenol contaminated water is technically feasible. Insights into the key mechanisms that would occur in the system have been given. Further work into operationalizing these processes is still needed.

Acknowledgements

I am especially thankful to my principal supervisor, Dr. Robert McLaughlan, for his guidance, continuous encouragement and support throughout of this study. His valuable ideas and comments helped me to develop my knowledge and skills of doing this research. I would like to thank Professor Saravanmuthu Vigneswaran and my co-supervisor Associate Professor Huu Hao Ngo for their valuable and thoughtful suggestions. Thanks are extended to Associate Professor James Edward Ball for his support and Dr. Shon for encouragement.

I would like to thank my colleagues Lazlo. Othman, Javeed, Than, Wen, Yousef, Ibrahim, Thamer, Johir, Chinu, Sherub and Tahir.

I am grateful for financial support from The CRC for Contamination Assessment and Remediation of the Environment (CARE). I wish to thank the academic and technical staff in the University of Technology Sydney (UTS) to their academic support especially Rami Haddad, David Hooper, Rod Hungerford and Phyllis Agius.

Special thanks to my wife Jinnat Ara for her generosity and help. Thanks to my mother Sufia Begum, daughter Lamia Nureen, son Yusuf Mahdi and all family members.

TABLE OF CONTENTS

Abbreviations

2-CP	: 2-Chlorophenol
3-CP	: 3-Chlorophenol
4-CP	: 4-Chlorophenol
2,4-DCP	: 2,4-Dichlorophenol
2,6-DCP	: 2,6-Dichlorophenol
2,4,6-TCP	: 2,4,6-Trichlorophenol
AOPs	: Advanced Oxidation Processes
BET	: Brunauer-Emmett-Teller
CP	: Chlorophenol
DOC	: Dissolved Organic Carbon
FC	: Filter Coal
GAC	: Granular Activated Carbon
HW	: Hardwood
ISCO	: In-Situ chemical Oxidation
LOD	: Limit of Detection
MDL	: Minimum Detection Limit
NPI	: National Pollutant Inventory
NOD	: Natural Oxidant Demand
PRB	: Permeable Reactive Barrier
PV	: Pore Volume
PVC	: Polyvinyl Chloride

Principal Notation

C_e : equilibrium concentration (mg L^{-1})

C_o : initial concentration (mg L^{-1})

D_{ow} : octanol-water distribution coefficient

K_{ow} : octanol-water partition coefficient

k_{th} : Thomas rate constant (L min^{-1} mg^{-1})

k_{yn} : Yoon-Nelson rate constant (min^{-1})

q_t : amount of sorbate at any time t (mg g^{-1})

q_e : amount of sorbate at equilibrium (mg g^{-1})

Q : volumetric flow rate (mL min^{-1})

r^2 : correlation coefficient

k_y : Yan rate constant (L min^{-1} mg^{-1})

LIST OF FIGURES

LIST OF TABLES

CHAPTER 1

Introduction

1Introduction

1.1 Introduction

Chlorophenols have been widely used in various industries such as raw materials in the manufacturing of herbicides, pesticides, insecticides, fungicides, synthetic dyes and pharmaceutical products. Chlorophenols have low biodegradability and have caused widespread contaminant to soils, surface waters and ground waters. They have been designated as priority toxic pollutants by the United States Environmental Protection Agency. Due to toxicity and odors of chlorophenols, research is needed to develop suitable methods for their removal from water.

Various methods such as reverse osmosis, oxidation, ion-exchange, sorption, electrochemical oxidation and photocatalytical degradation exist for the removal of chlorophenols from aqueous solution. To remediate contaminated subsurface water has traditionally relied on “pump and treat” method. However this method is expensive, often lengthy, and not always effective and has often proved unsuccessful for a number of harmful chemicals. A relatively novel approach is groundwater remediation using a permeable reactive barrier. This involves digging a trench (perpendicular to the groundwater flow) and filling it with permeable reactive material. The contaminant plume moves along the groundwater flow through the reactive wall and contaminant can be removed by several treatment processes (Suthersan, 1999). The reactive materials in permeable barriers are either decomposed to other, transform less dangerous compounds or efficiently fixed to the reactive material (Simon and Meggyes, 2000). Permeable reactive barriers that degrade the contaminants typically use zero-valent iron (ZVI). Although these barrier systems are fairly recent there has been considerable research

into ZVI. Permeable reactive barriers for the treatment of organic contaminants such as chlorinated ethenes is well documented but few studies are available for the treatment of chlorophenols with this technology (Simon and Meggyes, 2000; Choi et al., 2007).

There has been relatively little research into sorption barriers. Previous studies have shown that sorption with granular activated carbon (GAC) is an effective processes for both potable and waste water treatment. However traditional sorbents such as GAC can be expensive and more cost effective sorbents are needed in practice, especially for large scale in-situ groundwater treatment barriers. Woody biomass contains various organic compounds (lignin, cellulose and hemicellulose) with polyphenolic groups that might be useful for binding phenolic compounds through different mechanisms (Ahmaruzzaman, 2008). Having a low cost sorbent that can be regenerated in-situ is ideal since it is not practicable to remove them for ex-situ regeneration.

Using permeable reactive barriers (PRBs), where a reactive barrier immobilised (sorbed) or degrades (oxidised) contaminants in-situ without having to bring them to the surface, could be a better way of treating chlorophenol contaminated site. While extensive studies are carried out in an individual sorption (Nelson and Yang, 1995; Severtson and Banerjee, 1996) and chemical oxidation (Zhang et al., 2003; He et al., 2010) process for the treatment of chlorophenol but combined process are complex and rarely carried out. There is not enough quantitative information of the mechanism of chlorophenols sorption onto woody materials available and a lack of kinetic data about the degradation rates of chlorophenols under various permanganate concentrations at neutral pH in un-buffered solutions. This study carried out sorption, oxidation and oxidation of sorbed organic contaminant (e.g. chlorophenol) in water in a single

component system. Based on the batch and column results the benefits of combined sorption-oxidation for treatment of organic contaminant instead of single treatment process are conceptualised in a proposed alternative permeable reactive barrier system. Such a cost-effective barrier design process requires the knowledge of (1) environmentally acceptable chemical oxidant including their consumption, reaction kinetic and by-product (2) selection of cost-effective sorbent materials including their sorption capacity, particle size and oxidant demand. Therefore each treatment process should be studied to assess and design the proposed integrated system. Specially, oxidant will compete for the organic contaminant and sorbent materials in the sorption-oxidation system is an interesting phenomenon that will reduce overall oxidant consumption and will increase sorbent longevity by regeneration to achieve treatment goal for the removal of organic.

1.2 Research objectives

- Providing an overall conceptual framework with regard to reactions and process for successful in-situ implementation of this technology within a permeable subsurface barrier system which could be implemented from stormwater or groundwater.

The overall objective of this research was to develop a conceptual framework for in-situ subsurface oxidation-sorption barrier treating chlorophenol (CP) contaminated water. This required investigating the mechanisms which would occur in an oxidation-sorption barrier. This water was expected to be a neutral pH, poorly buffered groundwater or stormwater.

Specifically the research objectives were to

- Develop any necessary analytical methodologies to undertake the work.
- Determine a suitable oxidant for the proposed sorption-oxidation barrier and investigate oxidation of both dissolved and sorbed chlorophenol. This included investigations into oxidation kinetics and reaction by-products.
- Investigate reactions between the oxidant and the sorbent (woody material).
- Determine suitable low-cost sorbents for the proposed sorption-oxidation barrier and investigate sorption-desorption mechanisms with chlorophenol. This involved understanding the impact of sorption kinetics, sorbent characteristics, reactor conditions, sorption capacities and desorption upon the processes likely to occur in a barrier system.
- Investigate the sorption-oxidation system both in batch as well as under dynamic flow conditions.

1.3 Scope of research

The development of a subsurface oxidative-sorption barrier to treat organic contaminated water is a large, complex undertaking. This research study was to focus on aspects of an oxidative-sorption barrier which used woody biomass to treat chlorophenol contaminated water.

Therefore the scope of this work was limited to;

- Bench scale batch and column experiments.
- Treating chlorophenol as the sole contaminant
- Using spectrophotometric methods for the analytical work

1.4 Thesis outline

This thesis is divided into five main sections and introduction, literature review, experimental methodology, results and discussion, and conclusions. Two chapters studied the chlorophenol quantification during oxidation and oxidative kinetics of chlorophenols. Another two chapters examined the sorption-desorption of chlorophenols on selected sorbents and column experiment for 2,4-DCP sorption. A chapter on batch and column experiment which examine the permanganate consumption within a chlorphenol contaminated pine.

Chapter 1 presents the introduction of the study.

Chapter 2 describes a literature study in order to obtain an overview of in-situ remediation technology. It presents different organic contaminants, oxidizing agents, chemical kinetics, permeable barrier system, formation of MnO_2.

Chapter 3 investigates experimental method. It described in details of materials, chemicals, procedure, analytical technique and reaction devices.

Chapter 4 studies the method development for the quantification of chlorophenols during chemical oxidation

Chapter 5 presents the kinetic data of organic contaminants and permanganate which determines pseudo-first-order and second-order rate constants.

Chapter 6 presents the sorption-desorption of CP on to GAC, FC, pine and HW

Chapter 7 investigates batch column experiments to examine the ability to sorb 2,4-DCP on to pine.

Chapter 8 examines the ability of permanganate oxidation with chlorophenol in sorbed-pine by batch and column experiments.

Chapter 9 provides a summary, conclusions and suggestion to further research

1.5 Contribution to knowledge

The investigation of mechanisms occurring in an oxidative-sorption barrier is novel even though the primary mechanisms (sorption, oxidation) are commonly researched, however, their application to chlorophenols and woody biomass are not well researched. The advances made in this work have and will make contributions to the published literature.

The ability to cost-effective research on oxidation of chlorophenols relies on analytical methods to quantify the chlorophenol and a complimentary quenching agent to halt the oxidation process at pre-determined interval. A method was developed for this research and published.

> Hossain, S. M. G. and McLaughlan, R. G. (2010). Spectrophotometric method for the determination and kinetics of chlorophenols oxidation by potassium permanganate. 14th Annual Environmental Research Event (ERE), Rockhampton, Queensland, 27–30 June 2010.

> Hossain, S. M. G. and McLaughlan, R. G. (2012). Oxidation of chlorophenols in aqueous solution by excess permanganate. Water, Air, and Soil Pollution, 223, 1429–1435.

The oxidation rates of chlorophenols in aqueous solutions have been researched but little work relevant to stormwater/groundwater at poorly buffered, neutral pH has been done. This work was published. During this work it was also found that there had been

no fundamental work into the kinetics of various permanganate concentrations under these conditions. A paper has been submitted for publication.

> Hossain, S. M. G.and McLaughlan, R. G. (2010). Kinetics of the oxidation of chlorophenols in aqueous solution by potassium permanganate**.** 5th IWAYoung Water Professional Conference (YWPC), UNSW, Sydney, 5–7 July 2010.

> Hossain, S. M. G. and McLaughlan, R. G. (submitted). Kinetic investigations of oxidation of chlorophenols by permanganate, Journal of Environmental Chemistry and Ecotoxicology.

A key area of investigation in this research was the oxidation of chlorophenols in a reactive filtration media. This work is very novel since it investigates oxidation of both dissolved and sorbed chlorophenols as well as oxidation of a woody biomass sorbent. It includes both batch and column studies. This work we believe is publishable and will be submitted in due course.

Another area of investigation in the research was sorption. Knowledge of interactions of chlorophenols with woody biomass is still poorly researched. Contributions to the literature have been made in this area.

> G. S. M. Hossain and R. G. McLaughlan. (2012). Sorption of chlorophenols from aqueous solution by granular activated carbon, filter coal, pine and hardwood, Environmental Technology, 33, 1839–1846.

Hossain, S. M. G. and McLaughlan, R. G. (2009). Sorption of 2-chlorophenol, 4-chlorophenol and 2, 4-dichlorophenol from aqueous solutions using low-cost sorbents. 3rd International Contaminated Site Remediation Conference, Adelaide, South Australia, 27–30 September 2009.

During investigations into sorption the effects of biomass particle size on sorption were performed. This study identified that the elongate nature of the wood particles causes the lack of relationship between sorbent particle size and solute uptake. This work is novel and has been submitted for publication as a short communication.

Hossain, S. M. G. and McLaughlan, R. G. (submitted). Effect of wood particle size on chlorophenol uptake, Bioresource Technology.

This research has already made some contributions to the published literature and will contribute to improve understanding of chlorophenol sorption and permanganate oxidation processes both during in-situ remediation as well as in specifically designed permeable reactive barriers. Fundamental knowledge on the oxidation of chlorophenols as well as their sorption has been generated and will provide the basis for further fundamental and pilot scale studies. The use of woody biomass for chlorophenol sorption barriers have been shown to be feasible and their use in an oxidation-sorption barrier has the potential to be a cost-effective method for remediation of groundwater contaminated by chlorophenols.

CHAPTER 2

Literature review

2 Literature review

2.1 Introduction

This chapter reviews the organic compounds, chlorophenol in particular, present in water and their treatment processes. To represent these treatment processes for organic removal, a number of topics that are closely related to this study are reported in the literature and will be reviewed, such as in situ remediation technologies, permeable reactive barriers, sorption and chemical oxidation methods.

2.2 In-situ treatment technology

There are many techniques used in the remediation of contaminated soil and groundwater. One of the most common techniques is pump-and-treat, which is relatively cheap to install and safe to operate, although operation and maintenance costs are generally high. In this method, contaminated groundwater is drawn from the aquifer and treated on site. The treated water may then be re-injected to the aquifer, discharged to the surface water, or transferred to a water treatment plant. The contaminant concentration in the pumping wells decreases with operation time, however, and can become uneconomic. This has led to an increase in innovative remediation technologies for the in situ treatment of both soil and groundwater. The in situ technologies involve chemical, biological or physical treatment processes into the subsurface to degrade, remove or immobilize contaminants without bringing them above ground. The two most widely used in situ technologies for remediation are the permeable reactive barrier (Striegel et al., 2001) and chemical oxidation (Siegrist et al., 2001; ITRC, 2005).

2.2.1. Permeable reactive barriers/zones

The permeable reactive barriers (PRBs) are a new, cost-effective and innovative technology for a contaminated site. Common types of permeable reactive barriers are chemical reaction, biological and sorption. In the case of a chemical reaction barrier, the contamination is removed through an oxidation/reduction reaction. A biological barrier uses a compound which releases oxygen and nitrogen, enhancing microbial degradation. Lastly, a sorption barrier uses a sorbent to remove the contaminant.

PRB principles

Permeable reactive barriers (PRBs) enable in-situ remediation of contaminated groundwater by means of reactive materials. The reactive materials are placed in underground trenches downstream of the contamination plume. The plume is forced to flow across the reactive materials and the contaminants are immobilised or degraded. This cost-effective clean-up technology impairs the environment much less than other methods and does not require a continuous input of energy. It is cost-effective compared to the expensive pump and treat method (Scherer et al., 2000).

The principle of groundwater remediation using the permeable reactive barrier method is in digging a trench (perpendicular to the groundwater flow) and filling it with permeable reactive material. The contaminant plume moves along the groundwater flow (Figure 2.1) through the reactive wall, and contaminants can be removed by several treatment processes (Suthersan, 1999). The reactive materials in permeable barriers are either decomposed to other, less dangerous compounds or efficiently fixed to the reactive material (Simon and Meggyes, 2000).

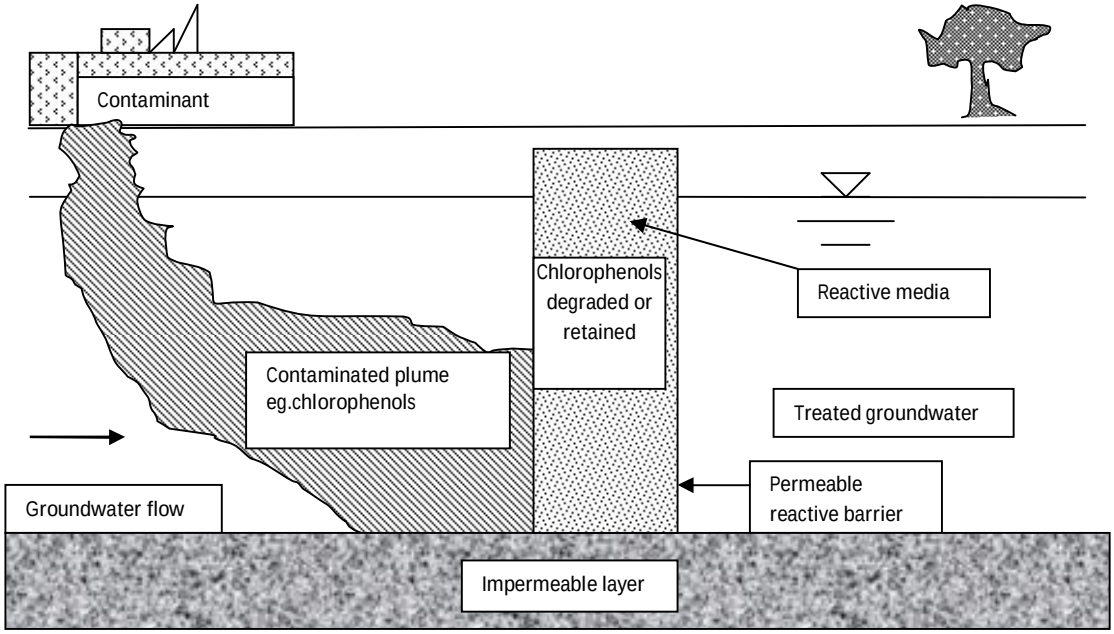

Figure 2.1 Groundwater remediation using PRB

Subsurface barriers are constructed to restrict or control the movement of contaminant plumes in groundwater (Striegel et al., 2001). A subsurface sorption barrier consists of reactive material, and the contaminant plume moves through the reactive barrier where the contaminants are either sorbed or chemically degraded to less toxic substances by the reactive material within the barrier (USEPA, 1997). A typical subsurface sorption barrier is shown in Figure 2.2.

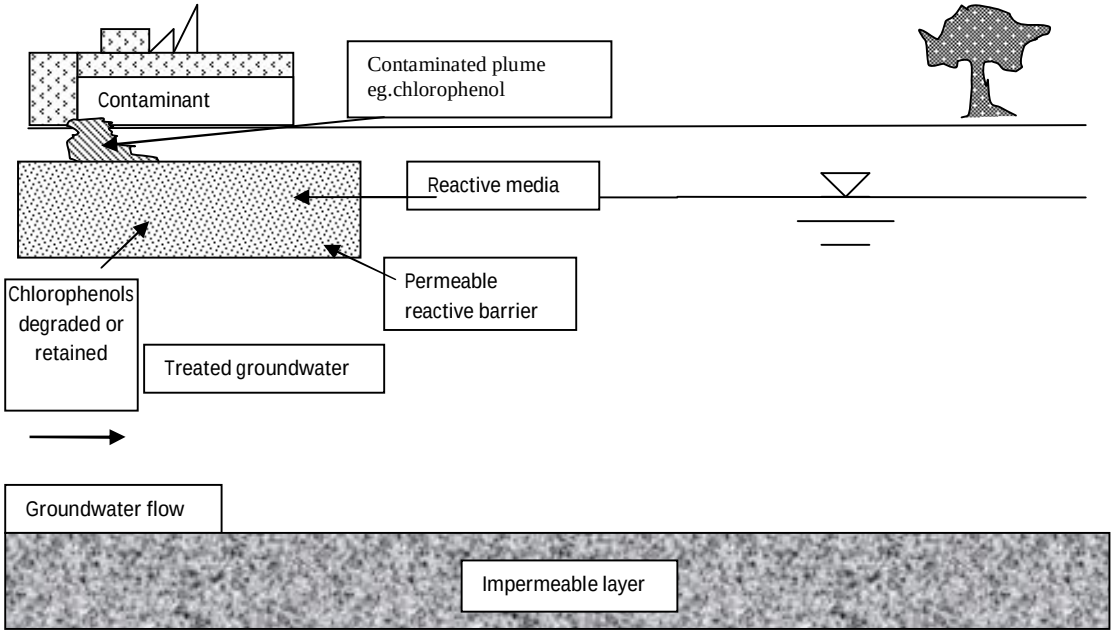

Figure 2.2 Groundwater remediation using horizontal subsurface barriers

PRB Reactive media selection

Reactive media types

Several treatment processes are applicable for the treatment of contaminants with reactive material in a PRB. These processes are discussed below:

- Sorption – The removal of contaminants from the solution using sorption and ion exchange by the reactive material. The most common sorption materials used in PRB are zeolite, granular activated carbon and peat for the removal of organic contaminants and heavy metals (Suthersan, 1999; ITRC, 2005). Traditional sorbents such as activated carbon can be expensive for large subsurface barriers, but alternatives like pine and hardwood can be used as low cost sorbents and do not require a pre-treatment step before application.

However, there are many factors to consider for groundwater remediation, such as price, environmental impact, contaminant properties, specific site restrictions and public acceptance.

- Chemical degradation – In this process, the contaminants are converted to less harmful compounds through chemical reaction. For example, dissolved chlorinated hydrocarbon can be degraded to non-toxic end products by zero-valent iron (Fe^{o}). The chemical degradation technique can prove expensive, however, and there is also the possibility that zero-valent iron (ZVI) barriers will clog the pore space or serve as a physical barrier to reactive surface sites during the oxidation of ferrous iron and the precipitation of oxides (Simon and Meggyes, 2000). So far, few documented case studies dealing with the application of ZVI for chlorophenols removal are available.
- Biological (aerobic or anaerobic) reactions – Volatile organic hydrocarbons (VOCs) can be degraded by means of biological reactions through aeration via a PRB (ITRC, 2005). Biological treatment is often the most economical, but the current conventional biodegradation method is unsatisfactory for chlorophenol removal.

The selection of reactive media for treating contaminants depends on many factors including the contaminant type, distribution and composition (Suthersan, 1999; ITRC, 2005). Examples of reactive materials are shown in Table 2.1:

Table 2.1 Reactive materials used in PRBs

Reactive Medium	Removal Mechanism	Contaminant removed	References
Coal, powdered activated carbon, peat, sawdust	Sorption	Benzene	Rael et al., 1995
Zero-valent metals (Fe)	Metal-enhanced reductive dechlorination for organic compounds	Chlorinated ethenes, ethanes, methanes, and propanes; chlorinated pesticides, Freons, nitrobenzene	ITRC, 2005
Oxygen releasing compounds, Nitrate releasing compounds	Microbial degradation	BTEX	Bianchi-Mosquera et al.,1994 Borden et al., 1997 Kao and Borden, 1997
Surfactant-Modified soils	Sorption	Nonpolar organics	Burris and Antworth, 1992 Lee et al., 1989 Wagner et al., 1994
Surfactant-Modified Clays	Sorption	Nonpolar organics	Smith and Galan, 1995, Smith and Jaffe, 1994 Smith et al., 1990
Surfactant-Modified zeolite	Sorption	Nonpolar organics	Bowman et al., 1995
Organic mulch (cypress bark, hardwood bark and pine bark nuggets)	Sorption and biodegradation	Polyaromatic hydrocarbons (PAHs)	Seo et al., 2007

Sawdust (Rael et al., 1995) and organic mulch (Seo et al., 2007) contains various biopolymers (such as cellulose and lignin) were used in PRB to remove organics. Pine wood contains cellulose and lignin. It indicates that wood chips can also be used as a suitable sorbent media in PRB to remove organic such as chlorophenol. In addition,

wood is inexpensive and readily available. This makes interests in studying the feasibility of using low-cost materials.

Design issues

The main purpose of a PRB is to capture contaminated groundwater and provide sufficient residence time in the reactive media to achieve the desired cleanup goals. The following main factors impact PRB design (ITRC, 2005):

- Suitable reactive media
- Configuration, shape, dimension, size and thickness of permeable reactive wall
- Groundwater flow
- Influence on hydrogeological regime
- Hydrologic modelling

A hydraulic model for designing a permeable reactive barrier is very important for the following reasons (ITRC, 1999):

- Determination of an approximate location and configuration of the permeable reactive barrier with respect to groundwater flow, plume movement and flow velocity through the In Situ Treatment Zone (ISTZ).
- Determination of the dimensions of the permeable reactive barrier and ISTZ
- Estimation of the hydraulic capture zone
- Determination of location and sample frequency of monitoring wells
- Evaluation of the hydraulic effects of potential losses in porosity, flow bypass, underflow, overflow, or flow across aquifers.

2.2.2 In situ chemical oxidation in a reaction zone

In situ reactive zones are based on the creation of a subsurface zone where the contaminants are immobilized or degraded into harmless compounds. The design of reactive zones is required to consider the following two reactions (Suthersan, 1999):

- Reactions between the injected reagents and the contaminants
- Reactions between the injected reagents and the subsurface environment.

The effectiveness of the reactive zone is determined by the relationship between the kinetics of target reactions and the rate at which the contaminants pass through the zone with the groundwater flow. An effective reactive zone also requires proper reagents which should mix uniformly within the reactive zone and have fewer side reactions (Suthersan, 1999).

The process of in situ destruction of contaminated organic sources in the aquifer using chemical oxidation is referred to as in situ chemical oxidation (ISCO) (Al et al., 2006). ISCO is a technique in which chemical oxidant is injected into the subsurface to treat organic contaminated soils and groundwater, producing fewer toxic or harmless substances such as carbon dioxide, oxygen and water (ITRC, 2005). ISCO reduces the target contaminant mass by lowering the concentration of aqueous phase contaminants which in turn increases the concentration gradient, thereby increasing the rate of mass transfer (Schnarr et al., 1998).

The treatment of organic compounds such as chlorophenols into harmless simple species using advanced oxidation processes such as ozone, ozone and ultraviolet, and Fenton's reagent has been reported to be effective (Pera-Titus et al., 2004), although the cost for such treatment is high. Nonetheless, in some cases ozone reacts with bromide to

form carcinogenic brominated by-products (Gimeno et al., 2005). The optimum pH for Fenton oxidation is in the acidic range, approximately pH 3.0, which limits the applicability of this environmental technology (Georgi et al., 2007). Moreover, oxidizing agents such as ozone, Fenton's Reagent and hydrogen peroxide have significantly shorter residence time in the subsurface compared to permanganate (Huang et al., 1999). Therefore, cost-effective and environmentally suitable chemical oxidation methods are needed. Other studies show that ethylenes can be treated successfully with ISCO in the field due to their higher reactivity with $KMnO_4$ (Schnarr et al., 1998). In the case of in situ chemical oxidation (ISCO), large excess permanganate is required, greater than the amount needed to treat the organic contaminant based on reaction stoichiometry due to the subsurface background matrix.

The design of a permanganate reactive barrier involves a series of vertical wells into which the $KMnO_4$ is injected. The $KMnO_4$ spreads out from the well casing by diffusion; the contaminant plume passes the PRBs, and in situ oxidation will destroy the contaminant and prevent further spreading (Figure 2.3). This semi-passive reactive barrier was proposed by Devlin and Barker (1999).

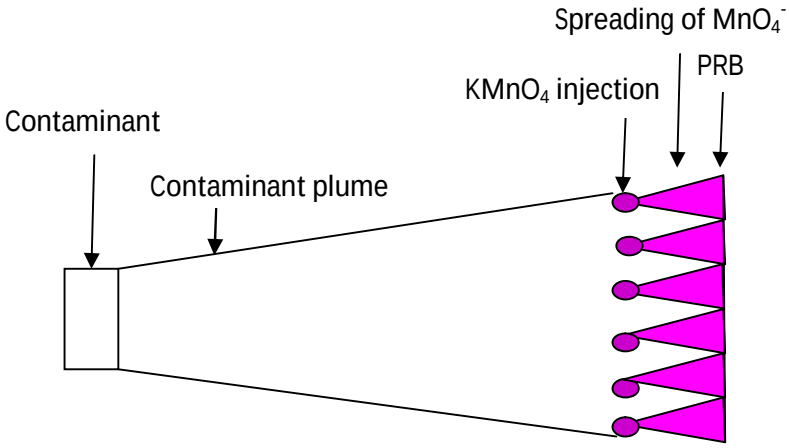

Figure 2.3 Design of the permanganate reactive barrier system

Design issues

Chemical oxidation is a widely used method for the remediation of groundwater contaminated by toxic chemicals. The most commonly used oxidants are permanganate, peroxide, persulfate and ozone, which are able to rapidly and completely destroy many toxic organic chemicals (USEPA, 2000). It reacts with natural organic matter more quickly; hence these oxidants are decreased within days while permanganate can last in the subsurface for several months before reaching the target material.

The rate and extent of degradation of a target organic contaminant depends on the properties of the chemical and its susceptibility to oxidative degradation, as well as the matrix condition such as pH, temperature, electrode potential (Eh), ionic strength and composition, and the generation of MnO_2 solids, the concentration of the oxidant and the concentration of other oxidant-consuming substances such as natural organic matter, reduced minerals and free radical scavengers. Therefore, the amount of permanganate consumption also increases (USEPA, 2000). The mass of oxidant needed will be equal

to the natural organic demand (NOD) plus the demand determined from the reaction stoichiometry (SERDP, 2006). In some aquifer systems, the NOD is large compared to the oxidant demand of the contaminant. Consequently, the high cost of the large quantity of oxidant required to overcome the NOD may limit the use of ISCO for the treatment of contaminant under such conditions.

The transport and oxidation process of oxidants such as potassium permanganate or hydrogen peroxide to the subsurface may change the soil matrix and permeability. Permeability losses can occur as a result of (1) the detachment and redeposition of colloids and particulate matter as a result of high rate fluid injection, (2) the production of reaction products CO_2 or MnO_2, or (3) the production of MnO_2 which may also lower the permeability of the soil matrix and/or may form a coating on dense non-aqueous phase liquid (DNAPL) (ITRC, 2005). Permeability increases can occur in certain formations where the acidity produced by chemical reactions can lower the pH and dissolve components such as $CaCO_3$ (SERDP, 2006). This may cause the mobilization of metals within the treatment zone and the formation of toxic by-products (USEPA, 2000). Other oxidation effects are the evolution of heat and gas, biological perturbation and reaction chemistry.

PRB technology with zero-valent iron (ZVI) is an effective method for remediation of contaminated groundwater (Jeen et al., 2006). ZVI can use in the degradation of chlorinated hydrocarbons. ZVI acts as reducing agent and it is oxidised to the ferrous ion (Fe^{2+}) with dissolved oxygen present in water. Dissolved oxygen is rapidly consumed at the entrance of an iron bearing barrier and further oxidation which leading to the formation of iron hydroxides, carbonates and sulphides in the wall causes

clogging and fouling in the reactive media reduced the permeability (Simon and Meggyes, 2000; ITRC, 2005). It was found that in situ chemical oxidation (ISCO) using $KMnO_4$ for groundwater treatment contaminated with chlorinated ethenes is effective. There are some limitations on the use of $KMnO_4$ for ISCO, the formation of MnO_2, which can affect the permeability (Crimi and Siegrist, 2004). Well clogging is expected due to precipitation of MnO_2 solids during oxidant injection at higher oxidant concentrations ~2% $KMnO_4$ (127 mM) (USDOE, 1999). However this is fine sand.

Although the groundwater remediation using reactive barriers is considered to be a promising technology, the longevity of barriers installed in subsurface systems is unknown because of the novelty of the technology, the reactivity of the aging barrier due to the formation of precipitants on the surface, and the effect of groundwater geochemistry and flow velocity on the performance of the reactive barrier, are still uncertain. It has been proven PRBs using ZVI systems can last for 15 years (ITRC, 2011). However, non-ZVI-based PRBs have not yet been proven to function for 15 years but several biowalls (wood chips barriers) have shown successful performance up to 5 years (Molin et al., 2009). Wood contains similar characteristics of biopolymer compounds (cellulose and lignin) like organic mulch can be expected longevity will be 3-5 years like biowall where organic mulch is a reactive media.

The oxidant injection design concentration and volume is determined by considering several factors (ITRC, 2005):

- The total oxidant dose required to degrade contaminants in the sorbed, dissolved, and nonaqueous (i.e., NAPL) phases, in excess of the losses caused by reactions with natural reductants and oxidant scavengers (i.e., organic carbon, reduced minerals, carbonates).

- Oxidant reaction rates and subsurface persistence can limit the radius of oxidant delivery and the desired radius of influence.
- The injection volume is directly related to the subsurface pore volume of the target area for treatment and the contaminants should not be displaced outside of the treatment zone by the injection (ITRC, 2005).
- If the dosing of permanganate concentration is increased, the rate of organic degradation increases. It is necessary to add excess oxidant to overcome the oxidant demand of non-target compounds. In some cases, the kinetics of these non-target reactions are fast, such that non-target reductants can often compete with the target contaminants for the available oxidant (ITRC, 2005).

2.2.3 Sorption-oxidation

Sorption-oxidation is an alternative in situ technique for soil and groundwater remediation. This technique is based on two mechanisms, sorption (Scherer et al., 2000) and chemical oxidation (Siegrist et al., 2001). Several factors must be considered when choosing a new remediation technique. The main factors to affect sorption-oxidation are the characteristics of sorbents, the properties of sorbate, the condition of the solution and the suitability of the oxidant.

Proposed conceptual design of sorption-oxidation reactive barrier

A major disadvantage of a sorption barrier is that sorption materials need to be replaced or to regenerate, which makes a sorption barrier rather expensive and not attractive compared to other options. By considering this aspect of a sorption barrier, this study proposed a permanganate-pine reactive barrier. In this processs, the contaminant will initially be sorbed by pine and subsequently, oxidized with permanganate. Saturated

pine will be regenerated by $KMnO_4$ through the oxidation of contaminants. In this way oxidation and regeneration will take place continuously as long as both $KMnO_4$ and pine exist in the barrier system.

The focus of this research is to better understand the processes that occur in an oxidative-sorption barrier. The conceptual design uses permanganate as oxidant and woody biomass (eg. pine-hardwood) as the sorbent. It is conceived that intermittent injection of $KMnO_4$ would occur. An oxidisable organic contaminant (eg., chlorophenol) would flow into the barrier and be sorbed to the media and then intermittent oxidised through permanganate injection. This sorption-oxidant barrier system was designed based on the concept of USEPA (1998) and Devlin and Barker (1999) PRBs (Figure 2.4).

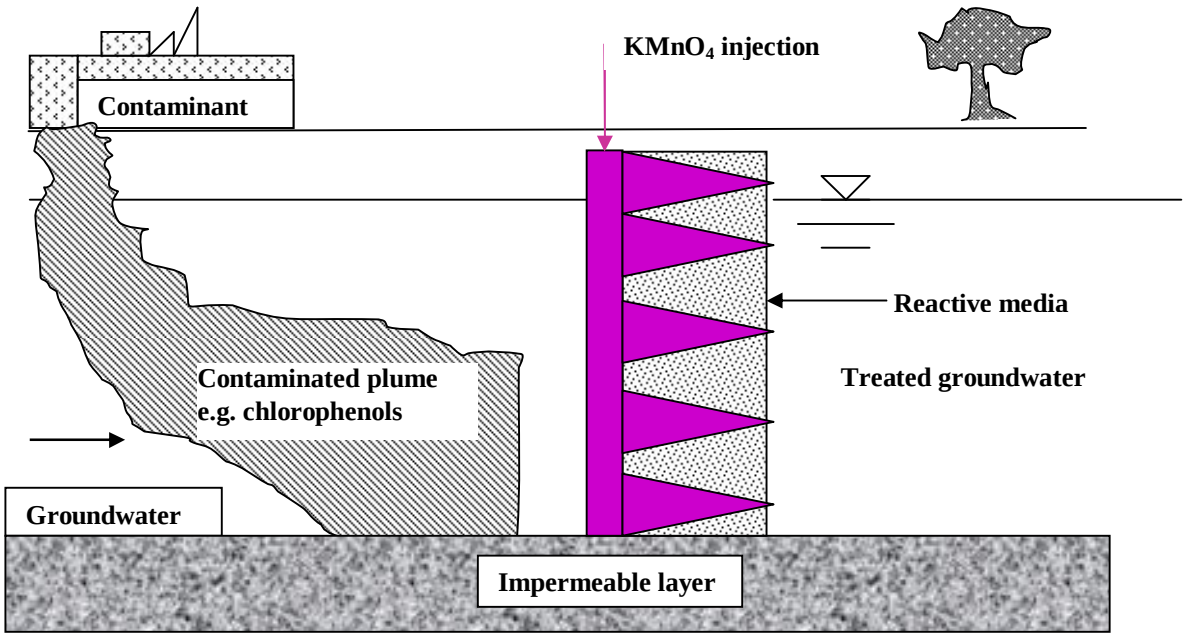

Figure 2.4 Conceptual design of permanganate-pine barrier (Groundwater)

A subsurface system sorption barrier could also be placed horizontally over the aquifer. The contaminant plume would pass through the sorption barrier and the contaminants retained by the woody biomass. Subsequently, $KMnO_4$ would be injected into the barrier where it would oxidise the sorbed contaminant and simultaneously regenerate the woody material. The proposed PRB in a subsurface system is shown in Figure 2.5

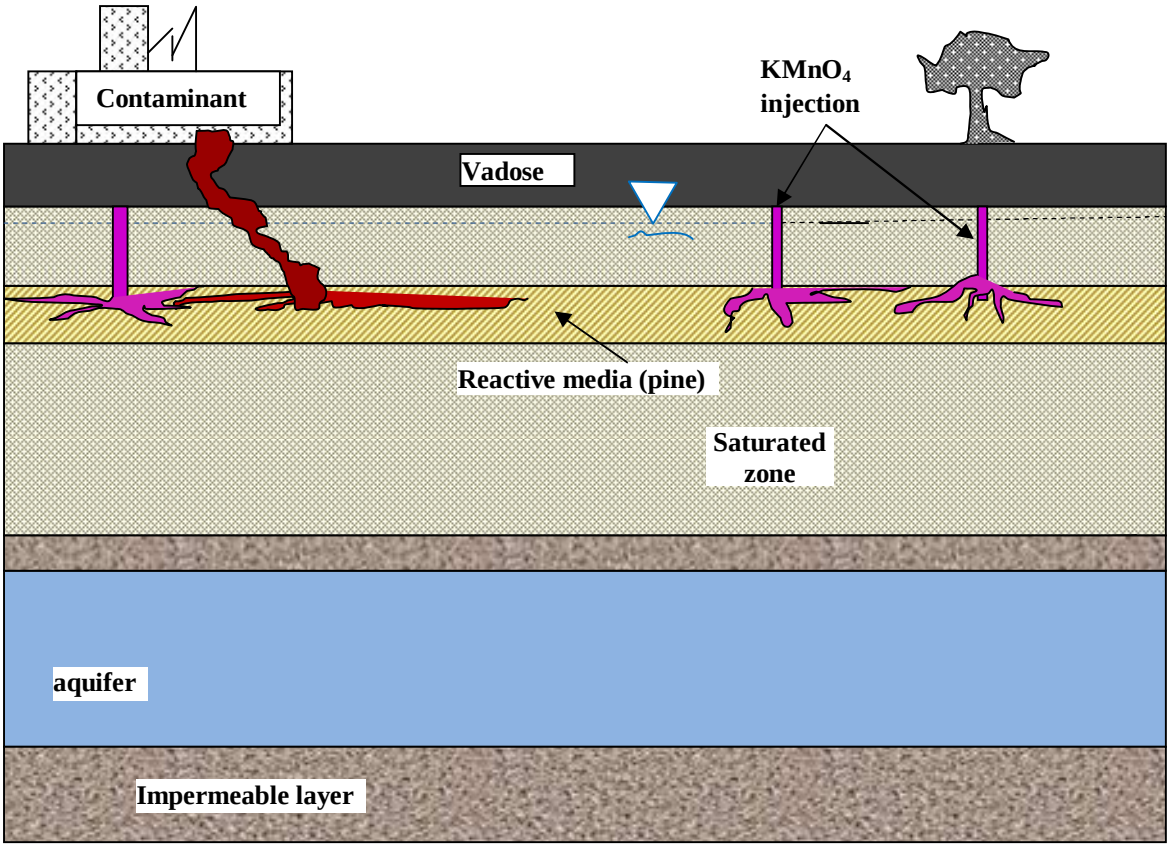

Figure 2.5 Conceptual design of permanganate-pine barrier (Subsurface)

A comparative study of the proposed pine-permanganate reactive barrier with other barrier systems is shown in Table 2.2.

Table 2.2 Comparative study of the proposed pine-permanganate reactive barrier with other barrier systems

	Sorption barrier (sorbent)	Oxidation barrier ($KMnO_4$)	Sorption-oxidation (pine and $KMnO_4$)
Contaminant removal	Contaminant plume will be sorbed by sorbent	Contaminant plume will be oxidised by $KMnO_4^-$ to harmless compounds.	Contaminant plume will be sorbed by pine and oxidised with $KMnO_4$. The saturated pine will be regenerated by $KMnO_4$ through oxidation with the contaminant which will take place continuously until $KMnO_4$ and pine remain.
Permanganate dosing	Sorbent needs to be replaced or regenera-ted frequently and might desorp through groundwater flow after saturation.	Needs higher $KMnO_4$ dose to maintain continuous residual $KMnO_4$.	Low $KMnO_4$ dosing expected to maintain continuous residual $KMnO_4$.
Oxidation	No oxidation occurs. Contaminant remains in sorbent or may be desorbed due to groundwater flow.	Oxidation occurs. Residual $KMnO_4$ does not exist for long due to groundwater flow.	Residual $KMnO_4$ exists for a long time.
Contaminant interaction	Contaminant interacts with existing sorbent during groundwater flow.	$KMnO_4$ reacts with existing contaminant plume during groundwater flow direction where $KMnO_4$ retention time is less.	$KMnO_4$ reacts with contaminant plume in a confined barrier system which maximises $KMnO_4$ utilization.

The advantages of the proposed pine permanganate barrier are as follows:

1. It would reduce $KMnO_4$ consumption.
2. It effects maximum utilization of $KMnO_4$.
3. Saturated pine can be regenerated and used for a long time.

2.3 Organic matter

Organic matter in surface and groundwater is a mixture of organic compounds. Organic matter in natural water can be divided into dissolved organic carbon (DOC) smaller than 0.45 µm and particulate organic carbon (POC) greater than 0.45 µm. Generally, DOC is greater abundance than POC. Dissolved organic carbon is approximately 90% of the total organic carbon of most contaminated waters (Aiken and Kuniansk, 2002). Langwaldt et al. (2005) studied the composition and content of organic matter present in groundwater and found that groundwater was contaminated with 60-2650 µmole L^{-1} of DOC, of which up to 98% was accounted for chlorophenols (CPs). Many studies (Simon and Meggyes, 2000; Choi et al., 2012) have been carried out on organic compound removal in surface and groundwater treatment because of contaminant toxicity. The types of organic pollutants detected in groundwater include pesticides, solvents, degreasers, petroleum components and industrial by-products. Some of these chemicals (e.g., chlorinated ethenes, phenolic compounds and poly aromatic hydrocarbons) are extremely toxic. The environmental distribution of organic compounds in the aquatic system depends mainly on their solubility physical-chemical factors affecting the partition between sorbent-sorbate phases (Esteves da Silva and Marques, 2007).

2.3.1 Chlorophenol contamination in surface and groundwater

Chlorophenols are contaminants in soils, sediments, surface water and groundwater because of their utilization as wood preservatives and general biocides in industry and agriculture (Cortés-Martínez et al., 2007). These compounds are carcinogens and exhibit considerable water solubility and high toxicity (Choi et al., 2012). Because they are harmful to organisms at low concentrations, many of them have been classified as hazardous pollutants because of their potential harm to human health. Their toxicity and persistence can directly impact the health of ecosystems and present a threat through the contamination of water bodies (Ahmed et al., 2011). Currently, ISCO with permanganate is available for decontaminating chlorinated ethenes. To evaluate the potential effectiveness of in situ chemical oxidation at field scale and provide design guidance for the implementation of this technology within a permeable barrier system, it is necessary to know the oxidation rates of chlorophenols. The oxidation of chlorophenols with permanganate is carried out by many researchers (Lee and Sebastian, 1981; Waldemer and Tratnyek, 2006; He et al., 2010).

Chlorophenols were detected in both surface and ground waters (Howard, 1989). Typical chlorophenol concentration in the groundwater was found in Finland contaminated site in the range from 10 to 40 mg L^{-1} (Puhakka, 2010). Chlorophenol concentration in groundwater for 2,4,6-trichlorophenol was found 7-11 mg L^{-1} (Jarvinen et al., 1994). High concentrations of 43.8 µg L^{-1} and 36.5 µg L^{-1}, respectively, were found for 2-CP and 2,4-DCP in surface water (Jones and Watts, 1997). A range of chlorophenols such as 2-CP, 4-CP and 2,4-DCP were found in ground water at an industrial site near Perth, Western Australia (Devis et al., 2008). The concentration of 2,4-DCP was in the range of 200–380 µ g L^{-1} whereas 4-CP concentration was

higher in the range of 250-15000 µg L^{-1} with depth range 7.5 to 13 m (Devis et al., 2008) detected in Perth.

In the environment, the distribution of chlorophenols varies depending on the source, e.g. air, land or water. The National Pollutant Inventory (NPI) records data for all sources of chlorophenols emissions in Australia, and since 2005/2006, the total industrial emission of chlorophenol has increased from 380 kg to 2600 kg in 2009/2010 (NPI, Australia) (Figure 2.6).

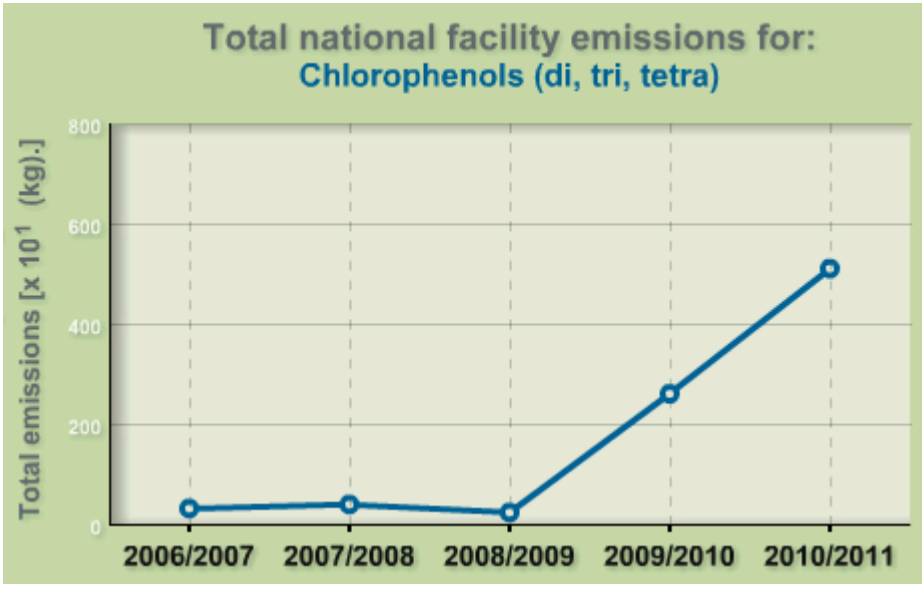

Figure 2.6 Chlorophenol emissions in Australia (Source: www.npi.gov.au)

According to Australian drinking water guideline values, the maximum allowable of 2,4-DCP is 0.2 mg L^{-1} and 2,4,6-TCP is 0.02 mg L^{-1}(NPI, Australia).

2.4 Sorption

In sorption, soluble organic molecules are attracted by solid sorbents through physical and chemical interaction. Physical interaction is mainly caused by Van der Waals dispersion forces, i.e. the molecular attraction between sorbent and sorbate molecules. It is reported that the sorption of phenols and chlorophenols may involve electron donor-acceptor complexes or dispersion forces between π-electrons in phenols and π-electrons in activated carbons (Coughlin and Ezra, 1968).

During sorption, soluble substances are sorbed onto the sorbent, and over a particular period of time, some soluble substances desorb. This is continued until the sorption and desorption rates are the same, i.e. initially, pseudo-equilibrium is achieved, and finally absolute equilibrium is reached between the sorbent and the sorbate. They are called isotherms because sorption experiments are generally carried out at constant temperature. There are several factors affecting the rate of sorption (Dabrowski et al., 2005) such as:

- sorbent: particle size, pore structure and surface area.
- sorbate: concentration, molecular size, molecular shape, solubility, ionization and hydrophobicity
- experimental condition: temperature, solution pH, contact time and ionic strength.

2.4.1 Sorbents

The main characteristics of good sorbents are their high porosity and large surface area which result in less time being required to reach equilibrium. Activated carbon has been effectively employed for the removal of chlorophenols by many researchers (Nelson and Yang, 1995; Furuya et al., 1997). Currently, there is a growing interest in using low cost sorbents for the removal of chlorophenols. A large variety of low-cost materials such as red mud (Gupta et al., 2004), paper mill sludge (Calace et al., 2002) and wood pulp (Severtson and Banerjee, 1996) are feasible substitutes for activated carbon for the removal of chlorophenols from contaminated water.

Sorbents contain pores that are classified by width into three sub-groups: micropores (pore size < 2 nm), mesopores (2–50 nm) and macropores (>50 nm), according to the definition of the International Union of Pure and Applied Chemistry (IUPAC) system. The width of the pores of filter coal, pine and hardwood sorbents are in a range between 7.6 nm and 23.2 nm and correspond to the mesoporous (Table 3.1 and Table 3.2). Granular activated carbon (GAC) may be classified as mesoporous or microporous carbon. Micropores usually account for over 95% of the total surface area of common activated carbons (Nassar and El-Geundi, 1991).

Granular Activated Carbon

Granular activated carbon (GAC) is a commonly used sorbent for the removal of organic contaminants from groundwater and waste water. It has a surface area greater than 900 m^2 g^{-1} and consists of microcrystallites of graphite stacked layers with the mircopores being formed by the spaces between crystals. The aromatic rings in the

graphite crystals provide the hydrophobic properties of the micropore surface (Snoeyink and Weber, 1967). This aromatic ring has a π-electron orbital below and above the plane of six carbon atoms (Morrison and Boyd, 1992), and the sorption of the phenolic molecule is a result of the interaction of aromatic π-electrons of the phenolic molecule and the π-electrons of the GAC aromatic ring (Furuya et al., 1997).

Sorption capacities for commercial GAC with 2-CP, 4-CP and 2, 4-DCP is typically in the order of 280–420 mg g^{-1} (Nelson and Yang, 1995; Aksu and Yener, 2001; Hamdaoui and Naffrechoux, 2007). The sorption capacity of chlorophenols on GAC mainly involve hydrogen-bonding between solutes and sorbents (Mattson et al., 1969). The sorption of phenols has been found to be rapid, with 60% to 80% of sorption achieved within the first hour of contact, followed by a slow approach to the final equilibrium stage, which requires five to seven days (Zogorski et al., 1976).

Organic material in permeable reactive barrier (PRB) is used for the treatment of contaminated groundwater through sorption and biological degradation. Granular activated carbon (GAC) is an example of a sorbent, and a surface for bacterial growth where bioremediation takes place to treat organic contaminant (ITRC, 2005). GAC mixed with zero-valent iron was used as a reactive media in PRB for the degradation of groundwater contaminants such as chlorophenols, chlorinated hydrocarbons and others at on laboratory and field scale (Farrell et al., 2000, Choi et al., 2007; Yang et al., 2010).

Filter Coal

Coal is a complex heterogeneous rock which is a mixture of organic and inorganic components and has a very complicated pore structure (Gurdal and Yalcin, 2001).

Walker and Mahajan (1993) reported that pores in coal are isolated from one another and sorption can only occur by diffusion through the solid glassy macromolecular coal. Sorption of phenol by coal was carried out by Ishaq et al. (2007) who reported that the significant phenol sorption in the case of virgin coal was due to the porosity in the coal matrix as well as to the interactions and donor-acceptor complex formation at the surface and within the pores because of functional groups.

There are relatively few published studies on the sorption of chlorophenols on coal. The micropores and macropores within coal may be responsible for sorption (Gan et al., 1972). However, even though the coal may have significant surface area, the utilization of the micropore is poor because of diffusion issues (Walker and Mahajan, 1993). To address this, many techniques have been proposed to improve the sorption capacity by modifying the coal surface. Ahmaruzzaman and Sharma (2005) studied 4-CP sorption onto coal. In untreated coal, the sorption process was controlled by external mass transfer followed by intra-particle diffusion mass transfer. They reported that pre-treated coal was found to be a better sorbent than untreated coal for chlorophenol removal. In the removal of phenol by untreated lignite coal, it was found that hydrogen-bonding of the phenolic –OH with the oxygen sites on the lignite surface was the most likely mechanism for sorption with most of the surface area due to the macrocracks (Polat et al., 2006). A sorption capacity of 10 mg g^{-1} and long equilibrium times (> 8 days) were obtained.

Wood (Pine and Hardwood)

Wood is used extensively as a fuel, construction material and industrial raw material in many countries. Researchers have found that wood is a good sorbent of a variety of

organic compounds, such as organochlorine pesticides (Bras et al., 1999), or monoaromatic and polyaromatic hydrocarbons (MacKay and Gschwend, 2000; Boving and Zhang, 2004). Wood consists of three major components: cellulose, hemicellulose and lignin. Cellulose and hemicellulose are responsible for hydrogen bonding because of their polyhydroxyl and polycarbonylic structure, whereas lignin's phenylpropane units may provide for relatively hydrophobic regions, which attract hydrophobic compounds (Huang et al., 2006). Extensive hydrogen bonding within the cellulose makes the cellulose molecule rigid and allows the molecule to sorb shock by subsequently breaking and reforming, i.e. the C-C and C-O bonds distort the ring structure (Rowell, 2005).

In a recent review of low cost sorbents for phenolic removal, it was noted that sawdust has proven to be a promising low-cost material (Shukla et al., 2002; Jadhav and Vanjara, 2004; Nenkova and Radev, 2004; Ahmaruzzaman, 2008). It contains various organic compounds (lignin, cellulose and hemicellulose) with polyphenolic groups that might be useful for binding phenolic compounds through different mechanisms. Studies on the sorption of other organic compounds to wood (MacKay and Gschwend, 2000; Boving and Zhang, 2004) also found it had promise as a sorbent. In a study on chlorophenol sorption (2,4-DCP) to wood pulp, it was found that sorption was unaffected by the fiber surface area (Severtson and Banerjee, 1996).

Sorption capacities of different sorbents

The value of the sorption capacity of chlorophenols on some low-cost sorbents is shown in Table 2.3. This indicates that the proposed novel sorbents have potential for chlorophenol sorption capacity.

Table 2.3 Chlorophenol sorption on various low-cost sorbents

Compounds	Sorbents	Sorption capacity mg g^{-1}	References
2-CP	Coal, Fly ash	0.8–1	Kao et al., 2000
2-CP	Bituminous Shale	3.1	Tutem et al., 1998
2-CP	Cokebreeze	2.95	Ahmaruzzaman and Sharma, 2005
2,4-DCP	Coal, Fly ash	1.5–1.7	Kao et al., 2000
2,4-DCP	Bituminous Shale	4.2	Tutem et al., 1998
2,4-DCP	Paper mill sludge	4.49	Calace et al., 2002

2.4.2 Quantifying sorption/desorption

Sorption equilibrium data can be expressed in the form of a sorption isotherm with the mass of sorbate sorbed per unit of dry mass of sorbent q_e (mg g^{-1}) on the y-axis and the mass of sorbate C_e (mg L^{-1}) in the aqueous solution on the x-axis at constant temperature. The equilibrium solid phase and liquid phase concentration can be calculated by using mass balance as follows:

The amount sorbed q_t (mg g^{-1}) at time t was calculated according to equation 2.1:

$$q_t = V (C_o - C_t) /W \qquad (2.1)$$

where C_o is the initial concentration (mg L^{-1}), C_t is the residual concentration (mg L^{-1}) at time t; V is the volume of the solution (L) and W is the mass of the sorbent (g).

Equilibrium sorption capacity, q_e (mg g^{-1}), was calculated by equation 2.2:

$$q_e = V (C_o - C_e) /W \quad (2.2)$$

where C_e (mg L^{-1}) is the equilibrium concentration in the liquid phase.

A desorption isotherm is important for determining the extent of irreversibility because it provides information about the strength of the sorbent-sorbate bond. The equilibrium solid-phase loading on pine and HW were calculated after desorption by equation 2.3:

$$q_e = (q_o W - C_e V)/W \quad (2.3)$$

where q_o is the equilibrium solid-phase loading after the initial sorption (mg g^{-1}), W is the mass of the sorbent (g), V is the volume of the solution (L), C_e (mg L^{-1}) is the equilibrium concentration in the liquid phase after desorption and q_e is the equilibrium solid-phase loading after desorption (mg g^{-1}).

Differences between sorption-desorption behaviour were evaluated using several different hysteresis indexes. Cox et al. (1997) proposed a hysteresis co-efficient H expressed as equation 2.4:

$$H = \frac{n_d}{n_a} . 100 \quad (2.4)$$

where n_d and n_a are the Freundlich exponents for desorption and adsorption respectively.

Zhu and Selim (2000) proposed a hysteresis index based on the difference in area between the adsorption and desorption isotherms by equation 2.5:

$$\lambda = \left(\frac{n_a + 1}{n_d + 1} - 1 \right) . 100 \quad (2.5)$$

When desorption occurs at the same rate as sorption, there is no hysteresis and H=100 and λ=0. Positive hysteresis occurs when the desorption rate is slower than sorption and is indicated by $H < 100$ and $\lambda > 0$.

2.4.3 Modelling equilibrium sorption

There are various models (Freundlich, 1906; Langmuir, 1916; Butler and Ockrent, 1929) for single component and multicomponent sorption systems. In a single component system, one contaminant is dissolved in water and this contaminant is assumed to be unaffected by the water. Therefore, sorption from a single contaminant is treated as a single component sorption, and polluted water containing more than one contaminant is multicomponent sorption equilibrium. This study will examine the equilibrium relation to single component equilibrium. A number of model isotherms have been documented to represent the single component sorption. The most widely used isotherms are the Langmuir isotherm and Freundlich isotherm, which have been used to discuss the equilibrium characteristics of the sorption process. The Freundlich isotherm is used for a heterogeneous surface, whereas the Langmuir model is basically obtained from the ideal assumption of a homogeneous sorption surface. The constant parameters of the isotherm equations for this sorption process were calculated by non-linear regression analysis and compared against experimental data for goodness of fit.

Langmuir isotherm

The Langmuir isotherm assumes a homogeneous surface energy distribution (Langmuir, 1916). According to this theory, it is assumed that the sorbent surface has fixed individual active sites. Each site is assumed to be capable of binding one molecule of

sorbate and a monolayer surface coverage is formed without interaction between the molecules sorbed. The Langmuir isotherm is defined by equation 2.6:

$$q_e = Q_m b C_e / (1+bC_e) \quad (2.6)$$

The linear form of the Langmuir isotherm equation is represented by equation 2.7:

$$C_e/ q_e = 1/ Q_m b + C_e/ Q_m \quad (2.7)$$

where C_e is the equilibrium concentration in the liquid phase (mg L^{-1}) and q_e is the equilibrium sorption capacity of the sorbent (mg g^{-1}). Parameters Q_m represent the maximum sorption capacity with the monolayer coverage on the sorbent particle and b is the Langmuir constant related to free energy of sorption. From the linear plot between C_e/q_e versus C_e, Q_m (mg g^{-1}) and b (L mg^{-1}) can be determined from the slope and intercept, respectively.

Freundlich isotherm

The sorption isotherm commonly used for liquid phase sorption on a surface having heterogeneous energy distribution is the Freundlich isotherm (Freundlich, 1906). The Langmuir model is based on the assumption that all sorption sites have the same energy of distribution on the surface. To develop the Langmuir theory, Freundlich considered that the energy of sorption may vary in a real situation because of surface heterogeneity, where intermolecular attractions might exist between the sorbate molecules. The Freundlich isotherm is expressed by the following equation 2.8:

$$q_e = K_F C_e^{1/n} \quad (2.8)$$

A logarithmic linearized form of Freundlich equation is expressed as equation 2.9:

$$\log q_e = \log K_F + 1/n \log C_e \quad (2.9)$$

where K_F and 1/n Freundlich constants are related to sorption capacity and are a measure of surface heterogeneity respectively. The Freundlich constants K_F and 1/n can be calculated from the slope and intercept of the linear plot between log q_e and log C_e.

2.4.4 Model for kinetic sorption

The rate of sorption is required to design the batch sorption system and to establish the sorption mechanism in a range of experimental conditions. Kinetic rate model equations are applied to the experimental data. The sorption kinetic data in this study was analysed using kinetic models such as the pseudo-first-order, pseudo-second-order and intra-particle diffusion.

Pseudo-first-order equation

The pseudo-first-order equation is expressed (Gerente et al., 2007) by equation 2.10:

$$q_t = q_e (1 - e^{-kt}) \quad (2.10)$$

where q_e and q_t are the sorption capacities (mg g^{-1}) at equilibrium and time t respectively, and k_1 is the rate constant of pseudo-first-order sorption (h^{-1}).

Pseudo-second-order equation

The pseudo-second-order equation is expressed (Gerente et al., 2007) by equation 2.11:

$$\frac{1}{(q_e - q_t)} = \frac{1}{q_e} + k_2 t \quad (2.11)$$

where q_e and q_t are the sorption capacities (mg g^{-1}) at equilibrium and time t respectively, and k_2 is the rate constant of pseudo-second-order sorption (g mg^{-1} h^{-1}).

Intra-particle diffusion

The effect of intra-particle diffusion on sorption can be determined (Weber and Morris, 1963) by equation 2.12:

$$q_t = k_{id} t^{0.5} + c \quad (2.12)$$

where k_{id} is the intra-particle diffusion rate constant (mg g^{-1} $h^{-0.5}$), q_t is the amount sorbed per unit sorbent at time t (mg g^{-1}). Plots of q_t against $t^{0.5}$ give a linear line where a slope is k_{id} and c is the intercept.

2.4.5 Equilibrium vs. non-equilibrium sorption processes

Column experiments are cost-effective and time efficient, and the parameters obtained from breakthrough curves (BTCs) are commonly considered to apply at a field level. BTCs are used to determine the parameters for the physicochemical processes of solute transport in porous media. The asymmetric shape and lack of tailing of the breakthrough curve (BTC) are due to equilibrium solute transport. By contrast, the asymmetric shape with early peaks and BTC tailing are due to non-equilibrium solute transport. The transport of many contaminants in the subsurface can be influenced by several rate limited processes. Brusseau et al. (1997) reported that both rate limited sorption and nonlinear sorption can cause breakthrough curves to exhibit fronting and tailing (Figure 2.7).

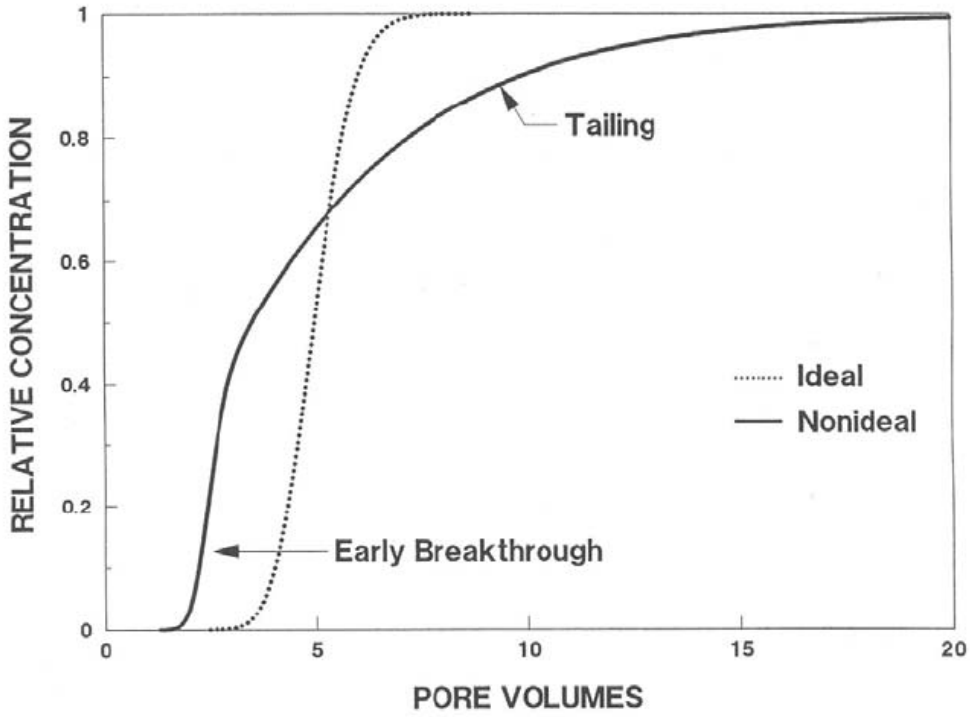

Figure 2.7 Breakthrough curves for ideal and non-ideal transport (Source: Brusseau et al., 1997)

Rate limited sorption is related to intra-sorbent diffusion as well as physical and chemical non-equilibrium processes (Brusseau and Rao, 1989). Physical non-equilibrium affects the transport of both reactive and non-reactive solutes.

2.4.6 Batch vs. column studies

Column sorption is more effective than batch sorption system for the cycle operation of sorption/desorption, and in some cases, regeneration. One advantage is that in column operation, the sorbents are continuously in contact with fresh solute solution, while in the batch system the concentration of solute in contact with sorbent decreases as sorption proceeds. In a column sorption system, the filtering material is packed in a column and influent passes through the column. During sorption, the sorbent located closest to the inlet of the column is saturated first, and a sorption zone with decreasing

concentration is observed near the exit of the bed. Many factors are associated with the column operation including diffusion, fluid effects, medium effects, fluid-medium interactions and boundary/initial condition (Sternberg, 2004). A column tracer test is used to estimate the effective porosity while one pore volume is injected when the effluent concentration (C) reaches 50% of the injected fluid concentration (C_o). The sorption capacity for column operation is determined by using the breakthrough curves (BTCs). Simple models such as the Thomas model (Thomas, 1944), the Yoon and Nelson model (Yoon and Nelson, 1984), the Bohart-Adams model (Bohart-Adams, 1920) and the Yan model (Yan et al., 2001) usually have applied to describe the sorption process in a sorption column.

2.5 Chemical oxidation

Usually chemical reaction involves through the oxidation-reduction simultaneously. The removal of electrons from contaminant to the oxidant is termed contaminant is oxidized and the oxidant as electron acceptor is termed reduced. In this study we will use the term “oxidation”.

2.5.1 Chemical oxidizing reagents

There are four commonly employed oxidants:

- Permanganate
- Hydrogen peroxide/Fenton’s reagent
- Persulfate
- Ozone

All these oxidants are strong oxidizing agents that are able to destroy many toxic organic chemicals. Oxidants can be applied for ISCO, depending on the type of

contaminant and soil character. The relative strength of common oxidants is shown in Table 2.4:

Table 2.4 Standard oxidation potential for oxidants used for in situ chemical oxidation

Chemical species	Standard oxidation potential (volts)	Remarks
Hydroxyl radical ($OH^{\cdot}$)	2.8	Hydroxyl radical is formed when ozone and hydrogen peroxide are decomposed, or from Fenton's reagent
Sulfate radical ($SO_4^{\cdot}$)	2.6	Sulfate radical is formed when persulfate is decomposed.
Ozone	2.1	
Persulfate	2.0	
Hydrogen peroxide	1.8	
Permanganate (Na/K)	1.7	

(Source: Siegrist et al., 2001; ITRC, 2005)

2.5.2 Permanganate

Permanganate is a strong oxidizing agent. Its advantages over other oxidants include its ability to react over a wide pH range, cost-effectiveness, stability in the subsurface and ease of handling (Vella and Munder, 1993; ITRC, 2005). Its use with a number of organic compounds (e.g., perchloroethylene, trichloroethylene and methyl-tert-butyl ether) has been reported (Huang et al., 2001; Damm et al., 2002). In the case of in situ chemical oxidation (ISCO), a large amount of permanganate is required in excess of the amount needed to treat the organic contaminant, based on reaction stoichiometry due to the subsurface background matrix. Little data is available for the oxidation of chlorophenols by permanganate. Waldemer and Tratnyek (2006) determined pseudo-first-order rate constants using excess chlorophenol with permanganate. Therefore, a kinetic study of chlorophenol oxidation with excess permanganate is important for

remediation. The findings of rates and half-lives can be useful for predicting the reduction of chlorophenols during permanganate oxidation.

Permanganate (MnO_4^-) has been used in wastewater treatment for decades (Drescher et al., 1998; Marley et al., 2002) and for the oxidation of nuclear wastes containing chelating ligands (Chang et al., 2006). The use of MnO_4^- for in situ remediation was started about 10 years ago (Gates et al., 1995; Hood et al., 2000). The effectiveness of MnO_4^- for the degradation of chlorinated solvent (Gates-Anderson et al., 2001; Schnarr and Farquhar, 1992; Stewart, 1965; Schnarr et al., 1998) and the reaction mechanisms and kinetics (Yan and Schwartz, 2000; Huang et al., 1999; Hood et al., 2000) are well documented. Permanganate may be used in the form of either $KMnO_4$ or $NaMnO_4$ salt (Al et al., 2006). It reacts rapidly with many organic contaminants. Its solubility in water ranges from 40 to 50 g L^{-1} at typical groundwater temperature (5–10 ^oC), and its aqueous solutions are immiscible with most hydrocarbons (Hood et al., 2000).

The reaction of permanganate oxidation is an electron transfer rather than a free radical process that characterizes oxidation by persulfate, hydrogen peroxide or ozone. It is applicable over a wide pH range. Under acidic conditions (pH <3.5) it involves a five-electron transfer process, as shown in equation 2.13, and in the pH range 3.5–12 the reaction follows the three-electron transfer in equation 2.14, with MnO_2 as a by-product. Finally, at high pH (pH >12), a single-electron transfer occurs, as given in equation 2.15. In acidic conditions, the Mn^{4+} in MnO_2 is also reduced slowly to Mn^{2+} as shown in equation 2.16 (ITRC, 2005). Pure potassium permanganate can also react with water but at very slow rate; the reaction follows equation 2.17.

$$MnO_4^- + 8H^+ + 5e^- \longrightarrow Mn^{2+} + 4H_2O \quad (2.13)$$

$$MnO_4^- + 2H_2O + 3e^- \longrightarrow MnO_2 + 4OH^- \quad (2.14)$$

$$MnO_4^- + e^- \longrightarrow MnO_4^{2-} \quad (2.15)$$

$$MnO_2 + 4H^+ + 2e^- \longrightarrow Mn^{2+} + 2H_2O \quad (2.16)$$

$$4MnO_4^- + 2H_2O \longrightarrow 3O_2 + 4MnO_2 + 4OH^- \quad (2.17)$$

Permanganate persists in the subsurface for months (ITRC, 2005) and is thus able to diffuse over greater distances into the soil system (USEPA, 2006). MnO_4^- also reacts with non-target reactants, mainly organic matter and reduced chemical species (i.e. ferrous, manganese and sulphide), which may limit the effectiveness of ISCO (USEPA, 2006).

Permanganate oxidation of organic chemicals and kinetics

Permanganate has been extensively used as an oxidizing agent for over a century but its reaction mechanism during oxidation process is still not clear. An aqueous solution of permanganate ion reacts rapidly with carbon-carbon double bonds (alkene) to form a cyclic hypomanganate (V) ester (Figure 2.8) (Huang et al., 2001). Further oxidation to form >CO< compounds, glycols, ketones and carboxylic acid depends on pH and oxidant concentration.

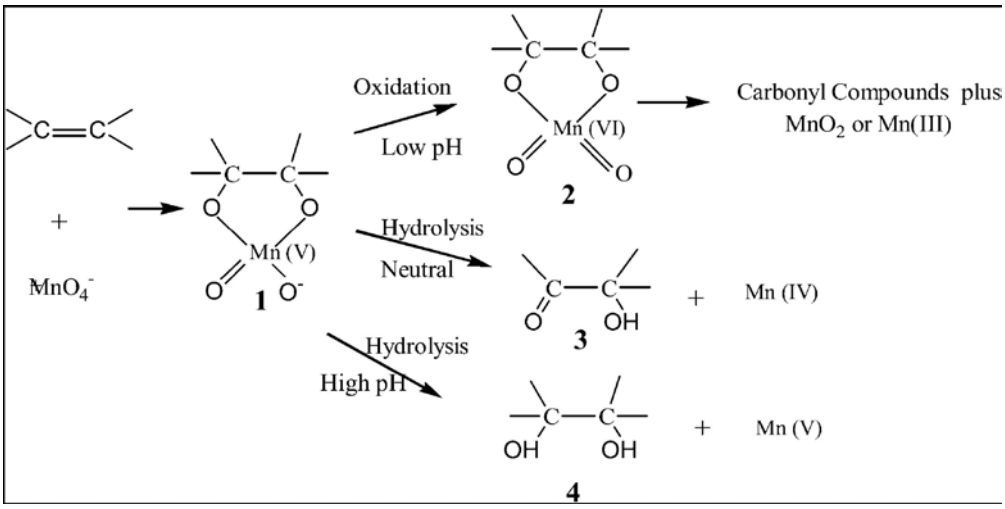

Figure 2.8 Reaction pathways of oxidation of alkenes with permanganate (Lee and Brownridge, 1974)

The oxidation of perchloroethylene (PCE) was carried out with excess $KMnO_4$ concentration by Hood et al. (2000) who found that the reaction between PCE and $KMnO_4$ is first-order with respect to both PCE and $KMnO_4$ and is second-order rate constant 2.45±0.65 M^{-1} min^{-1}. Schnarr et al. (1998) also demonstrated that high concentration of $KMnO_4$ enhances the oxidation of TCE and PCE. They observed that all chlorine bound with the initial chlorinated solvent was released after oxidation, indicating the complete destruction of the solvent. They proposed the following oxidation reaction in equation 2.18 and 2.19:

$$3C_2Cl_4 + 4MnO_4^- + 4H_2O \longrightarrow 6CO_2 + 12Cl^- + 4MnO_2 + 8H^+ \quad (2.18)$$

$$C_2Cl_3H + 2MnO_4^- \longrightarrow 2CO_2 + 3Cl^- + 2MnO_2 + H^+ \quad (2.19)$$

The oxidation of methyl tert-butyl ether (MTBE) by permanganate is second-order overall and first-order individually with respect to permanganate and MTBE (Damm et al., 2002). Damm et al. (2002) found that second-order rate constant was 1.426×10^{-6} M^{-1} h^{-1} and pH has no significant effect on the rate of reaction. The rate of MTBE oxidation by permanganate is slower than other oxidants. The stoichiometric reaction is expressed by equation 2.20:

$$21\ MnO_4^- + 2C_5H_{12}O \longrightarrow 21MnO_2 + 10CO_2 + 24OH^- \qquad (2.20)$$

It has been found that the rate of oxidation of some organic compounds (methanol, ethanol) is greater in alkaline permanganate than in acid media; Benerjee and Sengupta (1964) concluded that the log of rate constant exhibits a linear relationship at different pH values. The presence of a neutral salt like K_2SO_4 has no effect on the rate of reaction. Benerjee and Sengupta (1964) found that the oxidation rate increased in presence of excess organic compounds such as methanol or ethanol (R.CHOH where R= H or CH_3), but it decreased with the increasing concentration of oxidant due to the formation of stronger complexes in the presence of excess oxidant, i.e. permanganate. The oxidation reaction can be represented by equation 2.21:

$$5R.CHOH + 2MnO_4^- + 6H^+ \longrightarrow 5R.CHO + 2Mn^{2+} + 8H_2O \qquad (2.21)$$

Permanganate oxidation was carried out with a mixture of six poly aromatic hydrocarbons (PAHs). The greatest reduction was observed for benzo(a)pyrene (72.1%), pyrene (64.2%), phenanthrene (56.2%), and anthracene (53.8%). A minimal reduction was observed for fluoranthene (13.4%) and chrysene (7.8%) (Brown et al., 2003). Permanganate has been used for the oxidation of nuclear wastes at high pH

containing chelating agents such as ethylenediaminetetraacetic acid and nitrilotriacetic acid (EDTA and NTA). It has been shown that the maximum quantity of radionuclides and heavy metals are separated from the wastes. The reaction product indicates that permanganate reacts with the ethylene group in EDTA in alkaline conditions (Chang et al., 2006). In acidic solution, the oxidation of EDTA and permanganate produced ethylenediamine-N, N, N,-triacetic acid (ED3A), CO_2 and Mn^{2+} as the final product (Bose et al., 1991). Oxidation of EDTA by permanganate at high pH produced MnO_2 precipitation and via adsorption of metal on MnO_2 were examined (Korshin et al., 2007). It has been proved that a soluble form of colloidal manganese dioxide is produced from the reaction of potassium permanganate with trimethylamine in a phosphate buffer solution. The solubility of colloidal manganese dioxide is increased by the adsorption of phosphate ion on its surface and as such, it inhibits the flocculation of MnO_2 (Mata-Perez and Perez-Benito, 1985). The reaction kinetics of the oxidation of MCCR (Microcystine-RR) by permanganate indicates that the reaction is second-order overall and first-order with respect to both permanganate and MCRR. The second-order rate constant ranges from 0.154 to 0.225 L mg^{-1} min^{-1}. Degradation rates are increased with temperature and oxidant concentration. No pH adjustment is required and the half-life of the rate is less than one minute; approximately 99.5% of MCRR was degraded within ten minutes (Chen et al., 2005).

2.5.2.1 Permanganate oxidation of chlorophenols

Chemical oxidation involves the breaking of chemical bonds and the abstraction of electrons from the organic contaminant to the oxidant, where the contaminants are oxidized and the oxidant is reduced as an electron acceptor simultaneously. Permanganate oxidation may occur through different pathways such as electron

abstraction, hydrogen abstraction and oxygen donation, depending on the structure of the organic compound and the acidity of the solution (Chen et al., 2005). The hydroxyl group is a strongly activating ortho- and para-directing substituent in electrophilic aromatic substitution reaction (McMurry, 2008), so the oxidation kinetics of chlorophenols with permanganate may be influenced by the substituted electron-withdrawing chlorine in the para- and ortho- position on the aromatic ring and with the increasing number of substituted chlorine (Figure 2.9).

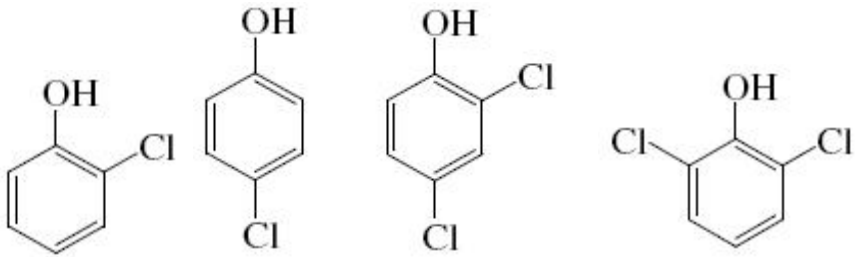

2-chlorophenol 4-chlorophenol 2,4-dichlorophenol 2,6-dichlorophenol

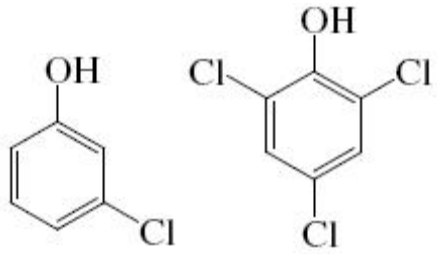

3-chlorophenol 2,4,6-trichlorophenol

Figure 2.9 Structure of selected chlorophenols

The presence of electron-withdrawing chlorine in the aromatic ring and its interaction with the hydroxyl group through the phenolic ring influences the relative acidities, and

hence the reactivity, of the chlorophenols (Aitken et al., 1994; Zhang et al., 2003; Han et al., 2005). Therefore, clarification on the expected resulting reaction sequence for various monochlorophenols (2-CP, 4-CP, 3-CP), dichlorophenols (2,4-DCP, 2,6-DCP) and 2,4,6-trichlorophenol (2,4,6-TCP) were investigated.

The oxidation of chlorophenol with $KMnO_4$ has been carried out by many researchers. Lee and Sebastian (1981) determined oxidation of 2-CP, 3-CP, 4-CP, 2,4-DCP and 2,4,6-TCP with permanganate. They found that the permanganate-chlorophenol reaction was second-order in an un-buffered alkaline (0.1M NaOH) environment and first order with respect to chlorophenol and permanganate. While Waldemer and Tratnyek (2006) determined that the reaction was second-order in a neutral, phosphate buffered solution. Jiang et al. (2009) found that a phosphate buffer significantly enhanced permanganate oxidation of 2,4-dichlorophenol. Other author (He et al., 2010) has determined second-order rates from pseudo-first-order rates by assuming the reaction was second-order, based on the work of Lee and Sebastian (1981). Therefore, the reactions of chlorophenols with permanganate under un-buffered conditions are assumed to be second-order and first-order with respect to each reactant. The summary of their second-order rate constants are shown in Table 2.5.

Table 2.5 Summary of rate constants for chlorophenol compounds in the $KMnO_4$ oxidation processes

Chlorophenols	Solvent condition, pH	T (^oC)	k (M^{-1} s^{-1})	References
2-CP	0.1M NaOH	25	10.8	Lee and Sebastian, 1981
2-CP	Phosphate buffer, pH 7.0	25	74	Waldemer and Tratnyek, 2006
2-CP	Un-buffered, pH 7.0	19	13.6	He et al., 2010
3-CP	0.1M NaOH	25	9.73	Lee and Sebastian, 1981
3-CP	Phosphate buffer, pH 7.0	25	13.4	Waldemer and Tratnyek, 2006
4-CP	0.1M NaOH	25	189	Lee and Sebastian, 1981
4-CP	Un-buffered, pH 7.0	16	59	Zhang et al., 2003
4-CP	Un-buffered, pH 7.0	19	8.4	He et al., 2010
2,4-DCP	0.1M NaOH	25	2.44	Lee and Sebastian, 1981
2,4-DCP	Un-buffered, pH 7.0	16	44	Zhang et al., 2003
2,4-DCP	Phosphate buffer, pH 7.0	25	142	Waldemer and Tratnyek, 2006
2,4-DCP	Un-buffered, pH 7.0	19	16.2	He et al., 2010
2,4-DCP	Un-buffered, pH 7.0	23	19.1	Jiang et al., 2009
2,4-DCP	Phosphate buffer, pH 7.0	23	45	Jiang et al., 2009
2,6-DCP	Un-buffered, pH 7.0	16	32	Zhang et al., 2003
2,6-DCP	Un-buffered, pH 7.0	19	19.6	He et al., 2010
2,4,6-TCP	0.1M NaOH	25	1.3	Lee and Sebastian, 1981
2,4,6-TCP	Phosphate buffer, pH 7.0	25	120	Waldemer and Tratnyek, 2006
2,4,6-TCP	Un-buffered, pH 7.0	19	19.4	He et al., 2010
2,4,6-TCP	pH 7.6	20	17-21	Bastos et al., 2008

The second-order rate constants (k_2) for the oxidation of CP and $KMnO_4$ at 22 °C and initial pH 7 are ~8–20 M^{-1} s^{-1} obtained by He et al. (2010) and for 2,4,6-TCP (17–21 M^{-1} s^{-1}) at pH 7.6 with permanganate was found by Bastos et al. (2008) (Table 2.5). It is noted that higher second-order rate constant of 2-CP (74 M^{-1} s^{-1}), 3-CP (13.4 M^{-1} s^{-1}), 2,4-DCP (142 M^{-1} s^{-1}) and 2,4,6-TCP (120 M^{-1} s^{-1}) determined by Waldemer and Tratynek (2006) (Table 2.5). However, Waldemer and Tratynek (2006) obtained

second-order rate constant (k_2) from pseudo-first-order conditions by measuring decreasing concentration of permanganate in a continuous system with excess chlorophenols in phosphate buffered system. Jiang et al. (2009) also found that the second-order rate constant for 2,4-dichlorophenol (45 M^{-1} s^{-1}) at pH 7 in 50 mM phosphate buffer was much higher than without phosphate buffer (19 M^{-1} s^{-1}). The second-order rate constant values for 2-CP (10.8 M^{-1} s^{-1}) and 2,4-DCP (2.44 M^{-1} s^{-1}) was determined by Lee and Sebastian (1981) in alkaline conditions. The reactivity of chlorophenol depends on its structure. The position of chlorine in the phenolic ring can influence the reactivity of chlorophenols towards $KMnO_4$ oxidation by inductive and resonance effects (Deborde and Von Gunten, 2008). Also the presence of chlorine in the phenolic ring and its interactions with the hydroxyl groups influences the oxidation kinetics of chlorophenols with $KMnO_4$ (Han et al., 2004).

2.5.2.2 Permanganate oxidation of woody materials

A permanganate measurement was carried out for pulp (unbleached pine) kappa number determination by Chai and Zhu (1999) in strongly acidic conditions, to eliminate MnO_2 interference during spectrophotometric analysis. They calculated the volume of 0.02 mole L^{-1} potassium permanganate consumed by one gram of moisture-free pulp. They mentioned that kappa number is not only related to the lignin content in pulps but also to lignin reactivity. As a strong oxidizing agent, permanganate degrades lignin easily and this is the basis for the determination of the kappa number of pulps (Garves, 1997). The oxidation of lignocellulosic substrate with $KMnO_4$ was performed by Jolly et al. (2006) at pH 2 and the concentration of permanganate was determined using UV-visible spectrophotometry at 526 nm. The lignin oxidation reaction was examined by Tong et al. (2000). They found that permanganate consumption was rapid in the initial stage,

indicating the amount of permanganate consumed by the easily oxidisable parts of lignin. Rowell (2005) reported that strong acid such as H_2SO_4 greatly affects the strength of wood fibre. Also, he mentioned that acid with pH values above 2.0 and bases with pH values below 10 do not degrade wood fibre for short period of time. Most of the oxidation of permanganate and woody material was carried out in strong acidic media. This study was carried out to estimate the consumption of permanganate with woody materials (pine) and sorbed CP in pine, in un-buffered neutral conditions.

2.5.2.3 Manganese oxides formed as an oxidation by-product

Permanganate has been used in ISCO for the treatment of organic contaminants at various hazardous waste sites (USEPA, 1998; Siegrist et al., 2001). The effects of precipitation of MnO_2 particles were studied in the presence of a different organic contaminant concentration i.e. TCE, at various permanganate concentrations, at different pH by Crimi and Siegrist (2004). They discovered that permanganate was depleted and manganese oxide was generated during the reaction with the organic contaminant by UV-visible spectrophotometry measurements of 525 and 418 nm respectively.

2.5.3 Peroxide

Hydrogen peroxide has been used for in situ chemical oxidation (ISCO), and for 30 years, the oxidizing agent has been studied both in the laboratory (Gates and Siegrist, 1995; Watts et al., 1990; Tyre et al., 1991; Gates-Anderson et al., 2001) and in the field (Kauffman et al., 2002; Cline et al., 1997; Cho et al., 2002). Hydrogen peroxide itself is a weak oxidant due to its high activation energy and it is not effective for certain

contaminants at high concentration because of a low reaction rate. To increase the reactivity of hydrogen peroxide, a ferrous iron salt, referred to as Fenton's reagent (Neyens and Baeyens, 2003) is added at pH 2–4. Traditionally, in Fenton's system a low concentration peroxide/iron mixture is insufficient for an in situ system because of the presence of competing organics and mineral surfaces that are reactive to hydrogen peroxide. More concentrated solutions are therefore used (4–20%) with iron in acid solution to accomplish the desired oxidation of the target organic contaminants. This is referred to as the Modified Fenton's system (ITRC, 2005).

Chemical oxidation using Fenton's reagent yields free radicals $HO^{\cdot}$ that can rapidly react with organic contaminants. The Fenton's application to soil and groundwater systems involves several competing reactions. The overall reactions can be described by the following equations, equation 2.22 to equation 2.30 (Pignatello et al., 2006; Neyens and Baeyens, 2003; Chen et al., 2001; Jones, 1999)

$$Fe^{2+} + H_2O_2 \longrightarrow Fe^{3+} + OH^- + OH^{\cdot} \quad (2.22)$$

$$Fe^{2+} + OH^{\cdot} \longrightarrow Fe^{3+} + OH^- \quad (2.23)$$

$$OH^{\cdot} + H_2O_2 \longrightarrow H_2O + OOH^{\cdot} \quad (2.24)$$

$$OH^{\cdot} + OH^{\cdot} \longrightarrow H_2O_2 \quad (2.25)$$

$$Fe^{3+} + H_2O_2 \longrightarrow Fe^{2+} + OOH^{\cdot} + H^+ \quad (2.26)$$

$$OH^{\cdot} + RH \longrightarrow H_2O + R^{\cdot} \text{ (chain propagation)} \quad (2.27)$$

$$R^{\cdot} + H_2O_2 \longrightarrow ROH + OH^{\cdot} \text{ (chain propagation)} \quad (2.28)$$

$$R^{\cdot} + R^{\cdot} \longrightarrow RR \text{ (non-chain termination)} \quad (2.29)$$

$$R^{\cdot} + Fe^{3+} \longrightarrow Fe^{2+} + \text{product (regenerate } Fe^{2+} \text{ for chain initiation)} \quad (2.30)$$

Hydrogen peroxide can also auto-decompose in aqueous solution with accelerated rates (equation 2.31) upon contact with mineral surfaces and carbonate and bicarbonate surfaces (Siegrist et al., 2001).

$$H_2O_2 \longrightarrow H_2O + O_2 \quad (2.31)$$

Chemical oxidation using Fenton's reagent is most effective under very acidic pH, i.e. pH 2–4, and becomes ineffective under moderate to strongly alkaline conditions (Siegrist et al., 2001; Chen et al., 2001). According to Fenton's conditions, it is necessary to reduce the pH of the soil and groundwater below 4, which may also lead to bringing naturally occurring ferrous iron into solution. This is because at higher pH, iron may precipitate as $Fe(OH)_3$ and will decompose the H_2O_2 to oxygen. But if due to the presence of high content of carbonate (CO_3^{--}) in the soil it can make it difficult to acidify. Consequently, free radical scavengers i.e. CO_3^{--} will retard the Fenton's reaction. Also, the oxidation reaction in Fenton's reaction is extremely rapid and is strongly exothermic (ITRC, 2005). An exothermic reaction with stronger H_2O_2 (10–17%) can evolve more heat and gas and may affect existing environmental conditions.

2.5.4 Sodium persulfate

Sodium persulfate is an oxidant currently used for ISCO (USEPA, 2006). Persulfate salts dissociate in water to persulfate anions ($S_2O_8^{2-}$) which are kinetically slow in destroying many organic contaminants (ITRC, 2005). Sodium persulfate can be used for ISCO using either direct or indirect oxidation. Direct oxidation (equation 2.32) has high

oxidation potential (Table 2.4), comparable to ozone, hydrogen peroxide and permanganate, but at high atmospheric temperature it is not very effective (Huang et al., 2002a). To enhance persulfate to sulphate radical oxidation mechanisms, it is used with high temperature (equation 2.33), or the addition of Fe^{2+} (equation 2.34) can activate the decomposition of persulfate (ITRC, 2005; Huang et al., 2002a). The metal activator can be naturally occurring or may be injected with persulfate to perform the free radical formation of $S_2O_8^{2-}$ to SO_4^{2-}. In the field, iron has been used to catalyse the persulfate anion while maintaining a slightly reduced condition and soluble Fe^{2+} (USEPA, 2006).

$$S_2O_8^{2-} + 2e^- \longrightarrow 2SO_4^{2-} \quad (2.32)$$

$$S_2O_8^{2-} + \text{heat} \longrightarrow 2SO_4^{\cdot-} \quad (2.33)$$

$$S_2O_8^{2-} + 2Fe^{2+} \longrightarrow 2SO_4^{\cdot-} + 2Fe^{3+} \quad (2.34)$$

$$SO_4^{\cdot-} + RH \longrightarrow R^{\cdot} + HSO_4^- \quad (2.35)$$

$$SO_4^{\cdot-} + H_2O \longrightarrow OH^{\cdot} + HSO_4^- \quad (2.36)$$

$$SO_4^{\cdot-} + Fe^{2+} \longrightarrow SO_4^{2-} + Fe^{3+} \quad (2.37)$$

The reaction involving radicals can be either chain-propagating or chain-terminating. A chain-propagating reaction (equation 2.35, 2.36), takes place with the SO_4^- radical which is formed from the chain-initiating reaction (equation 2.33, 2.34). Fe^{3+} is used in both chain-initiating (equation 2.34) and chain-terminating reactions (equation 2.37) (ITRC, 2005). Chloride, as well as bicarbonate/carbonate, can act as a free radical scavenger and will retard the persulfate reaction (Waldemer et al., 2007). Studies have shown effective oxidation of chlorinated ethenes by heat-activated persulfate (Waldemer et al., 2007) and iron activated persulfate (Liang et al., 2004).

2.5.5 Ozone

Ozonation is a very common municipal water treatment technology. The concept of using ozonation for treating complex organic pollutants has evolved over the past 15 years. The use of ozone in ISCO involves the application of a gas (ozone) posing different design and operation issues than those experienced with other oxidants (ITRC, 2005). Ozone oxidizes organic contaminants by either direct or indirect oxidation (Choi et al., 2002). Direct oxidation (equation 2.38) is normally used in water treatment, and indirect oxidation (equation 2.39) is applied for ISCO through the product of hydroxyl radicals (ITRC, 2005).

$$O_3 + 2H^+ + 2e^- \longrightarrow O_2 + H_2O \quad (2.38)$$

$$O_3 + OH^- \longrightarrow O_2 + OH^\cdot \quad (2.39)$$

To enhance hydroxyl radical formation, hydrogen peroxide is often added to the ozone/water system (equation 2.40) (ITRC, 2005).

$$2O_3 + H_2O_2 \longrightarrow 3O_2 + 2OH^\cdot \quad (2.40)$$

Ozone may be applied in situ, either as a vadose zone injection of ozone gas (Choi et al., 2002; ITRC, 2005), or through ozone sparging below the water table ((ITRC, 2005). Due to its high reactivity, the possibility of diffusion into the subsurface soil must be limited. In addition, the naturally occurring non-target chemical species, i.e. reduced minerals, organic matter; hydroxyl ion, etc., reacts rapidly with ozone and limits the effectiveness of ozone oxidation (USEPA, 2006).

2.5.6 Oxidation kinetic model

The rate of chemical reaction is defined as the rate of decrease of the concentration of reactants or the rate of increase of the concentration of products (Avery, 1974). The general rate equation is 2.41:

$$A \longrightarrow B + C \qquad (2.41)$$

where, A = reactant, B and C = products

The rate of reaction is (equation 2.42),

$$\text{Rate} = -d[A]/dt \qquad (2.42)$$

The rate of reaction (equation 2.42) is equal to the rate of decrease in the concentration A with time. Alternatively, the rate of increase in the concentration of product B or C can be written as follows (equation 2.43):

$$\text{Rate} = d[B]/dt = d[C]/dt \qquad (2.43)$$

The rate of reaction depends on the concentration of the reactants; as the concentration of A in the above reaction decreases, the rate of reaction also decreases. This can be expressed in equation 2.44:

$$\text{Rate} \propto [A]^n \qquad (2.44)$$

where, n is the order of reaction

by combining, equation 2.42 and equation 2.44, a new equation can be written as equation 2.45:

$$-d[A]/dt = k[A]^n \quad (2.45)$$

where, k is a rate constant for a particular temperature and is called rate constant.

Equation 2.45 indicates that the rate of reaction varies with the concentration of reactants, not with the concentration of product. The rate constant is a useful measure of the rate of chemical reaction in particular conditions. Its units depend on the order of reaction (Avery, 1974).

Zero-order reaction

Consider a chemical reaction in which reactant c is written as the equation 2.46:

$$c \longrightarrow \text{Product} \quad (2.46)$$

The rate of reaction changes at time t is in equation 2.47:

$$-dc/dt = k \quad (2.47)$$

Integration between the limits of $c = c^o$ when $t = 0$ and $c = c$ when $t = t$ gives the integrated zero-order rate equation (2.48) (Connors, 1990):

$$c = c^o - kt \quad (2.48)$$

In a zero-order reaction, a linear plot of c vs. t gives slope –k. The slope of the plot will be the zero-order rate constant of which units is moles per litre-second ($M\ s^{-1}$).

A reaction is of zero-order when the rate of reaction is independent of the concentration of reactants. The rate of reaction is a constant when the limiting reactant is completely consumed and reaction will stop immediately. In fact, a zero-order reaction is possible if the reactant concentration is not changed as the reaction proceeds, but this is uncommon, so zero-order reaction is rarely found. An electrode reaction might be an example of a zero-order reaction where material adsorbed on the surface of the electrode can react. In this case, if the reactant is strongly adsorbed from the solution it can adsorb as a unimolecular layer, i.e. the surface covered by that layer of molecules at any realistic concentration in the electrolyte solution. The surface concentration, which is adsorbed from electrolytic solution and is the only concentration of the reactant directly involved in the reaction, will then remain constant even though the electrolytic concentration varies over orders of magnitude. Zero-order reaction also arises as a result of several successive steps in more complex reaction mechanisms (Plambeck, 1996).

First-order reaction

Equation 2.49 is an elementary first-order reaction:

$$A \longrightarrow Z \tag{2.49}$$

where, A = is a reactant, Z = is a product

The corresponding differential rate equation 2.50 is

$$-dc_A/dt = kc_A \tag{2.50}$$

Separating the variables and integrating between the limits shown below gives equation 2.51, 2.52, 2.53 and 2.54 as equivalent forms of the integrated first-order-rate equation (Connors, 1990):

$$\int_{c^{o}_{A}}^{c_A} dc_A/c_A = -k \int_{0}^{t} dt \quad (2.51)$$

$$\ln c_A/c^{o}_{A} = -kt \quad (2.52)$$

$$\log c_A/c^{o}_{A} = -kt/2.303 \quad (2.53)$$

$$c_A = c^{o}_{A}e^{-kt} \quad (2.54)$$

Therefore, a plot of $\ln c_A/c^{o}_{A}$ vs. t is linear and first-order rate can be obtained from the slope; the usual unit is per second (s^{-1}).

The half-life can be defined using equation 2.52 with the substitution $c_A = c^{o}_{A}/2$ and $t = t_{1/2}$ as follows:

$$t_{1/2} = \ln 2/k = 0.693/k \quad (2.55)$$

Second-order reaction

The rate of a second-order reaction is proportional to either the concentration of a reactant squared or the product of the concentration of two reactants (Boekel, 2008).

Second-order reaction (case 1)

If the initial concentrations of the two reactants are equal the rate law,

$$d[A]/dt = d[A]/dt = -k[A]\,[A] \quad (2.56)$$

separating the variables and integration

$$\int_{[A]_o}^{[A]} d[A]/[A]^2 = -k \int_{t_o}^{t} dt \quad (2.57)$$

or,

$$1/[A] = kt + C \quad (2.58)$$

Provided that $[A] = [A]_o$ at $t = 0$, the constant C becomes equal to $1/[A]_o$ thus the second order integration rate equation is

$$1/[A] - 1/[A]_o = kt$$

or,

$$1/[A] = 1/[A]_o + kt \quad (2.59)$$

A plot $1/[A]$ vs. t , produces a straight line with slope k and intercept $1/[A]_o$.

For second-order reaction, a plot of $1/[A]$ vs. t is linear and the slope is equal to k. The usual units of a second-order rate constant are litres per mole-second ($M^{-1} s^{-1}$).

Second-order reaction (case 2)

In the case of reaction A and B

$$A + B \longrightarrow \text{Product} \quad (2.60)$$

If the starting concentration of the two reactants is different

Then the rate law is

$$d[A]/dt = d[B]/dt = -k[A][B] \quad (2.61)$$

By integration

$$\ln [B]\,[A]_o/[B]_o[A] = ([B]_o - [A]_o)\,kt \qquad (2.62)$$

where $[A]_o$ and $[B]_o$ are the initial concentration of at time t = 0. [A] and [B] are the concentration at time t. If [A] and [B] are measured then plot $\ln [B]\,[A]_o/[B]_o[A]$ vs t should yield a straight line with a slope equal to k ($[B]_o - [A]_o$). From this second-order rate, (k) can be calculated.

In a second order reaction rate, the concentration of two reactants must be followed simultaneously, which is difficult, or one must be measured and the other calculated as the difference, which is less precise. A common solution for this problem is pseudo-first-order approximation. In this case, the stoichiometric excess of one of the reactants is necessary.

Pseudo-first-order reaction

The oxidation reaction of CP and $KMnO_4$ can be expressed using rate law (Boekel, 2008) as equation 2.63:

$$d[KMnO_4]/dt = d[CP]/dt = -k[KMnO_4][CP] \qquad (2.63)$$

where, $[KMnO_4]$ = the concentration of permanganate

[CP] = the concentration of chlorophenol

k = second-order rate constant

t = time

The rate law for the degradation of CP by $KMnO_4$ is assumed to be the form:

$$d[CP]/dt = – k[KMnO_4][CP] \quad (2.64)$$

If the initial concentration of the reactant $KMnO_4$ is much larger than the concentration of CP, then $KMnO_4$ remains constant. The expression may be written as:

$$d[CP]/dt = – kC\,[CP] \quad (2.65)$$

where C = the unchanging $KMnO_4$ concentration.

Since the two constants k and C can always be combined into one constant, the above expression is equal to

$$d[CP]/dt = – k_{app}[CP] \quad (2.66)$$

where $k_{app} = kC$

From the above equation, it can be seen that the degradation of CP will follow first-order kinetics; that is, the reaction will appear to be a first-order reaction dependent only on the concentration of one reactant, i.e. CP.

The integrated form of a first-order rate expression is,

$$\ln[CP]_t = \ln[CP]_o – k_{app}t$$

or,

$$\ln[CP]_t / [CP]_0 = – k_{app}t \quad (2.67)$$

Where, $[CP]_t$ = the amount of chlorophenol remaining at time t.

$[CP]_o$ = initial concentration of CP

k_{app} = the apparent first-order rate constant.

t = time of sampling

Plot of $\ln[CP]_t / [CP]_o$ vs. t should yield a straight line with a slope equal to $- k_{app}$.

The experimentally determined first-order rate constant (k_{app}) can be related to the true second-order rate constant by the expression,

$$k_{app} = k [KMnO_4] \quad (2.68)$$

Then the value of k_{app} (apparent first-order rate constant) can be divided by the known constant concentration of the excess ($KMnO_4$) and compared to obtain the true constant second-order rate k.

$$k = k_{app} / [KMnO_4] \quad (2.69)$$

2.6 Chemical analysis method

A number of techniques such as high performance liquid chromatography (HPLC) methods and gas chromatography have been reported for the estimation of chlorophenols after permanganate oxidation. HPLC methods often require a pre-treatment step such as liquid-liquid extraction and solid phase extraction; this separation method is expensive and often time-consuming. An ideal quenching agent will preferentially consume excess oxidant and not produce adverse chemical by-products or other interferences which could impact the analytical method used. Commonly used quenching agents for oxidants include sodium sulfite, peroxide, sodium thiosulfate and hydroxylamine hydrochloride. He et al. (2010) used sodium thiosulfate as a quenching agent for permanganate with subsequent analysis by HPLC using UV detection at 270–305 nm. Zhang et al. (2003) used sodium sulfite as a quenching agent followed by gas chromatography. In spite of their higher sensitivity, spectrophotometric methods are more versatile and easier to apply for the rapid routine analysis of environmental samples.

2.7 Summary

The various treatment processes have been reviewed: permeable reactive barrier, sorption, chemical oxidation and sorption-oxidation system. Organic compound removal from surface and groundwater is an environmental issue because of their toxicity. Some of these compounds are carcinogenic and extremely toxic such as chlorinated ethenes, poly aromatic hydrocarbons and phenolic compounds. The distribution of organic compounds in the aquatic system depends on their physico-chemical properties.

Instead of pump-and-treat, permeable reactive barriers (PRBs) enable in-situ remediation of contaminated groundwater by means of reactive materials. The reactive materials are placed in underground trenches where the contaminants are removed from an aquifer by flow through a reactive barrier, so the contaminants are treated without soil excavation or groundwater pumping. Generally, this cost-effective technology for in situ clean-up impairs the environment much less than other methods do.

GAC has been used as sorbent extensively for the treatment of organic contaminated water. It has extended surface area, high sorption capacity and microporous structure. Wood can be used as low-cost sorbent because of their physicochemical characteristics and availability in large quantity. It contains various organic compounds (lignin, cellulose and hemicellulose) with polyphenolic groups that might be useful for binding phenolic compounds through different mechanisms. Coal is other low-cost sorbent which consists of complicated pore structure. The micropores and macropores within the coal may be responsible for sorption. Temperature, solution pH, contact time and ionic strength can play a major role in sorption processes. There are some other factors

affecting the rate of sorption such as: sorbent: particle size, pore structure and surface area, sorbate: concentration, molecular size, molecular shape, solubility, ionization and hydrophobicity. Langmuir and Freundlich models in literature used curve fitting techniques to predict equilibrium sorption. Kinetic sorption indicates the transport of solute in sorbent. Most of the previous work used kinetic models such as pseudo-first-order, pseudo-second-order and intra-particle diffusion to analyse the kinetic data. Sorption-desorption processes were evaluated using hysteresis indexes.

Permanganate, Hydrogen peroxide/Fenton's reagent, persulfiate and ozone are strong oxidizing agents that are able to destroy many toxic organic chemicals. Potassium permanganate has advantages over other oxidants, its ability to react over a wide pH range, cost-effectiveness, stability in the subsurface and ease of handling. The studies which used a combination of sorption-oxidation for the treatment of organic contaminant in water are evaluated. The main factors of sorption-oxidation depend on the characteristic of oxidant and sorbents. Integration of such a process for contaminant removal is an advantageous conceptually rather than single treatment processes.

The oxidation of permanganate with woody material is reviewed. The lignocellulosic material can be easily oxidized by permanganate. The progress of the oxidation was evaluated on the basis of permanganate consumption by the lignin.

CHAPTER 3

Experimental work and methodology

3 Experimental work and methodology

3.1 Introduction

This chapter provides a description of materials used and the procedures followed for various experiment throughout the study.

3.2 Composition and types of sorbents

The wood sorbents used in this study were Pine and Hardwood (HW) which were supplied by Soilco Pty. Ltd., Australia. The wood chips obtained were approximately 10–35 mm in length (Figures 3.1 and 3.2) and ground before being used for experiments. The characteristics of the Pine and HW are presented in Table 3.1.

Figure 3.1 Pine wood chips

Figure 3.2 Hardwood chips

Table 3.1 Characteristics of wood used

Specification	Pine 0.6 mm	Pine 1.18 mm	Pine 2.36 mm	Pine 4.75 mm	HW 1.18 mm
BET surface area ($m^2 g^{-1}$)	0.65	0.45	-	0.79	0.55
Pore volume ($cm^3 g^{-1}$)	0.0018	0.0011	-	0.0031	0.0016
Pore width (nm)	11.1	12.1	-	15.6	7.6
Total carbon (%)	-	48.7	-	-	48.3
CEC (cmol kg^{-1})	-	6.2	-	-	3.5
Carbon-nitrogen ratio	-	428	-	-	364
Lignin (%)	-	23	-	-	13
Cellulose (%)	-	57	-	-	61
Hemicellulose (%)	-	14	-	-	14
Residue (%)	-	6	-	-	12
Ash (%)	-	0.3	-	-	0.2

The granular activated carbon (GAC) and filter coal (FC) samples (Figures 3.3 and 3.4) used in this study were obtained from James Cumming & Sons Pty. Ltd., Australia. The main physical properties of these sorbents are shown in Table 3.2.

Figure 3.3 GAC

Figure 3.4 Filter coal

Table 3.2 Physical properties of granular activated carbon (GAC) and filter coal (FC)

Specification	GAC	FC
Particle size (mm)	1.18	1.18
BET surface area ($m^2 g^{-1}$)	954	1.33
Micropore area ($m^2 g^{-1}$)	485.2	0.2966
External surface area ($m^2 g^{-1}$)	468.8	1.0282
Bulk density (kg m^{-3})	280-320	650
Pore volume ($cm^3 g^{-1}$)	0.212	0.00012
Pore width (nm)	2.6	23.2

3.2.1 Sorbent material preparation

Any bark in the wood samples was removed by sorting, and the remaining wood was ground to the required particle size (Figure 3.5) using a hammer mill (Model No. ADEB80N2, John Morris Pty. Ltd.).

Pine 4.75 mm Pine 2.36 mm Pine 1.18 mm

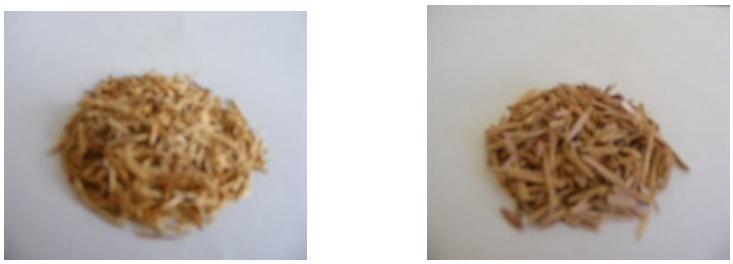

Pine 0.6 mm HW 1.18 mm

Figure 3.5 Particle sizes of woody materials

All sorbents were sieved such that the 4.75 mm material passed though a 6.5 mm sieve but was retained over a 4.75 mm mesh sieve. The 2.36 mm material passed though a 4.75 mm sieve but was retained over a 2.36 mm mesh sieve. The 1.18 mm material passed though a 2.36 mm sieve but was retained over a 1.18 mm mesh sieve. The 0.6 mm material passed though a 1.18 mm sieve but was retained over a 0.6 mm mesh sieve. All samples were washed to remove fines and leachable organic carbon.

The sieved GAC and FC were washed with warm distilled water to remove carbon fines (Figure 3.6) and then repeatedly washed with distilled water until the electrical conductivity, UV absorbance same or within 10% and the pH were the same as in distilled water. The GAC and FC were then dried for 24 h at 110 °C, cooled and stored in airtight desiccators, along with silica gel, before use.

Initial leaching was carried out for pine and HW to reduce the dissolved organic carbon (DOC) (Figure 3.6) in batch mode. The sieved pine and HW were further prepared by mixing with 0.6 mm glass beads (Burwell Abrasive Blasting Equipment, Australia) and then leached using tap water in a continuous flow column until the UV absorbance and electrical conductivity were at steady state conditions (seven days). Samples were then washed with distilled water and dried in an oven at 50 °C for 48 h, then stored in airtight desiccators at room temperature until use.

FC GAC Pine, HW

Figure 3.6 Sorbent leaching

3.2.2 Sorbent treated with $KMnO_4$ for column study

The $KMnO_4$-treated pine was prepared by flushing the pine (4.75 mm) with an aqueous solution of $KMnO_4$ ~3.8 mM (~600 mg L^{-1}) in a column at flow rate 5 and 10 mL min^{-1}. Flushing was continued until a residual concentration of $KMnO_4$ was measured (~50%) and the effluent concentration of $KMnO_4$ was changed less than 2% of the previous reading. This indicated the samples had undergone significant reaction. Then the columns were drained and flushed with distilled water at 22 °C until $KMnO_4$ was not found in the flushing solution**.**

3.3 Sorbates

Six phenolic (99%) compounds 2-chlorophenol (2-CP), 3-chlorophenol (3-CP), 4-chlorophenol (4-CP), 2,4-dichlorophenol (2,4-DCP), 2,6-dichlorophenol (2,6-DCP) and 2,4,6-trichlorophenol (2,4,6-TCP) were used in this research. They were purchased from Sigma-Aldrich Chemical Company. The properties of chlorophenols are given in Table 3.3.

Table 3.3 Main physicochemical properties of chlorophenols ([#]Ma et al., 1993; Czaplicka, 2004)

Compounds	Molecular weight (g $mole^{-1}$)	Solubility (g L^{-1}) at 20 °C	log K_{ow}	pK_a
2-CP	128.56	28	2.12–2.17	8.3–8.6
3-CP	128.56	26	2.48–2.50	8.8–9.1
4-CP	128.56	27	2.35–2.44	9.1–9.4
2,4-DCP	163.00	4.5	2.75–3.30	7.5–8.1
2,6-DCP	163.00	2.6[#]	2.57–2.86	6.7–7.8
2,4,6-TCP	197.45	0.434	3.60–4.05	6.0–7.4

3.4 Preparation of solutions

Individual (~ 0.52–0.78 mM) stock solutions of chlorophenol were prepared for batch oxidation and for sorption experiment (~6.1–7.8 mM). Working solutions were prepared from the stock solutions with Milli-Q water. A 10-mM stock solution of permanganate was prepared for batch study in an amber colour glass bottle and standardized with oxalic acid. The $KMnO_4$ influent solution (~3.8 mM) and working solutions (~ 1.84 mM) of 2,4-DCP were prepared for column study. Water used for the column study was distilled water due to large volumes needed. All the stock solutions were kept in a screw-capped, amber colour glass bottle while stored in a refrigerator at 4 °C for up to one month.

A stock solution for DOC analysis was prepared by dissolving reagent grade potassium hydrogen phthalate. The ionic strength (I = 0.02-0.2 M) was controlled using KCl. Analytical grade reagent $KMnO_4$, oxalic acid, KCl, silver nitrate, $Na_2S_2O_3$, Na_2SO_3, $NH_2OH.HCl$, NaOH, HNO_3, H_2SO_4, HCl and H_2O_2 (50%, v/v) were obtained from Chem-Supply.

3.5 Physical measurements

3.5.1 Particle size classification and distribution

Particle size classification of sorbent materials were analysed using ASTM D422-63 Standard Test Method for particle-size analysis (ASTM, 1998). The sorbents were dried in an oven at 50 °C for 48 h and sieved through the following sieves: 6.5 mm, 4.75 mm, 2.36 mm, 1.18 mm and 0.6 mm. The particle size distribution of woody materials according to length and width was determined using a micro-meter and by weighing the each sieved size fraction.

3.5.2 Physical analysis of GAC and FC

The specific surface area and pore characteristics of solid-phase media were measured using BET/N_2 (Micromeritics Tristar) and the BET surface area, t-plot external surface area, t-plot micropore volume and BJH adsorption average pore width were analysed for GAC and FC by Particle and Surface Sciences Pty. Ltd., Australia.

3.5.3 Physical analysis of woody materials

Lignin, cellulose, and hemicellulose were determined in the Wagga Wagga Feed Quality Testing Laboratory (Department of Primary Industries, NSW) using methods for Acid Detergent Fibre, Acid Detergent Lignin-Neutral Detergent Fibre (AFIA, 2010). Total carbon and nitrogen for all solid materials were determined in duplicate using a Truspec Carbon Nitrogen determinator. Ash content was measured using the method for Total Volatile Solids (APHA/AWWA/WEF, 1998) at 550 °C. The cation exchange capacity (CEC) was measured using saturated ammonium extractants at pH 7 method

(Rayment and Higginson, 1992). This was done by Southern Cross University. The specific surface areas and pore characteristics of solid phase media were measured using BET/N_2 (Micromeritics Tristar) at Particle Analysis Service, Commonwealth Scientific and Industrial Research Organisation (CSIRO). The measured pine and HW surface areas and pore volume data was found similar to other reported values (Papadopoulos et al., 2003; Seelsaen et al., 2007).

3.5.4 Bulk density

Bulk density was calculated by dividing the weight of column packing materials when dry by the total volume of materials.

3.5.5 Effective porosity

The effective porosity of the column was calculated by dividing the pore volume which is determined from a tracer experiment by the total internal volume of column.

3.5.6 pH measurement

A pH (TPS WP-81) meter was used to determine the pH of the sample. The meter was calibrated with two buffer solutions at pH 4 and 7.

3.5.7 Electrical conductivity

Conductivity was measured using either a conductivity meter (TPS W-81) or online Lab pro conductivity meter. It was calibrated with TPS standard KCl solution (147 µS cm^{-1}).

3.5.8 Zeta potential

Zeta potentials were measured with a Malvern Zetasizer.

3.6 Chemical analysis

3.6.1 Chlorophenol analysis for oxidation tests

Chlorophenols were analysed directly with UV–visible spectrophotometer (Shimadzu, Model UV-1700, Japan) using a 10-mm quartz cell. The analysis were carried out using maximum absorption wavelengths at pH 12 for 2-CP (294 nm), 3-CP (292 nm), 4-CP (298 nm), 2,4-DCP (305 nm), 2,6-DCP (299 nm) and 2,4,6-TCP (312 nm). The calibration plot was constructed for trichlorophenol, dichlorophenols and monochlorophenols over a concentration range 0.0054–0.52 mM, 0.0064–0.61 mM and 0.0073–0.78 mM, respectively, and found absorptivity for 2-CP is 3.42 cm^{-1} mM^{-1}, for 3-CP is 3.05 cm^{-1} mM^{-1}, for 4-CP is 2.38 cm^{-1} mM^{-1}, for 2,4-DCP is 3.60 cm^{-1} mM^{-1}, for 2,6-DCP is 4.90 $cm^{-1}mM^{-1}$ and for 2,4,6-TCP is 5.17 $cm^{-1}mM^{-1}$. The required pH 12 for CP analysis was adjusted using 1 M NaOH. The detection limits were in the range 0.0006-0.0008 mM for trichlorophenol, dichlorophenols and monochlorophenols. The detection limit was determined using the formula (Ermer, 2001): LOD (Limit of Detection) = 3.3*σ/S where σ and S are the standard deviation and slope of the calibration line. All samples were centrifuged at 3000 rpm for 5 minutes and then filtered using 0.2 μm Whatman filter paper to remove any manganese dioxide precipitates present. Any remaining MnO_2 may oxidize the phenolate ion but at pH 12 the rate of reaction is much slower than permanganate oxidation of CP and has no influence on the kinetics of the initial reaction (Lee and Sebastian, 1981). The filtrate

was analysed for residual chlorophenol concentration with the spectrophotometer at pH 12. The absorbance data were converted into CP concentration by use of a previously prepared calibration curve.

3.6.2 Chlorophenol analysis for sorption tests

Concentrations of chlorophenols were determined by mixing 1 mL of sample solution with 3 mL of Milli-Q water in a glass vial and centrifuged at 3000 rpm for 10 min to remove particulates. The solutions were then analysed for residual chlorophenol concentration with a UV-visible spectrophotometer using 10 mm quartz cells. A control sample from the batch and column experiments was used to adjust background absorbance values to account for any colour leaching from the sorbents; however, extensive pre-treatment of sorbents minimized the influence of leaching as described in the section 3.2.1. The maximum measured absorption wavelengths were 274 nm (2-CP), 280 nm (4-CP) and 284 nm (2,4-DCP) at pH 5.6–5.8. During analysis samples were adjusted with HCl or NaOH to pH 5.6–5.8 if required. The chlorophenol concentration was determined from Equation 3.1:

$$\text{Concentration (mg L}^{-1}) = \text{Maximum Absorbance / Absorptivity} \qquad (3.1)$$

The calculated absorptivity (ε) value was 0.0147 cm^{-1} mg^{-1} (1.89 cm^{-1} mM^{-1}) for 2-CP, 0.0119 cm^{-1} mg^{-1} (1.53 cm^{-1} mM^{-1}) for 4-CP and 0.0132 cm^{-1} mg^{-1} (2.15 cm^{-1} mM^{-1}) for 2,4-DCP. The calibration data was generated in triplicate and the mean value used**.** The calibration data showed an excellent straight line fit ($r^2 > 0.99$) over the range of sample concentration (1–100 mg L^{-1}) for all chlorophenols. The detection limits were 0.0019–0.0037 mM for 2-CP, 4-CP and 2,4-DCP.

3.6.3 Permanganate analysis

Concentrations of permangnate were analysed with UV-visible spectrophotometer using a 10-mm quartz cell. The maximum absorption wavelengths for $KMnO_4$ at pH 5.6 were 525 nm. Calibration for permanganate was performed over a range 1–1.5 mM, and the measured absorptivity was 2.47 cm^{-1} mM^{-1}. The calibration data was generated in triplicate and the mean value used. The regression coefficient value (r^2) for all the calibration curves resulted in a straight line fit ($r^2 > 0.99$).

To minimise the impact light scattering from any manganese dioxide colloids present in solutions, the samples were collected and then filtered using 0.2 μm Whatman filter paper. The samples were then diluted with Milli-Q water and centrifuged at 3000 rpm for 5 min and analysed using UV-visible spectrophotometer at 525 nm. A minimum detection limit (MDL) for MnO_4^- of 0.003 mM was determined during method development.

3.6.4 Chloride analysis

The concentration of chloride was determined for tracer test using UV-visible spectrophotometer at a wavelength 420 nm. Experimental 50 mL samples were taken and 5 mL of nitric acid solution (65 % v/v) added to each of them to acidify the sample. 1 mL of 0.5% silver nitrate solution was then added in one of them and mixed thoroughly. It was allowed to react for 10 min and then measured using UV-visible spectrophotometer. Standard solutions for chloride were prepared according to Standard Method (APHA, 1998).

A calibration curve was made from potassium chloride (KCl) standard solution over a range 0.028–0.84 mM. Chloride concentration was also estimated from electrical conductivity using 11 point calibration curve. The calibration data were generated in triplicate and the mean value was used. The regression coefficient value (r^2) for the calibration curves were straight line fit ($r^2 > 0.99$).

3.6.5 Dissolved organic carbon (DOC) analysis

A 100 g oven dried (100 °C) pine (2.36 mm) were taken in one-litre bottle, mixed with Milli-Q water and shaken at 150 rpm for 70 h. Leachate samples were filtered using 0.2 μm Whatman filter paper to remove particulates and tested for DOC using a Multi N/C 2000 TOC analyser (Analytik Jena AG). A stock solution for DOC analysis was prepared by dissolving reagent grade potassium hydrogen phthalate in Milli-Q water and standard solutions were prepared according to Standard Method (APHA, 1998). The calibration data were generated in duplicate and the mean value was used.

3.6.6 Manganese oxide (MnO_2) analysis

Aliquot of sample solution was transferred to a 10 mm quartz cell cuvette and put in the UV-visible spectrophotometer. The absorbance was measured at wavelength 418 nm.

3.7 Experimental methods

3.7.1 Chlorophenols in different solvent condition

To determine UV absorbance at pH ~ 5.6, ~pH 12.0 and in methanol, solutions of 2-CP (1-100 mg L^{-1}), 3-CP (1-100 mg L^{-1}), 4-CP (1-100 mg L^{-1}), 2,4-DCP (1-100 mg L^{-1}),

2,6-DCP (1-100 mg L^{-1}) and 2,4,6-TCP (1-100 mg L^{-1}) were prepared at pH 5.6 and at pH 12.0 using Milli-Q water. Solutions of 2-CP (1-100 mg L^{-1}), 4-CP (1-100 mg L^{-1}), 2,4-DCP (1-100 mg L^{-1}) and 2,4,6-TCP (1-100 mg L^{-1}) were prepared in methanol. The pH was adjusted using HCl or NaOH to maintain pH. The data acquisition was carried out using a UV-visible spectrophotometer with software UV probe. All experiments were carried out in triplicate at temperature 22 °C.

3.7.2 Solid phase extraction procedure

Phenomenex Strata (500 mg) cartridges were used for the solid phase extraction (SPE) process (Figure 3.7). The cartridges washed with 4 mL of methanol followed by 4 mL of 2M H_2SO_4 to adjust the pH to 2-3. The washing water passed through the cartridges by gravity. The water sample (4 mL) with an initial concentration ~1 mg L^{-1} was placed into the cartridge. The sample was allowed to drain slowly and was rinsed with 4 mL of 2M H_2SO_4, at pH 2. The cartridges were dried using a vacuum pump for 5 min. The chlorophenols were then eluted with 4 mL methanol and the eluent was collected in a cuvette and analysed directly by a UV-visible spectrophotometer.

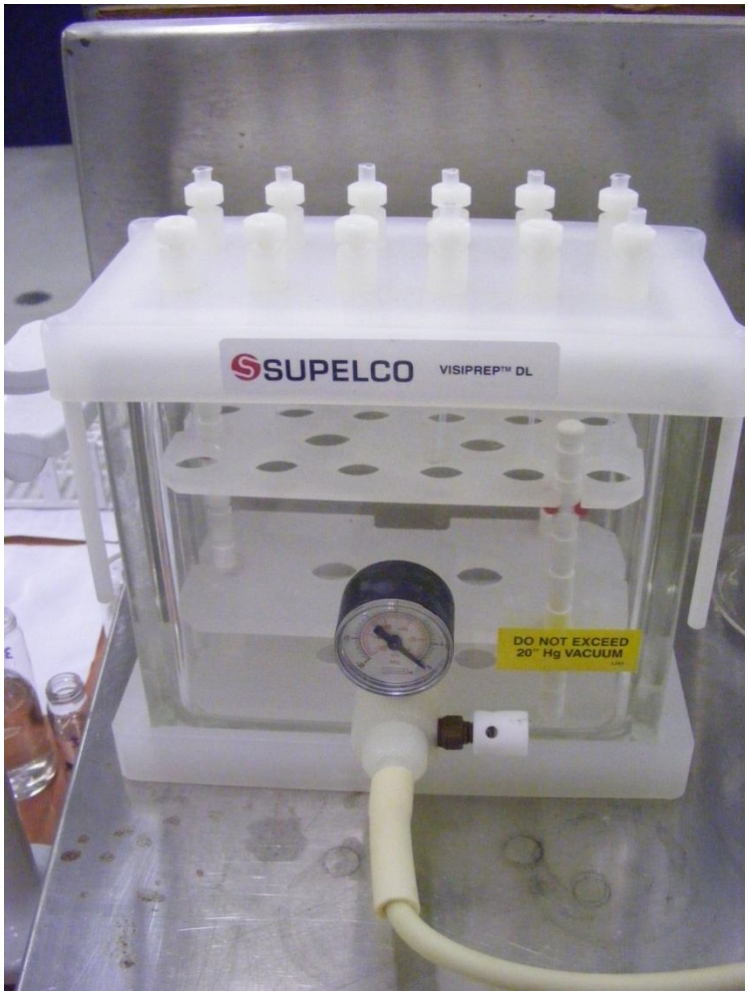

Figure 3.7 Solid phase extraction

3.7.3 Quenching reagent

Accurately measured aliquots of CP solution (~0.16 mM) were transferred into 25 mL glass vials. Approximately, 0.1–0.25 mL of 1M of each quenching reagent ($Na_2S_2O_3$, Na_2SO_3, $NH_2OH.HCl$ and H_2O_2) was added into the vials separately and diluted to 20 mL. The contents of each vial were mixed well and the absorbance was recorded. The experiments were conducted for 20 minutes, without added pH buffer and in duplicate at 22 °C.

3.7.4 Kinetic method for oxidation of chlorophenols by permanganate

The rate at which the chlorophenol compounds were degraded was measured using two methods. For all the reactions $KMnO_4$ was maintained excess compared to chlorophenol. In the first method, the concentrations of $KMnO_4$ and CP were fixed. In the second method the concentration of $KMnO_4$ was varied while the concentration of chlorophenol was constant. Again, the $KMnO_4$ concentration was constant and the concentration of chlorophenol was varied.

3.7.4.1 Fixed $KMnO_4$ and CP fixed concentration

The permanganate concentration was maintained in excess of stoichiometric requirements to create a pseudo-first-order reaction. The oxidation reaction was initiated by mixing 10 mL of CP (~0.16 mM) and 10 mL $KMnO_4$ (1.5 mM) in glass vials (25 mL) which were then sealed. At selected time intervals (0.17, 0.5, 1, 1.5, 2, 3, 4, 5, 10, 15 and 20 min) 0.15 mL of 1 M of Na_2SO_3 solution was added immediately into each vial to quench the reaction (Figure 3.8). All the reactions were conducted without added pH buffer in triplicate and 22 °C. Un-buffered solutions were used since it was believed this would better represent a groundwater environment than a well buffered neutral solution. The samples were then analysed (Section 3.6.1). The initial and final pH of experiments was 5.3 – 6.2 which is less than the pK_a values of chlorophenols (Table 3.3) and therefore reflects the non-ionised form of CP during the oxidation reactions.

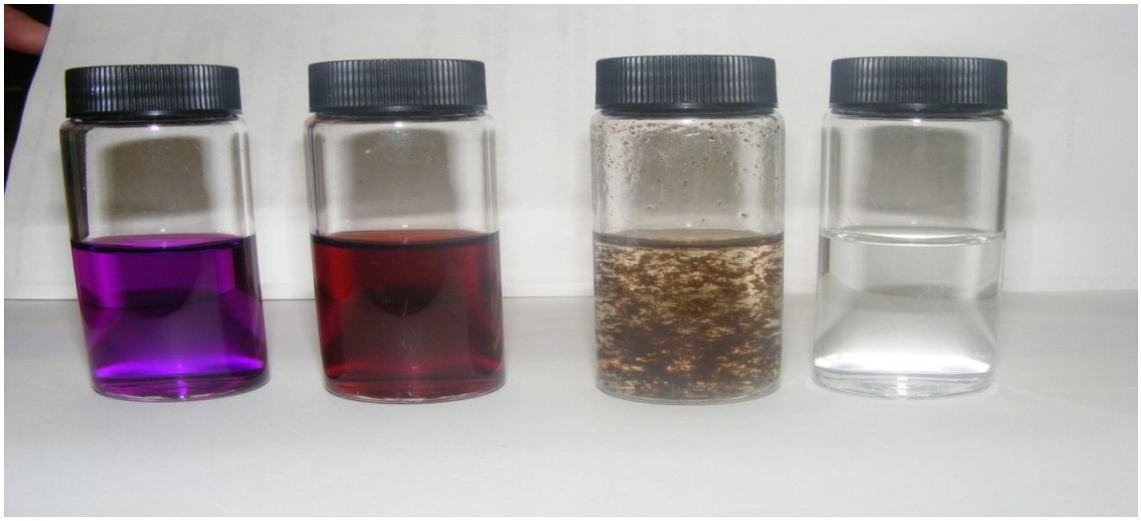

Figure 3.8 Chemical reactions of $KMnO_4$ and chlorophenol

3.7.4.2 $KMnO_4$ and CP varied

This comprised two experiments:

- excess varied $KMnO_4$ and fixed CP concentration
- excess fixed $KMnO_4$ and varied CP concentration

Batch experiments were carried out in an aqueous solution by varying the reactant concentration under pseudo-first-order condition where permanganate was in excess. Initial concentrations were varied in the range 0.8–3.2 mM for permanganate and 0.04–0.24 mM for chlorophenols. Oxidative reactions were initiated by mixing CP and $KMnO_4$ in a series of screw-capped amber colour glass bottles (18 mL) with a headspace to aqueous phase ratio of 1:8 by volume. At preselected time intervals, 0.1–0.15 mL of 2M Na_2SO_3 solution was added immediately into the vials to quench the reaction. All the reactions were conducted without added pH buffer in duplicate and the

reported data were an average of these values. The samples were analysed by UV–visible spectrophotometry (section 3.6.1). The ionic strength (0.02-0.2M) was maintained with the addition of KCl. The initial pH of the experiment was 7.0 ± 0.05 and adjusted using sulphuric acid or sodium hydroxide, as required.

3.7.5 Spectral study of MnO_2

Aliquot of $KMnO_4$ (0.2 mM) solution were transferred to 10 mm quartz cell cuvette and put in the spectrophotometer. Chlorophenol solution was then added quickly using a microliter syringe and successively scanned with a wavelength ranging from 400 to 700 nm during the reaction.

3.7.6 Batch sorption kinetic procedure

Batch experiments were conducted by placing the sorbent and solution in screw capped amber colour glass bottle with a headspace. The headspace of the bottles was not investigated for chlorophenol volatilization since previous studies (Colella et al., 1998) indicated that disappearance of dissolved chlorophenol was due to sorption and not volatilization. To verify this, calculated values for the fraction of chlorophenol in the headspace for these experiments was found to be less than 0.115% based on published Henry's constants. Different masses of solute and sorbent were used for each material due to the vastly different sorbent and solute properties. All weights reported in this thesis are as dry matter. Samples of 4 g of FC in 100 mL of solution with initial sorbate concentration 300 mg L^{-1} were placed in a 200 mL bottle. Fixed amounts of GAC (0.13 g) in 100 mL of solution with initial concentration 200 mg L^{-1} were placed in a 200 mL bottle. Sorbent (pine, HW) for 2-CP, 4-CP (1 g) and 2, 4-DCP (0.75 g) in 40 mL

solution at an initial concentration 100 mg L^{-1} were placed in a 75 mL bottle. The bottles were shaken immediately in an orbital shaker in a dark condition at 150 rpm. A small quantity of liquid was withdrawn from the bottles at different pre-determined time intervals for analysis.

3.7.7 Batch sorption equilibrium procedure

Batch studies were conducted to obtain the equilibrium data. The experiments were carried out by equilibrating 4 g of FC in 100 mL of solution with different initial sorbate concentrations (20–300 mg L^{-1}) and placed in a series of 200 mL bottles. Different masses of GAC (0.01–0.12 g) in 100 mL of solution with fixed initial sorbate concentration (200 mg L^{-1}) were placed into a series of 200 mL bottles. Sorbent (pine, HW) for 2-CP, 4-CP (2 g) and 2, 4-DCP (1.5 g) in 40 mL solution with different initial concentration (20–300 mg L^{-1}) were placed into a series of 75 mL glass bottles. The bottles were kept in an orbital shaker in a dark condition and continuously mixed at 150 rpm for 3 d (pine, HW), 6 d (GAC) and 11 d (FC). These concentrations and equilibrium contact time were established from the preliminary investigations.

All experiments were performed at room temperature (22 °C) and carried out without adding any pH buffer. Control samples showed no loss of solute during the experimental period. The pHs of the solution before and after the sorption process were measured. The initial and final pHs for GAC, pine and HW were 4.5–5.2 while filter coal varied from 5.3–6.3. This is below the pKa values of 2-CP, 4-CP and 2, 4-DCP (Table 3.3) and therefore reflects sorption of the non-ionised form of the solute. If pH is below the pK_a value, sorption has been found to be relatively independent of pH

(Nelson and Yang, 1995; Kao et al., 2000). Each sorption experiment was conducted in duplicate and the mean values have been reported. The maximum deviation from the mean on any sample was less than 5% (Appendix B).

3.7.8 Batch desorption kinetic procedure

Batch desorption kinetics experiments consisted of equilibrating 2 g of sorbent for 2-CP, 4-CP and 1.5 g for 2,4-DCP with particle size 1.18 mm at a nominal chlorophenol concentration of 100 mg L^{-1} of 40 mL solution in a 75 mL serum bottle. The bottles were shaken immediately in an orbital shaker in a dark condition at 150 rpm and 22 °C. Following equilibrium, the liquid and solid phases were separated by centrifugation and decantation and then 40 mL of Milli-Q water were added to the bottle. The bottles were shaken at 150 rpm and samples (1-2 mL) were withdrawn at pre determined time intervals. The samples were analysed as per section 3.6.2.

3.7.9 Batch desorption equilibrium procedure

Equilibrium batch desorption experiments were carried out to quantify desorption hysteresis for 2-CP, 4-CP and 2,4-DCP. An equilibrium time of 72 h was selected based on the desorption kinetics test showing there was less than a 4% daily change in residual concentrations after 72 h. The sorbents were equilibrated (72 h) with each solution of chlorophenols (~300 mg L^{-1}) using the sorption experimental procedure described in section 3.7.7. Following equilibrium a desorption study was carried out by four sequential decant-refill steps. After equilibrium, 20 mL of solution were removed from the solution and replaced by 20 mL of Milli-Q water. Then the bottles were shaken at 150 rpm for each desorption cycle (72 h) and analysed for residual chlorophenol. The

equilibrium solid phase loading on the sorbent was calculated by the difference of total amount sorbed and the amount desorbed in each step per unit sorbent.

3.7.10 Fitting isotherms

The errors for the isotherms parameters of CP sorption on pine, HW, GAC and FC were obtained by calculating the sum of squares error. Sorption isotherm models were fitted against experimental data using nonlinear regression within a Microsoft Excel spreadsheet (Bolster and Hornberger, 2007). This approach was used rather than linearization of the equations since linearization may result in improperly weighted data points during the analysis (Billo, 2007) and limit the accuracy of the fit (Bolster and Hornberger, 2007). The mathematical models were optimized for best fit using sum of error squares (SSE). Parameter fits with the lowest SSE values was considered best-fit. Regression co-efficient (r^2) were also calculated.

The sum of error squares (SSE) was calculated (Tseng et al., 2003) by equation 3.2:

$$\mathrm{SSE} = \sqrt{\frac{\sum (q_{e,exp} - q_{e,calc})^2}{N}} \qquad (3.2)$$

where, $q_{e,exp}$ and $q_{e,calc}$ are the sorption capacity (mg g^{-1}) obtained from experiment and calculation, respectively, and N is the number of data points.

3.7.11 Permanganate oxidation of pine and sorbed-CP

Batch experiments were carried out to measure the consumption of permanganate with untreated pine and CP treated pine. Sorption under equilibrium condition was first

carried out (section 3.7.7) and after equilibrium had been reached the whole solution was removed, centrifuged and then decanted.

Oxidation of pine and sorbed CP at initial pH 6.15: The concentration of permanganate was maintained in excess to create pseudo-first-order reaction on the basis of sorbed chlorophenols concentration. The oxidant (MnO_4^-) at 100 mL of ~4 mM (~630 mg L^{-1}) was added to each bottle containing pine and pine with sorbed CP (pine were treated with 2-CP, 4-CP and 2,4-DCP) and mixed at temperature 22 °C. The bottles were covered with aluminium foil to prevent photo-induced degradation of MnO_4^-. Small quantities of liquid samples were withdrawn at selected time intervals. A control was prepared with the same $KMnO_4$ solution without pine. Since the residual MnO_2 may interfere with the determination of permanganate, the absorbance of MnO_2 (418 nm) is deducted from $KMnO_4$ (525 nm) absorbance and therefore does not affect the permanganate concentration calculation. All experiments were carried out in duplicate and without adding any pH buffer. The solution pH was varied between 6.15-7.05 units during oxidation. The maximum deviation at absorbance 525 nm from the mean on any sample was less than 2%.

Oxidation of pine at initial pH ~2: Batch experiments were also conducted to investigate the reaction of $KMnO_4$ and pine at pH 2. About 5 g of pine (size 4.75 mm) were taken into a 300 mL amber colour glass bottle. The oxidant (MnO_4^-) at 250 mL of ~61 mM was added into the bottle and mixed in an orbital shaker at 150 rpm and 22 °C. Small quantities of liquid samples were withdrawn at preselected time intervals and analysed as described section 3.6.3. All experiments were carried out in duplicate.

3.7.12 Preparation of in-situ MnO_2 and reaction with CP

Manganese dioxide was prepared by the reaction of $KMnO_4$ with oxalic acid (Cao and Suib, 1994). The reaction was carried out by mixing dissolved $KMnO_4$ (0.079 g) with dissolved oxalic acid (0.114 g) in a 75 mL vials using Milli-Q water. MnO_2 was precipitated and started to coagulate and slowly settled down as coagulation is referred to in-situ form MnO_2. The flushing was carried out with frequent centrifugation until no $KMnO_4$ was detected, conductivity steady (4.4 µS cm^{-1}) and pH ~ 5.2. Then CP solution was added into the bottle (after decantation) and mixed in an orbital shaker at 150 rpm. It is difficult to separate MnO_2 from the aqueous medium. Therefore it was quantified as dry weight. The CP concentration further confirmed after instant addition into the in-situ formed MnO_2 to consider dilution effect. Samples are withdrawn at preselected time intervals and analysed as described section 3.6.2.

3.7.13 Column test

The experiments were carried out in PVC class 18 with internal diameter 5.3 cm and 56 cm in height with end caps constructed of PVC fittings and sealed with silicone. The bottom and top ends were drilled and affixed with plastic tube couplers. Both inlet and outlet of the column coupler joints were fitted with a mesh screen to prevent filtering material of the column from escaping. All columns were packed by mixing 66 g of pine and 1665 g of 0.6 mm glass beads (~20–25% v v^{-1} pine) with a bed depth of approximately 54 cm and bulk density 1.5 g cm^{-3}. The reactive media were added to the column in increments with continuous column vibration, without using any compaction over the filtration media surface (Oliviera et al., 1996). The filtration media were confined in the column by an inert plastic screen, at the bottom and column packing at

the top of the bed. Both ends of the column were packed by a layer of 1.5 cm each of glass bead (3 mm) to ensure uniform flow. The column was clamped to an upright position and was operated from bottom to top flow condition through the fixed-bed with peristaltic pump (Masterflex, Cole Parmer Instrument Company Ltd.). The inlet solutions were pumped from a 25 L plastic container using Silastic tubing (I.D 4.8 mm) extended to the outlet of the column. The control column was packed with glass bead and no significant evidence for the sorption of 2,4-DCP and consumption of $KMnO_4$ was found due to contact with the experimental apparatus. The flow rate of the column was controlled through the pump rpm and modifying outlet pipe diameter using a clamp and checked with a graduated cylinder. Before start-up, the column was operated for approximately 12–24 h by passing distilled water until the steady flow, stable conductivity and colour occurred. The column setup is shown in Figure 3.9:

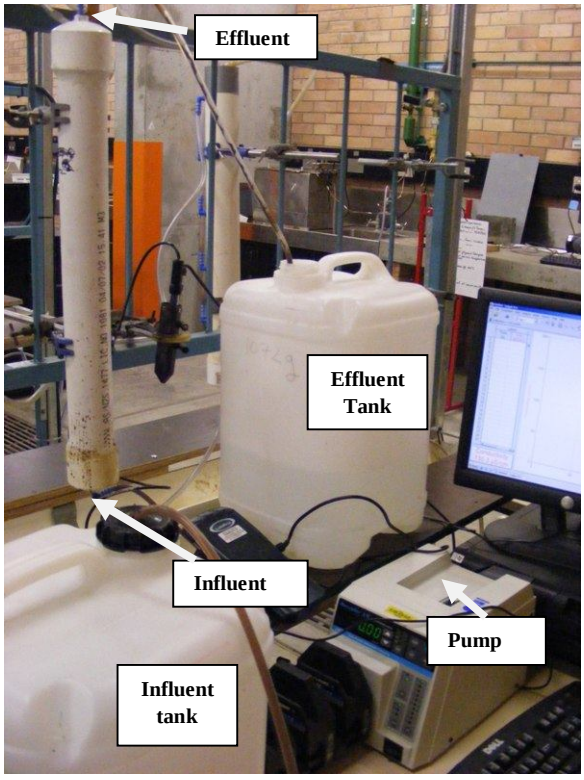

Figure 3.9 Column setup

Seven column (Col) experiments were conducted to investigate sorption of 2,4-DCP and the effect of an oxidizing agent ($KMnO_4$) on woody material (pine) in a dynamic sorption system. Col-1 (Run-1), Col-2 (Run-1), Col-3 (Run-1) and Col-6 (Run-1) were conducted to examine the sorption of 2,4-DCP onto pine at initial solution pH 5.22–5.45. The flushing was stopped until the effluent concentration was changed relatively slowly. The experimental conditions for column sorption are shown in Table 3.4.

Table 3.4 Experimental conditions of column sorption experiments at 22 °C

Column No	Run No	Sorbate	Influent conc. (mM)	Flow (mL min^{-1})	Pine particle Size (mm)	Sorbent
Col-1	Run-1	2,4-DCP	~1.84	5	1.18	Pine
Col-2	Run-1	2,4-DCP	~1.84	5	4.75	Pine
Col-3	Run-1	2,4-DCP	~1.84	10	4.75	Pine
Col-4	Run-1	$KMnO_4$	~3.8	10	4.75	Pine
Col-4	Run-2	2,4-DCP	~1.84	10	4.75	[a]Pine
Col-5	Run-1	$KMnO_4$	~3.8	5	4.75	Pine
Col-5	Run-2	2,4-DCP	~1.84	5	4.75	[a]Pine
Col-6	Run-1	2,4-DCP	~1.84	5	4.75	Pine
Col-6	Run-2	$KMnO_4$	~3.8	5	4.75	[b]Pine
Col-7	Run-1	$KMnO_4$	~63.0	5	4.75	Pine

[a]$KMnO_4$ modified pine
[b]Pine with sorbed 2,4-DCP (on modified pine)

Col-4 (Run-1) and Col-5 (Run-1) were initially flushed with $KMnO_4$ at an initial pH 5.65–5.82 at flow rates 10 and 5 mL min^{-1} respectively, to investigate different residence time. The flushing was stopped until the effluent concentration of MnO_4^- was

changed relatively slowly. Thus the, MnO_4^- has to migrate through uncontaminated pine prior to the reaction with 2,4-DCP. Then the columns were drained and flushed with distilled water until the steady flow, conductivity, pH and minimal leachate reached and no MnO_4^- was detected in the effluent. Then 2,4-DCP solution was passed to Col-4 (Run-2) and Col-5 (Run-2). This process has continued until the effluent concentration started to increase and finally become increases slowly.

Col-6 (Run-2) and Col-7 (Run-1) were flushed with the $KMnO_4$ solution. Col-7 experiments were conducted to investigate the reaction of $KMnO_4$ and pine at pH ~2. Finally, after the completion of experiment, Col-4 (Run-1), Col-5 (Run-1), Col-6 (Run-2) and Col-7 (Run-1) were again drained and flushed with distilled water until MnO_4^- was no longer detected in the effluent. Then a tracer test (section 3.7.14) was carried out to check the porosity of the filtering media.

Effluent samples were collected from the outlet of the column at various time of interval for chemical analysis. Experiments were carried out at different flow rates, sorbent particle sizes and the effect of $KMnO_4$ was evaluated in sorption of 2,4-DCP on pine and consumption of $KMnO_4$ by pine. All experiments were carried out at 22 °C and an un-buffered condition.

3.7.14 Column Studies: tracer experiment

A conservative tracer was used to determine the pore volume and porosity for all columns. Approximately 72 mg L^{-1} of conservative tracer (KCl) was prepared using distilled water. This solution was pumped at a specified flow rate through the column. KCl solution was used rather than NaCl solution, because the potassium and chloride

ion mobilities are almost the same, which minimizes the liquid junction potential (Sternberg, 2004). Tracer solutions were passed through a flow cell containing an electrical conductivity electrode attached to a data logger. Data were collected at pre-determined intervals.

3.7.15 Column Studies: Breakthrough data processing

Chloride breakthrough curves were constructed by plotting relative concentration (effluent concentration divided by influent concentration) versus cumulative effluent volume (Figure 3.10).

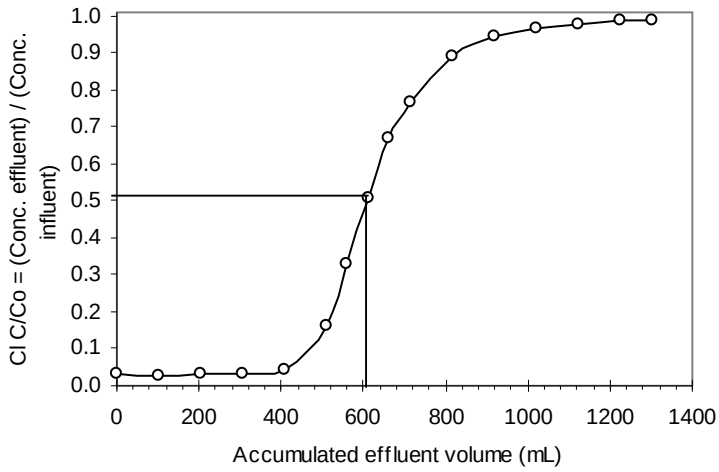

Figure 3.10 Chloride (Cl) breakthrough curve for wood column

The influent concentration (C_o) is used in normalizing the effluent concentration (C). The cumulative effluent volume corresponding to the relative concentration at 0.5 of the tracer input ($C/C_o = 0.5$) can be used to determine the pore volume for constant flux experiments (Barry and Parker, 1987). The effective porosity for the column filtration media was calculated from the total internal column volume and the pore volume with

relative concentration (C/C_o) at 0.5 which is one pore volume (Figure 3.10). The data were adjusted to account for inlet and outlet tubing which are not a part of porous media. Thus the effective pore volume as determined by the tracer test is used in normalizing the accumulated effective volume.

3.7.16 Column Studies: Leaching test

Leaching test was conducted to minimize the dissolved organic carbon (DOC) concentration leaching from pine to aqueous solution for the columns used distilled water. The leaching test was completed when the DOC of the effluent samples measured at 254 nm reached a low level. This minimised the effect of DOC on measured absorbance for both the CPs and permanganate. During UV-visible analysis no significance absorbance at 254 nm were found for sorbent (pine) leaching used for this study. The measured DOC for leaching samples at different experimental wavelength is shown in Table 3.5.

Table 3.5 Leaching absorbance from pine

Pine particle size (mm)	Flow (mL min^{-1})	Wavelength (nm)	Absorbance	DOC mg L^{-1}
1.18	5	254	0.0101	1.13
1.18	5	284	0.009	1.00
1.18	5	420	0.0005	1.25
4.75	5	254	0.0072	0.81
4.75	5	284	0.0011	0.12
4.75	5	420	0.0001	0.25
4.75	10	254	0.0004	0.05
4.75	10	284	0.0002	0.02
4.75	10	420	0.0001	0.25

3.7.17 Column Studies: Colloid growth measurements

Permanganate (MnO_4^-) has a peak at a wavelength at 525 nm while transparent at 418 nm. Thus manganese (Mn) colloids (primarily MnO_2) were continuously measured using the effluent samples at wavelength 418 nm using a UV-visible spectrophotometer. To measure the surface charge, Zeta potential is used, which shows the repulsive forces of the colloidal particles.

CHAPTER 4

Method development to quantify chlorophenols during permanganate oxidation

4 Method development to quantify chlorophenols during permanganate oxidation

4.1 Introduction

Current analytical techniques for the determination of chlorophenols during oxidation with permanganate in aqueous solutions are lengthy, using HPLC and gas chromatography. In this kinetic study, a large number of samples need to be analysed. Despite of their lower sensitivity, spectrophotometric methods are more versatile and easier to apply. The spectroscopic method for the determination of phenols with 4-aminoantipyrine (4-AAP) is well established but 4-chlorophenol shows negligible response with 4-AAP (Kang et al., 2000). In many cases, the quantity of chlorophenol compound in water may be too small to detect in a UV-visible spectrophotometer. Therefore, methods are needed for their separation and concentration. The sensitivity, separation and concentration using solid phase extraction and use of spectrophotometer for chlorophenol estimation are also proposed in this chapter.

A spectrophotometric method was developed at pH 12.0 for the quantification of chlorophenols in water and during permanganate oxidation. A comparison with methanol using liquid-liquid extraction for the separation and concentration of chlorophenols from aqueous solutions and their determination by UV-visible spectrophotometer were also studied. The method development involved improving analytical sensitivity through optimising the analysis pH and the absorption wavelengths in order to eliminate interferences from permanganate, its by-products as well as the quenching agents.

4.2 Results and discussion

4.2.1 Spectral analysis for CP

Spectral and calibration data for the CP compounds at different solvent conditions were studied. In the first step of the experiment, measured absorbance as a function of concentration for each single CP compound were used to determine the calibration parameter by linear regression analysis. In the second step the recovery efficiency was estimated for four chlorophenols from prepared water solutions (~ 1 mg L^{-1}) by use of methanol extraction (see section 3.7.2) and in the third step method development for the quantification of chlorophenol during oxidation was under taken.

In the first stage, this experiment involved the measurement of absorbance of chlorophenol in three different solvent conditions (see section 3.7.1). The neutral form of chlorophenol has observed at pH 5.6 since it is lower than the pK_a while the anionic forms occurs at pH 12 since it is higher than the pK_a (Table 3.3). The values of absorption data were taken into consideration in order to determine correlation with concentrations (1-100 mg L^{-1}) for all six chlorophenols. For all CP linear dependence and regression coefficients (r^2) were > 0.99. The minimum detection limits (MDL) was determined experimentally for all cases. The intensity of this absorbance depends on solution concentration. The more concentrated a solution the greater the absorbance. The detection limit was determined using the formula (Ermer, 2001): LOD (Limit of Detection) = $3.3*\sigma/S$ where σ and S are the standard deviation and slope of the calibration line.

Spectra for 2-CP in water at pH 5.6, showed the absorption curves were placed between 250–274 nm with a maximum absorbance at wavelength 274 nm (Figure 4.1). When methanol is used as a solvent the shape of spectra is different and shifted in the range 276–292 nm with a maximum absorbance at 276 nm for each concentration (Figure 4.1). In the case of a water solution at pH 12.0, the spectra shape vs. sample concentrations (i.e. with respect to absorbance) is more evident at wavelength range 294–350 nm (Figure 4.1).

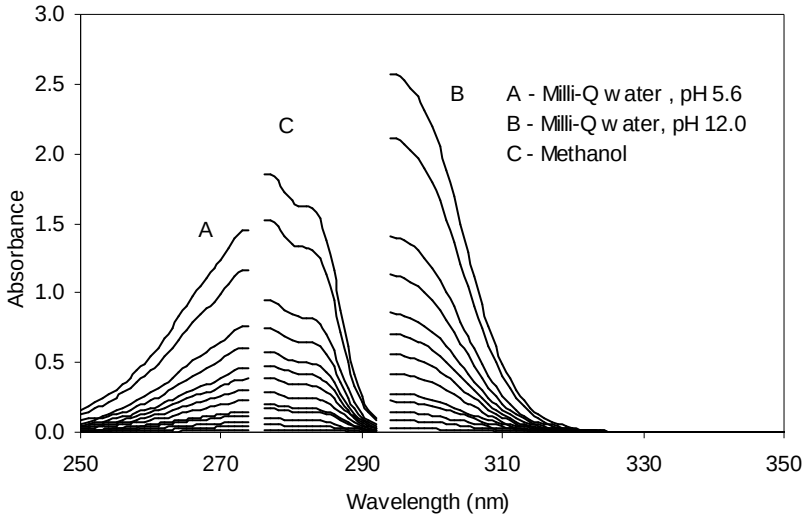

Figure 4.1 UV-visible spectra for 2-CP in water and methanol

The UV-visible absorbance in order to determine the concentration at pH 5.6, at pH 12.0 and in methanol were made 274 nm, 294 nm and 276 nm, respectively, (Table 4.1).

Table 4.1 Spectral and calibration data for 2-CP compounds: initial concentration 0.0063–0.77 mM, 22 °C

Solvent	Wavelength λ_{max} (nm)	Absorbance range	Absorptivity (ε) (cm^{-1} mM^{-1})	r^2	MDL (mM)
Milli-Q water at pH ~5.6	274	0.012–1.454	1.89	0.999	0.0037
Milli-Q water at pH ~12.0	294	0.025–2.571	3.42	0.997	0.0006
Methanol	276	0.018–1.856	2.41	0.999	0.0017

MDL- minimum detection limit

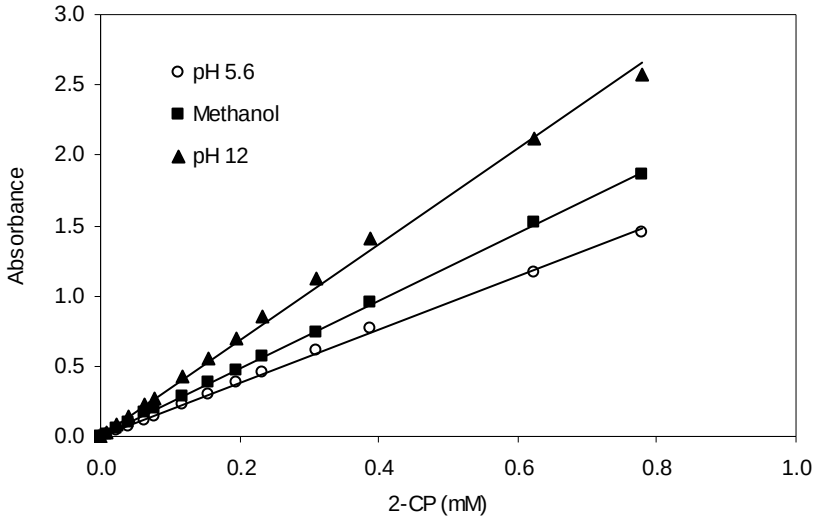

Figure 4.2 UV-visible absorbance for 2-CP in water and methanol

From the UV-visible spectral analysis, it was observed that for the same initial concentration of 2-CP a solution at pH 12.0 has values of absorbance greater than pH 5.6 and methanol (Figure 4.2). Therefore, the measurements were carried out at solution pH 12.0 and wavelength at 294 nm to obtain the higher 2-CP sensitivity.

Spectra for 3-CP in water at pH 5.6, showed the absorption curves were placed between 250–274 nm with a maximum absorbance at wavelength 274 nm (Figure 4.3). In case of

water solution at pH 12.0, the spectra shape vs. sample concentrations (i.e. with respect to absorbance) is more evident at wavelength range 292–350 nm (Figure 4.3).

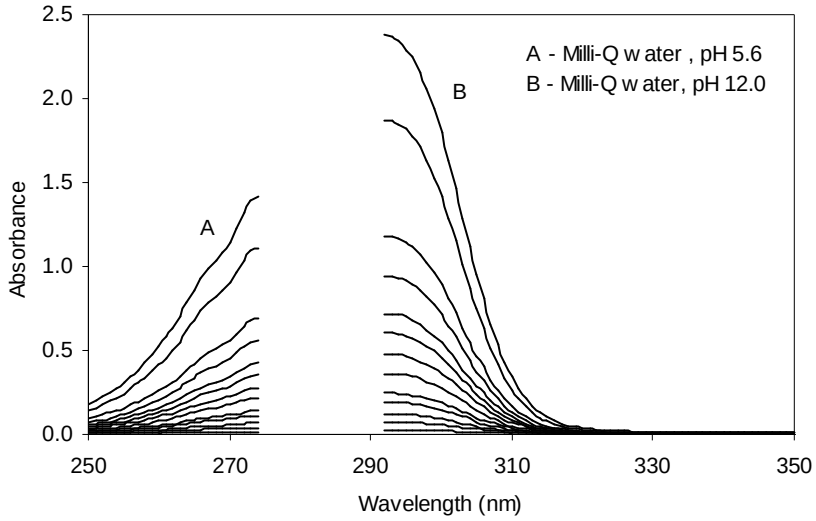

Figure 4.3 UV-visible spectra for 3-CP in water

The UV-visible absorbances in order to determine concentration in water at pH 5.6 and at pH 12.0 were made 274 nm and 292 nm (Table 4.2).

Table 4.2 Spectral and calibration data for 3-CP compounds: initial concentration 0.0078–0.79 mM, 22 °C

Solvent	Wavelength λ_{max} (nm)	Absorbance range	Absorptivity (ε) (cm^{-1} mM^{-1})	r^2	MDL (mM)
Milli-Q water at pH ~5.6	274	0.014–1.414	1.80	0.999	0.0007
Milli-Q water at pH ~12.0	292	0.026–2.376	3.05	0.999	0.0006

MDL- minimum detection limit

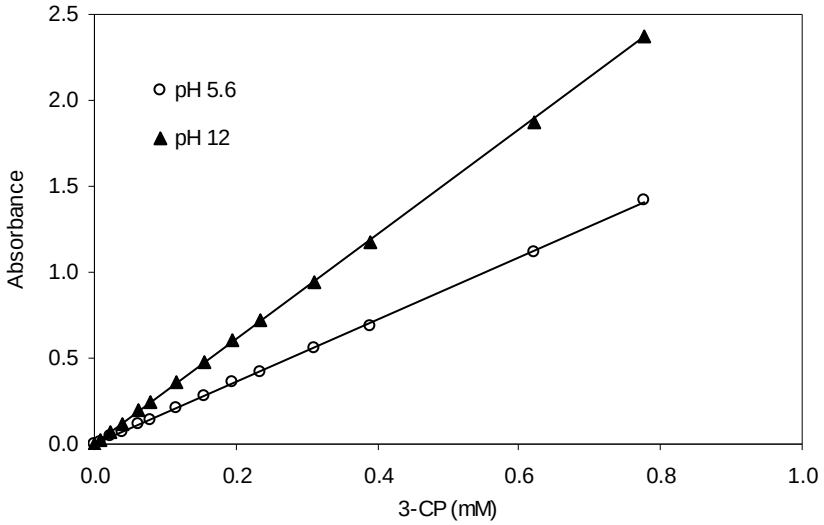

Figure 4.4 UV-visible absorbance for 3-CP in water

From the UV-visible spectral analysis, it was observed that for the same initial concentration of 3-CP a solution at pH 12.0 has values of absorbance greater than pH 5.6 (Figure 4.4). Therefore, the measurements were carried out at solution pH 12.0 and wavelength at 292 nm to obtain the higher 3-CP sensitivity.

Spectra for 4-CP in water at pH 5.6, showed the absorption curves were placed between 250–280 nm with a maximum absorbance at wavelength 280 nm (Figure 4.5). When methanol is used as a solvent the shape of spectra is different and shifted in the range 283–296 nm with a maximum absorbance at 283 nm for each concentration (Figure 4.5). In case of water solution at pH 12.0, the spectra shape vs. sample concentrations (i.e. with respect to absorbance) is more evident at wavelength range 298–350 nm (Figure 4.5).

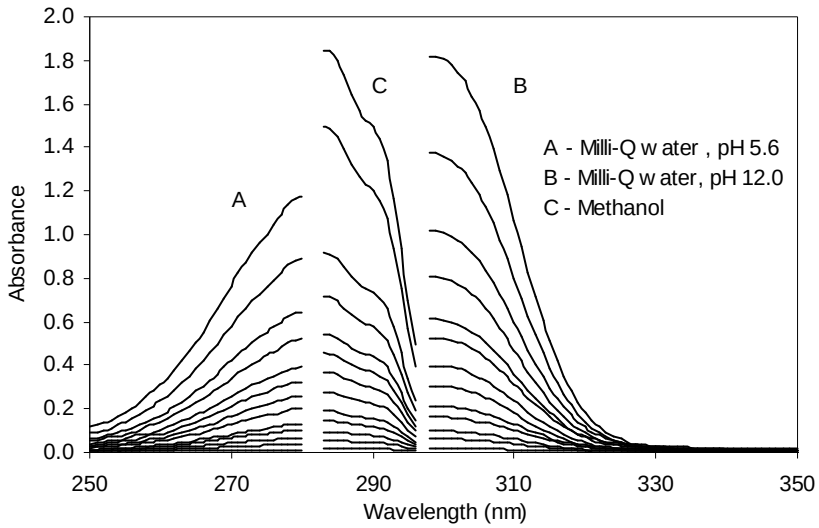

Figure 4.5 UV-visible spectra for 4-CP in water and methanol

The UV-visible absorbance in order to determine concentration in water at pH 5.6, at pH 12.0 and in methanol were made 280 nm, 298 nm and 283 nm, respectively, (Table 4.3).

Table 4.3 Spectral and calibration data for 4-CP compounds: initial concentration 0.0076–0.78 mM, 22 °C

Solvent	Wavelength λ_{max} (nm)	Absorbance range	Absorptivity (ε) (cm^{-1} mM^{-1})	r^2	MDL (mM)
Milli-Q water at pH ~5.6	280	0.013–1.176	1.53	0.997	0.0026
Milli-Q water at pH ~12.0	298	0.018–1.815	2.38	0.999	0.0006
Methanol	283	0.019–1.847	2.37	0.991	0.0014

MDL- minimum detection limit

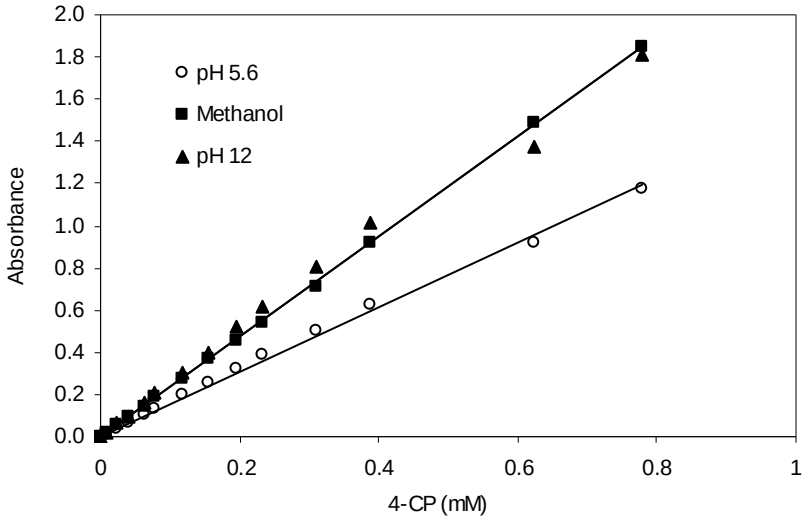

Figure 4.6 UV-visible absorbance for 4-CP in water and methanol

From the UV-visible spectral analysis, it was observed that for the same initial concentration of 4-CP a solution at pH 12.0 has values of absorbance greater than pH 5.6 but almost similar in methanol (Figure 4.6). However, due to lower minimum detection limit (MDL) (Table 4.3), the measurements were carried out at solution pH 12.0 and wavelength at 298 nm to obtain the higher 4-CP sensitivity.

Spectra for 2,4-DCP in water at pH 5.6, showed the absorption curves were placed between 250–284 nm with a maximum absorbance at wavelength 284 nm (Figure 4.7). When methanol is used as a solvent the shape of spectra is different and shifted in the range 287–303 nm with a maximum absorbance at 287 nm for each concentration (Figure 4.7). In case of water solution at pH 12.0, the spectra shape vs. sample concentrations (i.e. with respect to absorbance) is more evident at wavelength range 305–350 nm (Figure 4.7).

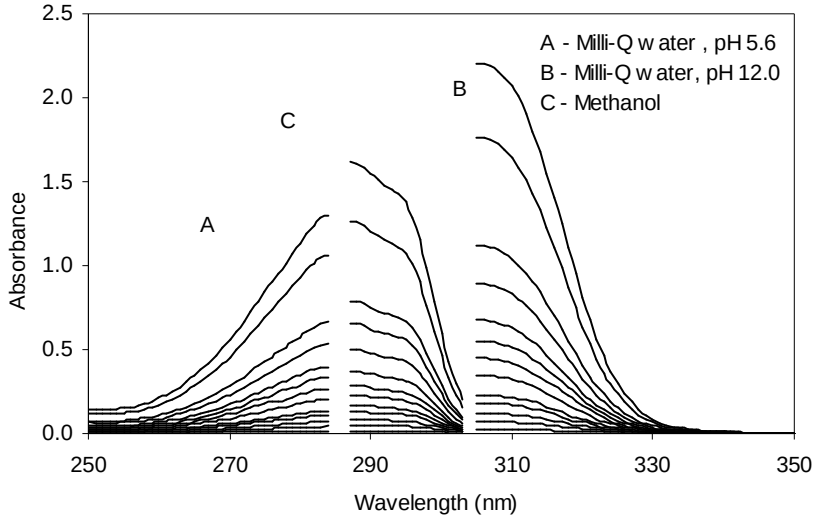

Figure 4.7 UV-visible spectra for 2,4-DCP in water and methanol

The UV-visible absorbance in order to determine concentration in water at pH 5.6, at pH 12.0 and in methanol were made 284 nm, 305 nm and 287 nm, respectively, (Table 4.4).

Table 4.4 Spectral and calibration data for 2,4-DCP compounds: initial concentration 0.0062–0.62 mM, 22 °C

Solvent	Wavelength λ_{max} (nm)	Absorbance range	Absorptivity (ε) (cm^{-1} mM^{-1})	r^2	MDL (mM)
Milli-Q water at pH ~5.6	284	0.014–1.301	2.15	0.999	0.0019
Milli-Q water at pH ~12.0	305	0.023–2.205	3.60	0.999	0.0008
Methanol	287	0.016–1.614	2.60	0.998	0.0011

MDL- minimum detection limit

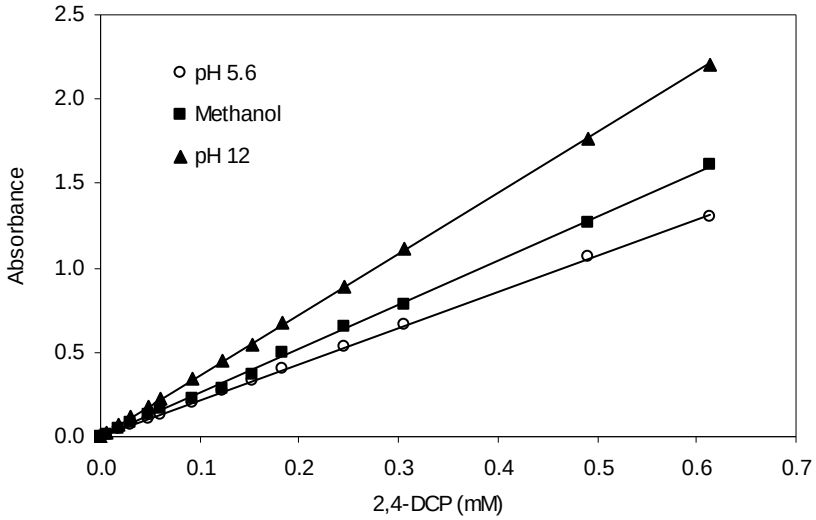

Figure 4.8 UV-visible absorbance for 2,4-DCP in water and methanol.

From the UV-visible spectral analysis, it was observed that for the same initial concentration of 2,4-DCP a solution at pH 12.0 has values of absorbance greater than pH 5.6 and methanol (Figure 4.8). Therefore, the measurements were carried out at solution pH 12.0 and wavelength at 305 nm to obtain the higher 2,4-DCP sensitivity.

Spectra for 2,6-DCP in water at pH 5.6, showed the absorption curves were placed between 250–283 nm with a maximum absorbance at wavelength 283 nm (Figure 4.9). In case of water solution at pH 12.0, the spectra shape vs. sample concentrations (i.e. with respect to absorbance) is more evident at wavelength range 299–350 nm (Figure 4.9).

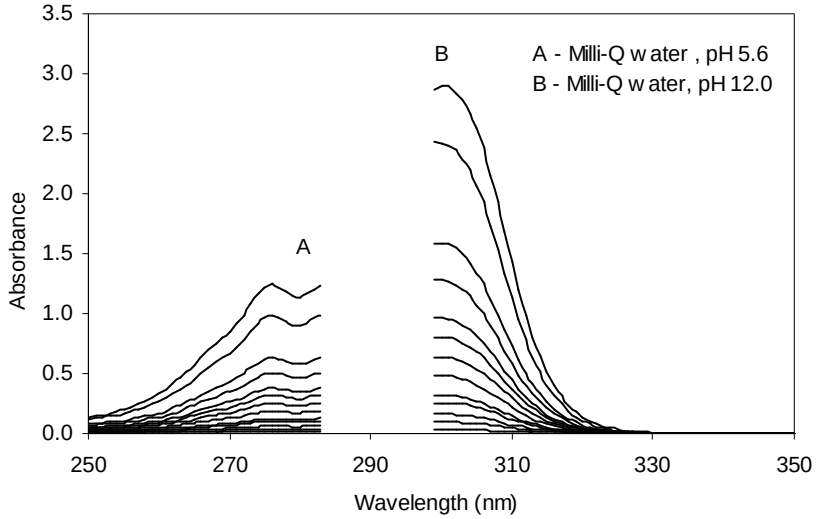

Figure 4.9 UV-visible spectra for 2,6-DCP in water

The UV-visible absorbances in order to determine concentration in water at pH 5.6 and at pH 12.0 were made 283 and 299 nm **(**Table 4.5).

Table 4.5 Spectral and calibration data for 2,6-DCP compounds: initial concentration 0.0067–0.61 mM, 22 °C

Solvent	Wavelength λ_{max} (nm)	Absorbance range	Absorptivity (ε) (cm^{-1} mM^{-1})	r^2	MDL (mM)
Milli-Q water at pH ~5.6	283	0.014–1.232	2.02	0.999	0.0004
Milli-Q water at pH ~12.0	299	0.033–2.872	4.90	0.996	0.0006

MDL- minimum detection limit

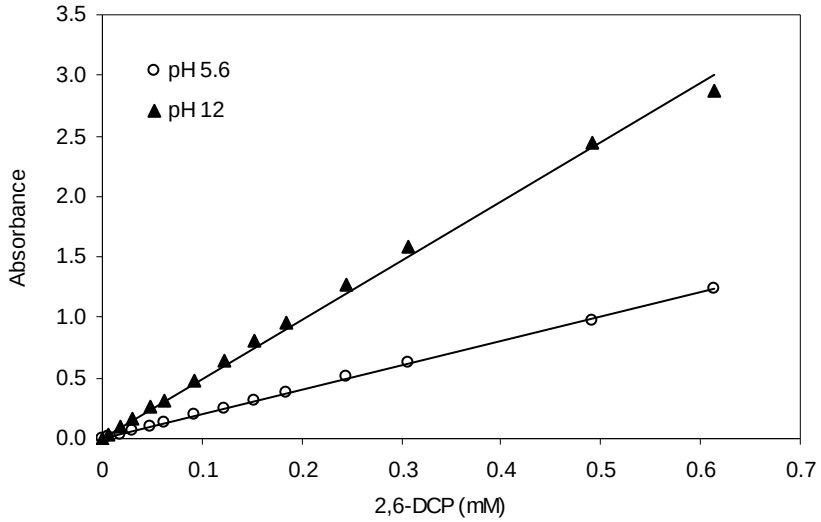

Figure 4.10 UV-visible absorbance for 2,6-DCP in water

From the UV-visible spectral analysis, it was observed that for the same initial concentration of 2,6-CP a solution at pH 12.0 has values of absorbance greater than pH 5.6 (Figure 4.10). Therefore, the measurements were carried out at solution pH 12.0 and wavelength at 299 nm to obtain the higher 2,6-DCP sensitivity.

Spectra for 2,4,6-TCP in water at pH 5.6, showed the absorption curves were placed between 250–294 nm with a maximum absorbance at wavelength 294 nm (Figure 4.11). When methanol is used as a solvent the shape of spectra is different and shifted in the range 296–310 nm with a maximum absorbance at 296 nm for each concentration (Figure 4.11). In case of water solution at pH 12.0, the spectra shape vs. sample concentrations (i.e. with respect to absorbance) is more evident at wavelength range 312–350 nm (Figure 4.11).

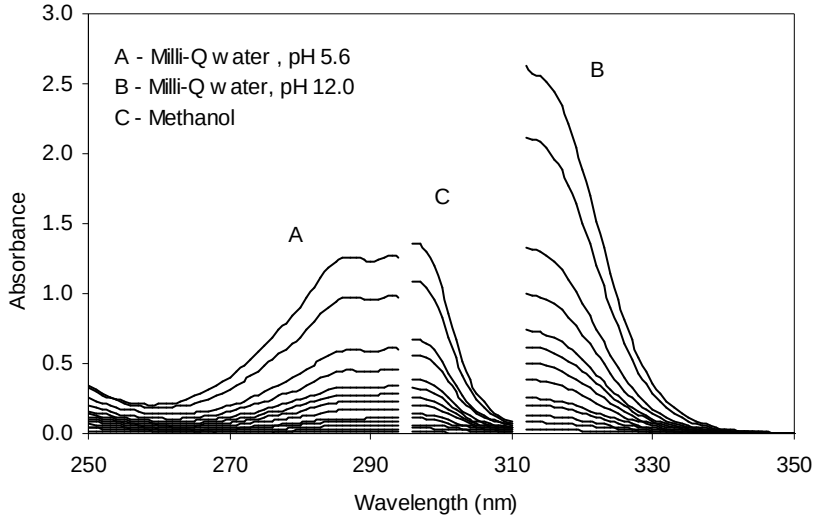

Figure 4.11 UV-visible spectra for 2,4,6-TCP in water and methanol

The UV-visible absorbance in order to determine concentration in water at pH 5.6, at pH 12.0 and in methanol were made 294 nm, 312 nm and 296 nm, respectively, (Table 4.6).

Table 4.6 Spectral and calibration data for 2,4,6-TCP compounds: initial concentration 0.0034–0.52 mM, 22 °C

Solvent	Wavelength λ_{max} (nm)	Absorbance range	Absorptivity (ε) (cm^{-1} mM^{-1})	r^2	MDL (mM)
Milli-Q water at pH ~5.6	294	0.013–1.257	2.41	0.998	0.0010
Milli-Q water at pH ~12.0	312	0.028–2.624	5.17	0.999	0.0007
Methanol	296	0.009–1.359	2.67	0.999	0.0020

MDL- minimum detection limit

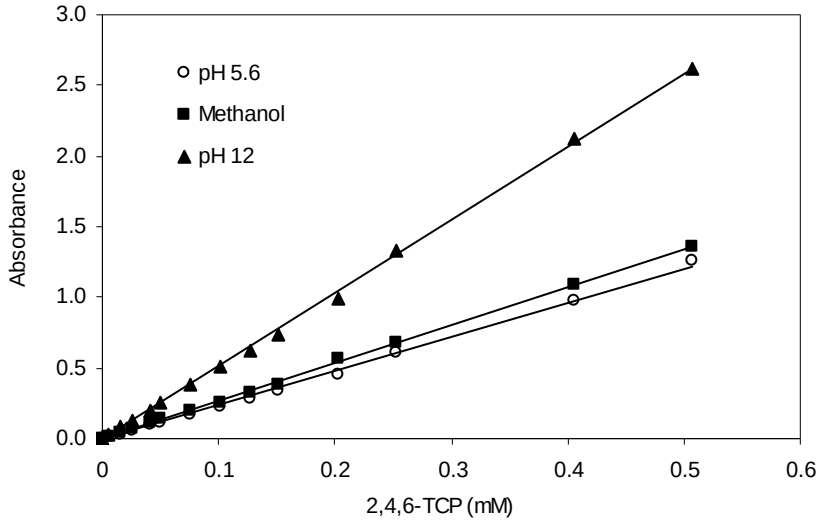

Figure 4.12 UV-visible absorbance for 2,4,6-TCP in water and methanol.

From the UV-visible spectral analysis, it was observed that for the same initial concentration of 2,4,6-TCP a solution at pH 12.0 has values of absorbance greater than pH 5.6 and methanol (Figure 4.12). Therefore, the measurements were carried out at solution pH 12.0 and wavelength at 305 nm to obtain the higher 2,4,6-TCP sensitivity.

Thus, for all chlorophenols in water solution at pH 5.6, λ_{max} was found in the range 274–294 nm and at pH 12.0 in the range 292–312 nm. When methanol was used as solvent λ_{max} for 2-CP, 4-CP, 2,4-DCP and 2,4,6-TCP were in the range from 276–296 nm. The absorbance was measured at pH 12.0 at wavelength range 292-312 nm to obtain the higher chlorophenol sensitivity.

For example, the measurements of absorbance in methanol, Milli-Q water at pH 12 and pH 5.6 for initial concentration ~1 mg L^{-1}. The results indicated that chlorophenols showed comparable absorption with methanol at the wavelength range 274–312 nm (Table 4.7).

Table 4.7 Comparison of absorbance at concentration ~1 mg L^{-1} for chlorophenols

Solvent condition	2-CP mg L^{-1} /Abs.	3-CP mg L^{-1} /Abs.	4-CP mg L^{-1} /Abs.	2,4-DCP mg L^{-1} /Abs.	2,6-DCP mg L^{-1} /Abs.	2,4,6-TCP mg L^{-1} /Abs.
Milli-Q water at pH ~5.6	0.82/0.012	1.0/0.014	1.09/0.013	1.06/0.014	1.11/0.014	1.07/0.013
Milli-Q water at pH ~12.0	0.94/0.025	1.08/0.026	0.97/0.018	1.04/0.023	1.09/0.033	1.07/0.028
Methanol	0.96/0.018	----	1.09/0.019	1.01/0.016	---	0.67/0.009

From Table 4.7, it was observed that in most cases the chlorophenol concentration at pH 12.0 shows a maximum absorbance in the range 292–312 nm with an initial concentration ~1 mg L^{-1} when compared with the solvent at pH 5.6 and methanol.

When the absorption value is too strong (>100 mg L^{-1}) deviation from Lambert-Beer law occurs or when it is too week (< 1mg L^{-1}) the sensitivity of absorbance was too low. By considering this issues absorbance measurement for calibration were made in the range 1–100 mg L^{-1}. The average detection limit was 0.1 mg L^{-1} which is an order of magnitude higher than HPLC (0.01 mg L^{-1}) (Ye and Shen, 2004). This method can be useful to analyse un-buffered neutral water sample. The concentration of residual chlorophenol can be determined by UV-visible spectrophotometer at higher wavelength 292-312 nm, and before the determination, the pH value of the solution will be adjusted to pH 12.

4.2.2 Analytical recovery

A solid phase extraction (SPE) process was applied (section 3.7.2) for the separation and pre concentration of organic compounds from water samples. The recovery for each

chlorophenol was calculated by comparison of the absorbance of the extracted and non-extracted (as measured calculated by concentration) compounds (Table 4.8, 4.9).

Table 4.8 Concentration of CP before and after solid phase extraction (SPE)

No. of sample	2-CP (mg L^{-1})		4-CP (mg L^{-1})		2,4-DCP (mg L^{-1})		2,4,6-TCP (mg L^{-1})	
	Before SPE	After SPE	Before SPE	After SPE	Before SPE	After SPE	Before SPE	After SPE
1	0.96	0.90	1.09	0.92	1.01	0.82	0.67	0.44
2	0.96	0.80	1.09	1.03	1.01	0.94	0.67	0.52
3	0.96	0.90	1.09	0.98	1.01	0.94	0.67	0.52
4	0.96	0.85	1.09	0.87	1.01	0.88	0.67	0.44

Table 4.9 The recovery (%) of CP by extraction with methanol from water solution and identification by UV-visible spectrophotometry

No of Sample	% of recovery			
	2-CP	4-CP	2,4-DCP	2,4,6-TCP
1	94	84	81	66
2	83	94	93	78
3	94	90	93	78
4	89	80	87	66
Mean value	90	87	89	72

In conclusion, it was found that absorbance vs. concentration obeys the Lambert-Beer law for the concentration range (1-100 mg L^{-1}) of these chlorophenols. The minimum detectable concentration and their corresponding absorbance were determined. The recovery efficiency after extraction with methanol showed poor result for 2,4,6-TCP (72%).

4.2.3 Analysis method development

The spectra showed that during the oxidation of permanganate a reaction by-product colloidal manganese dioxide is produced. It is believed that CP (mono or dichlorophenol) and permanganate oxidation proceeded according to equation 4.1:

$$C_6H_3Cl_2OH / C_6H_4ClOH + KMnO_4 \longrightarrow CO_2 + KCl + H_2O + MnO_2 \qquad (4.1)$$

4.2.4 Effect of pH on CP absorbance

Since the studied CP are un-dissociated at pH 5.6 and dissociated at pH 12 a bathochromic shift appears between acidic and basic solutions which can be used for phenolic compound detection to get higher sensitivity. The measured bathochromic shifts ($\Delta\lambda_{max}$) for first peak and second peak at various pH is shown in Table 4.10. The bathochromic shifts ($\Delta\lambda_{max}$) in this study for the un-dissociated chlorophenol is between 16–21 nm (Table 4.10) for the second peak which is consistent with other studies (Thomas and Burgess, 2007).

Table 4.10 Measured maximum absorbance of CP (~0.16 mM) at various pH, 22 °C

CP	pH 5.6	pH 12		pH 5.6	pH 12	
	1st peak λ_{max} (nm)	1st peak λ_{max} (nm)	Bathochromic shift $\Delta\lambda_{max}$ (nm)	2nd peak λ_{max} (nm)	2nd peak λ_{max} (nm)	Bathochromic shift $\Delta\lambda_{max}$ (nm)
2-CP	214	238	24	274	294	20
3-CP	218	239	21	274	292	18
4-CP	226	244	18	280	298	18
2,4-DCP	220	245	25	284	305	21
2,6-DCP	223	240	17	283	299	16

CP-chlorophenol

For example the spectrum of 4-CP in aqueous solution at pH 5.6 shows maximum absorption band at 226 and 280 nm while at pH 12 it exhibits maximum absorption bands at 244 and 298 nm. The peak at the lower wavelength is more intense in both the cases than the peak at the higher wavelength (Figure 4.13).

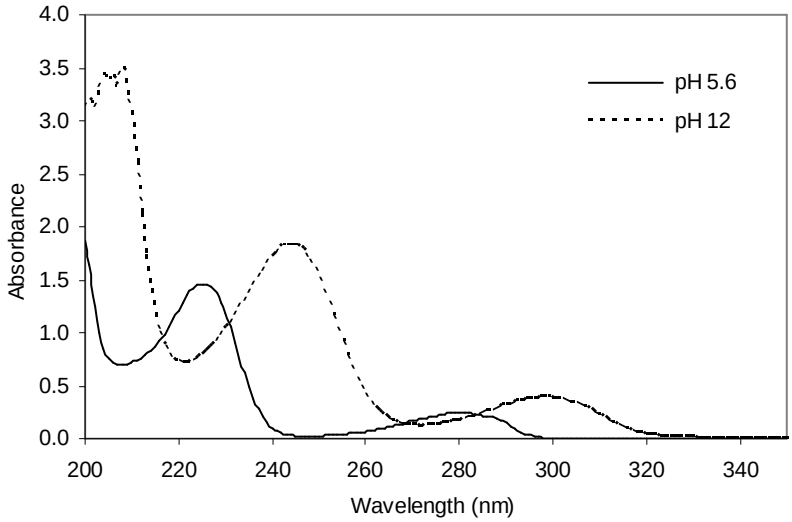

Figure 4.13 Spectra of 4-CP (~ 0.16 mM) at various pH

Similarly, maximum absorbance was found at pH 12.0 for 2-CP, 3-CP, 2,4-DCP and 2,6-DCP (Table 4.10). It was observed that at pH 12 the absorption peak did not change with time which indicates each CP is stable at this pH. Measurements were carried out at a higher wavelength to avoid interference and the determination of chlorophenol was made at pH 12 for higher sensitivity. The pH of aqueous solution of CP was 5.6 and the experimental initial pH was 5.3. The pH change of up to 0.3 units did not have a significant influence of the rate of reaction.

4.2.5 Effect of quenching agents on CP absorbance

Commonly used quenching agents ($Na_2S_2O_3$, Na_2SO_3, $NH_2OH.HCl$ and H_2O_2) were evaluated. For example, the addition of an aqueous solution of each quenching agent ($Na_2S_2O_3$, Na_2SO_3 and H_2O_2) can cause a change in the absorption spectrum from the 4-CP control. At 226 nm, increased absorbance occurs (Table 4.11). However $NH_2OH.HCl$ causes minimal change from the 4-CP control. At 280 nm all the quenching agents cause minimal deviation from the absorbance due to 4-CP (Figure 4.14). There was no change in absorbance with time (i.e. up to 20 min) which indicates the selected quenching agents do no react with 4-CP at pH 5.6.

Table 4.11 Absorbance of 4-CP (~0.16 mM) with quenching agent, reaction time 20 min, pH 5.6 (22 °C)

Reagents	(226 nm)	(280 nm)
4-CP (control)	1.4600	0.2483
4-CP + Na_2SO_3	1.8650	0.2455
4-CP + $Na_2S_2O_3$	3.8060	0.2471
4-CP + $NH_2OH.HCl$	1.4319	0.2413
4-CP + H_2O_2	2.1321	0.2848

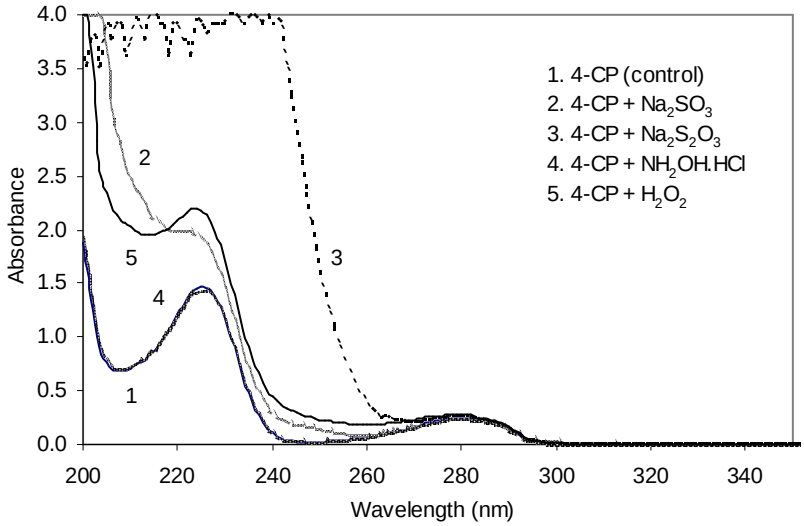

Figure 4.14 Spectra of 4-CP (~ 0.16 mM) with quenching agent, pH 5.6, 22 °C

4.2.6 Selection of the quenching agent

Using the analytical method of 4-CP analysis during oxidation by permanganate, the other CP analysis during oxidation was also examined. Since the measured absorbance of the chlorophenols was greater at pH 12 than at pH 5.6, it was decided to further evaluate the impact of the quenching agents and reagent at this pH. The reagent blank containing $NH_2OH.HCl$, H_2O_2, $Na_2S_2O_3$ and Na_2SO_3 showed higher absorption at the wavelength range 238–245 nm, and lower absorbance at wavelength range 292–305 nm at pH 12 (Figure 4.15).

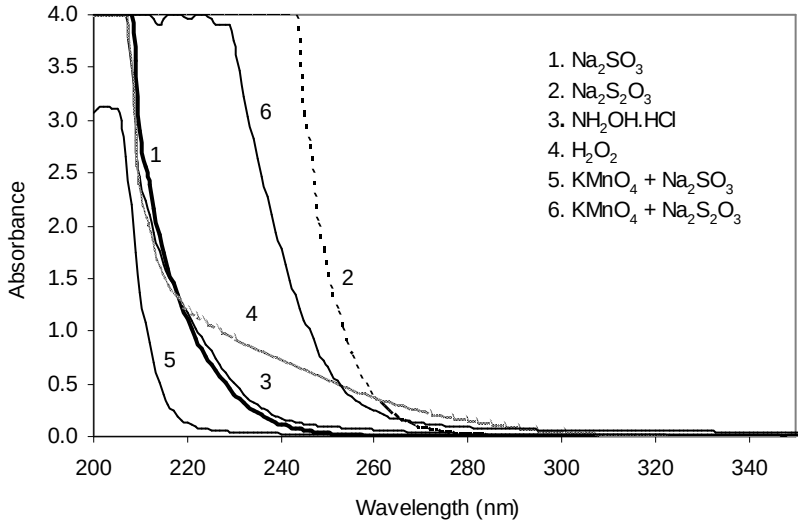

Figure 4.15 Spectra of quenching agent and reagent blank at pH 12

The data are shown in Table 4.12 and 4.13. Therefore, absorbance was measured at the higher wavelengths (292–305 nm) to minimise the impact of absorbance due to the quenching agents.

Table 4.12 Absorbance for various reagents and solutions, pH 12, 22 °C at wavelength range 238–245 nm

Reagents	2-CP 238	3-CP 239	4-CP 244	2,4-DCP 245	2,6-DCP 240
CP (~0.16 mM)	1.2041	1.3914	1.8490	1.5645	0.9779
$KMnO_4$ (1.5 mM)	2.1499	2.0846	1.7102	1.6326	2.0139
Na_2SO_3 (1M)	0.1555	0.1367	0.0695	0.0602	0.1198
$Na_2S_2O_3$ (1M)	3.999	3.999	3.655	3.0726	3.999
$NH_2OH.HCl$ (1M)	0.2135	0.1930	0.1259	0.1177	0.1748
H_2O_2 (1M)	0.7771	0.7568	0.6577	0.6385	0.7367
$KMnO_4$ + Na_2SO_3	0.0298	0.0291	0.0254	0.0248	0.0282
$KMnO_4$ + $Na_2S_2O_3$	2.1052	1.9370	1.2208	1.1061	1.7743

Table 4.13 Absorbance for various reagents and solutions, pH 12, 22 °C at wavelength range 292–305 nm

Reagents	2-CP 294	3-CP 292	4-CP 298	2,4-DCP 305	2,6-DCP 299
CP (~0.16 mM)	0.5414	0.4733	0.3885	0.5807	0.7692
$KMnO_4$ (1.5 mM)	1.8019	1.6232	2.1143	2.4738	2.1766
Na_2SO_3 (1M)	0.0001	0.0001	0.0001	0.0001	0.0001
$Na_2S_2O_3$ (1M)	0.0002	0.0002	0.0002	0.0002	0.0002
$NH_2OH.HCl$ (1M)	0.022	0.0222	0.0212	0.0143	0.0163
H_2O_2 (1M)	0.069	0.0789	0.0544	0.0349	0.0513
$KMnO_4$ + $Na_2S_2O_3$	0.0670	0.0693	0.0637	0.0586	0.0632
$KMnO_4$ + Na_2SO_3	0.0127	0.0128	0.0127	0.0126	0.0126

The higher absorbance for $NH_2OH.HCl$ and H_2O_2 makes them unsuitable as quenching agents compared with $Na_2S_2O_3$ and Na_2SO_3. Higher absorbance would increase the detection levels for the chlorophenol detection at the chosen wavelength. A solution containing Na_2SO_3 or $Na_2S_2O_3$ with $KMnO_4$ after filtration at pH 12 shows negligible absorbance of Na_2SO_3 (0.0126–0.0128) and higher absorbance for $Na_2S_2O_3$ (0.0586–0.0693). $Na_2S_2O_3$ had the same absorbance at 525 nm as Na_2SO_3 which shows that the permanganate had reacted to the same extent but greater absorbance at 418 nm which can be attributed to MnO_2, even though both samples had been filtered using 0.2 μm Whatman filter paper. Na_2SO_3 was therefore chosen as the preferred quenching agent for CP due to its lower absorbance through the 292–305 nm range. The detection limits were 0.0006 and 0.0008 mM for dichlorophenols and monochlorophenols, respectively. The determination of minimum detection limit was described in section 4.2.1.

Thus the spectral interference for the quenching agent (Na_2SO_3) and reagent condition may be neglected at spectral range 292–305 nm (Table 4.13) while the higher absorption spectrum with new characteristics bands shows at 238–245 nm (Table 4.12). Therefore residual CP analyses during oxidation were made at pH 12.

4.2.7 Analysis of 4-CP during oxidation

In order to measure the 4-CP concentration during permanganate oxidation, it was necessary to quench the reaction at a specific time. A quenching agent (Na_2SO_3) was added to eliminate interference caused by residual permanganate to the measurement of UV absorbance. It reacts with residual permanganate only and therefore the target residual analyte (4-CP) remains unchanged. The filtrate was analysed for residual 4-CP at pH 12. The disappearance of peaks at 244 nm and 298 nm indicates degradation of 4-CP after reaction with permanganate (Figure 4.16). At pH 12 measurements were carried out at 298 nm to avoid the interferences.

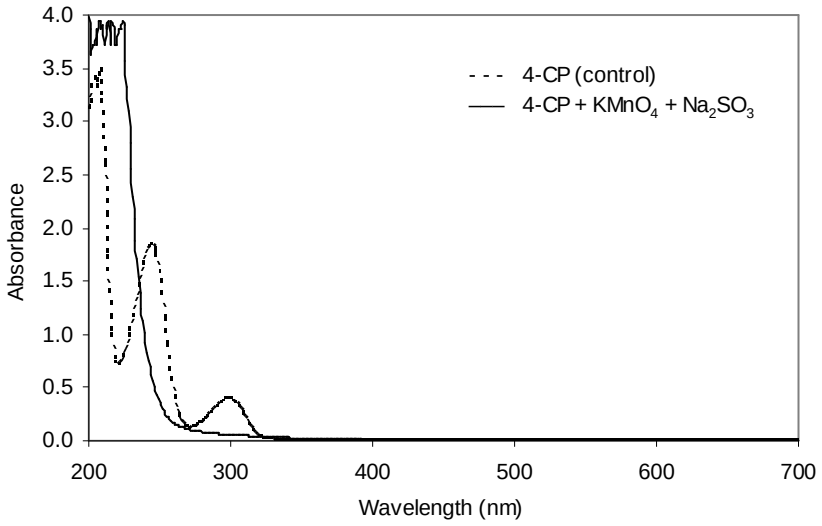

Figure 4.16 Absorption spectra after reaction of 4-CP (~ 0.16 mM) and $KMnO_4$ (1.5 mM) using quenching agent Na_2SO_3, pH 12, 22 °C

Thus the absorbance measurements for the determination of CP concentration were made at pH 12 for 294 nm (2-CP), 292 nm (3-CP), 298 nm (4-CP), 305 nm (2,4-DCP) and 299 nm (2,6-DCP) in order to obtain higher sensitivity during permanganate oxidation and to avoid interference from the absorption of quenching agent. Therefore CP degradation during oxidation could be determined by measuring the decrease in absorbance at wavelength range 292–305 nm as a function of time.

4.2.8 Permanganate decomposition and their spectral studies

4.2.8.1 Reactions between $KMnO_4$ and 4-CP

To obtain spectroscopic evidence of $KMnO_4$ consumption during 4-CP oxidation, the solution was successively scanned by UV-visible spectrophotometer. Figure 4.17 shows the spectrum changes during the oxidation of 4-CP with permanganate over time. The absorbance of MnO_4^- has significant peaks at both 525 and 546 nm (see blue line in Figure 4.17) and is therefore representative of the initial concentration of MnO_4^-. The absorption intensity in the region 460-600 nm is attributable to $KMnO_4$ and it decreased as the reaction proceeded due to the consumption of permanganate.

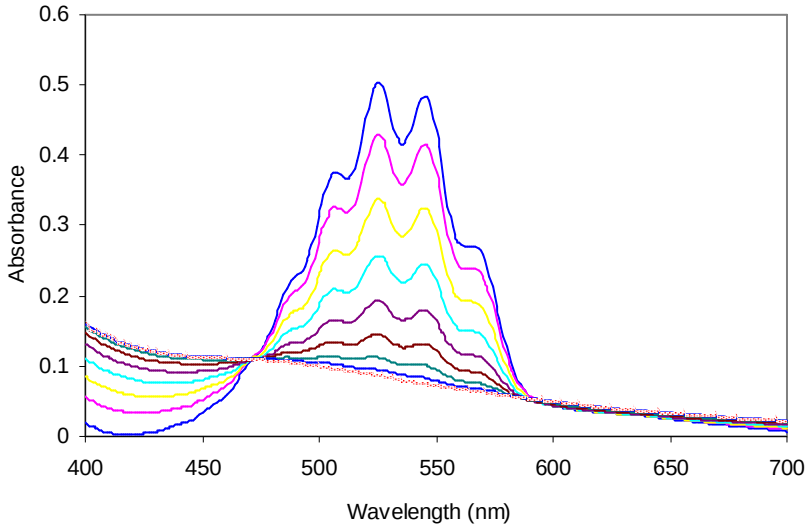

Figure 4.17 Spectral changes during the oxidation of 4-CP (~ 0.23 mM) with $KMnO_4$ (~ 0.2 mM) at time intervals of 45 sec, initial pH 5.3, 22 °C. The blue line is the initial $KMnO_4$ spectrum and the dotted line is the final due to a reaction with CP and MnO_2 is produced.

4.2.8.2 Formation of MnO_2

Spectroscopic evidence for the formation of MnO_2 was observed (Figure 4.17) when the 4-CP and permanganate solution was scanned by UV-visible spectrophotometer during the reactions (equation 4.1). Between 400 and 460 nm, the absorbance increased as the reaction proceeded. The absorption at 418 nm increased from 0.003 to 0.132 within 6 min, indicating the formation of species other than permanganate because permanganate has no absorbance at this wavelength. Similar results were found by Yan and Schwartz (1999) during oxidation of TCE-permanganate and they concluded that the produced species was colloidal MnO_2.

4.2.8.3 Isosbestic point

A sharp isosbestic point was found during successive scans of the reaction (Figure 4.17) an isosbestic point indicates that MnO_2 behaves according to Beer's Law. The isosbestic point was found at 473 nm. Almost similar isosbestic points were found for TCE at 467 nm (Waldemer and Tratnyek, 2006) and for trimethylamine at 470 nm (Mata-Pereze and Perez-Benito, 1985) during oxidation with permanganate. A sharp isosbestic point also implies that Beer's law is fulfilled and no long lived intermediates are formed during the reaction (Lee and Perez-Benito, 1985). A linear relationship between the absorbance at 525 nm (where both permanganate and manganese dioxide absorb) and the absorbance at 418 nm (where only manganese dioxide absorbs) was found when both reactant (MnO_4^-) and product (MnO_2) absorb light are plotted (Figure 4.18) indicates Beer's Law obeyed.

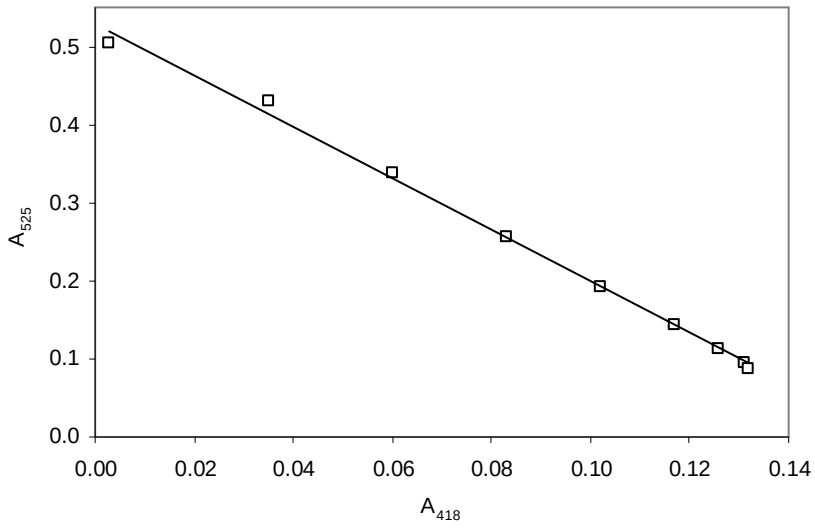

Figure 4.18 A linear relationship between absorbances at two wavelength A_{525} and A_{418}

During CP degradation in un-buffered condition it is possible that the formation of organic intermediates may occur. However, during the analysis I ensure this did not occur. In this study I analysed residual CP which showed negligible interference from intermediates. This is demonstrated by a sharp isosbestic point which implies that Beer's law is fulfilled and therefore no long lived intermediates are formed during the reaction. This has also been shown in other studies (Lee and Perez-Benito, 1985; He et al,. 2010)

4.2.9 Chlorophenol kinetics

Kinetic experiments of the oxidation of CP with $KMnO_4$ were carried out in un-buffered conditions. The results indicated that the oxidation of chlorophenol by permanganate is second-order overall, and first-order with respect to either CP or $KMnO_4$, and can be expressed as equation 4.2:

$$-d[CP]/dt = k_2[MnO_4^-][CP] \quad (4.2)$$

where, k_2 is the second-order rate constant (M^{-1} s^{-1}). As the permanganate is present in excess compared with CP, it can be considered a constant. The reaction then becomes pseudo-first-order and equation 4.2 can be written in the form of equation 4.3 and 4.4:

$$-d[CP]/dt = k_1[CP] \quad (4.3)$$

$$k_1 = k_2[MnO_4^-]_o \quad (4.4)$$

where k_1 is the pseudo-first-order rate constant (s^{-1}), $[MnO_4^-]_o$ is the initial permanganate concentration (M). The second-order rate constant (k_2) can be calculated from equation 4.4 (Zhai et al., 2006; He et al., 2010).

For all chlorophenols when reacted with excess $KMnO_4$ the reaction rate is pseudo-first-order with respect to CP (Figure 4.19).

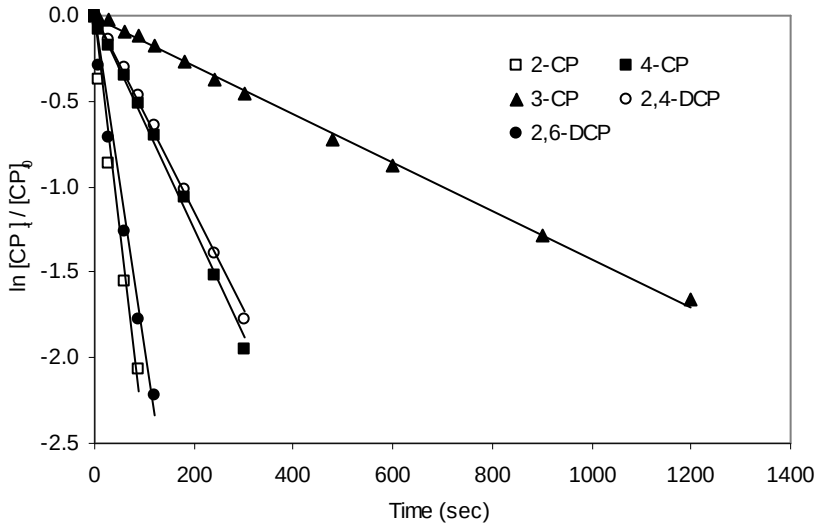

Figure 4.19 Degradation of chlorophenols by $KMnO_4$. $[CP]_o$ ~0.16 mM, Initial $KMnO_4$ 1.5 mM, pH 5.3, 22 °C

The plot $\ln[CP]_t/[CP]_o$ versus reaction time for all CP degradation are well fit with a pseudo-first-order decay model (i.e., $r^2 > 0.98$). Errors estimated are based on a 95% confidence interval using the mean value of k_1. The reaction order is 2-CP > 2,6-DCP > 4-CP ~ 2,4-DCP > 3-CP. The observed first-order rate constant and calculated second-order rates constant are shown in Table 4.14.

Table 4.14 Rate constants for chlorophenol (~0.16 mM) oxidation by $KMnO_4$ (1.5 mM): initial pH 5.3, 22 °C

Compounds	[a]k_1 ($\times 10^{-3}$ s^{-1})	[b]k_2 (M^{-1} s^{-1})
2-CP	24.3 ± 0.206	16.2
3-CP	1.42 ± 0.0011	0.95
4-CP	6.26 ± 0.022	4.2
2,4-DCP	5.74 ± 0.0479	3.8
2,6-DCP	19.4 ± 0.0627	12.9

[a]k_1 = pseudo-first-order rate constant = the mean value ± 95% confidence interval
[b]k_2 = second-order rate constant is calculated by $k_2 = k_1/[KMnO_4]_o$ using the mean k_1 value

The second-order rate constant (k_2) was calculated (using the equation 4.4) from the measured pseudo-first-order rate constant (k_1) with respect to CP with initial $KMnO_4$ concentration (1.5 mM). Second-order rate constants are more general and more useful than pseudo-first-order rate constants. The rates from this study (~4–16 M^{-1} s^{-1}) are similar to that reported by He et al. (2010) (~8–20 M^{-1} s^{-1}) and except for 4-CP are within an order of magnitude of those reported by Zhang et al. (2003) and Waldemer and Tratnyek (2006). Our reaction sequences are similar to those of He et al. (2010) and Waldemer and Tratnyek (2006) but differ from Zhang et al. (2003). It was found that 3-CP is the most resistant to oxidation. The oxidation kinetics may be influenced by the interaction of electron-withdrawing chlorine and hydroxyl groups, the resonance of the phenolic anion, the steric effect of chlorine and the acidities of chlorophenols (Zhang et al., 2003; Han et al., 2004).

4.3 Conclusion

The proposed analytical method for chlorophenol quantification is simple, inexpensive and does not require any major pre-treatment procedure prior to analysis. The values of absorption are higher at pH 12.0 compared to other solvent conditions. Solid phase

extraction followed by measurement of the UV absorption value for quantification of chlorophenol from water may be used for routine on-site sample analysis. It is suited for the relatively high chlorophenol concentrations found at sites with significant groundwater contamination. The kinetics of permanganate oxidation of CP was found to be pseudo-first-order with respect to the reductant in un-buffered conditions. Future studies should determine second-order reactions rates under a range of environmental conditions. The relatively rapid reaction rates between permanganate and chlorophenol suggests that permanganate may potentially be used for treatment of chlorophenol contaminated water. Any toxic by-products formed during the oxidation processes should be identified. The determined second-order rate constant can be useful to predict the reaction rates of CP with permanganate during practical soil and groundwater remediation work. The rate constants are not same for all chlorophenols with nearly the same initial concentration of both the permanganate and CP. This indicates that the structure of chlorophenols may have influence on their oxidation kinetics. The spectral analysis indicated that the wavelength at 418 nm is useful in quantification of the oxidation level as the permanganate has minimal impact in this region.

CHAPTER 5

Kinetic investigations of oxidation of chlorophenols by permanganate

5 Kinetic investigations of oxidation of chlorophenols by permanganate

5.1 Introduction

Previous chapter (Chapter 4) have determined second-order rates from pseudo-first-order rates assuming the reaction was second-order based on the work of Lee and Sebastian (1981). Also, Waldemer and Tratnyek (2006) determined the permanganate-chlorophenol reaction was second-order in a neutral, phosphate buffered solution, there is still a lack of kinetic data about the degradation of chlorophenols under various oxidant concentrations at neutral pH in un-buffered solutions. Therefore, this study aims to verify whether the permanganate-chlorophenol reaction is second-order under neutral pH, un-buffered conditions and determine the reaction rates, and to investigate the relationships between rates of reaction and structural properties of the chlorophenols. Un-buffered neutral solutions were used since it was believed this would better represent a groundwater environment than a well buffered neutral solution.

This study examined the kinetics of oxidation of various chlorophenols in relation with chemical kinetics, oxidant and contaminant concentration at which excess permanganate (0.8–3.2 mM) oxidizes an aqueous solution of chlorophenols (0.04–0.24 mM) in un-buffered solution with ionic strength ~0.02 M. The effect of pH and ionic strength on second-order reaction of 4-CP (as model compound) were also investigated.

5.2 Reaction order

The kinetics of oxidation of chlorophenols by $KMnO_4$ were studied in un-buffered solution with ionic strength ~0.02 M under pseudo-first-order conditions as described in section 3.7.4.2. Batch experiments were performed to verify the oxidation of CP by $KMnO_4$ is second-order overall, and first-order with respect to either CP or $KMnO_4$. For all this experiments first-order rate constants were determined by evaluating the CP degradation rates.

According to equation 4.1 (section 4.2.3), the oxidation reaction of CP and $KMnO_4$ can be expressed using rate law (Boekel 2008) as equation 5.1:

$$r = -d[CP]/dt = k_2 [CP]^{\alpha} [MnO_4^-]^{\beta} \quad (5.1)$$

where r is the reaction rate, k_2 represents the second-order rate constant ($M^{-1} s^{-1}$), [CP] is the concentration of chlorophenol (M), $[MnO_4^-]$ is the concentration of permanganate (M), α and β are the reaction orders with respect to [CP] and $[MnO_4^-]$, respectively. The reactions are assumed to be second-order overall, and first-order with respect to either CP or $KMnO_4$ based on previous kinetic studies on the oxidation of CP by $KMnO_4$ (Lee and Sebastian, 1981; Waldemer and Tratnyek, 2006; He et al., 2010). Therefore, the reaction order for both α and β are expected to be one. The equation 5.1 can be rewritten as equation 5.2:

$$r = -d[CP]/dt = k_2 [CP] [MnO_4^-] \quad (5.2)$$

As the permanganate is present in excess and its concentration is assumed to be constant, the reaction then becomes pseudo-first-order and equation 5.2 can be simplified (Huang et al., 2001) to equation 5.3 and 5.4:

$$r = -d\,[CP]/dt = k_1\,[CP] \tag{5.3}$$

$$k_1 = k_2\,[MnO_4^-]_o \tag{5.4}$$

where k_1 is the (observed) pseudo-first-order rate constant (s^{-1}) for CP, $[MnO_4^-]_o$ is the initial permanganate concentration (M). k_2 the second-order rate constant ($M^{-1}\ s^{-1}$) calculated from equation 5.4 (Yan and Schwartz, 1999; Huang et al., 2002; Zhai et al., 2006). The above hypotheses are verified through the experimental data.

In the situation where α and β are the reaction orders with respect to [CP] and $[MnO_4^-]$ respectively, equation 5.3 and 5.4 can be re-written to equation 5.5 and 5.6:

$$r = k_1\,[CP]^{\alpha} \tag{5.5}$$

$$k_1 = k_2\,[MnO_4^-]^{\beta} \tag{5.6}$$

At different initial concentration of [CP] and measuring the reaction rate, the order α with respect to [CP] can be determined by using natural log transform of the equation 5.5, see equation 5.7:

$$\ln r = \ln k_1 + \alpha \ln [CP] \tag{5.7}$$

Again, at different initial concentration of $[MnO_4^-]_o$ and measuring k_1, the order β with respect to $[MnO_4^-]$ can be obtained by using natural log transform of the equation 5.6, see equation 5.8:

$$\ln k_1 = \ln k_2 + \beta \ln [MnO_4^-]_o \quad (5.8)$$

To avoid complications from subsequent reactions or catalysis, an initial rate method (Casado et al. 1986) was used here and equation 5.7 can be expressed by equation 5.9:

$$\ln r_o = \ln k_1 + \alpha \ln [CP]_o \quad (5.9)$$

where r_o is initial rates,

k_1 are obtained by integrating equation 5.3 (from 0 to t), see equation 5.10:

$$\ln [CP]_t = - k_1 t + \ln [CP]_o \quad (5.10)$$

where $[CP]_o$ and $[CP]_t$ are the concentrations of CP at beginning and at time t, respectively.

Based on equation 5.8 and 5.9 order of reaction (α, β) can be determined.

Two sets of batch kinetic experiments were carried out to determine α and β values for chlorophenol oxidation. In the first set of experiment, the pseudo-first-order reaction rate with respect to CP was determined with various initial CP concentrations (0.04–0.24 mM). The initial excess permanganate was fixed for 2-CP, 2,6-DCP and 2,4,6-TCP (~1.2 mM) and 3-CP, 4-CP and 2,4-DCP (~1.5 mM) while initial concentration was varied for 2-CP (0.08–0.2 mM), for 3-CP, 4-CP and 2,4-DCP (0.05–0.16 mM), for 2,6-

DCP (0.08–0.24 mM) and 2,4,6-TCP (0.04–0.1 mM). The initial reaction rates were measured from the tangent of the CP concentration-time curve. For example, Figure 5.1 shows a typical graph for concentration-time curve of 4-CP. Similarly, for 2-CP, 3-CP, 2,4-DCP, 2,6-DCP and 2,4,6-TCP concentration-time curve is shown in Figures A1-A5 in Appendix A.

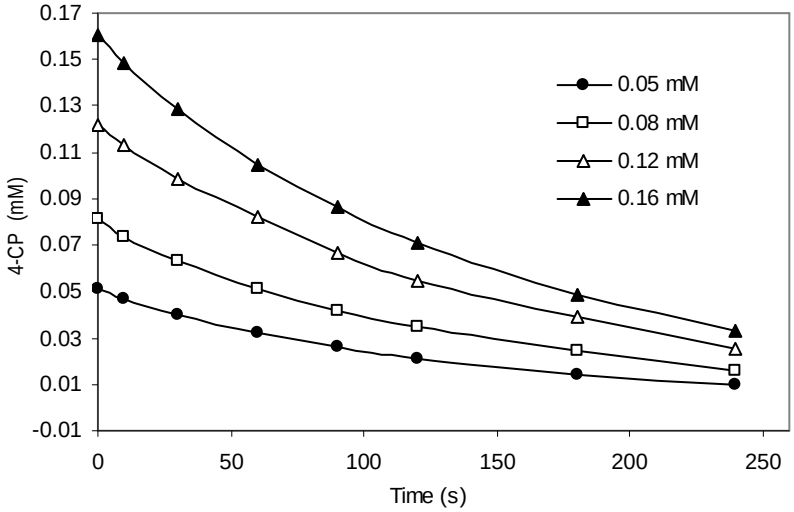

Figure 5.1 Degradation of 4-CP under various initial 4-CP concentration with fixed $KMnO_4$: $[4\text{-CP}]_o$ ~ (0.05–0.16) mM, $[MnO_4^-]$ ~ 1.5 mM, I ~0.02 M, initial pH 7.0 (22 °C)

A plot of ln r_o vs. ln $[CP]_o$ gives a linear curve with slope (i.e. α) close to 1.0 (Figure 5.2), indicating first-order reaction with respect to CP concentration (0.04–0.24 mM) with a good fit (Table 5.1).

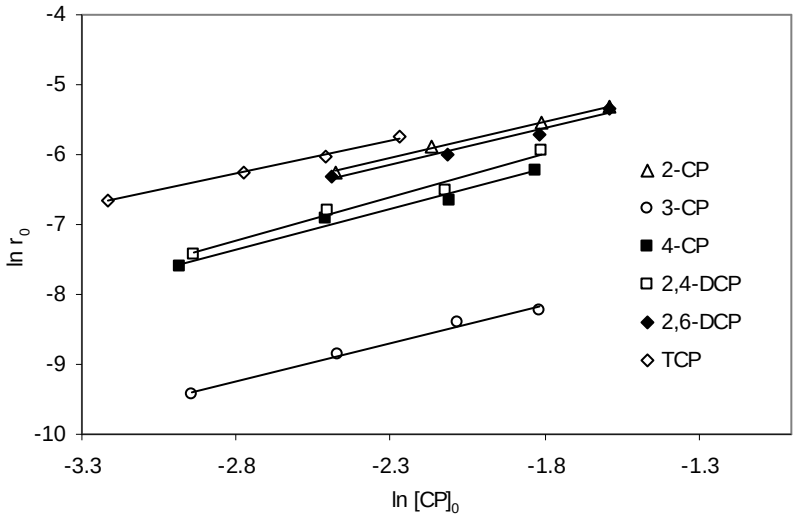

Figure 5.2 Plot of initial rate ln r_o versus initial concentration of CP ln$[CP]_o$: $[CP]_o$ ~ (0.04–0.24 mM), $[MnO_4^-]_o$ ~ 1.2 for 2-CP, 2,6-DCP and 2,4,6-TCP, ~1.5 mM for 3-CP, 4-CP and 2,4-DCP, I ~ 0.02 M, Initial pH 7.0 (22 °C)

Table 5.1 Reaction order alpha (α) with respect to the [CP]: I ~ 0.02 M, Initial pH 7.0 (22 °C)

Compound	α	r^2
2-CP	1.05	0.995
3-CP	1.10	0.989
4-CP	1.14	0.977
2,4-DCP	1.24	0.984
2,6-DCP	1.05	0.979
2,4,6-TCP	0.94	0.994

Equation 5.4 shows that k_1 is proportional to $[MnO_4^-]_o$ and almost constant when used in excess during each reaction. Therefore, the degradation rate of CP at various initial excess $KMnO_4$ concentrations (0.8–3.2 mM) was determined to investigate the influence of oxidant concentration on the first-order rate constants and to verify the reaction order with respect to $KMnO_4$. So the different experimental values of pseudo-

first-order rate constant (k_1) for each CP degradation from various initial excess concentration of $[MnO_4^-]_o$ can be obtained using equation 5.10. The value of β was then estimated based on equation 5.8.

Experimentally the initial excess permanganate concentration was varied for 2-CP, 2,6-DCP from 0.8 to 2 mM, for 3-CP, 4-CP and 2,4-DCP from 1.2 to 3.2 mM and for 2,4,6-TCP from 0.97 to 2.0 mM while the initial concentration of CP was fixed for 2-CP, 3-CP, 4-CP, 2,4-DCP, 2,6-DCP at ~0.16 mM and for 2,4,6-TCP at ~0.08 mM. A plot of ln k_1 against ln $[MnO_4^-]_o$ gives a linear curves ($r^2 > 0.98$) with slopes in the range from 0.91 to 0.98 i.e. close to one (Table 5.2, β = ~1) indicating that the reaction order is first-order for all chlorophenols with respect to $KMnO_4$ when reacting with fixed CP (Figure 5.3).

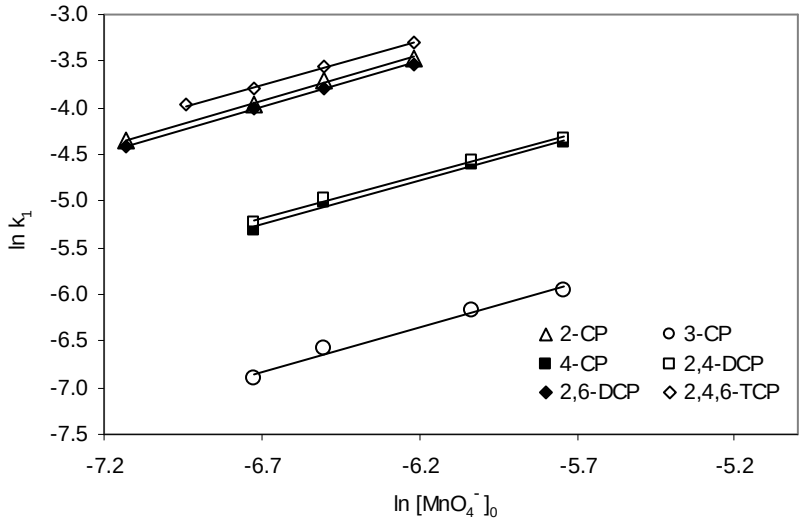

Figure 5.3 Plot of pseudo-first-order rate constant ln k_1 versus initial concentration of permanganate ln$[MnO_4^-]_o$: $[CP]_o$ ~0.16 mM, except 2,4,6-TCP ~0.08 mM, $[MnO_4^-]_o$ (0.8–3.2 mM), I ~0.02 M, Initial pH 7.0 (22 °C)

Table 5.2 Reaction order beta (β) with respect to [MnO_4^-]: I ~ 0.02 M, Initial pH 7.0 (22 °C)

Compound	β	r^2
2-CP	0.98	0.997
3-CP	0.95	0.982
4-CP	0.95	0.992
2,4-DCP	0.91	0.998
2,6-DCP	0.97	0.999
2,4,6-TCP	0.95	0.999

The results from both the Figures 5.2, 5.3 and Table 5.1, 5.2 indicated that the initial reaction between CP and $KMnO_4$ is a second-order reaction with $\alpha = \sim 1$ and $\beta = \sim 1$. The rate law for the CP oxidation can be expressed as equation 5.2. Thus, the reaction between CP and $KMnO_4$ was of second-order overall, and first-order with respect to each reactant. The second-order rate constants (k_2) for all chlorophenols can be determined using equation 5.4 are shown in Table 5.3.

Table 5.3 Rate constants for the oxidation of chlorophenols (CP) with various concentrations of $KMnO_4$: I ~0.02 M, Initial pH 7.0 (22 °C)

$[CP]_o$ ($\times 10^{-3}$ M)	$[KMnO_4]_o$ ($\times 10^{-3}$ M)	r^2	[a]k_1 ($\times 10^{-3}$ s^{-1})	[b]k_2 (M^{-1} s^{-1})	[c]k_2 (M^{-1} s^{-1})
2-CP (~0.16)	0. 8	0.996	13.4 ± 0.010	16.8	16.2± 0.502
2-CP (~0.16)	1.2	0.997	18.8 ± 0.215	15.7	
2-CP (~0.16)	1.5	0.996	24.6 ± 0.244	16.4	
2-CP (~0.16)	2.0	0.995	31.4 ± 0.258	15.7	
3-CP (~0.16)	1.2	0.996	1.0 ± 0.019	0.83	0.86± 0.050
3-CP (~0.16)	1.5	0.998	1.4 ± 0.003	0.93	
3-CP (~0.16)	2.4	0.994	2.1 ± 0.036	0.88	
3-CP (~0.16)	3.2	0.998	2.6 ± 0.066	0.81	
4-CP (~0.16)	1.2	0.999	4.9 ± 0.079	4.1	4.2± 0.160
4-CP (~0.16)	1.5	0.998	6.6 ± 0.141	4.4	
4-CP (~0.16)	2.4	0.993	9.9 ± 0.069	4.1	
4-CP (~0.16)	3.2	0.994	12.7 ± 0.165	4.0	
2,4-DCP (~0.16)	1.2	0.998	5.4 ± 0.074	4.5	4.4± 0.168
2,4-DCP (~0.16)	1.5	0.996	6.9 ± 0.054	4.6	
2,4-DCP (~0.16)	2.4	0.996	10.4 ± 0.128	4.3	
2,4-DCP (~0.16)	3.2	0.994	13.3 ± 0.153	4.2	
2,6-DCP (~0.16)	0. 8	0.999	12.0 ± 0.011	15.0	14.9± 0.158
2,6-DCP (~0.16)	1.2	0.998	18.1 ± 0.360	15.1	
2,6-DCP (~0.16)	1.5	0.989	22.3 ± 0.108	14.9	
2,6-DCP (~0.16)	2.0	0.995	29.3 ± 0.291	14.7	
2,4,6-TCP (~0.08)	0.97	0.998	18.8 ± 0.141	19.4	19.0± 0.305
2,4,6-TCP (~0.08)	1.2	0.993	22.7 ± 0.157	18.9	
2,4,6-TCP (~0.08)	1.5	0.989	28.5 ± 0.229	19.0	
2,4,6-TCP (~0.08)	2.0	0.985	37.1 ± 0.329	18.6	

[a]k_1 (pseudo-first-order rate constant) = the mean value ± 95% confidence interval.
[b]k_2 (second-order rate constant) is determined from $k_2 = k_1 / [MnO_4^-]_o$ using the mean of $k_1$values
[c]k_2 (second-order rate constant) = the mean value ± 95% confidence interval.

The observed pseudo-first-order rate constants increased for 2-CP, 3-CP, 4-CP, 2,4-DCP, 2,6-DCP and 2,4,6-TCP with an increased permanganate dosage (Table 5.3). This indicates that the rate of reaction between CP and $KMnO_4$ is faster with a higher concentration of $KMnO_4$, which shows that the rate of reaction varies with oxidant

concentration. An increase in oxidation rate with oxidant concentration was also reported in the literature (Huang et al., 1999). In all the experiments, the r^2 value for zero-order were in the range 0.56–0.94 and for second-order were in the range 0.73–0.94 (data not shown). The pseudo-first-order was in the range 0.98–0.99 (Table 5.3). This suggests that the pseudo-first-order kinetic model was best fit to the observed CP data. For example, Figure 5.4 shows a typical graph for the degradation of 4-CP by excess $KMnO_4$ during the experiments.

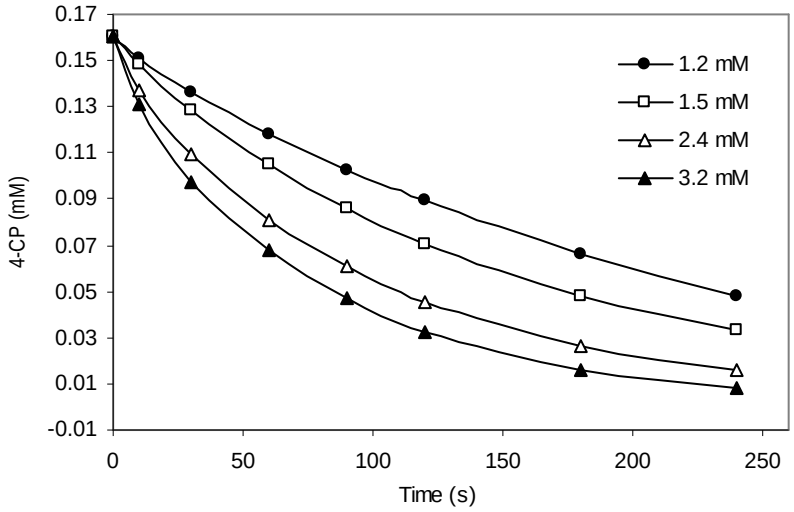

Figure 5.4 Degradation of 4-CP under various concentration of $KMnO_4$: $[4\text{-CP}]_o$ ~ 0.16 mM, $[MnO_4^-]$ ~(1.2–3.2 mM), I ~ 0.02 M, Initial pH 7.0 (22 °C)

The oxidation of 4-CP by $KMnO_4$ in all runs shows a linear relationship which shows it behaves according to a pseudo-first-order kinetic model where $r^2 > 0.99$. Pseudo-first-order rate constants were calculated from the results in Figure 5.5.

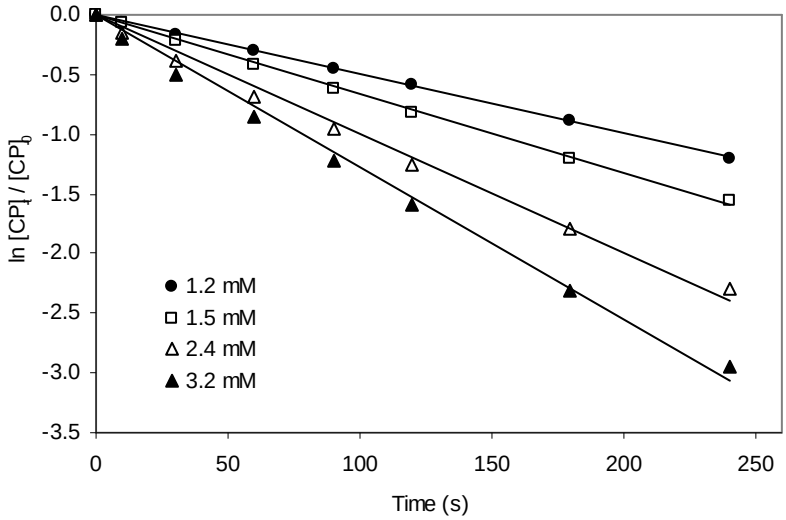

Figure 5.5 Oxidation fit curves of 4-CP at various concentration of $KMnO_4$: $[4\text{-CP}]_o$ ~0.16 mM, $[MnO_4^-]$ ~ (1.2–3.2 mM), I ~0.02 M, Initial pH 7.0 (22 °C)

The pseudo-first-order reaction rate increased from $(4.9 – 12.7) \times 10^{-3}$ s^{-1} for 4-CP, with the increasing permanganate dosage (1.2–3.2 mM) which indicated that the rate of reaction has a relationship with oxidant concentration. Similarly, the pseudo-first-order reaction rate was increased for 2-CP, 3-CP, 2,4-DCP, 2,6-DCP and 2,4,6-TCP under different excess initial permanganate concentration and are shown in Table 5.3 and Figures A6–A15 in Appendix A.

The pseudo-first-order kinetic data of CP degradation at various initial CP concentrations (0.04–0.24 mM) with excess fixed permanganate are also investigated to determine the effect of CP concentration on the rate constant. It is observed that the pseudo-first-order rate constants for 2-CP, 3-CP, 4-CP, 2,4-DCP, 2,6-DCP and 2,4,6-TCP did not change significantly at various initial CP concentrations (Table 5.4). This indicates that the rate of reaction between CP and $KMnO_4$ was not impacted by initial CP concentrations. At various initial CP concentrations with excess $KMnO_4$, the r^2

value for zero-order were in the range 0.78–0.94 and for second-order were in the range 0.89–0.94 (data not shown). The pseudo-first-order was in the range 0.98–0.99 (Table 5.4). This suggests that the pseudo-first-order kinetic model was the best fit to the observed CP data. For example, the degradation of 4-CP concentration at various initial 4-CP concentrations is shown in Figure 5.6. The data at various initial 4-CP concentrations with a fixed excess permanganate dosage (1.5 mM) exhibits pseudo-first-order kinetic behaviour with $r^2 > 0.99$.

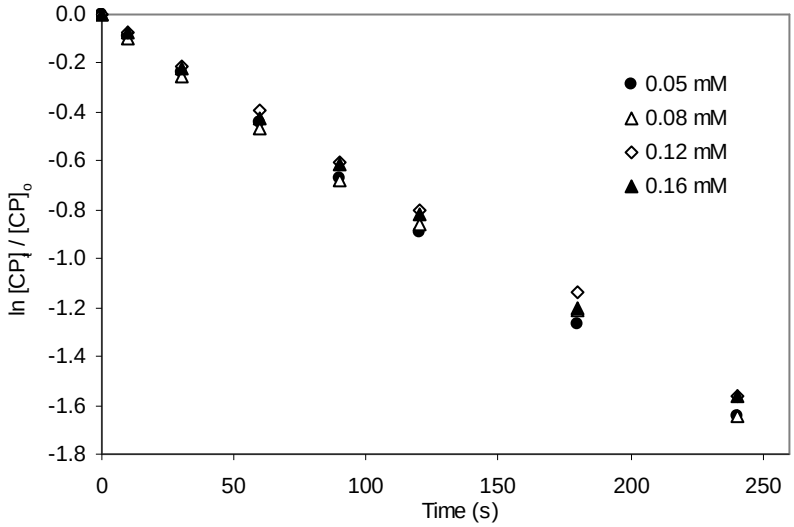

Figure 5.6 Oxidation fit curves of 4-CP at various initial 4-CP concentration with fixed $KMnO_4$: $[4\text{-CP}]_o$ ~ (0.05–0.16 mM), $[MnO_4^-]$ ~ 1.5 mM, I ~ 0.02 M, Initial pH 7.0 (22 °C)

The pseudo-first-order rate was not changed significantly for 4-CP (6.52–6.99) × 10^{-3} s^{-1} at various initial 4-CP concentrations (0.05–0.16 mM) with fixed excess permanganate (1.5 mM), indicating that the oxidation rate of 4-CP has little effect with the various initial 4-CP concentrations. In the same way, the pseudo-first-order rate was almost constant for 2-CP, 3-CP, 2,4-DCP, 2,6-DCP and 2,4,6-TCP at various initial CP

concentrations (0.04–0.24 mM) with excess permanganate as shown in Table 5.4 and Figures A16–A20 in Appendix A.

Table 5.4 Rate constants for the oxidation of chlorophenols (CP) with fixed concentrations of $KMnO_4$ solutions: I ~ 0.02 M, Initial pH 7.0 (22 °C)

$[CP]_o$ ($\times 10^{-3}$ M)	$[KMnO_4]_o$ ($\times 10^{-3}$ M)	r^2	$^a k_1$ ($\times 10^{-3}$ s^{-1})	$^b k_2$ (M^{-1} s^{-1})	$^c k_2$ (M^{-1} s^{-1})
2-CP (~0.08)	1.2	0.996	19.0 ± 0.008	15.80	15.7 ± 0.089
2-CP (~0.11)	1.2	0.998	18.9 ± 0.039	15.75	
2-CP (~0.16)	1.2	0.996	18.7 ± 0.215	15.58	
2-CP (~0.20)	1.2	0.998	18.8 ± 0.107	15.67	
3-CP (~0.05)	1.5	0.997	1.45 ± 0.020	0.97	0.95± 0.016
3-CP (~0.08)	1.5	0.999	1.43 ± 0.003	0.95	
3-CP (~0.13)	1.5	0.998	1.40 ± 0.004	0.93	
3-CP (0.16)	1.5	0.998	1.44 ± 0.003	0.96	
4-CP (~0.05)	1.5	0.997	6.99 ± 0.066	4.66	4.52 ± 0.150
4-CP (~0.08)	1.5	0.996	6.97 ± 0.077	4.65	
4-CP (~0.12)	1.5	0.998	6.52 ± 0.021	4.35	
4-CP (~0.16)	1.5	0.998	6.60 ± 0.141	4.40	
2,4-DCP (~0.05)	1.5	0.997	7.04 ± 0.035	4.69	4.67± 0.050
2,4-DCP (~0.08)	1.5	0.996	7.10 ± 0.033	4.73	
2,4-DCP (~0.12)	1.5	0.995	7.0 ± 0.067	4.67	
2,4-DCP (~0.16)	1.5	0.996	6.9 ± 0.054	4.60	
2,6-DCP (~0.08)	1.2	0.996	18.2 ± 0.045	15.17	15.21± 0.238
2,6-DCP (~0.12)	1.2	0.987	18.1 ± 0.062	15.08	
2,6-DCP (~0.16)	1.2	0.998	18.0 ± 0.450	15.00	
2,6-DCP (~0.24)	1.2	0.997	17.5 ± 0.001	14.58	
2,4,6-TCP (~0.04)	1.2	0.996	22.64 ± 0.037	18.87	18.86 ± 0.097
2,4,6-TCP (~0.06)	1.2	0.996	22.74 ± 0.080	18.95	
2,4,6-TCP (~0.08)	1.2	0.993	22.71 ± 0.157	18.91	
2,4,6-TCP (~0.10)	1.2	0.999	22.45 ± 0.205	18.71	

[a] k_1 (pseudo-first-order rate constant) = the mean value ± 95% confidence interval.
[b] k_2 = second-order rate constant is calculated by $k_2 = k_1/[MnO_4^-]_o$ using the mean k_1 value
[c] k_2 (second-order rate constant) = the mean value ± 95% confidence interval

The second-order rate constant (k_2) can also be obtained using at various initial CP concentrations with fixed $KMnO_4$. A plot of ln $[CP]_t$ / $[CP]_o$ vs. time gives the pseudo-

first-order constant (k_1) in the range 1.40–22.74 s^{-1} and $r^2 \geq 0.98$ (Table 5.4). Dividing the mean value of pseudo-first-order constant (k_1) by the fixed $KMnO_4$ concentration the second-order rate constants are within the range 0.93–18.95 $M^{-1} s^{-1}$.

The second-order rate constants (k_2) (Table 5.3 and 5.4) for the oxidation of CP and $KMnO_4$ at 22 °C and initial pH 7 are comparable to ~8–20 $M^{-1} s^{-1}$ obtained by He et al. (2010) at much lower concentrations of $KMnO_4$ and CP than those used in this study. The second-order-rate constant for 2,4,6-TCP (17–21 $M^{-1} s^{-1}$) at pH 7.6 with permanganate found by Bastos et al. (2008) is also comparable to this study. It is noted that our second-order rate constant was lower for 2-CP, 3-CP, 2,4-DCP and 2,4,6-TCP than the rate constant of 2-CP (74 $M^{-1} s^{-1}$), 3-CP (13.4 $M^{-1} s^{-1}$), 2,4-DCP (142 $M^{-1} s^{-1}$) and 2,4,6-TCP (120 $M^{-1} s^{-1}$) determined by Waldemer and Tratynek (2006). However, Waldemer and Tratynek (2006) obtained second-order rate constant (k_2) from pseudo-first-order conditions by measuring decreasing concentration of permanganate in a continuous system with excess chlorophenols in phosphate buffered system. But this study obtained second-order rate constant (k_2) by measuring decreasing concentrations of chlorophenols with excess permanganate in un-buffered system. Jiang et al. (2009) also found that the second-order rate constant for 2,4-dichlorophenol (45 $M^{-1} s^{-1}$) at pH 7 in 50 mM phosphate buffer was much higher than without phosphate buffer (19 $M^{-1} s^{-1}$). The second-order rate constant values for 2-CP (10.8 $M^{-1} s^{-1}$) and 2,4-DCP (2.44 $M^{-1} s^{-1}$) determined by Lee and Sebastian (1981) in alkaline conditions are close to this study. Our second-order reaction sequences are 2,4,6-TCP > 2-CP ~2,6-DCP > 2,4-DCP ~ 4-CP > 3-CP and are similar to those of He et al. (2010) and Waldemer and Tratnyek (2006) but differ from Zhang et al. (2003). The reactivity of chlorophenol depends on its structure. The position of chlorine in the phenolic ring can influence the reactivity of

chlorophenols towards $KMnO_4$ oxidation by inductive and resonance effects (Deborde and Von Gunten, 2008). Also the presence of chlorine in the phenolic ring and its interactions with the hydroxyl groups influences the oxidation kinetics of chlorophenols with $KMnO_4$ (Han et al., 2004).

5.3 Reactivity of chlorophenols

Lee and Sebastian (1981) mentioned that oxidation is initiated by transfer of an electron from the phenolate ion to permanganate as in equation 5.11.

$$PhO^- + MnO_4^- \longrightarrow PhO^{\cdot} + MnO_4^{2-} \qquad (5.11)$$

Han et al. (2004) mentioned that the acidity of chlorophenol is a measure of its ability to release a proton from the hydroxyl group to water by its lone pair attraction through the formation of hydrogen bonding. Consequently, the hydroxyl bond length is increased while the hydroxyl bond strength is decreased. Also, they mentioned that all ortho isomers (2-CP, 0.9668 Å) have relatively longer O-H bond lengths and lower pK_a values whereas meta (3-CP, 0.9630 Å) or para (4-CP, 0.9628 Å) isomers have shorter O-H bond lengths and higher pK_a values (Table 3.3). The longer O-H bond length enhances the release of the proton from the hydroxyl hydrogen and has increased the acidity of the chlorophenols. The induction of chlorine in an ortho position is most effective due the presence of intramolecular hydrogen bonding in the syn conformers (Figure 5.7) of an ortho chlorophenol. Consequently the acidities of all ortho chlorophenols are stronger than other chlorophenols.

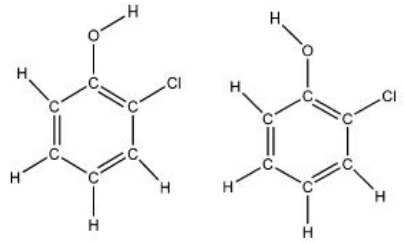

2-CP syn conformer 2-CP anti conformer

Figure 5.7 Conformer of 2-CP

Therefore, Han et al. (2005) suggest that the acidity of ortho chlorophenol is higher than corresponding para or meta to ortho position for mono chlorophenol. The complexes with di-ortho substitution, the larger deviation of hydrogen bond angles (148^0) were observed which may be due to the repulsion from the ortho chlorine next to the water. This reflects di-ortho substitutions (2,6-DCP) have different properties from those with the mono-ortho substitution (2-CP). This causes the decrease in binding energy with di-ortho substitution which influences the steric hindrance for the hydrogen bonding in the complexes (Han et al., 2005). This might be the reason for slightly lower acidity in the di-ortho chlorophenol. This is the good agreement with our results where we found slightly higher rate constant for 2-CP than 2, 6-DCP.

The 3-CP is shown to be most resistant to oxidation (Table 5.3 and 5.4). The high deficiency of electrons in the carbon-carbon double bond, induced by meta-chloro substituent in 3-CP reduces the oxidation rate. The fact the meta-chloro substitution is unable to participate in π-resonance interactions and their effect on reactivity is dominated by their σ-electron-acceptor only (Ulrich and Stone, 1989). Therefore, 3-CP oxidation is slow and its rate constant is small compared to others. The higher reactivity of 4-CP and 2,4-DCP was found than 3-CP which may be due to the π-resonance

interaction through electron donating conjugative effect which is partially counteracted with the σ-electron withdrawing effect (Stone, 1987).

A higher reactivity of mono-ortho (2-CP) and di-ortho (2,6-DCP) degradation compared to other chlorophenol (eg. 4-CP and 2,4-DCP) was found (Table 5.3, 5.4). It indicates that a significant steric effect was evident in the reaction by the interaction of electron-withdrawing chlorine and hydroxyl group. Previous studies reported that permanganate first attacked on phenolate anion during the oxidation of potassium permanganate and chlorophenols (Zhang et al. 2003; Lee and Sebastian, 1981). So formation of phenolate ion accelerates the oxidation process. Han et al. (2004) suggested that acidities of all ortho chlorophenol are stronger than other chlorophenols. It means availability of PhO^- anion from all ortho chlorophenol is quicker than other chlorophenol (4-CP and 2,4-DCP). Consequently, higher oxidation rates for all ortho chlorophenol with permanganate may be applicable. Similarly, higher rate constants for mono-ortho (2-CP) and di-ortho (2,6-DCP) were obtained in this study and are consistent with this molecular theory. It should be noted that the acidity of 2,6-DCP may influence due to steric effect whereas the acidity of 4-CP and 2,4-DCP is influenced by the resonance of the phenolate anion and the steric effect of chlorine (Han et al., 2004). Bastos et al. (2008) also found the difference in rate between 2,4-diboromophenol (2,4-DBP) and 2,6-dibromophenol (2,6-DBP), where 2,6-DBP degraded three times as fast as 2,4-DBP during oxidation with potassium permanganate. They mention that, this is due to withdrawing of electron density around the phenoxy ion. These results are comparable with our work where the rate of 2,6-DCP is faster than that of 2,4-DCP and chlorine is the electron-withdrawing group. This is opposite to the order that was found by Zhang et al. (2003). They reported that the rate of oxidation for 2,4-DCP is faster than the rate

of oxidation of 2,6-DCP. The pK_a also affects the rate of reaction as the initial pH 7.0 used in this study is the closer value of ionization constant i.e. pK_a (Table 3.3) for 2,6-dichlorophenol and 2,4,6-trichlorophenol which may explain the rapid rate of reaction. In summary, the oxidation kinetics may be influenced by the interaction of electron-withdrawing chlorine and hydroxyl group, the effect of pK_a, the resonance of the phenolic anion, the steric effect of chlorine and the acidities of chlorophenols (Han et al., 2004).

5.4 Effect of water quality

Few published studies on the effect of water quality on CP degradation by $KMnO_4$ were found. The effects of ionic strength (0.02–0.2 M) and pH (5.5–8.5) on the oxidation of 4-CP by permanganate were investigated. These ionic strengths cover most of the natural subsurface groundwater (Huang et al., 2002).

5.4.1 Effect of ionic strength

Ionic strength ranges from 0.02 to 0.2 M using KCl were studied for 4-CP to see the effect of ionic strength on oxidation rate. The r^2 values for zero-order were in the range 0.89–0.92 and for second-order were in the range 0.87–0.94 (data not shown). The result indicated that oxidation studies with 4-CP by $KMnO_4$ at various ionic strength are best fitted with a pseudo-first-order model ($r^2 > 0.99$). The second-order rate constant was calculated using equation 5.4 and little effect of various ranges of concentration of ionic strength were found (Figure 5.8 and Table 5.5).

Table 5.5 Rate constants for 4-CP (~0.16 mM) oxidation by $KMnO_4$ (1.5 mM): I~0.02–0.2 M, Initial pH 7.0 (22 °C)

Ionic Strength (M)	[a]k_1 ($\times 10^{-3}$ s^{-1})	r^2	[b]k_2 (M^{-1} s^{-1})
0.0[c]	6.3 ± 0.031	0.996	4.2
0.02	6.6 ± 0.141	0.998	4.4
0.05	6.6± 0.021	0.998	4.4
0.15	6.5 ± 0.041	0.997	4.3
0.20	6.2± 0.010	0.999	4.1

[a]k_1 (Pseudo-first-order rate constant) = the mean value ± 95% confidence interval
[b]k_2 (second-order rate constant) is determined from $k_2 = k_1 / [MnO_4^-]_o$ using the mean of k_1 values
[c]Oxidation of CP by $KMnO_4$ in Milli-Q water

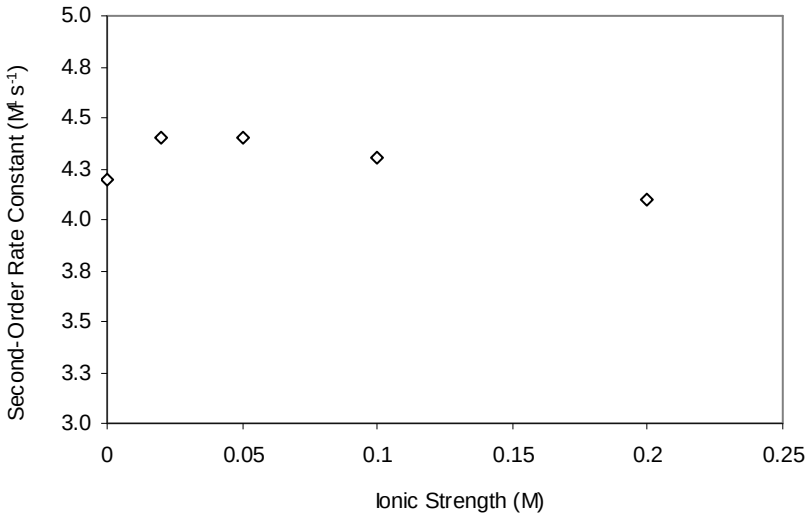

Figure 5.8 Oxidation of 4-CP by $KMnO_4$ in Milli-Q water and in solution at pH 7.0 with different ionic strength. 4-CP ~0.16 mM, $[MnO_4^-]$ ~1.5 mM, I ~0.02–0.2 M, Initial pH 7.0 (22 °C)

5.4.2 Effect of pH

The chosen pH ranges were below the pK_a = 9.1–9.4 (Czaplicka, 2004) for 4-CP. The r^2 values for zero-order were in the range 0.83–0.93 and for second-order were in the range 0.88–0.94 (data not shown). The results best fit with a pseudo-first-order model ($r^2 > 0.98$) and showed little effect due to variations of pH (Figure 5.9). The observed

pseudo-first-order rate and calculated second-order-rate constants are shown in Table 5.6.

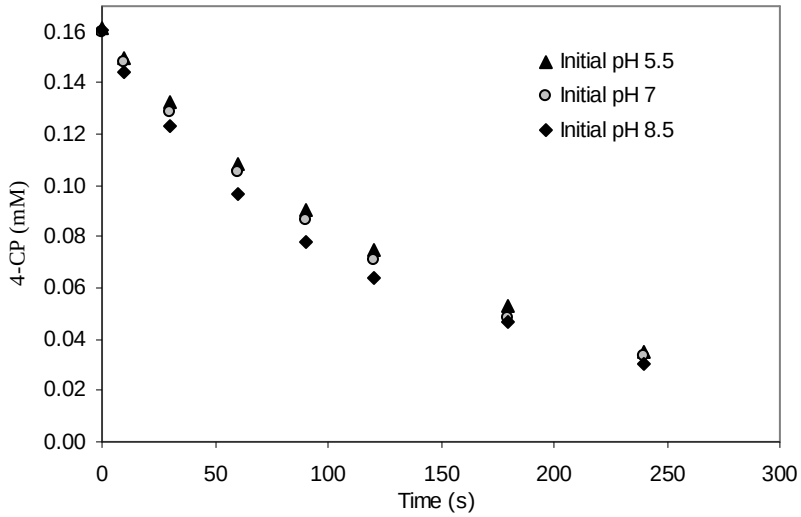

Figure 5.9 Effect of initial pH on 4-CP (~0.16 mM) degradation by $KMnO_4$ (1.5 mM), I ~0.02 M (22 °C)

Table 5.6 Rate constants for 4-CP (~0.16 mM) oxidation by $KMnO_4$ (1.5 mM) and at various initial pH (5.5–8.5): I ~0.02 M (22 °C)

Initial pH	[a]k_1 ($\times 10^{-3}$ s^{-1})	r^2	[b]k_2 (M^{-1} s^{-1})
5.5	6.4 ± 0.062	0.999	4.3
7.0	6.6 ± 0.141	0.998	4.4
8.5	7.2 ± 0.083	0.989	4.8

[a]k_1 (Pseudo-first-order rate constant) = the mean value ± 95% confidence interval
[b]k_2 (second-order rate constant) is determined from $k_2 = k_1 / [MnO_4^-]_o$ using the mean of k_1 values

Therefore, 4-CP oxidation with permanganate is relatively insensitive to pH within the range 5.5 to 8.5. Xiao et al. (2010) found little impact on the rate of 2,4-DCP degradation during permanganate assisted ozonation over an initial pH range of 5.5 to 8.5.

5.5 Conclusion

This work shows that chlorophenols can be rapidly degraded by permanganate in aqueous solution. The reaction of CP with permanganate is second-order in total and first-order individually with respect to CP and $KMnO_4$. The rate of reaction increases with the concentration of permanganate within this investigation range, confirming the independence of the second-order rate constant from the concentration of permanganate. The initial concentration of CP was found to have no significant affect on the rate constant determination for pseudo-first-order kinetic model with fixed excess permanganate concentration. The introduction of substituted chlorine is responsible for stabilizing the phenolate anion and therefore influences the acidity of the chlorophenol and hence reactivity. Further work on the effect of water quality (ionic strength, pH) should be undertaken across a range of CP. Also, the degradation by-product of CPs with permanganate should be quantified. The findings of this study can be valuable in designing in-situ treatment of chlorophenol-contaminated soil and groundwater.

CHAPTER 6

Batch chlorophenol sorption-desorption studies

6 Batch chlorophenol sorption-desorption studies

6.1 Introduction

Sorption is a widely used process for the removal of inorganic and organic contaminants from waters and wastewaters. It has been found that chlorophenol can be strongly sorbed by granular activated carbon but it can be expensive for large subsurface barriers. There is a growing interest in using low-cost sorbents (filter coal, pine and hardwood). Also, they do not require a major pre-treatment step before application. This study focused on both kinetics and equilibrium characteristics of chlorophenol absorption on FC, pine and HW and comparison with GAC.

6.2 Results and discussion

6.2.1 Sorption kinetics

A kinetic study was performed to measure the uptake rates of chlorophenols (2-CP, 4-CP and 2,4-DCP) and determine their equilibrium sorption time. Sorption is indicated by the decreasing concentration of sorbate in liquid phase. To reach equilibrium the contact time 3 days (pine, HW), 6 days (GAC) and 11 days (FC) were considered. These times are similar to other chlorophenol studies for GAC (Nelson and Yang, 1995) and wood pulp (Severtson and Banerjee, 1996).

Batch sorption kinetics results show that the sorption of chlorophenols onto GAC, pine and HW comprised two stages with an initial stage of rapid sorption with at least 50% of the final uptake achieved within 3 h followed by a slower second stage (Figures 6.1–

6.3). In contrast, FC achieved only 10% of the final uptake after 3 h (Figure 6.4). The amount of chlorophenol sorption, q_t (mg g^{-1}) at time t was calculated by equation 2.1.

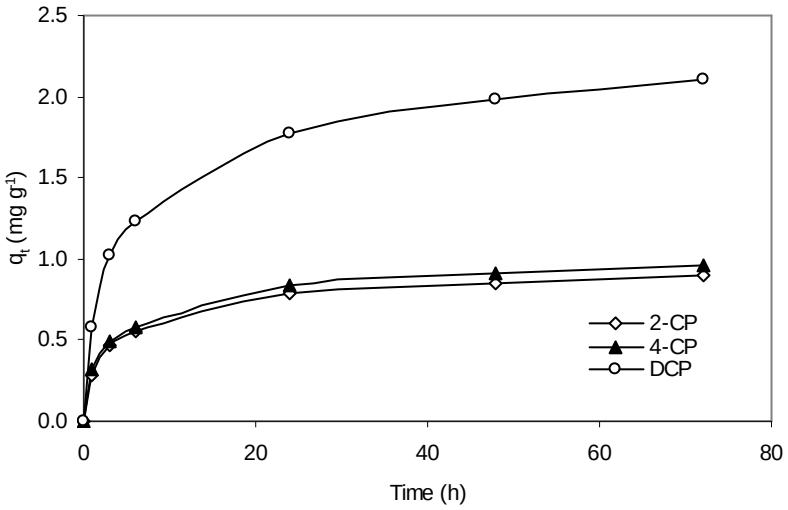

Figure 6.1 Kinetics of sorption of chlorophenols on pine

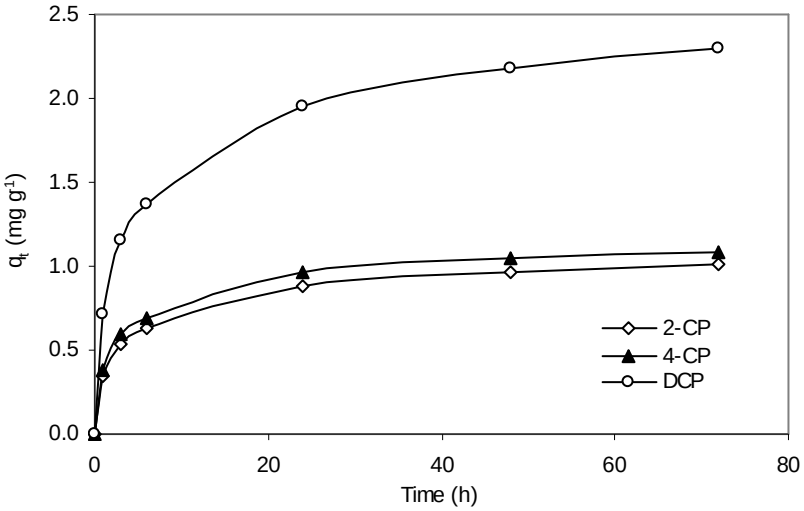

Figure 6.2 Kinetics of sorption of chlorophenols on HW

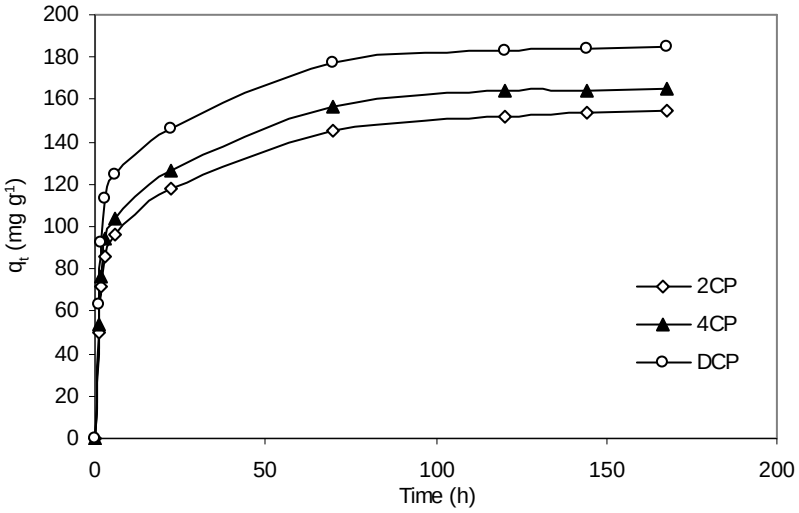

Figure 6.3 Kinetics of sorption of chlorophenols on GAC

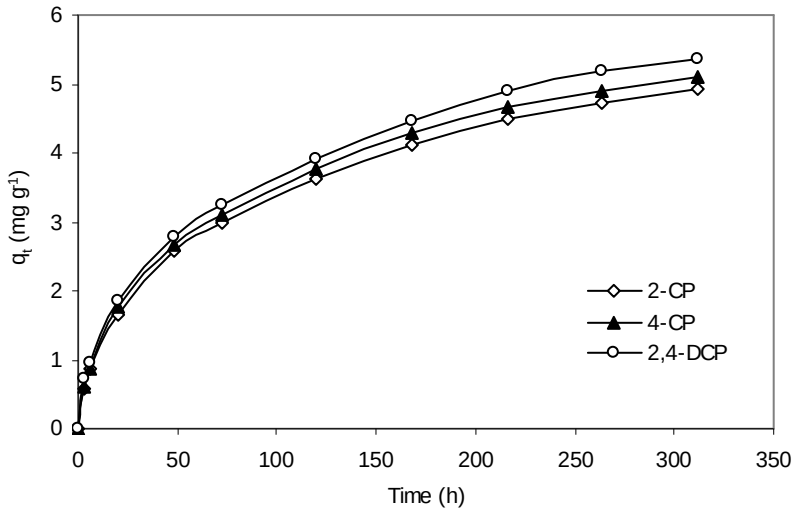

Figure 6.4 Kinetics of sorption of chlorophenols on FC

The initial rapid uptake stage is due to the availability of reaction sites on the sorbents. As a result this creates strong concentration gradients between the sorbate and sorbent in a heterogeneous system. But later on, after gradual occupancy of these sites the rate

of sorption becomes relatively slow. Three kinetic models pseudo-first-order (equation 2.10), pseudo-second-order (equation 2.11) and intraparticle diffusion model (equation 2.12) were considered to represent the sorption processes and rate-controlling step. The calculated kinetic parameters (Tables 6.1 and 6.2) show that there was a better fit to the FC, pine and HW experimental data compared with the GAC data. All sorbents had a marginally better fit to a pseudo-second-order model compared to the pseudo-first-order model. It is well documented that pseudo-second-order kinetic models have been successfully applied to many sorption systems (Gerente et al., 2007; Ho and McKay, 1999).

Table 6.1 Pseudo-first-order parameters for the sorption of chlorophenols on sorbents

Sorbents	Particle size (mm)	Sorbate	k_1 (h^{-1})	q_e (calc) (mg g^{-1})	r^2	SSE
GAC	0.6	2-CP	0.334	133	0.863	16.2
GAC	0.6	4-CP	0.332	153	0.881	14.0
GAC	0.6	2,4-DCP	0.377	174	0.894	14.2
GAC	1.18	2-CP	0.304	140	0.870	13.9
GAC	1.18	4-CP	0.312	144	0.869	15.8
GAC	1.18	2,4-DCP	0.355	169	0.883	15.0
GAC	2.36	2-CP	0.293	134	0.849	14.6
GAC	2.36	4-CP	0.311	139	0.864	16.0
GAC	2.36	2,4-DCP	0.344	165	0.884	14.7
FC	0.6	2-CP	0.019	4.8	0.977	0.31
FC	0.6	4-CP	0.019	5.0	0.981	0.32
FC	0.6	2,4-DCP	0.022	5.1	0.975	0.37
FC	1.18	2-CP	0.017	4.5	0.982	0.27
FC	1.18	4-CP	0.018	4.6	0.979	0.29
FC	1.18	2,4-DCP	0.017	4.9	0.979	0.33
FC	2.36	2-CP	0.016	4.2	0.982	0.26
FC	2.36	4-CP	0.017	4.4	0.980	0.29
FC	2.36	2,4-DCP	0.019	4.6	0.973	0.34
Pine	1.18	2-CP	0.24	0.84	0.935	0.07
Pine	1.18	4-CP	0.247	0.89	0.926	0.07
Pine	1.18	2,4-DCP	0.214	1.95	0.943	0.15
Pine	2.36	2-CP	0.220	0.83	0.953	0.06
Pine	2.36	4-CP	0.255	0.87	0.924	0.07
Pine	2.36	2,4-DCP	0.208	1.90	0.945	0.15
Pine	4.75	2-CP	0.211	0.81	0.951	0.06
Pine	4.75	4-CP	0.231	0.87	0.939	0.07
Pine	4.75	2,4-DCP	0.196	1.88	0.945	0.15
HW	1.18	2-CP	0.253	0.94	0.917	0.08
HW	1.18	4-CP	0.267	1.01	0.917	0.09
HW	1.18	2,4-DCP	0.234	2.12	0.925	0.18

Table 6.2 Pseudo-second-order parameters for the sorption of chlorophenols on sorbents

Sorbents	Particle size (mm)	Sorbate	k_2 (g mg^{-1} h^{-1})	q_e (calc) (mg g^{-1})	r^2	SSE
GAC	0.6	2-CP	0.0033	150	0.947	8.3
GAC	0.6	4-CP	0.0029	162	0.960	7.9
GAC	0.6	2,4-DCP	0.0030	183	0.967	7.7
GAC	1.18	2-CP	0.0028	148	0.953	8.2
GAC	1.18	4-CP	0.0027	159	0.952	8.8
GAC	1.18	2,4-DCP	0.0028	179	0.960	8.4
GAC	2.36	2-CP	0.0028	142	0.938	9.1
GAC	2.36	4-CP	0.0026	157	0.952	8.7
GAC	2.36	2,4-DCP	0.0028	175	0.960	8.4
FC	0.6	2-CP	0.0035	5.8	0.990	0.20
FC	0.6	4-CP	0.0037	5.9	0.989	0.21
FC	0.6	2,4-DCP	0.0048	6.0	0.986	0.24
FC	1.18	2-CP	0.0036	5.4	0.991	0.18
FC	1.18	4-CP	0.0035	5.6	0.990	0.19
FC	1.18	2,4-DCP	0.0034	5.9	0.987	0.23
FC	2.36	2-CP	0.0036	5.1	0.989	0.18
FC	2.36	4-CP	0.0037	5.3	0.988	0.20
FC	2.36	2,4-DCP	0.0041	5.5	0.984	0.23
Pine	1.18	2-CP	0.3723	0.90	0.979	0.04
Pine	1.18	4-CP	0.3721	0.95	0.973	0.04
Pine	1.18	2,4-DCP	0.1348	2.12	0.982	0.08
Pine	2.36	2-CP	0.3306	0.90	0.987	0.03
Pine	2.36	4-CP	0.3691	0.94	0.975	0.04
Pine	2.36	2,4-DCP	0.1318	2.08	0.982	0.08
Pine	4.75	2-CP	0.3167	0.89	0.986	0.03
Pine	4.75	4-CP	0.3442	0.94	0.979	0.04
Pine	4.75	2,4-DCP	0.1246	2.06	0.980	0.08
HW	1.18	2-CP	0.3606	1.00	0.969	0.05
HW	1.18	4-CP	0.3699	1.10	0.969	0.05
HW	1.18	2,4-DCP	0.1417	2.29	0.972	0.10

6.2.2 Analysis of uptake mechanism

The kinetic results (Figures 6.1–6.4) can be used to investigate the sorption mechanism. One approach to gaining an insight into chlorophenol sorption is to examine the sorption process. Rate controlling mechanisms can include (Zogorski et al., 1976; Koumanova et al., 2003; Gerente et al., 2007);

- Film diffusion: Diffusion/mass transport across the liquid film surrounding the particle.
- Intra-particle diffusion: Internal diffusion/mass transport within the particle boundary.
- Sorption onto the sites.

At any particular time, sorption kinetics will be controlled by the slower process of any of these mechanisms. Often sorption onto the sites is assumed to be rapid relative to the diffusion mechanisms. An appreciation of which diffusion processes controls sorption at any particular time can be obtained by applying the intra-particle diffusion model to the experimental data. Numerous studies on sorption show that initial curved portions of the intra-particle diffusion plot suggest film diffusion processes while linear portions suggest intra-particle diffusion (Gerente et al., 2007). A third stage may occur where intra-particle diffusion decreases due to a low solute concentration and the sorption rate plateaus. In reality these various stages may actually be a gradual transition. Weber and Morris (1963) reported if a linear relation is obtained and that line passes though the origin then intra-particle diffusion is the rate controlling step. However the rate controlling mechanism may change during the sorption process.

There appear to be three distinct patterns within the intra-particle diffusion plots (Figures 6.5 to 6.7). Both the pine and hardwood have relatively rapid initial uptake controlled by film diffusion followed by a curvi-linear stage which gradually goes to plateaus. The GAC also has a relatively rapid initial uptake but has a number of distinct linear sections before reaching a plateau. Other studies have attributed multiple linear sections to the diffusion of the solute into macropores, transitional pores and micropores (Koumanova et al., 2003; Dubinin, 1967). The diffusion plot for filter coal is nearly linear (Figure 6.8) with a line passing near the origin (r^2 = 0.98). This suggests that intra-particle diffusion of chlorophenol in filter coal was solely the rate controlling step over a long contact time period. The lack of any significant initial uptake is evident in that only 10% of the final chlorophenol uptake has occurred after 3 hours. Intra-particle diffusion is the only rate limiting mechanism for sorption onto coal contrasts with the other sorbents where film diffusion played a major role during early stages of the sorption process.

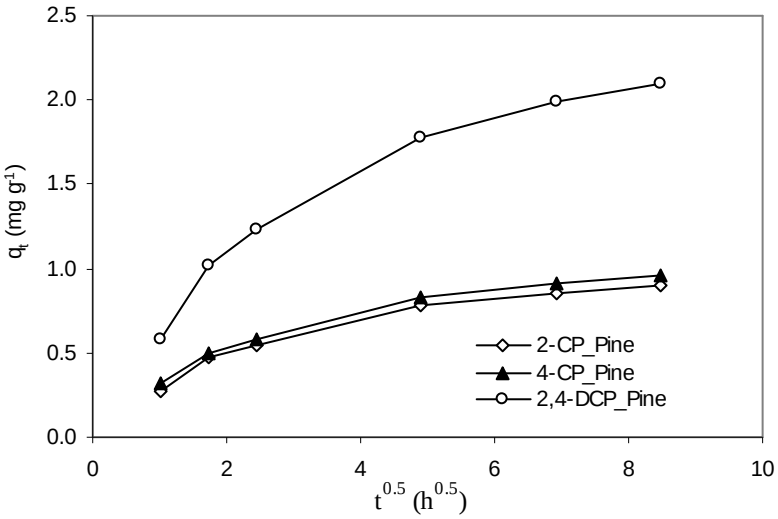

Figure 6.5 Chlorophenol uptake onto Pine

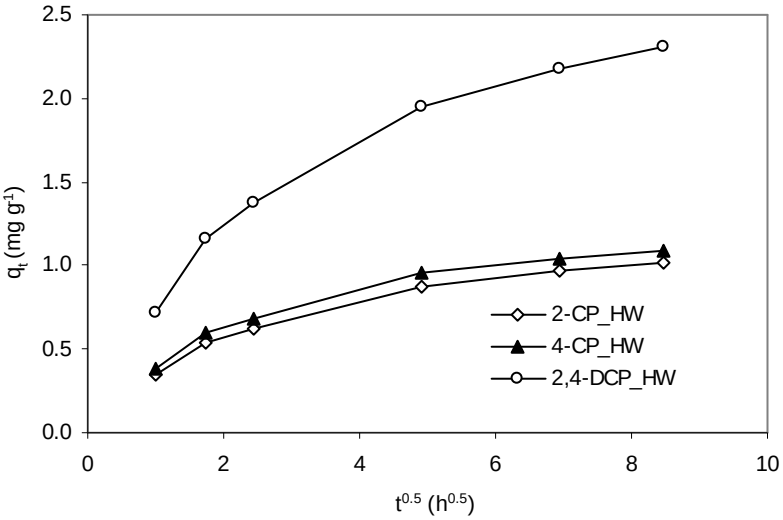

Figure 6.6 Chlorophenol uptake onto HW

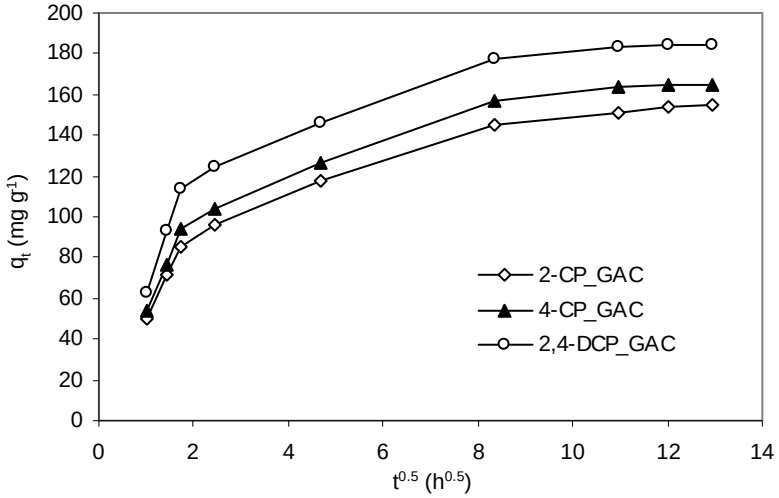

Figure 6.7 Chlorophenol uptake onto GAC

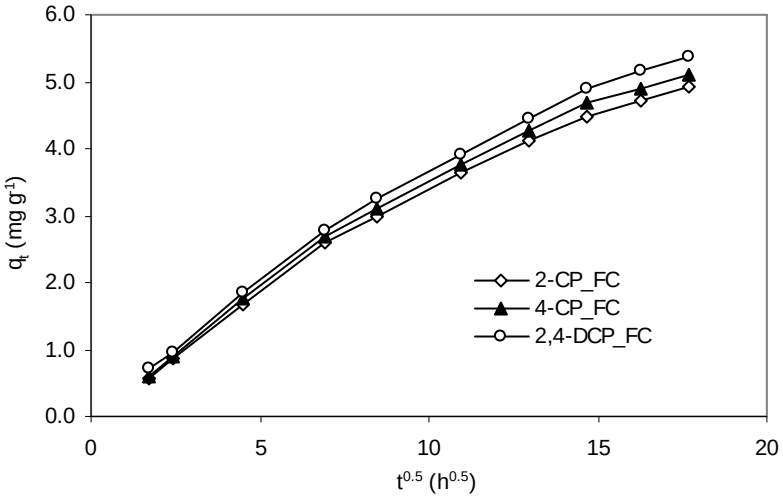

Figure 6.8 Chlorophenol uptake onto FC

6.2.3 Equilibrium sorption

Equilibrium sorption data provides the sorption capacity of the sorbents. Isotherm analysis is required to develop an equation which accurately represents these values. Isotherm equation parameters represent the surface properties and affinity of the sorbents and can be used to compare the sorption capacities of the sorbent for a particular sorbate. The amount of sorbed chlorophenol at equilibrium, q_e (mg g^{-1}) was calculated by equation 2.2.

6.2.3.1 Equilibrium sorption isotherm

A plot of equilibrium sorption isotherm curves for chlorophenol loading (q_e) against the residual concentration (C_e) of chlorophenol present in the solution after equilibrium is shown in Figures 6.9–6.11.

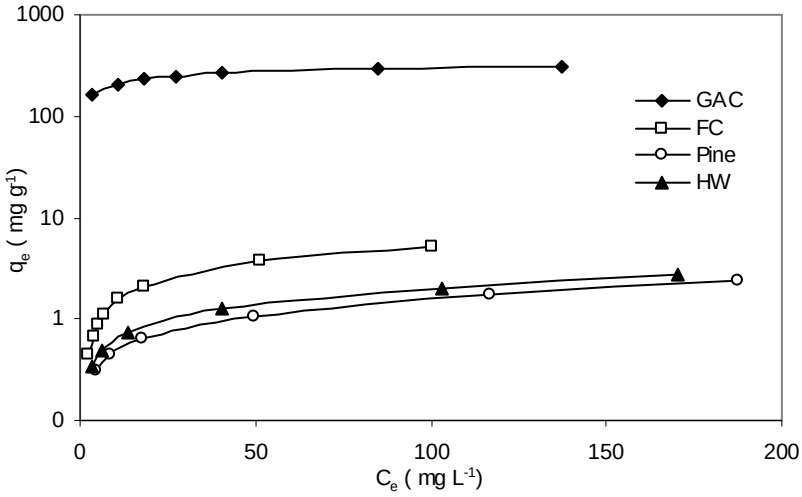

Figure 6.9 Equilibrium sorption isotherm for 2-CP onto the sorbents

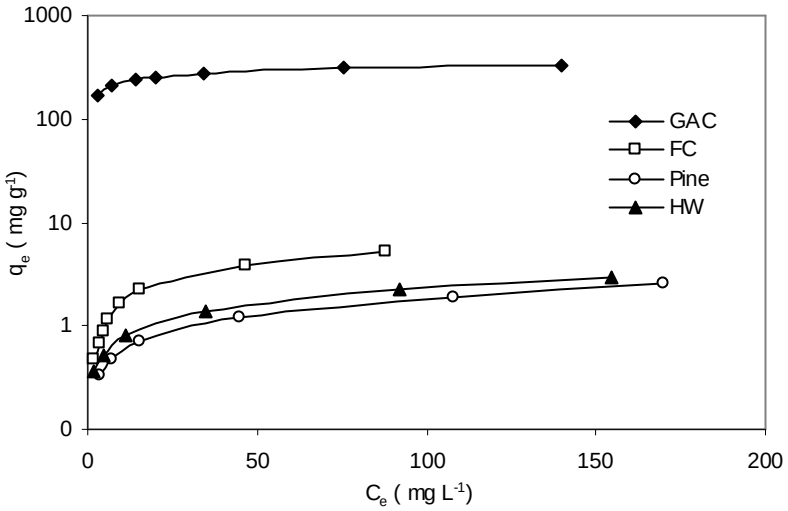

Figure 6.10 Equilibrium sorption isotherm for 4-CP onto the sorbents

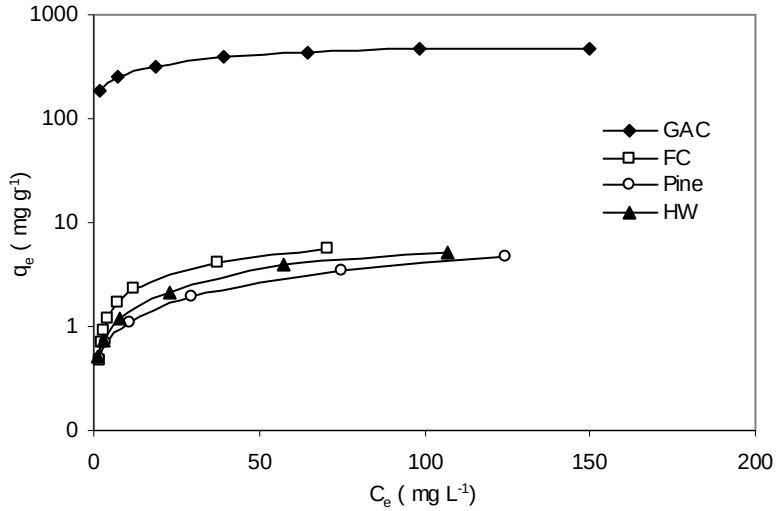

Figure 6.11 Equilibrium sorption isotherm for 2,4-DCP onto the sorbents

6.2.3.2 Equilibrium sorption isotherm model

The equilibrium sorption isotherm data was fitted to both Freundlich and Langmuir models (Figures 6.12–6.19, Tables 6.3 and 6.4).

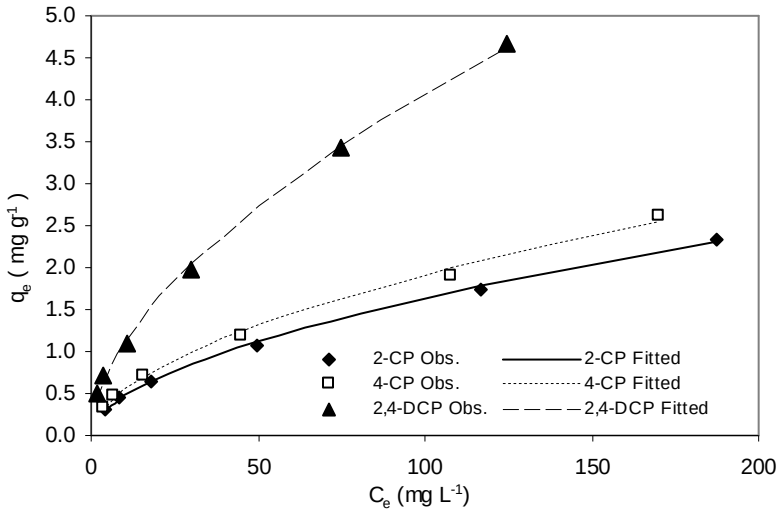

Figure 6.12 Prediction of Freundlich equilibrium sorption of chlorophenol onto Pine

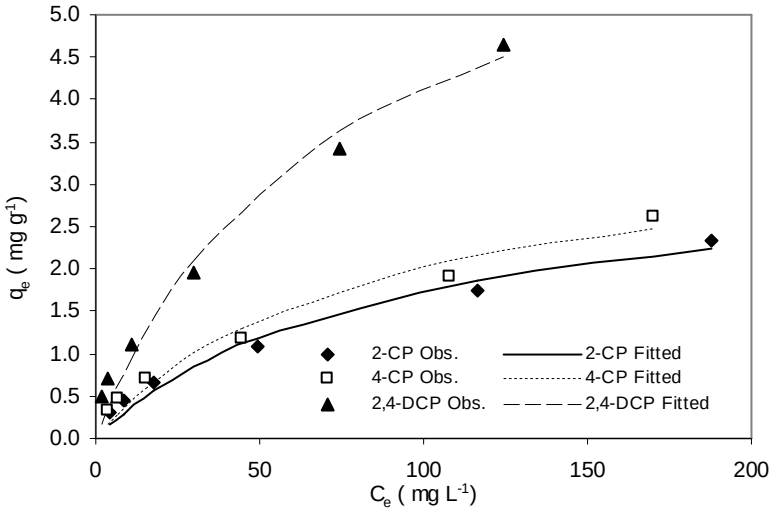

Figure 6.13 Prediction of Langmuir equilibrium sorption of chlorophenol onto Pine

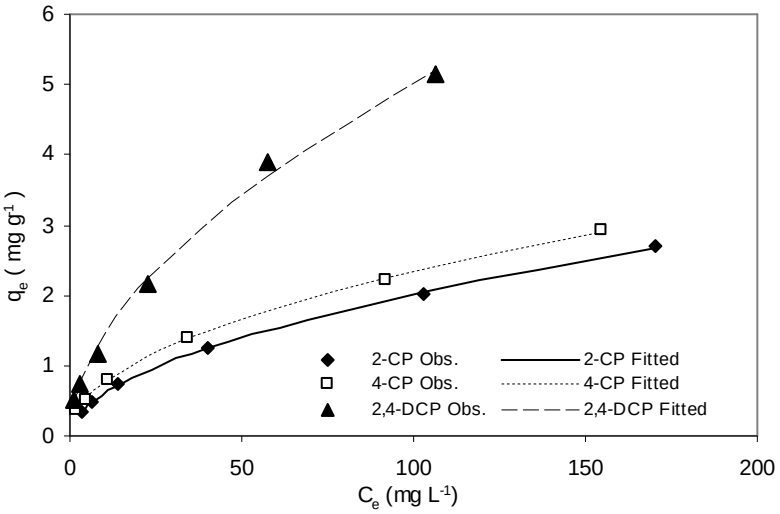

Figure 6.14 Prediction of Freundlich equilibrium sorption of chlorophenol onto HW

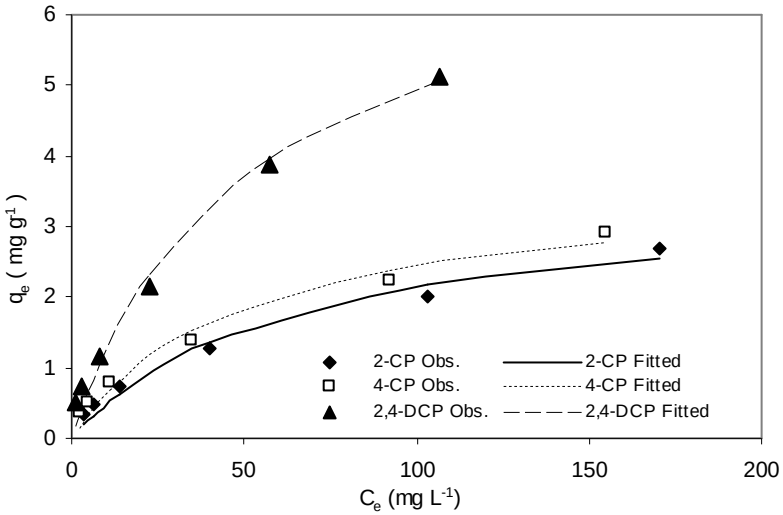

Figure 6.15 Prediction of Langmuir equilibrium sorption of chlorophenol onto HW

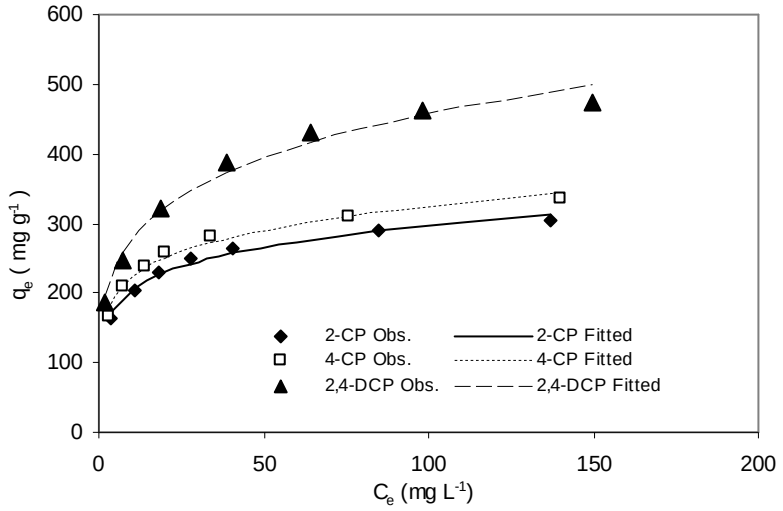

Figure 6.16 Prediction of Freundlich equilibrium sorption of chlorophenol onto GAC

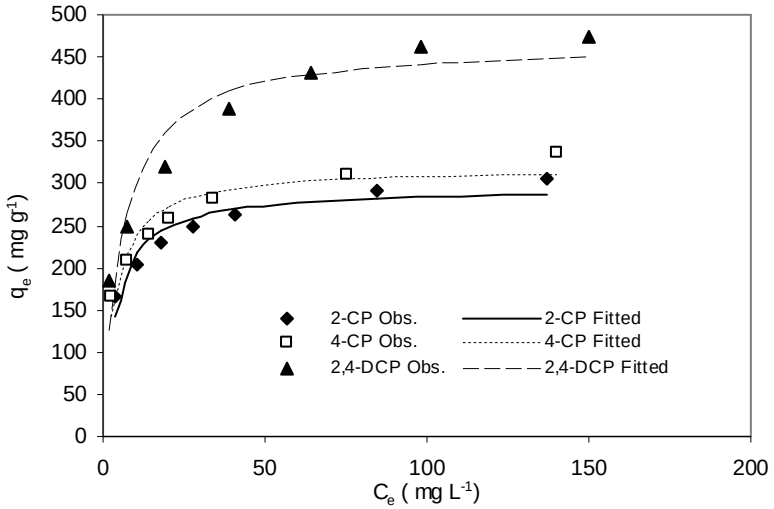

Figure 6.17 Prediction of Langmuir equilibrium sorption of chlorophenol onto GAC

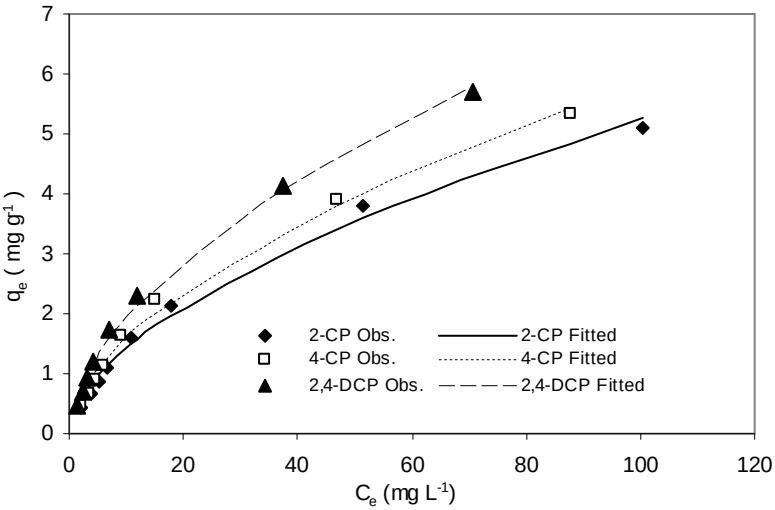

Figure 6.18 Prediction of Freundlich equilibrium sorption of chlorophenol onto FC

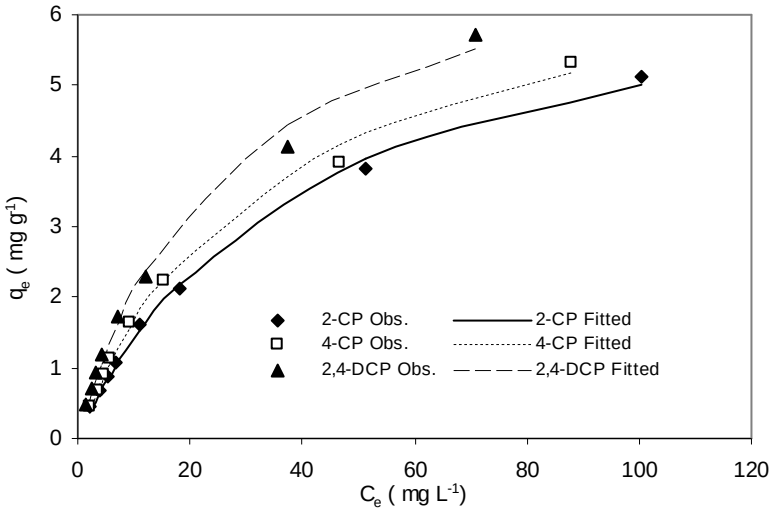

Figure 6.19 Prediction of Langmuir equilibrium sorption of chlorophenol onto FC

Table 6.3 Fitted sorption parameters from Freundlich isotherm

Sorbent	Sorbate	K_F	1/n	r^2	SSE
GAC	2-CP	141	0.162	0.983	6.0
GAC	4-CP	151	0.166	0.981	7.4
GAC	2,4-DCP	168	0.217	0.982	14.0
FC	2-CP	0.390	0.567	0.995	0.10
FC	4-CP	0.430	0.567	0.994	0.12
FC	2,4-DCP	0.530	0.560	0.994	0.13
Pine	2-CP	0.130	0.550	0.998	0.03
Pine	4-CP	0.150	0.550	0.996	0.05
Pine	2,4-DCP	0.290	0.570	0.998	0.07
HW	2-CP	0.180	0.525	0.999	0.02
HW	4-CP	0.240	0.494	1.000	0.02
HW	2,4-DCP	0.400	0.548	0.997	0.10

Table 6.4 Fitted sorption parameters from Langmuir isotherm

Sorbent	Sorbate	Q_m (mg g^{-1})	b (L mg^{-1})	r^2	SSE
GAC	2-CP	294	0.270	0.900	14.7
GAC	4-CP	319	0.288	0.906	16.5
GAC	2,4-DCP	467	0.182	0.904	31.8
FC	2-CP	7.0	0.025	0.992	0.14
FC	4-CP	7.2	0.030	0.993	0.13
FC	2,4-DCP	7.5	0.039	0.992	0.16
Pine	2-CP	3.2	0.012	0.969	0.13
Pine	4-CP	3.6	0.013	0.962	0.16
Pine	2,4-DCP	7.0	0.014	0.975	0.24
HW	2-CP	3.5	0.016	0.974	0.14
HW	4-CP	3.6	0.021	0.969	0.17
HW	2,4-DCP	7.4	0.020	0.983	0.22

The equilibrium sorption isotherm data was fitted to both Freundlich (Table 6.3) and Langmuir models (Table 6.4). The data from the equilibrium experiments show that both the calculated Freundlich and Langmuir models fitted the FC, pine and HW data better than the GAC data. The Freundlich model gave a marginally better fit than the Langmuir model. Another study (Colella et al., 1998) found a poor fit for sorption of same chlorophenols onto GAC using the Langmuir model**.**

6.2.4 Sorption capacity of different sorbents

The sorption capacities of the sorbents are indicated by the Langmuir constant Q_m and the Freundlich constant K_F. Another study using GAC found broadly similar values to this study for Q_m (303–370 mg g^{-1}) and K_F (58–129) with the same chlorophenols (Hamdaoui and Naffrechoux, 2007). It has been recognised the adsorption capacities of

GAC varies depending upon whether the carbon is wood, bituminous or lignite based (Colella et al., 1998; Sorial et al., 1993). In many cases the chemical nature of the surface functional groups dominates the influence of the pore size distribution on activated carbon (Dabrowski et al., 2005). Unfortunately there is little comparative data available for the other sorbents. The sorption capacities of the sorbents have a similar trend to the sorbent surface area with GAC (954 $m^2 g^{-1}$) >> FC (1.33 $m^2 g^{-1}$) > HW-pine (0.45–0.55 $m^2 g^{-1}$). However if sorption capacity per unit surface area is calculated, then the sorption capacity will be HW-pine (7.4–13.1 mg m^{-2}) > FC (5.3–5.6 mg m^{-2}) >> GAC (0.31–0.49 mg m^{-2}). This suggests that the wood sorbents has a much greater surface reactivity for the non-ionised chlorophenols than the other sorbents. This is consistent with results from phenol sorption onto coal and GAC (Polat et al., 2006). The sorption capacity ordering is found to be GAC > FC > HW > Pine (Figure 6.20).

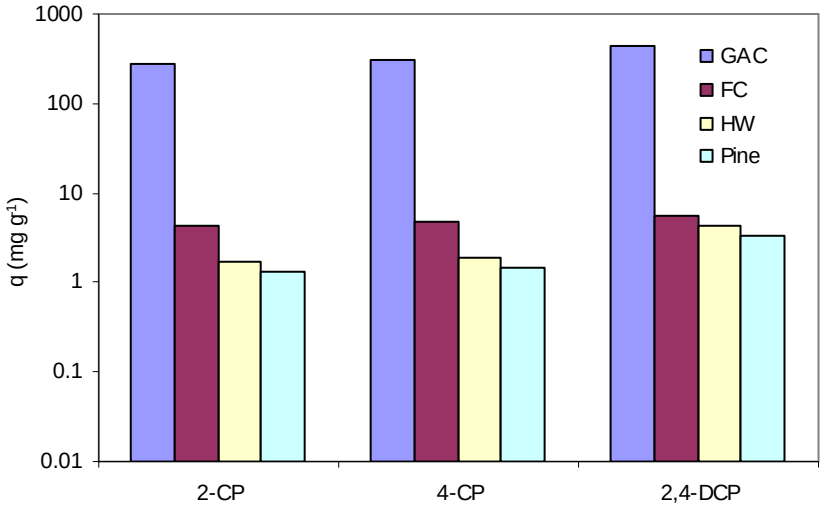

Figure 6.20 Sorption capacities at an equilibrium concentration of 70 mg L^{-1} for the chlorophenols using 1.18 mm sorbents

The magnitude of the exponent 1/n can give an indication on the favourability and capacity of the sorbent/sorbate system. Values $n > 1$ represents favourable sorption condition, with $1 < n < 10$ particularly beneficial (McKay et al., 1982). The GAC is a good sorbent for chlorophenols ($4.6 \leq n < 6.2$) while FC, HW and pine ($1.8 \leq n < 2.0$) are less beneficial (Table 6.3).

6.2.5 Effect of molecular size and pore structure

The pore size of the sorbents and the size of sorbate molecules should be considered for the sorption process. Sorption is dependent on the pore size distribution such as the number of micro-, meso- and macropores in the structure and the availability of pores of appropriate size. The calculated diameters of chlorophenols in this study were in the range of approximately 0.8–1nm (Jung et al., 2001). The values of average pore diameter of GAC, FC, pine and HW are higher (Table 3.1) than the calculated diameter of chlorophenol. It indicates that chlorophenol molecules can easily enter into the pores of these sorbents and sorb on the external surface.

6.2.6 Effect of benzene ring reactivity

The effect of benzene ring on sorption capacity was examined. The difference in sorption behaviour of chlorophenols is shown in Figures 6.1–6.4. The value of Q given in Table 6.4 indicates that the sorption capacity of 2-CP (0.02–2.3 mmol g^{-1}) and 4-CP (0.03–2.5 mmol g^{-1}) is lower than 2,4-DCP (0.04–2.9 mmol g^{-1}). Coughlin and Ezra (1968) indicated that the chlorophenols are sorbed to the surface of the sorbent through the interaction between π-electrons in the phenol ring and the π-electrons in the aromatic surface structure of the carbon. They mentioned that phenol sorption decreases

with increasing loading of oxygen complexes to the carbon due to the complex formation. Mattson et al. (1969) reported that the phenol sorption on carbon occurs by a donor-acceptor complex mechanism. In this mechanism, carbonyl oxygen group on the carbon surface acts as the electron donor and the aromatic ring of phenol acts as the acceptor. Mahajan et al. (1980) concluded that the effect of surface chemical properties on the sorption of phenol is more significant than the porosity of the carbon. 2,4-DCP showed higher sorption capacity, since the two electronegative chlorine atoms attract electrons towards the benzene ring, therefore, favour the formation of a bond between the surface of carbonyl groups and the electron-deficient aromatic ring of the phenol. This is consistent with results in this study that 2,4-DCP showed highest sorptive capacity.

6.2.7 Effect of hydrophobicity on sorption

The pK_a values of the compounds (Table 3.3) reveal that at the experimental pH range (4.5–6.3), sorption of chlorophenols occurred in their non-ionized form for all sorbents. The sorption capacities (Q_m, K_F) also show the sorption affinity for all sorbents except FC towards the chlorophenols are in the order 2,4-DCP (0.04–2.9 mmol g^{-1}) > 4-CP (0.03–2.5 mmol g^{-1}) > 2-CP (0.02–2.3 mmol g^{-1}). This is consistent with other studies (Jain and Jayaram, 2007; Jung et al., 2001). It reflects that for a particular sorbent the sorption capacity of phenolic compounds increases with an increase in the hydrophobicity of that compound as indicated by their increased log K_{ow} value. In contrast to the other sorbents the sorption affinity for the most hydrophobic compound (2,4-DCP) onto coal is much less relative to the less hydrophobic compounds. This could suggest that factors other than surface reactivity control the extent of uptake. The extremely slow rate of sorption kinetics observed in anthracite filter coal reacted with

organic contaminants has been attributed to condensed organic carbon which forms highly cross-linked micro-porous networks which leads to slow pore diffusion and a very slow relaxation of the sorption matrix (Andresen et al., 2004). The pore structure in coals is complex and diffusion of the reactants to coal surfaces is still a matter of debate (Walker and Mahajan, 1993).

6.2.8 Effect of particle size on sorption

The effect of particle size on the kinetics of CP sorption on pine (1.18–4.75 mm), GAC (0.6–2.36 mm) and FC (0.6–2.36 mm) were studied. The literature suggests that the larger particles have a lower sorption capacity than smaller particles (Gupta et al., 1990). The experimental kinetic curves are presented in Figures 6.21–6.29.

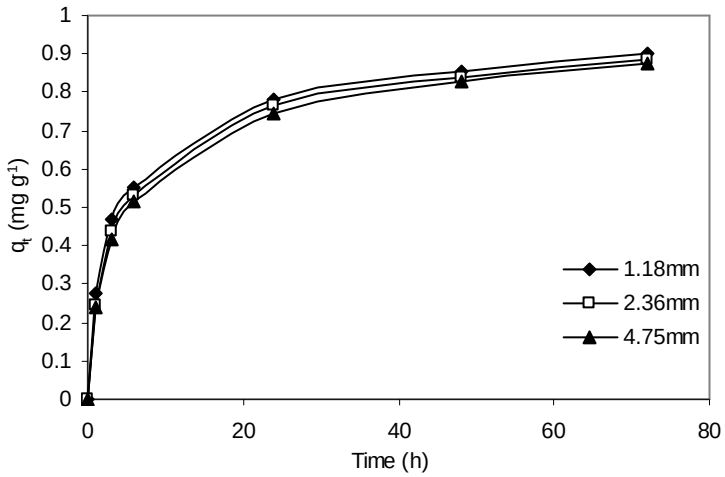

Figure 6.21 Effect of particle size on kinetics of 2-CP by pine

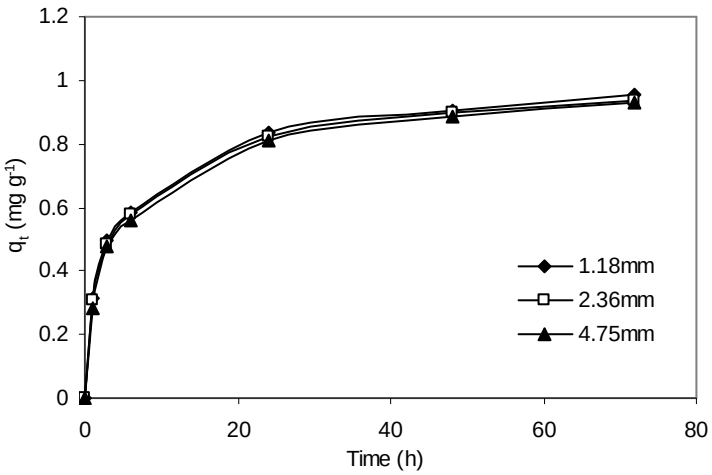

Figure 6.22 Effect of particle size on kinetics of 4-CP by pine

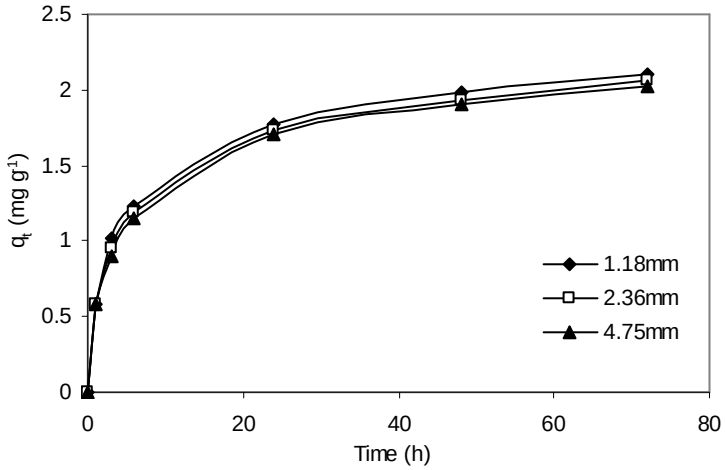

Figure 6.23 Effect of particle size on kinetics of 2,4-DCP by pine

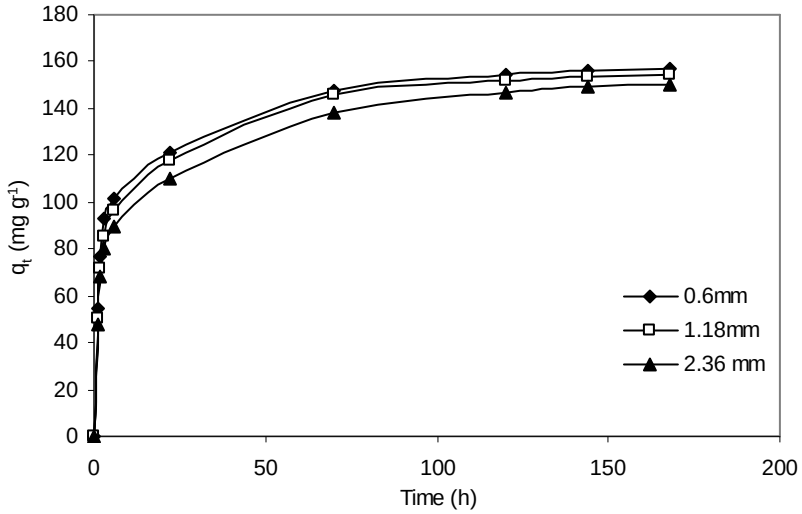

Figure 6.24 Effect of particle size on kinetics of 2-CP by GAC

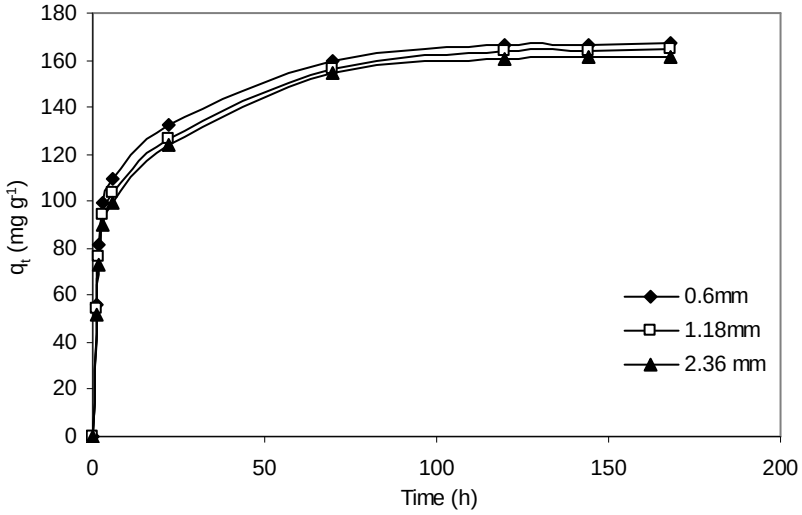

Figure 6.25 Effect of particle size on kinetics of 4-CP by GAC

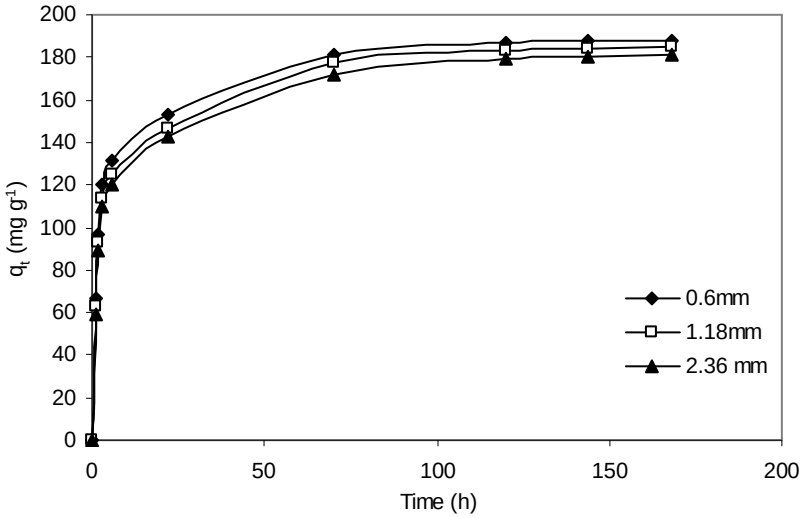

Figure 6.26 Effect of particle size on kinetics of 2,4-DCP by GAC

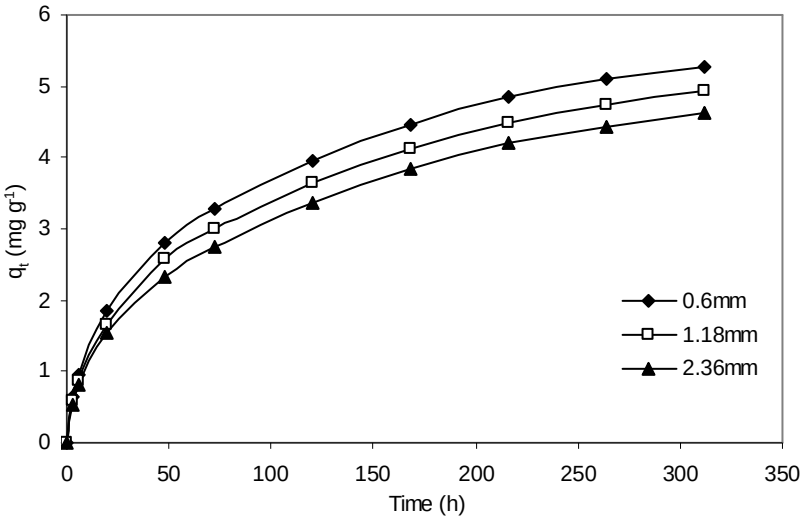

Figure 6.27 Effect of particle size on kinetics of 2-CP by FC

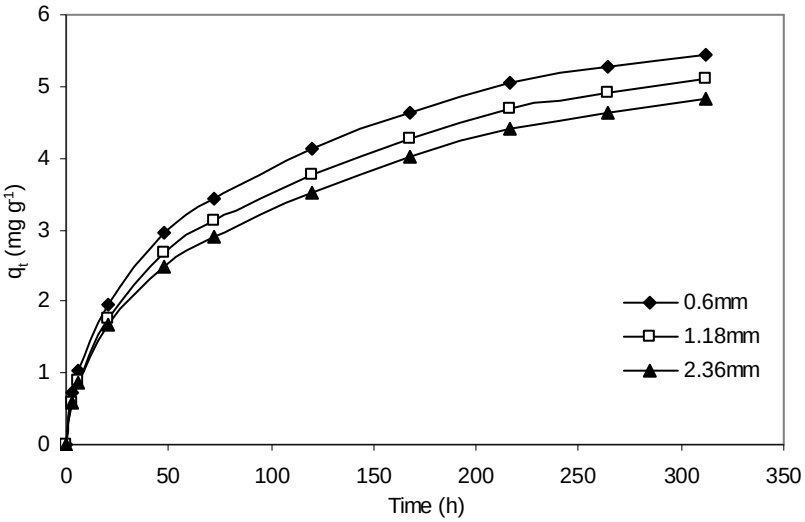

Figure 6.28 Effect of particle size on kinetics of 4-CP by FC

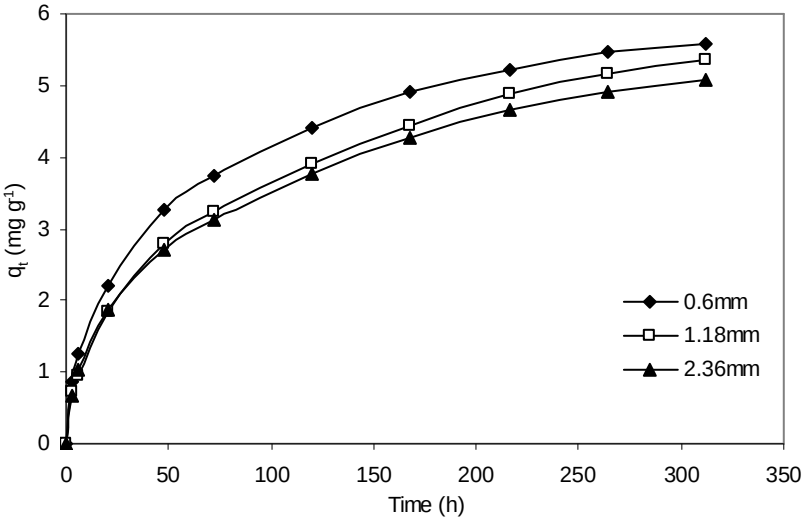

Figure 6.29 Effect of particle size on kinetics of 2,4-DCP by FC

The sorption capacities of GAC and FC from 0.6 to 2.36 mm showed little change. The pseudo-second-order rate constants (k_2) was also little affected in most cases by the particle size (Table 6.2). In fact, the smaller particles have greater specific surface area compared to larger particles; consequently there is more vacant active space available for the sorption of CP.

The low specific surface area and pore volume of pine (Table 3.1) indicates that only the external particle surface is available for sorption (Bras et al., 2005). The effect of particle size on chlorophenol sorption equilibrium was evaluated using four particle sizes of pine ranging from 0.6 to 4.75 mm. Although, sorption kinetics is slightly faster with decreasing particle size, equilibrium capacity was not affected by particle size. Sorption isotherms were parameterised and best fit results are presented (Table 6.5 and 6.6). The results show that the sorption isotherm parameters for a particular compound are similar at equilibrium for all particle sizes. This may seem counter-intuitive since it is often postulated that particle surface area increases with a decrease in the particle size for particles with minimal internal porosity. MacKay and Gschwend (2000) found monoaromatic hydrocarbon uptake on pine was the same regardless of particle size and shape. Their results contrast with Barrera-Garcia et al. (2008) who found a dependence of particle size with uptake. They attributed this to non-equilibrium conditions.

The range of particle sizes used in this study does not appear to significantly affect chlorophenol sorption, although larger particles associated with a slightly decreased sorption capacity for pine, GAC and FC.

Table 6.5 Best fit Langmuir isotherm parameters of different particle sizes for pine

Pine (mm)	Chlorophenols	Q_m (mg g^{-1})	b (L mg^{-1})	r^2	SSE
0.6	2-CP	3.3	0.012	0.980	0.11
0.6	4-CP	3.5	0.014	0.980	0.12
0.6	2,4-DCP	6.9	0.015	0.970	0.25
1.18	2-CP	3.2	0.012	0.969	0.13
1.18	4-CP	3.6	0.013	0.962	0.16
1.18	2,4-DCP	7.0	0.014	0.975	0.24
2.36	2-CP	3.1	0.010	0.979	0.10
2.36	4-CP	3.2	0.011	0.982	0.09
2.36	2,4-DCP	6.9	0.012	0.977	0.22
4.75	2-CP	3.2	0.009	0.979	0.10
4.75	4-CP	3.2	0.011	0.984	0.09
4.75	2,4-DCP	6.8	0.013	0.980	0.21

Table 6.6 Best fit Freundlich isotherm parameters of different particle sizes for pine

Pine (mm)	Chlorophenols	K_F	1/n	r^2	SSE
0.6	2-CP	0.14	0.541	0.999	0.02
0.6	4-CP	0.17	0.534	0.999	0.02
0.6	2,4-DCP	0.29	0.577	0.998	0.08
1.18	2-CP	0.13	0.550	0.998	0.03
1.18	4-CP	0.15	0.550	0.996	0.05
1.18	2,4-DCP	0.29	0.570	0.998	0.07
2.36	2-CP	0.11	0.559	0.999	0.02
2.36	4-CP	0.12	0.559	0.997	0.04
2.36	2,4-DCP	0.24	0.588	0.998	0.07
4.75	2-CP	0.11	0.568	0.998	0.03
4.75	4-CP	0.12	0.566	0.998	0.03
4.75	2,4-DCP	0.26	0.575	0.999	0.05

Table 6.7 Characteristics of wood particle shape

Specification	Pine 0.6 mm	Pine 1.18 mm	Pine 2.36 mm	Pine 4.75 mm	HW 1.18 mm
BET surface area ($m^2 g^{-1}$)	0.65	0.45	-	0.79	0.55
Average length (mm)	4.8	7.2	11.5	20.3	7.9
Average width (mm)	0.61	1.33	2.49	4.87	1.23
Length/width ratio	7.9	5.4	4.6	4.2	6.4
Interquartile distance (mm)	3	4	7	6	4

The effect of particle shape on chlorophenol sorption was evaluated on pine using four particle sizes (0.6 mm to 4.75 mm) and on HW (1.18 mm). Fitted sorption isotherm parameters for a particular compound are similar at equilibrium for all particle sizes (Table 6.5). This relatively uniform uptake trend is consistent with the similar surface area data for different particle sizes (Table 6.7). The poor correlation between particle size and surface area is due to the elongate nature of the particles. The particle width rather than particle length was found to be more closely aligned with the sieve mesh opening. This is consistent with the elongate particles passing through the mesh vertically and has been reported from horizontally screened samples (Hartmann et al., 2006). Of particular importance when designing large scale filtration systems is the dependence of sorption on particle size. Smaller particle sizes require greater pre-processing and therefore increased sorbent cost. Also it is difficult to handle and install in PRB system

6.2.9 Desorption

Desorption experiments were carried out in Milli-Q water on pine and HW in order to understand sorption irreversibility. Initial experiments were conducted using sorbed

chlorophenol to observe the desorption kinetics. Then experiments were carried out using 4 desorption cycles to determine the sorption-desorption isotherms.

6.2.9.1 Desorption kinetics

Desorption kinetic data decrease initially for one cycle of desorption (Figure 6.30 and 6.31) and were then considered to reach equilibrium. The rate of desorption was followed using the procedure as described in section 3.7.8. Desorption of 2-CP, 4-CP and 2,4-DCP from pine and HW followed a biphasic pattern with a fast desorption phase in the first 6 h (Figures 6.30 and 6.31) and followed by a slow phase. The trend between pine and HW was similar.

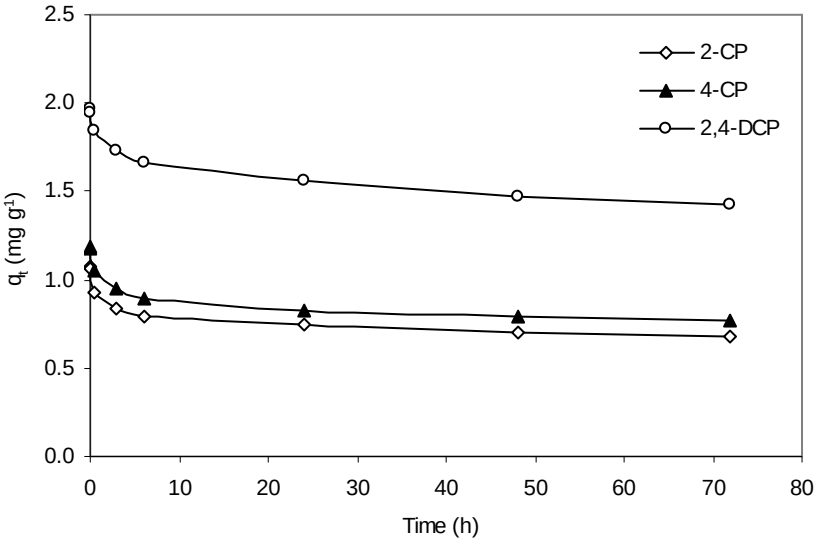

Figure 6.30 Changes of solid phase loading of CP with time during desorption by pine

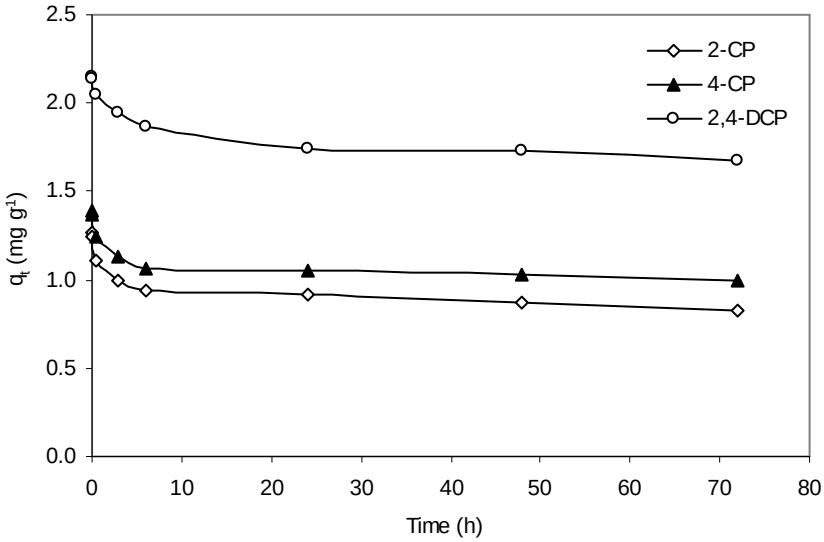

Figure 6.31 Changes of solid phase loading of CP with time during desorption by HW

6.2.9.2 Desorption equilibrium

Equilibrium based sorption-desorption experiments (section 3.7.7 and 3.7.9) were conducted to determine the extent of irreversible sorption for 2-CP, 4-CP and 2,4-DCP from woody materials. A plot of equilibrium solid-phase loading of sorption-desorption (q_e) against equilibrium liquid-phase chlorophenol concentration (C_e) of sorption-desorption is shown in Figures 6.32–6.37. The amount of equilibrium solid-phase loading after desorption was calculated by equation 2.3. It shows irreversible sorption. In the case of fully reversible sorption both isotherms coincide.

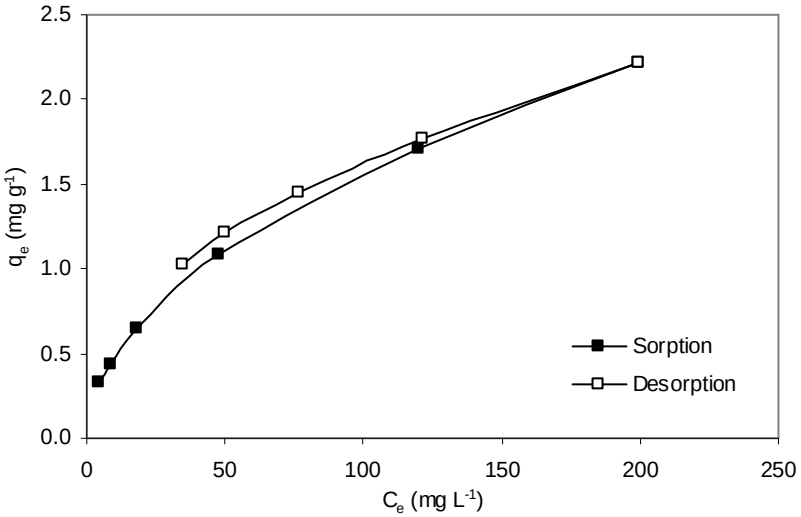

Figure 6.32 Sorption-desorption isotherms of 2-CP by pine

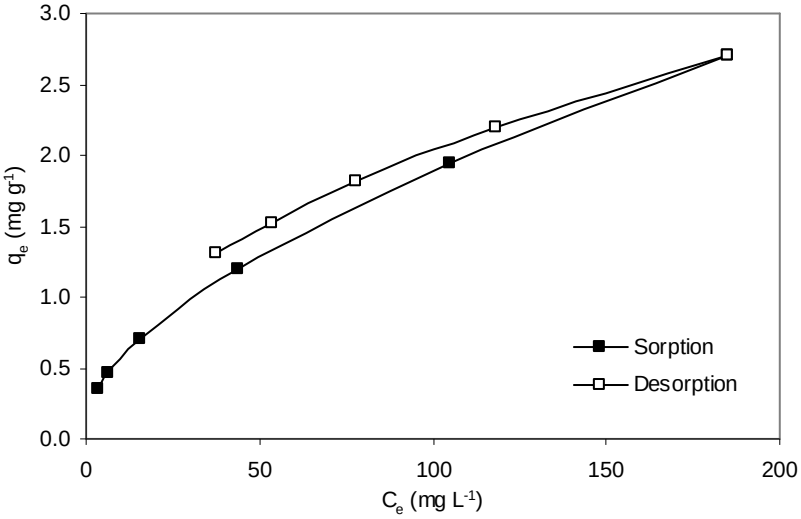

Figure 6.33 Sorption-desorption isotherms of 4-CP by pine

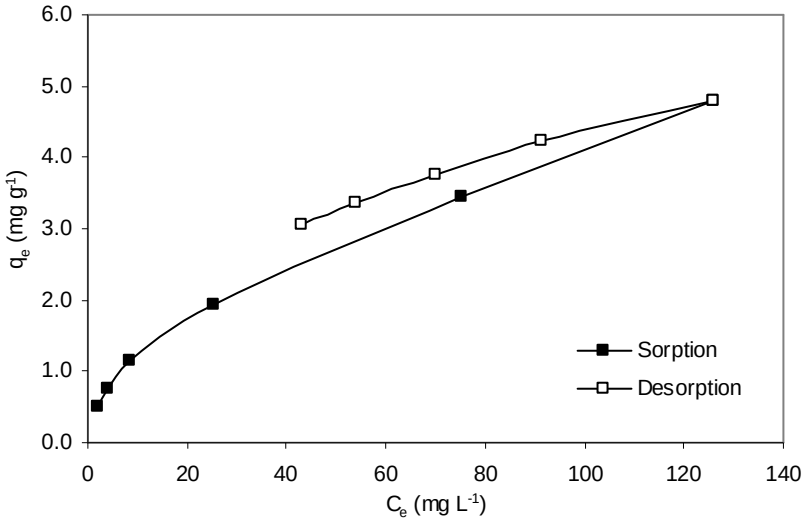

Figure 6.34 Sorption-desorption isotherms of 2,4-DCP by pine

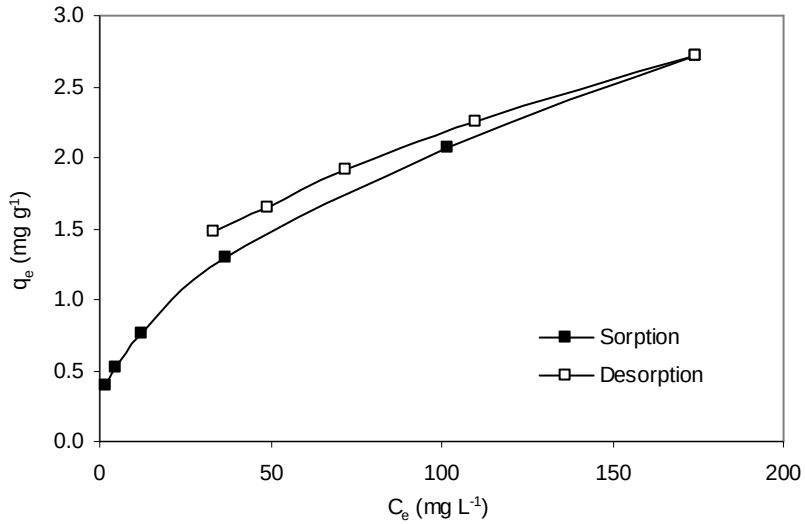

Figure 6.35 Sorption-desorption isotherms of 2-CP by HW

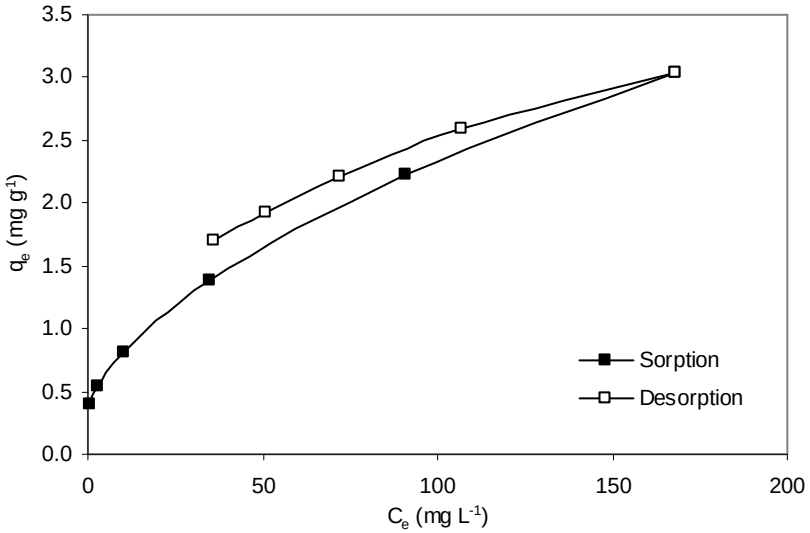

Figure 6.36 Sorption-desorption isotherms of 4-CP by HW

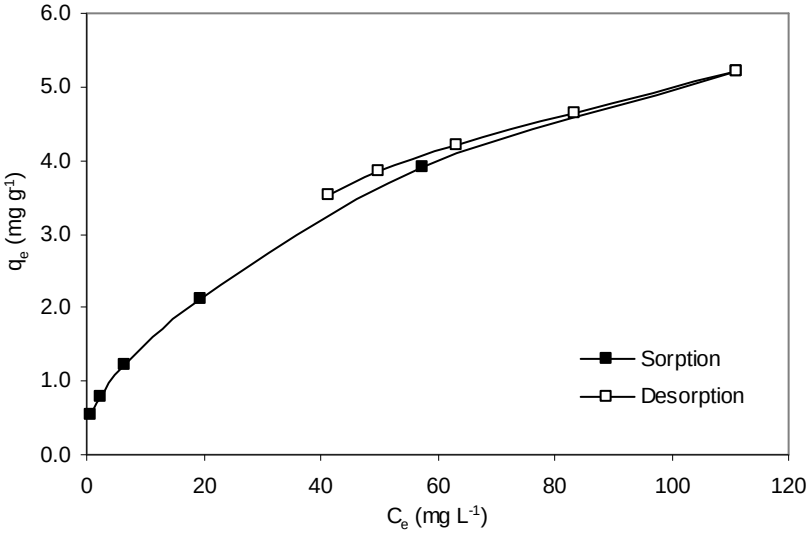

Figure 6.37 Sorption-desorption isotherms of 2,4-DCP by HW

The desorption parameters (section 2.4.2) for the Freundlich constants for both sorption and desorption isotherms are shown in Table 6.8 and Table 6.9. The desorption data for both pine and hardwood had a better fit to the Freundlich model compared to the Langmuir model which had on adequate fit (r^2 = 0.91–0.99) (data not shown).

Table 6.8 Fitted sorption parameters for desorption from Freundlich isotherm.

Sorbent	Sorbate	K_F	1/n	r^2	SSE
Pine	2-CP	0.15	0.508	1.000	0.01
Pine	4-CP	0.16	0.537	0.999	0.03
Pine	2,4-DCP	0.34	0.543	0.998	0.07
HW	2-CP	0.25	0.458	0.998	0.04
HW	4-CP	0.29	0.454	0.994	0.08
HW	2,4-DCP	0.50	0.501	0.997	0.09

Table 6.9 Freundlich parameters and hysteresis coefficients for desorption of chlorophenols on pine and hardwood.

Sorbent	Sorbate	K_{dF}	$1/n_d$	r^2	SSE	H	λ
Pine	2-CP	0.22	0.434	1.000	0.01	85	5.16
Pine	4-CP	0.25	0.459	0.999	0.01	85	5.35
Pine	2,4-DCP	0.62	0.424	0.999	0.02	78	8.36
HW	2-CP	0.38	0.378	0.998	0.02	83	5.81
HW	4-CP	0.43	0.381	0.999	0.01	84	5.29
HW	2,4-DCP	0.85	0.385	0.999	0.02	77	8.38

Data from the Freundlich isotherm are used to describe sorption-desorption behaviour. For both pine and hardwood, the sorption capacity during desorption (K_{dF}) was (1.46 to 1.8 times) greater than during sorption (K_F). This indicates there is a greater sorbed mass for a given solute concentration during desorption compared with that during a

sorption cycle. Also, the desorption K_{dF} values were consistently higher than those for sorption. This is indicative of sorption-desorption hysteresis as a result of partially irreversible sorption of chlorophenols onto a pine and HW. Adsorption-desorption behaviour can also be described in terms of hysteresis coefficients (section 2.4.2). The results from the Table 6.9 showed that $H < 100$ and $\lambda > 0$ which indicate positive hysteresis in the pine and HW. The lowest hysteresis was observed for 2,4-DCP which has a high sorption capacity and reflects its strong hydrophobicity. These data indicate that the degree of irreversibility increases from 2-CP~4-CP to 2,4-DCP.

Rodriguez-Cruz et al. (2008) studied sorption-desorption isotherms of pesticides (^{14}C-Linuron) by untreated pine. They found hysteresis coefficient for pesticides (^{14}C-Linuron) was 68. This is comparable with this study. The hysteresis coefficient in pine is lower for Linuron due to more hydrophobic (Log K_{ow} = 3.0) compared with pine for 2-CP and 4-CP which are less hydrophobic (Log K_{ow} = 2.12-2.44) and closer to pine for 2,4-DCP (almost similar hydrophobic, Log K_{ow} = 2.75-3.3).

Mattson et al. (1969) indicated that the formation of charge-transfer complexes between the sorbates and the functional groups of activated carbon surface is the possible reason for irreversible sorption. The degree of irreversibility is related to the number of high-energy (chemisorption) bonds. The hydroxyl group in phenolic is a strongly activating ortho- and para-directing substituent in electrophilic aromatic substitution reaction (McMurry, 2008). Therefore, electron density of a phenolic ring is strongly influenced by the nature of a substituent. Chlorine atoms act as an electron withdrawing group in the phenolic ring. Thus chlorine substituted phenolic ring acts as a acceptor in donor-

acceptor complexes. Hence, more chlorine atom in the phenolic ring formed stronger-complexes with a given donor. This might be the another reason for higher irreversibility of 2,4-DCP.

The quantity of chlorophenols desorbed after 4 desorption cycles from the wood (pine, HW) compared to that initially sorbed (Figure 6.38) varied between 44–53% for monochlorophenol and 31-37% for dichlorophenol. This indicated that a significant fraction of monochlorophenol is weakly sorbed on wood. On the contrary, 2,4-DCP molecules were less desorbed, because of strong hydrophobic interactions with wood.

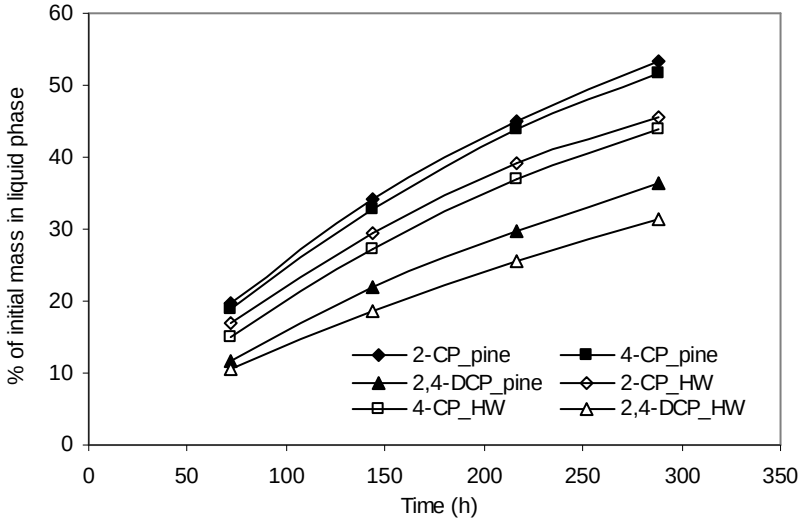

Figure 6.38 Desorbed percentages of chlorophenols from pine and HW. These percentages were calculated from the initially sorbed mass and after the 4 desorption cycle.

6.3 Conclusion

Granular activated carbon is a traditional sorbent widely used for chlorophenol removal from water. Both hardwood and pine and coal show promise as an alternative to

commercial GAC under natural pH and can be used with minimal pre-treatment which improves their cost-effectiveness. Whilst GAC has a much greater sorption capacity, other sorbents had a number of performance characteristics that may be desirable in some applications. The woody materials had a relatively rapid chlorophenol uptake, and high surface reactivity. The anthracite filter coal was found to have a similar equilibrium uptake of chlorophenol to the wood but had slow kinetics and would therefore suit applications where there was a long residence time such as groundwater barriers. Predictive modelling of contaminant uptake for the kinetic data suited a pseudo-second-order model and the equilibrium data for a Freundlich model. The calculated hysteresis coefficient indicated that there is a hysteresis in pine and HW. Lower desorption by the more sorptive compound indicates low hysteresis can be attributed to more irreversible due to strong hydrophobic interaction of 2,4-DCP with wood surfaces. Sorption kinetics with different particle sizes of sorbents was slightly affected while equilibrium capacity of pine did not change with changing particle size.

CHAPTER 7

Column sorption study: 2,4-dichlorophenol

7 Column sorption study: 2,4-dichlorophenol

7.1 Introduction

Few studies have been done on the sorption of 2,4-DCP with pine under flow rather than under batch conditions. Of the chlorophenols previously tested 2,4-DCP was chosen since it has the highest sorption capacity on wood (pine) as determined from the batch isotherm experiment. The isotherm and breakthrough data are important to evaluate the sorption process using pine. The aim of this study is to evaluate the potential of pine as a reactive media for the removal of 2,4-DCP in aqueous solution by column tests in a continuous flow system. The influence of flow rate, particle size and $KMnO_4$ on sorption was examined from the column test results. Various analytical models were used to evaluate the sorption process.

7.2 Column studies

The aim of the column experiments was to investigate the sorption of 2,4-DCP on pine and modified pine (the permanganate treated pine). The column experiments were carried out by passing 2,4-DCP solution with a flow rate 5 and 10 mL min^{-1} through a column (section 3.7.13). Particle sizes of 1.18 and 4.75 mm were used with glass beads for column operation. Therefore, the column did not get clogged due to mixing of glass beads with pine particles and the influent moved freely through the column. Column operation was continued until the effluent concentration of 2,4-DCP was changes less than 2% of the previous effluent reading.

Pore volume and effective porosity

Mass transport through the column experimentally was carried out by using a conservative tracer (KCl) (section 3.7.14). This information can be used to determine mass transport parameters for the column. Chloride breakthrough curves were constructed by plotting relative concentration (effluent concentration divided by influent concentration) versus cumulative effluent volume (Figure 7.1).

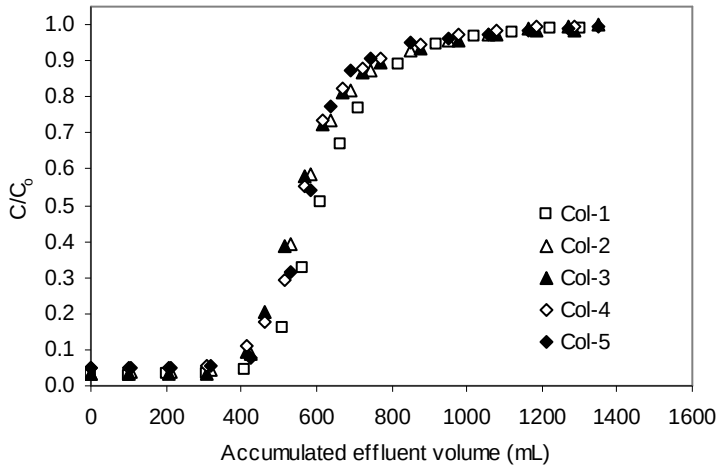

Figure 7.1 Chloride breakthrough curves for the pine column

The influent concentration (C_o) is used in normalizing the effluent concentration (C). The cumulative effluent volume corresponding to the relative concentration at 0.5 of the tracer input ($C/C_o = 0.5$) can be used to determine the pore volume for constant flux experiments (Barry and Parker, 1987). For example, when C/C_o is 0.5, the measured pore volume is equal 528 mL (Figure 7.1), that is the time required for the tracer to traverse the column when no interactions occur assuming no dispersion i.e. plug flow advection between tracer and filtration media (residence time) (Boulda et al., 2007). The

effective porosity for the column filtration media was calculated from the total column volume of 1232 mL and the pore volume with relative concentration (C/C_o) at 0.5 (Table 7.1).

Table 7.1 Column characteristics: mass of pine 66 g, mass of glass beads 1665 g

Column No.	Pine particle size (mm)	Flow (mL min^{-1})	Pore volume (mL)	Residence time (min)	Porosity
Col-1	1.18	~5	573	110	0.47
Col-2	4.75	~5	528	106	0.43
Col-3	4.75	~10	512	50	0.42
Col-4	4.75	~10	524	52	0.43
Col-5	4.75	~5	542	108	0.44

Breakthrough curve analysis

The characteristics shape of the breakthrough curve depends on the influent concentration, sorbent particle size, inlet flow rate and other column properties. The breakpoint and column exhaustion were used to evaluate the breakthrough curves. The total quantity sorbed in the column is calculated from the area above the breakthrough curve (outlet 2,4-DCP concentration, C/C_o versus time) multiplied by the flow rate. The uptake capacity (q) of the pine was calculated from the mass sorbed in the column divided by the mass of the sorbent (66 g) in the column. The column data were calculated at a fixed C/C_o (0.02 and 0.8) for all runs. This was done because of the tailing and the maximum capacity was only 0.8 of influent. This is common in non-equilibrium systems. All breakthrough curves had a similar shape. The initial and final pH varied between 5.2–5.5. The breakthrough curves for sorption of 2,4-DCP onto pine

was obtained by plotting C (effluent concentration) divided by C_o (influent concentration) against number of column pore volume. The effective column pore volume was determined by the chloride tracer. The point on the breakthrough curve at which the 2,4-DCP concentration reaches to $C/C_o = 0.02$ and $C/C_o = 0.8$ (i.e. 80% of the influent concentration) were considered break point and the point of column exhaustion, respectively.

7.3 Effect of flow rate

The effect of 5 and 10 mL min^{-1} flow on 2,4-DCP sorption by pine was studied by keeping the 2,4-DCP influent concentration and particle size constant. The plots of the ratio of effluent (C) to influent concentrations (C_o) versus pore volume at two different flow rates are shown in Figure 7.2.

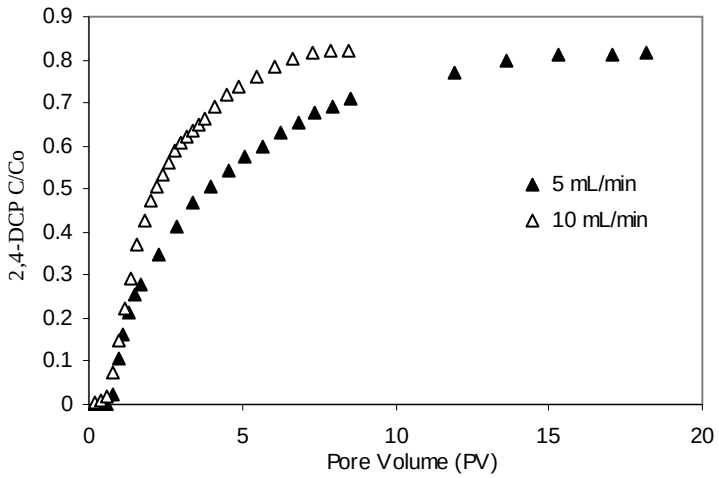

Figure 7.2 Breakthrough curves for different flow rates under the experimental condition Col-2 (Run-1) and Col-3 (Run-1) (2,4-DCP ~1.84 mM, pine 4.75 mm)

Figure 7.2 showed that the relative effluent concentration (C/C_o) of 2,4-DCP increased rapidly after the breakpoint and reaches 80% of the influent concentration i.e. exhaustion time. The breakthrough curves shifted from left to right as the flow rate decreases from 10 mL min^{-1} to 5 mL min^{-1}. Because the higher flow rate (10 mL min^{-1}) has a shorter residence time (50 min), the sorption to column decreases. But at a longer residence time (106 min) with 5 mL min^{-1} in the column, the 2,4-DCP had a longer time to interact with the pine. The column sorption data were evaluated. The breakpoint time, pore volume (PV), the total time at different flow rates and uptake (q) are shown in Table 7.2.

Table 7.2 Column data and parameters obtained at different flow rates, pine 4.75 mm

	Flow	C/C_o = 0.02		C/C_o = 0.8		
Column No.	(mL min^{-1})	Time (min)	No. of PV	Time (min)	No. of PV	q (mg g^{-1})
Col-2 (Run-1)	5	76	0.72	1440	13.6	18
Col-3 (Run-1)	10	30	0.60	335	6.7	9

PV - pore volume
q - uptake capacity

The breakthrough curve becomes steeper when the flow rate increased from 5 mL min^{-1} to 10 mL min^{-1}. The break point time (C/C_o = 0.02) and sorption of 2,4-DCP decreases at flow rate 10 mL min^{-1}. The probable reason is that when the residence time of 2,4-DCP solution in column is not long enough for sorption to reach exhaustion point (C/C_o = ~0.8) at that flow, the 2,4-DCP solution leaves the column before exhaustion occurs. Thus at a higher flow rate the contact time between 2,4-DCP and the surface of the pine decreases and results in a reduced uptake capacity. If the flow rate decreases the residence time then mass transfer limitations occur. Increased flow may decrease film

resistance (Ko et al., 2000) and therefore potentially increases mass transfer. However under these column conditions it does not appear important.

The results indicated that the sorption of 2,4-DCP onto pine was strongly influenced by flow rate. An earlier breakthrough time and exhaustion time were observed for a higher flow rate. The total breakthrough concentration was reached at 6.7 PV at a flow rate 10 mL min^{-1} while at flow rate 5 mL min^{-1} it is delayed until 13.6 PV (Table 7.2). The uptake capacity of 2,4-DCP was decreased from 18 mg g^{-1} to 9 mg g^{-1} when the flow rate was increased from 5 mL min^{-1} to 10 mL min^{-1} with the same particle size (4.75 mm). The measured value for q is not the equilibrium amount, it is the uptake capacity.

7.4 Effect of particle size

The sorption process was studied at particle sizes 1.18 and 4.75 mm while the influent concentration and flow rate were kept constant. The effluent concentration was monitored until the concentration changes relatively slowly (Figure 7.3 and Table 7.3).

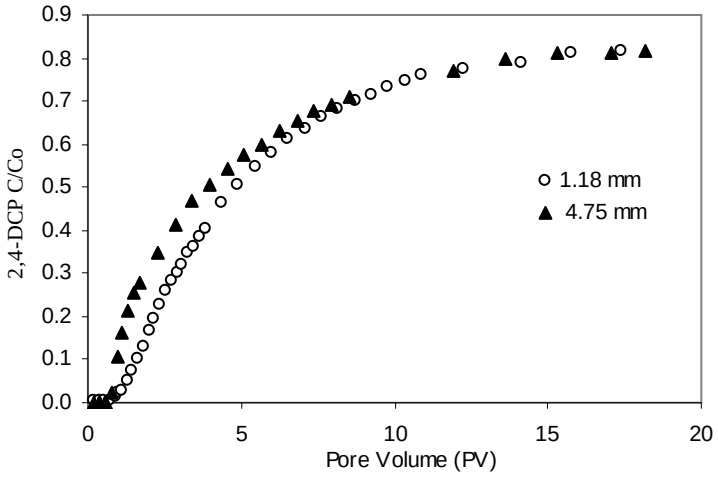

Figure 7.3 Breakthrough curves for different particle sizes under the experimental condition Col-1 (Run-1) and Col-2 (Run-1) (2,4-DCP ~1.84 mM, flow rate 5 mL min^{-1})

Table 7.3 Column data and parameters obtained at different particle sizes, flow 5 mL min^{-1}, 22 °C

		$C/C_o = 0.02$		$C/C_o = 0.8$		
Column No.	Particle size (mm)	Time (min)	No. of PV	Time (min)	No. of PV	q (mg g^{-1})
Col-1 (Run-1)	1.18	110	1.0	1560	14.2	21
Col-2 (Run-1)	4.75	76	0.72	1440	13.6	18

PV - pore volume
q - uptake capacity

The breakpoint ($C/C_o = 0.02$) and exhaustion point ($C/C_o = 0.8$) for the larger particle size occurred slightly earlier than for the smaller particle size. This indicates that 2,4-DCP sorption onto pine is higher for the smaller particle size than larger particle size. These results show a similar trend to the batch results where 2,4-DCP uptake is slightly higher for the smaller particle size (1.18 mm, 7 mg g^{-1}) than the larger particle size (4.75 mm, 6.8 mg g^{-1}) (Table 6.5).

After ~14 PV, they have the same exhaustion point ($C/C_o = 0.8$) but uptake was slightly higher for smaller particle size. This may be due to the higher sorption rate in the column for smaller particle size. These results were also recognised in the batch experiment, the sorption kinetics of smaller particle size was slightly faster but equilibrium capacity was not affected by the particle size.

7.5 Effect of $KMnO_4$-treatment of pine

Column sorption experiments using 2,4-DCP were carried out on both the Col-2 (Run-1), Col-3 (Run-1) for untreated pine and Col-4 (Run-2), Col-5 (Run-2) for permanganate treated (modified) pine (section 3.2.2). The 2,4-DCP data for the pine

and modified pine media under both high and low flow conditions are shown in Figures 7.4, 7.5 and Table 7.4.

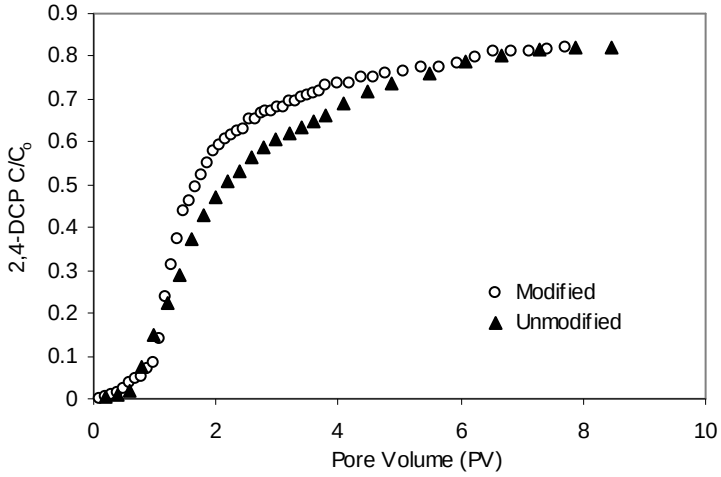

Figure 7.4 Breakthrough curves for 2,4-DCP sorption with respect to $KMnO_4$ modified and unmodified pine under the experimental condition Col-3 (Run-1) and Col-4 (Run-2) (2,4-DCP ~1.84 mM, $KMnO_4$ ~3.8 mM, flow rate 10 mL min^{-1})

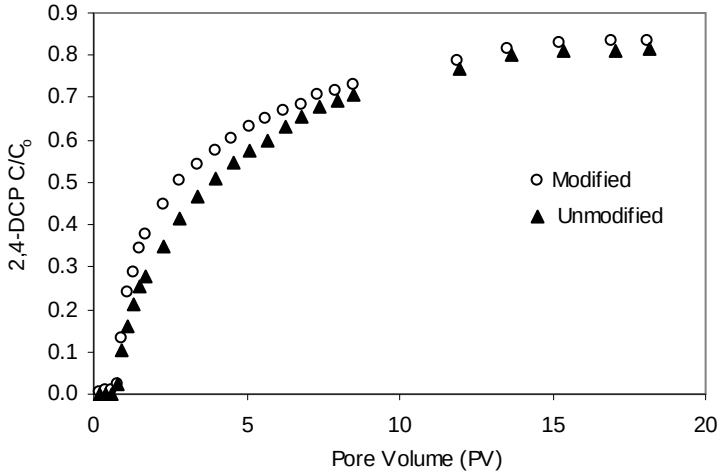

` Figure 7.5 Breakthrough curves for 2,4-DCP sorption with respect to $KMnO_4$ modified and unmodified pine under the experimental condition Col-2 (Run-1) and Col-5 (Run-2) (2,4-DCP ~1.84 mM, $KMnO_4$ ~3.8 mM, flow rate 5 mL min^{-1})

Table 7.4 Column data and parameters obtained at modified and unmodified pine, 22 °C

Column and Run No.	Pine condition	Flow (mL min^{-1})	C/C_o = 0.02 Time (min)	C/C_o = 0.02 No. of PV	C/C_o = 0.8 Time (min)	C/C_o = 0.8 No. of PV	q (mg g^{-1})
Col-3 (Run-1)	unmodified	10	30	0.60	335	6.7	9
Col-4 (Run-2)	modified	10	25	0.49	320	6.2	7
Col-2 (Run-1)	unmodified	5	76	0.72	1440	13.6	18
Col-5 (Run-2)	modified	5	72	0.68	1329	12.6	15

PV - pore volume
q - uptake capacity

The break through curves in the pine and modified pine are similar in shape. The column data (Table 7.4) suggest that the time required for unmodified pine to reach the breakpoint (C/C_o = 0.02) is slightly higher than the modified pine column. The time to reach exhaustion point (C/C_o = 0.8) is also slightly different. This suggests that 2,4-DCP sorption onto unmodified pine is slightly higher than modified pine.

The small decrease in 2,4-DCP uptake from 18 mg g^{-1} to 15 mg g^{-1} was observed for modified pine at flow rate 5 mL min^{-1} and 9 mg g^{-1} to 7 mg g^{-1} at flow rate 10 mL min^{-1}. This decrease in uptake may be due to the MnO_2 impregnated on pine. It indicates that $KMnO_4$ treatment of pine did not improve the 2,4-DCP sorption capacity of pine. This is because the permanganate has partially reacted with lignin on the pine and therefore has decreased a key component of the pine which is known as to cause sorption (section 2.5.2.2)

7.6 Comparison of batch and column sorption capacity

The sorption capacity of the pine obtained from the batch equilibrium studies was compared with the column sorption capacity. It was found that the column sorption

capacity of 2,4-DCP was higher than the equilibrium batch studies for smaller particle size (1.18 mm, 7 mg g^{-1}) and larger particle size (4.75 mm, 6.8 mg g^{-1}). The data shown 3:1 (i.e. 21:7 mg g^{-1} for 1.18 mm and 18:6.8 mg g^{-1} for 4.75 mm) ratio of column to batch capacity at both particle sizes at 5 mL min^{-1} and ~1.3:1 (i.e. 9:6.8 mg g^{-1} for 4.75 mm) ratio at the higher flow rate (10 mL min^{-1}). The decrease in ratio is due to greater mass transfer limited sorption in column studies at the higher flow rate. Other studies also found higher column sorption capacity than batch study for the removal of phenol and chlorophenol. Some examples are shown in Table 7.5.

Table 7.5 Examples of batch and column study

Sorbent	Sorbate	Batch capacity (mg g^{-1})	Column capacity (mg g^{-1})	References
Fertilizer waste	2,4,6-TCP	98.0	129.7	Gupta et al. (2000)
Fertilizer waste	4-CP	62	99.3	Gupta et al. (2000)
Activated carbon	phenol	33.33	76.6	Ekpete et al. (2011)
Activated carbon	2-CP	35.71	78.6	Ekpete et al. (2011)

A higher sorption capacity using treated fertilizer waste were obtained compared to the batch capacity for the removal of 4-CP (1.6 times) and 2,4,6-TCP (1.3 times) by Gupta et al. (2000). Ekpete et al. (2011) also found higher sorption capacity in the column study for the removal of phenol (2.3 times) and 2-CP (2.2 times) by commercial activated carbon. A higher sorption capacity in column studies is believed to be due to a uniform concentration gradient maintained at the interface of the sorption surface as the solute in the pore space is continuously replaced. However in batch studies the concentration gradient decreases with time as solute uptake occurs. This is one plausible reason for the greater uptake but further work is need.

7.7 Modelling column 2,4-DCP sorption

Effective design of a column sorption process is needed to predict the breakthrough curves and sorption capacities in a column dynamic system under different operational conditions. To interpret the breakthrough curves, three analytical models (Thomas, 1944; Yan et al., 2001; Yoon and Nelson, 1984) were applied**.** Whilst these models do have limitations when applied to these data, they do provide some insight. Numerical modelling using a non-equilibrium model was beyond the scope of this work.

7.7.1 Thomas model

Thomas model (Thomas, 1944) is widely used in column studies. This model is based on the Langmuir isotherm for equilibrium and second-order reversible reaction kinetics. In this study, it was used to calculate the sorption rate and capacity of 2,4-DCP from the column studies. The nonlinear form of the Thomas model can be expressed as equation 7.1:

$$\frac{C}{C_o} = \frac{1}{1 + \exp[k_{th}(q_{th} \times M - C_o \times V)/Q]} \qquad (7.1)$$

where C is the effluent 2,4-DCP concentration (mg L^{-1}), C_o is the initial 2,4-DCP concentration (mg L^{-1}) in the influent, k_{th} is the Thomas rate constant (L min^{-1} mg^{-1}), q_{th} is the maximum 2,4-DCP sorption capacity (mg g^{-1}), M is the mass of the sorbent (g), V is the effluent volume (L), and Q is the flow rate (mL min^{-1}).

The linearized form of the Thomas model can be expressed as equation 7.2:

$$\ln\left(\frac{C_o}{C} - 1\right) = \frac{k_{th} \times q_{th} \times M}{Q} - \frac{k_{th} \times C_o}{Q} \times V \qquad (7.2)$$

The constants k_{th} and q_{th} were determined from a plot of $\ln(C_o/C\text{-}1)$ against V at a given flow rate.

The column data obtained from the sorption of 2,4-DCP by pine was applied to equation (7.2) to determine the Thomas rate constant (k_{th}) and the maximum solid-phase concentration (q_{th}) from the slope and the intercept. A plot of $\ln(C_o/C - 1)$ versus V gives a straight line with a slope of $(-k_{th}C_o/Q)$ and intercept $(k_{th}q_{th}M/Q)$ (Appendix C 1-C 5). It was found that the linearity of the Thomas model was effective only for relative concentration $(C/C_o) > 0.05$ and <0.85 and their r^2 values are more than 0.80. The values of k_{th}, q_{th} and the correlation coefficients (r^2) at different flow rates, particle sizes and modified pine were obtained from the Thomas model is shown in Table 7.6.

Table 7.6 Predicted parameters from the Thomas model (linear, >0.05 and <0.85) of 2,4-DCP sorption on pine

Column and Run No	Flow (mL min^{-1})	Particle size (mm)	q_{BTC} (mg g^{-1})	k_{th} (L min^{-1} mg^{-1})	q_{th} (mg g^{-1})	r^2
Col-1 (Run-1)	5	1.18	21	0.0078	17	0.83
Col-2 (Run-1)	5	4.75	18	0.0052	13	0.81
Col-3 (Run-1)	10	4.75	9	0.0222	5.5	0.85
Col-4 (Run-2)	10	*4.75	7	0.0215	2.7	0.84
Col-5 (Run-2)	5	*4.75	15	0.0046	10	0.82

q_{th} - Thomas capacity
q_{BTC} - breakthrough curve capacity
*$KMnO_4$ modified pine

The difference between q_{BTC} and q_{th} is smaller (14-33%) at a lower flow rate compared to a higher flow rate (40-60%). This may reflect that at a higher flow rate, non-equilibrium effects are greater and therefore the model deviates from ideal conditions. In summary, the q values from the breakthrough curves (BTC) show lower uptake at higher flow rate, higher particle size and when using $KMnO_4$ modified pine.

From Table 7.6 the column sorption capacity (q_{th}) for 2,4-DCP was found to decrease and the Thomas rate constant (k_{th}) increase with increasing flow rate from 5 to 10 mL min^{-1} because sorption is usually controlled by mass transfer especially at a low flow rate (Aksu and Gonen, 2004). The results indicated that the Thomas rate constant (k_{th}) from 0.0078 to 0.0052 (L min^{-1} mg^{-1}) as the particle size increased from 1.18 to 4.75 mm with same flow rate (5 mL min^{-1}). This is consistent with the pseudo-second-order rate constant k_2 (Table 6.2).

7.7.2 Yoon-Nelson model

Yoon and Nelson (1984) can be expressed as following equation 7.3:

$$\ln \frac{C}{C_o - C} = k_{yn}t - \tau k_{yn} \qquad (7.3)$$

where k_{yn} is the Yoon-Nelson rate constant (min^{-1}), τ the time required for 50% sorbate breakthrough (min), and t is the breakthrough (sampling) time (min). The k_{yn} and τ can be determined from a plot of $\ln(C/(C_o - C))$ versus sampling time (t).

A plot of ln $C/(C_o-C)$ versus sampling time (t) gives a straight line according to equation (7.3) with a slope of (k_{yn}) and intercept (τ k_{yn}) (Figures Appendix C6-C10). It was found that the linearity of the Yoon-Nelson model was effective only for relative concentration (C/C_o) > 0.25 and <0.85 and their r^2 values are more than 0.82. The values of τ (half of breakthrough time) predicted by the Yoon-Nelson model is presented in Table 7.7:

Table 7.7 Predicted parameters from the Yoon-Nelson model (linear, >0.25 and <0.85) of 2,4-DCP sorption on pine

Column and Run No	Flow (mL min^{-1})	$k_{yn}(min^{-1})$	τ from BTC (min)	τ from Yoon-Nelson (min)	r^2
Col-1 (Run-1)	5	0.0015	540	543	0.87
Col-2 (Run-1)	5	0.0014	420	419	0.86
Col-3 (Run-1)	10	0.0061	110	106	0.88
Col-4 (Run-2)	10	0.0074	91	73	0.82
Col-5 (Run-2)	5	0.0012	330	356	0.84

The τ values estimated from experimental BTC curves (Figures 7.7-7.9) for Col-1 (Run-1), Col-2 (Run-1), Col-3 (Run-1), Col-4 (Run-2), and Col-5 (Run-2). The results show that the half of breakthrough time (τ) found from the Yoon-Nelson model is a reasonable prediction of the experimental data (Table 7.7).

7.7.3 Yan model

To predict the actual breakthrough curves, the Yan model (Yan et al., 2001) was employed and expressed as the following equation 7.4:

$$\frac{C}{C_o} = 1 - \frac{1}{1 + \left(\frac{Q^2 t}{k_y q_y M}\right)^{kyCo/Q}} \qquad (7.4)$$

where k_y is the Yan rate constant for the Yan model (L min^{-1} mg^{-1}), t is the time (min), Q is flow rate (mL min^{-1}), M is the mass of the sorbent (g) and q_y is the maximum sorption capacity (mg g^{-1}) of sorbent estimated by the Yan model.

The breakthrough curves of 2,4-DCP dynamic sorption with respect to the flow rate, particle size and modified pine were investigated using Yan model (Figures 7.6, 7.7, 7.8 and 7.9).

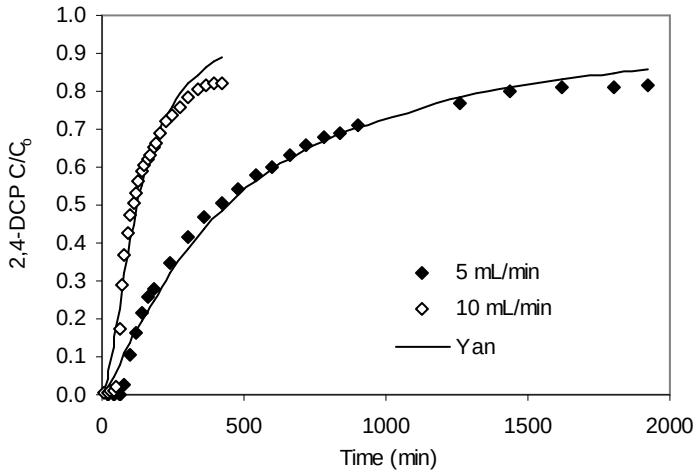

Figure 7.6 Effect of flow rate and predicted breakthrough curves of Yan model under the experimental condition Col-2 (Run-1) and Col-3 (Run-1)

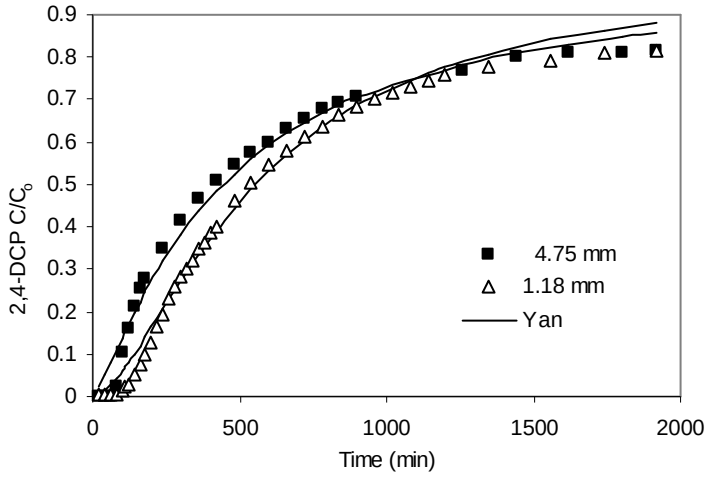

Figure 7.7 Effect of particle size and predicted breakthrough curves of Yan model under the experimental condition Col-1 (Run-1) and Col-2 (Run-1)

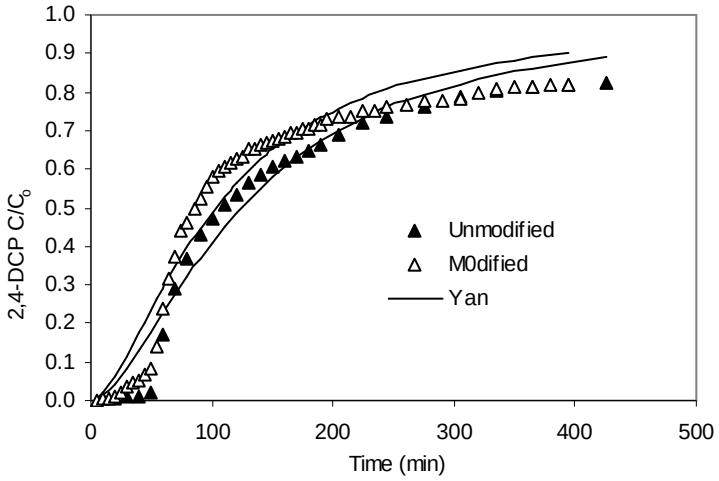

Figure 7.8 Effect of 2,4-DCP sorption on to unmodified and $KMnO_4$-modified pine and predicted breakthrough curves of Yan model under the experimental condition Col-3 (Run-1) and Col-4 (Run-2)

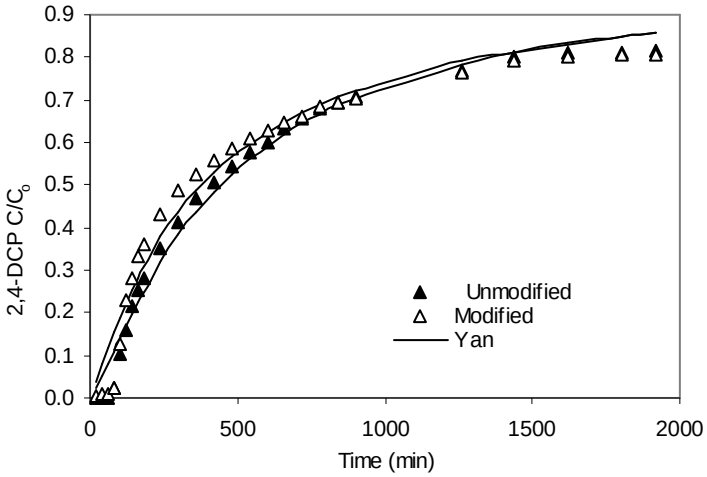

Figure 7.9 Effect of 2,4-DCP sorption on to unmodified and $KMnO_4$-modified pine and predicted breakthrough curves of Yan model under the experimental condition Col-2 (Run-1) and Col-5 (Run-2)

It was observed that a better fit at early and late column data occurred for the low flow rate while a poor fit at early and late data for the high flow rate. The various operating parameters such as effect of flow, particle size and modified pine can be predicted by the Yan model (Table 7.8):

Table 7.8 Predicted parameters from the Yan model (non-linear) of 2,4-DCP sorption on pine.

Column and Run No	Flow (mL min^{-1})	Particle size (mm)	k_y (L min^{-1} mg^{-1})	q_{BTC} (mg g^{-1})	q_y (mg g^{-1})	r^2
Col-1 (Run-1)	5	1.18	0.0273	21	8.1	0.99
Col-2 (Run-1)	5	4.75	0.0208	8	8.0	0.99
Col-3 (Run-1)	10	4.75	0.0582	9	3.4	0.96
Col-4 (Run-2)	10	*4.75	0.055	7	3	0.95
Col-5 (Run-2)	5	*4.75	0.0183	15	7.8	0.97

q_y – Yan capacity
q_{BTC} - breakthrough curve capacity
* $KMnO_4$ modified pine

The results show that the exhaustion time (C/C_o~0.8) (Figure 7.6) at flow rate 10 mL min^{-1} was earlier than the flow rate 5 mL min^{-1}. This suggests that the column sorption capacity (q_y) for 2,4-DCP was found to decrease with increasing flow rate from 5 to 10 mL min^{-1}. But the sorption capacity was not affected by changing the particle size and modified pine. The experimental breakthrough curves of 2,4-DCP are well fitted for all run by Yan model with r^2 values >0.95. The r^2 values at a flow rate 5 mL min^{-1} and different particle size are comparatively better fit than at the flow rate 10 mL min^{-1}. The predicted Yan capacity (q_y) is similar for col-2 (Run-1) and for other column the q_y (Yan capacity) is about 50% of the q_{BTC} (Table 7.8).

The parameters of three models and their r^2 values are given in tables 7.6, 7.7 and 7.8 respectively. It was observed that the Yan model gave the best fit to the experimental data with r^2 values are greater than 0.95. The difference between q_{BTC} and q_{th} is smaller compared to the Yan model. The values of τ (half of breakthrough time) by the Yoon-Nelson model are well predicted for all runs. It was found that Thomas model gave the best fit to the experimental data at smaller particle size (1.18 mm) which is more than 80% of the experimental values. Though the Yan model gives greater r^2 values (>0.95), Thomas model better predicted the column capacity.

7.8 Conclusion

Pine was found to be an effective sorbent in removing 2,4-DCP from aqueous solution. Sorption of 2,4-DCP was found to be dependent on the residence time and flow rate. The decrease in breakthrough time and sorption capacity of 2,4-DCP due to the increased flow rate reflects the shorter residence time in the column. The permanganate

modified pine and larger particle size showed decrease of 2,4-DCP sorption. However, modified pine may be used as a reactive media in permeable barrier system to remove dissolved metals as well as 2,4-DCP from aqueous solution. The results demonstrated that the Thomas model fitted the experimental data little better at lower flow rate. However, the data are valid of these analytical models for experimental conditions used in this study.

CHAPTER 8

Oxidation of sorbed chlorophenols: batch and column study

8 Oxidation of sorbed chlorophenols: Batch and column study

8.1 Introduction

In the proposed barrier system there are 6 processes that could occur

1. sorption of dissolved CP to pine
2. oxidation of dissolved CP by dissolved $KMnO_4$
3. oxidation of pine by dissolved $KMnO_4$
4. oxidation of pine with sorbed CP by dissolved $KMnO_4$
5. desorption of CP from pine
6. oxidation of CP by in-situ MnO_2

The reaction of permanganate with pine is complex. This study investigated the reaction of permanganate with pine and pine with sorbed CP. Batch and column experiments were designed and carried out to determine permanganate consumption. Batch experiments at a higher permanganate concentration at pH ~2 (to avoid MnO_2 interferences) were conducted to determine the permanganate consumption by pine. This can be used to determine the maximum oxidant demand by pine. Batch experiments with a lower concentration were designed to determine the permanganate consumption and kinetic behaviour with pine/sorbed CP at neutral pH environment. In this study 2-chlorophenol (2-CP), 4-chlorophenol (4-CP) and 2,4-dichlorophenol (2,4-DCP) were chosen for the batch experiment. Column experiments under dynamic in-situ conditions were used to determine permanganate transport and consumption for the treatment of pine and 2,4-DCP sorbed in pine. Two different flow rates were tested.

Each of these processes was investigated by batch or column studies prior conducting an integrated experiment where all processes would occur. However, it was not always possible to have just a single process occurring in an experiment.

8.2 Stoichiometry

The theoretical stoichiometric reaction for complete 2-CP or 4-CP oxidation can be described by equation 8.1. It assumed no intermediates were formed during the oxidation reaction.

$$3C_6H_4ClOH + 26KMnO_4 + 4H_2O \longrightarrow 18CO_2 + 3KCl + 23KOH + 26MnO_2 \qquad (8.1)$$

The percentage of destruction efficiency was calculated from the stoichiometry using equation 8.1 for 2-CP, 4-CP and 2, 4-DCP.

8.3 Batch studies

8.3.1 Sorption of dissolved CP to pine

For this experiment, to determine the CP sorption capacity of pine, initially, a kinetic study was performed to determine the equilibrium sorption time (section 3.7.6). The sorption capacity of pine was determined from equilibrium sorption (section 3.7.7). The equilibrium sorption capacities (q_e) of the chlorophenols are in the order 2, 4-DCP > 4-CP > 2-CP (Table 8.1) for the same initial concentration (~100 mg L^{-1}) of CP. It shows that the sorption capacity of phenolic compounds increases with an increase in the hydrophobicity of that compound as indicated by their increased log K_{ow} value (Table 8.1).

Table 8.1 Sorption of CP on pine: contact time 3 days, mixing rate150 rpm, 22 °C

particle size, mass (mm, g)	Compounds	log K_{ow}	C_e (mg L^{-1})	q_e (mg g^{-1})	q_e (mM)
1.18 (2)	2-CP	2.12–2.17	49	1.02	0.40
1.18 (2)	4-CP	2.35–2.44	44	1.13	0.44
1.18 (1.5)	2,4-DCP	2.75–3.30	39	1.62	0.37
4.75 (1.5)	2,4-DCP	--	31	1.83	0.42

8.3.2 Oxidation of dissolved CP by dissolved $KMnO_4$

The oxidation of CP with MnO_4^- was carried out in an aqueous solution. The observed first order rate constants are shown in Table 8.2 (data extracted and calculated from Table 5.3).

Table 8.2 Rate constants for chlorophenol (~0.16 mM) oxidation by $KMnO_4$ (1.5 mM): initial pH 7.0, 22 °C

Compounds	Reaction time (min)	k_1 (min^{-1})	r^2
2-CP	1.5	1.48 ± 0.244	0.996
4-CP	4	0.39 ± 0.141	0.998
2,4-DCP	4	0.41 ± 0.054	0.996

k_1= pseudo first order rate constant = the mean value ± 95% confidence interval

The oxidation of CP was rapid with excess MnO_4^- and follows first-order. Up to 73–86% oxidation was taking place within 4 min (section 5.2).

8.3.3 Oxidation of pine and pine with sorbed CP by dissolved $KMnO_4$

$KMnO_4$ consumption

The consumption of permanganate by pine and sorbed CP on pine was determined in batch experiments during oxidation (methods in section 3.7.11). Oxidation of pine

containing sorbed CP was carried out after equilibrium sorption (section 8.3.1). Both pine and sorbed CP on pine shows relatively rapid initial $KMnO_4$ consumption followed by a slow increase in $KMnO_4$ consumption (Figure 8.1).

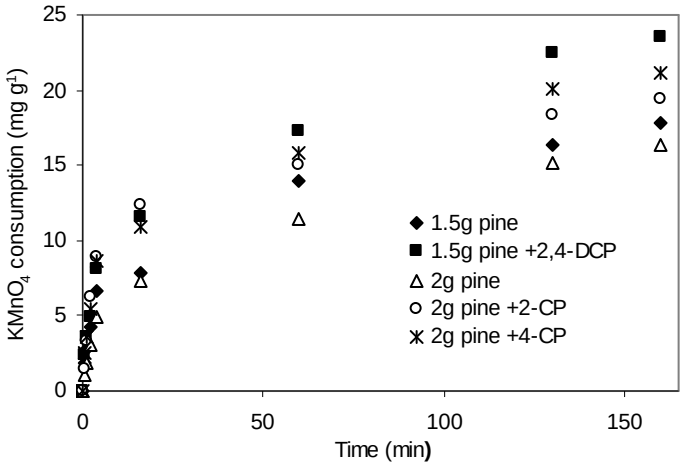

Figure 8.1 Consumption of $KMnO_4$ on pine (1.18 mm) and sorbed CP in pine: $KMnO_4$ ~4 mM, initial pH 6.15, 22 °C

The consumption of $KMnO_4$ by reaction with pine is the result of several stages of reaction. Each of these is likely to react at different rate. Permanganate concentrations and measured consumption after 160 min are presented along with the removal of CP determined from the stoichiometry relationship (equation 8.1) using $KMnO_4$ consumption data (Table 8.3).

Table 8.3 $KMnO_4$ consumption during oxidation of pine and sorbed-CP after 160 min reaction: $KMnO_4$ (~4 mM), initial pH 6.15, 22 °C

Particle size, mass (mm, g)	CP used	Sorbed CP From Table 8.1 (mg g^{-1})	MnO_4^- consumption: pine with sorbed CP (mg g^{-1})	MnO_4^- consumption: Total (mg g^{-1})	MnO_4^- consumption: sorbed CP (mg g^{-1})	*CP removed (%)
1.18 (1.5)	-	-	-	17.88	---	---
1.18 (1.5)	2,4-DCP	1.62	23.55	30.84	12.96	76%
4.75 (1.5)	-	-	-	14.34	---	---
4.75 (1.5)	2,4-DCP	1.83	21.28	28.98	14.64	73 %
1.18 (2)	-	-	-	16.33	---	---
1.18 (2)	2-CP	1.02	19.37	24.49	8.16	79%
1.18 (2)	4-CP	1.13	21.17	25.37	9.04	83%

*calculated by stoichiometry

The consumption of $KMnO_4$ by pine was slightly greater for the smaller particle size (16-18 mg g^{-1}) compared with the larger particle size (~14 mg g^{-1}). The results also show a greater MnO_4^- consumption when the pine has sorbed CP compared to just pine and a small decrease in consumption due to a larger sorbent particle size is seen when the $KMnO_4$ is linked to CP oxidation. Using stoichiometry, the results show that ~73–83% of sorbed CP can be destroyed. It appears the more strongly sorbed compounds i.e. 2,4-DCP < 2-CP < 4-CP have slightly lower rates of oxidation.

The results show that permanganate consumption by pine is comparable with the values used for Kappa number determination (Chai and Zhu, 1999). Chai and Zhu (1999) found, for example, 0.1403 g of wood pulp (unbleached pine) required 3.515 mL of $KMnO_4$ (4 mM) where Kappa number was 25.1. In this study, 0.1403 g pine required 5 mL of $KMnO_4$ for particle size 1.18 mm (Kappa No. 35.9) and 4.2 mL of $KMnO_4$ for

particle size 4.75 mm (Kappa No. 30.1) when calculated according to kappa determination.

Reaction kinetics

Initial tests with CP oxidation showed the process was best described by first-order kinetics under excess permanganate concentration. The concentration of $KMnO_4$ had approximately a 10-fold excess (~4 mM) than sorbed CP (Table 8.1). Earlier work also showed that permanganate is effective in oxidizing chlorophenols in aqueous phase (Chapter 5). It was observed that the oxidation of CP (2-CP, 4-CP and 2,4-DCP) was rapid with excess $KMnO_4$ and follow first-order within 1.5–4 min where 73–86% oxidation was takes place. Therefore, the initial linear (<4 min) portion of the curves was used to calculate rate constants from 160 min reaction time.

The analysis found the data had a poor fit to zero-order (r^2 = 0.88–0.93) and a reasonable fit to second-order (r^2 = 0.95–0.96) (data not shown). The first-order (r^2 = 0.97–0.98) kinetic model was a slightly better fit most of the cases to the observed CP data for particle size 1.18 mm. First-order kinetics was used within 4 min where 30–46% of the reaction occurred (Figure 8.2) to design the experiments. A plot of ln $[KMnO_4]_t/[KMnO_4]_o$ vs. time gives linear curves, the slope of which can be used to estimate first-order rate constants for the consumption of $KMnO_4$ (Figure 8.2).

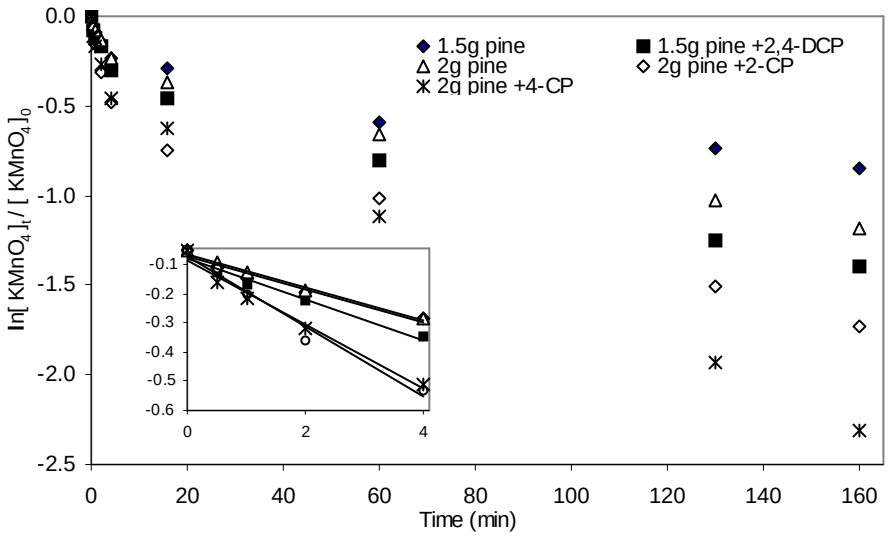

Figure 8.2 The kinetics of oxidation of $KMnO_4$ with pine and sorbed CP in pine: Reaction time 0-4 min (inset) and 0-160 min, Pine 1.18 mm, $KMnO_4$, (~4 mM), initial pH 6.15, 22 °C

Typical kinetic plots of $KMnO_4$ by pine and sorbed CP follows a similar pattern over 160 min of investigation (Figure 8.2). The rate of consumption of $KMnO_4$ slowed as the reaction proceeded and deviated from the linearity. Also, it was observed that the reaction between pine and sorbed CP still occurring at the end of the experimental period. The observed first-order rate constants were 0.0560–0.1211 min^{-1} for pine and sorbed CP within 4 min is shown in Table 8.4.

Table 8.4 First-order rate constants for pine (1.18 mm) and sorbed CP oxidation by $KMnO_4$ (~4 mM): initial pH 6.15, 22 °C

Pine mass (g)	CP used	Rate Constant 0–4 min $^{a}k_1$ (min^{-1})	r^2	Rate Constant 0–160 min $^{a}k_1$ (min^{-1})	r^2
1.5	-	0.0564 ± 0.0016	0.970	0.0048 ± 0.0001	0.909
1.5	2,4-DCP	0.0693 ± 0.0019	0.970	0.0082 ±0.0001	0.953
2	-	0.0559 ± 0.0040	0.984	0.0070 ± 0.0002	0.958
2	2-CP	0.1211 ± 0.0027	0.977	0.0097 ±0.0001	0.907
2	4-CP	0.1096 ± 0.0013	0.981	0.0133 ±0.0002	0.973

$^{a}k_1$ (first-order rate constant) = the mean value ± 95% confidence interval

The oxidation reaction kinetics is complex due to the heterogeneous interaction with pine. The greater reaction rate of pine with sorbed CP compared to pine alone within 4 min indicates that sorbed CP may be preferentially oxidised compared to just the lignin in the pine. The slower the reaction after 4 min may be due to the MnO_2 accumulated on the pine surface which might be the reason for the deviation from the pseudo-first-order conditions as the kinetics reaction proceeded. Another possibility is that $KMnO_4$ also becomes rate limiting, hence it shows as a second-order reaction.

8.3.4 Desorption of CP from pine

Following sorption equilibrium, the rate of desorption was carried out (section 3.7.8). Desorption kinetics shows that only 1.2–1.9% of total sorbed CP desorbs by 5 minutes (Table 8.5).

Table 8.5 Desorption of CP from pine

Time (min)	Compounds	Solid phase (pine) loading		% remaining in liquid phase after desorption
		before desorption q_{sorp} (mg g^{-1})	after desorption q_{desorp} (mg g^{-1})	
5	2-CP	1.08	1.06	1.9
5	4-CP	1.19	1.17	1.7
5	2,4-DCP	1.69	1.67	1.2

No significant desorption was found in the aqueous solution within 5 min which shows pine has a high level of non-reversible sorption. Therefore, it was thought that oxidation may have occurred through direct interaction of permanganate and sorbed CP in solid phase (pine) instead of desorption followed by oxidation in the liquid phase. The higher rate constant of pine sorbed with CP compared with pine alone indicated that sorbed CP can be easily oxidized by $KMnO_4$ during this rapid stage.

8.3.5 Oxidation of CP by in-situ MnO_2

The mass of MnO_2 formed in-situ as oxidation reaction by-product is difficult to quantify in an aqueous medium. It was measured by drying the in-situ MnO_2. This dry weight was used to estimate the in-situ MnO_2. The concentration of in-situ formed MnO_2 in this process was found ~0.034 mM. Experiments were carried out (section 3.7.12) with excess CP to create a pseudo-first-order kinetics. The r^2 values for zero-order were in the range 0.84–0.94 and for second-order were in the range 0.97–0.98 (data not shown). The r^2 for pseudo-first-order were in the range 0.98–0.99 slightly better fit with the observed kinetic data (Figure 8.3).

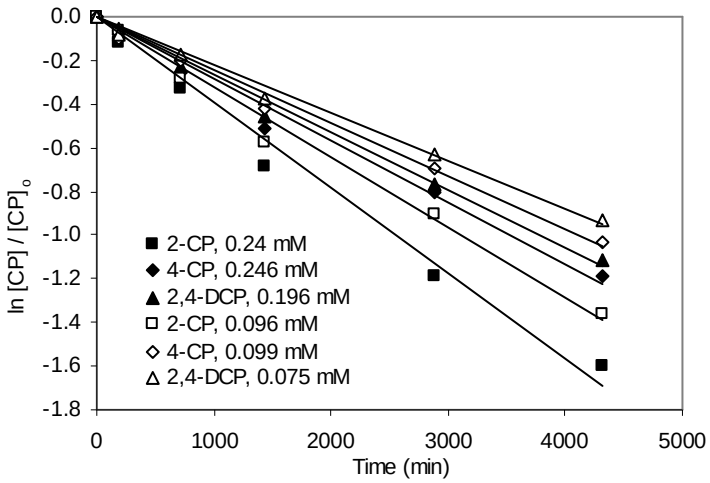

Figure 8.3 Oxidation fit curves of CP by in-situ MnO_2: [CP] ~0.075-0.246 mM, [MnO_2] ~0.034 mM, Initial pH ~5.0, 22 °C

Other studies found sorptive loss of 4-CP on MnO_2 was less than 10% of the total mass (4-CP) (Ko et al., 2007). They also mentioned that the decrease in 4-CP concentration in an aqueous medium is mainly due to the oxidative reaction with MnO_2. Therefore, CP reaction with MnO_2 was investigated to evaluate the kinetics (Table 8.6).

Table 8.6 Rate constant for CP oxidation by in-situ MnO_2 (~0.034 mM), initial pH ~5.0, 22 °C

CP	Conc. of CP (mM)	[a]k_1 ($\times 10^{-1}$ min^{-1})	r^2
2-CP	0.096	0.0032	0.988
2-CP	0.240	0.0039	0.985
4-CP	0.099	0.0024	0.988
4-CP	0.246	0.0028	0.984
2,4-DCP	0.075	0.0022	0.991
2,4-DCP	0.196	0.0027	0.992

[a]k_1-first-order rate constant

The reaction was relatively slow. The 2-CP shows higher reactivity towards oxidation by MnO_2 compared to other chlorophenols (4-CP, 2,4-DCP). The results of this study indicate that MnO_2 will not facilitate the oxidation of CP under these experimental conditions.

Conclusion

During the initial stage (4 min) the oxidation of sorbed CP with $KMnO_4$ is correlated with rapid permanganate consumption and consequently has a higher rate constant (Table 8.4) than pine alone. This indicates CP is the contributing reactant with regard to the consumption of $KMnO_4$. Also, it was found that the rate constant of the reaction of $KMnO_4$ and dissolved CP was higher (Table 8.2) than the rate constant of $KMnO_4$ and pine (Table 8.4) over the same period of time. This suggests that the oxidation of CP takes place regardless of any consumption of $KMnO_4$ interaction of pine materials. So, the reactions between permanganate and cellulosic materials (lignin, hemicellulose and cellulose) will dominate only after the oxidation reaction with CP. Both probably occur simultaneously however one finishes before the other and has a greater rate. However further work is needed to better understand this process. The rates of sorbed CP are 2,4-DCP < 2-CP ~4-CP while for the dissolved it is 2,4-DCP~4-CP < 2-CP. The reason for 4-CP having a relatively slower rate when is sorbed compared with this when it is dissolved is not currently understood. There is relatively little published work to compare these results.

8.3.6 Spectral evidence for $KMnO_4$ oxidation

8.3.6.1 Reaction between $KMnO_4$ and pine/sorbed 2,4-DCP

Spectral evidence was undertaken to prove that the decreased concentration of permanganate was due to oxidation. This was done by showing the occurrence of MnO_2. To obtain spectroscopic evidence of $KMnO_4$ consumption during pine and with sorbed 2,4-DCP oxidation, samples were successively scanned by a UV-visible spectrophotometer. The oxidation of permanganate caused a perceptible change in the spectrum during reaction of pine (Figure 8.4) and sorbed 2,4-DCP (Figure 8.5) with permanganate over time.

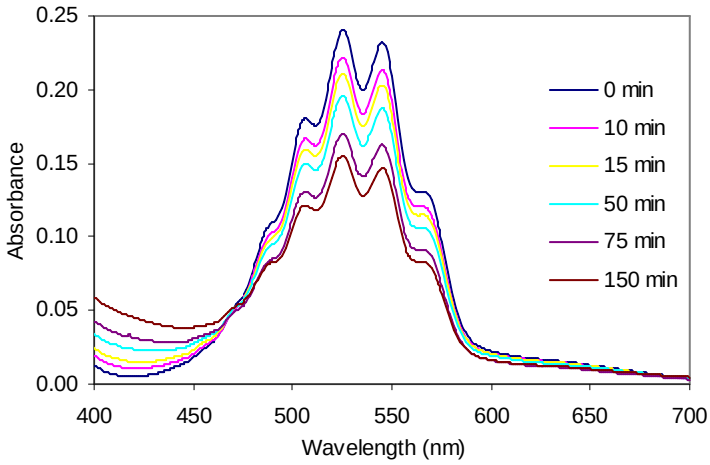

Figure 8.4 Spectral changes during the oxidation of MnO_4^- (~0.1 mM) and 1.5 g of pine (4.75 mm), 22 °C

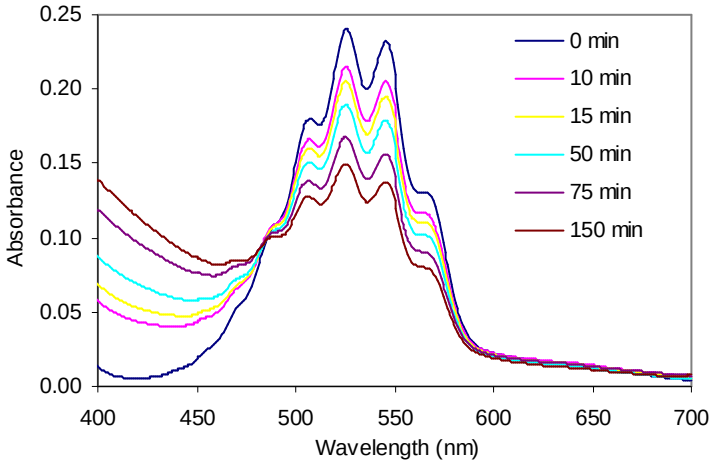

Figure 8.5 Spectral changes during the oxidation of MnO_4^- (~0.1 mM) and 1.5 g of pine (4.75 mm) sorbed with 2,4-DCP, 22 °C

The absorption intensity in the region 460–600 nm is attributable to $KMnO_4$ and it decreased as the reaction proceeded due to the consumption of permanganate. Therefore, the decrease in MnO_4^- concentration implies oxidation reaction with pine and with sorbed 2,4-DCP.

8.3.6.2 MnO_2 formation

Between 400 and 460 nm, the absorbance increased as the reaction proceeded. The absorption at wavelength 418 nm increased from 0.005 to 0.046 for pine and 0.005 to 0.116 for sorbed 2,4-DCP (Figures 8.4 and 8.5), indicating the formation of species other than permanganate because permanganate has no absorbance at this wavelength. Similar results were found by Yan and Schwartz (1999) during oxidation of TCE-permanganate and they concluded that the produced species was colloidal MnO_2. It was observed that MnO_2 gradually developed with pine as the reaction time increased (Figure 8.4). However, when reacts pine with sorbed 2,4-DCP the formation of MnO_2 was enhanced (Figure 8.5) as the reaction time increased. It was found that the MnO_2

formation was higher for sorbed 2,4-DCP than just pine. This suggests the oxidation rate of sorbed 2,4-DCP was higher by MnO_4^- as show in the rate constants (Table 8.4).

8.3.6.3 Isosbestic point

A sharp isosbestic point was found during successive scans of the reaction (Figures 8.4 and 8.5). A isosbestic point indicates that MnO_2 behaves according to Beer's Law. The isosbestic point was found at 475 nm for pine and 485 nm for sorbed 2,4-DCP during oxidation with permanganate. Almost similar isosbestic points were found for TCE at 467 nm (Waldemer and Tratnyek, 2006) and for trimethylamine at 470 nm (Mata-Perez and Perez-Benito, 1985) during oxidation with permanganate. A sharp isosbestic point also implies that Beer's law is fulfilled and no long lived intermediates are formed during the reaction (Lee and Perez-Benito, 1985). A linear relationship between the absorbance at 525 nm (where both permanganate and manganese dioxide absorb) and the absorbance at 418 nm (where only manganese dioxide absorbs) was found when both reactant (MnO_4^-) and product (MnO_2) absorb light are plotted (Figures 8.6 and 8.7), indicates Beer's Law obeyed.

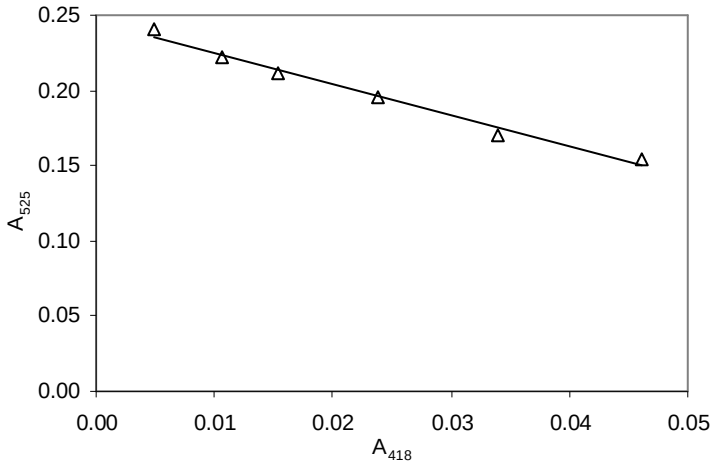

Figure 8.6 A linear relationship between absorbances at two wavelength A_{525} and A_{418} for pine and $KMnO_4$ reaction

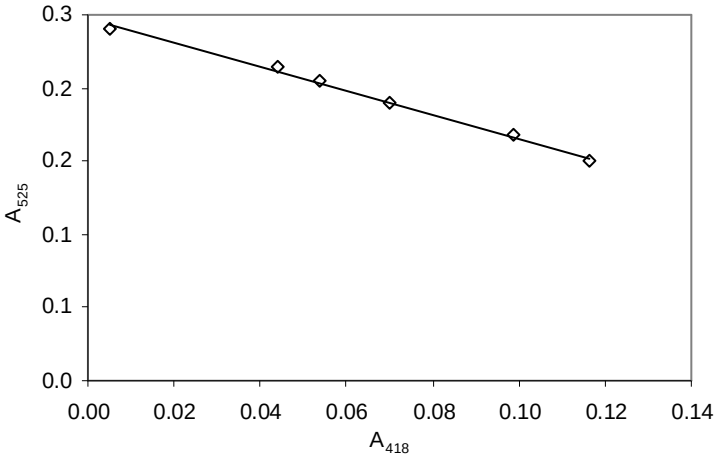

Figure 8.7 A linear relationship between absorbances at two wavelength A_{525} and A_{418} for sorbed 2,4-DCP and $KMnO_4$ reaction

8.4 Column studies

Column experiments were designed to investigate the effect of flow rate and reaction of sorbed-2,4-DCP on the consumption of $KMnO_4$ by pine.

Pore volume and effective porosity

Chloride breakthrough curves were constructed by plotting relative concentration (effluent concentration divided by influent concentration) versus accumulated effluent volume (Figure 8.8).

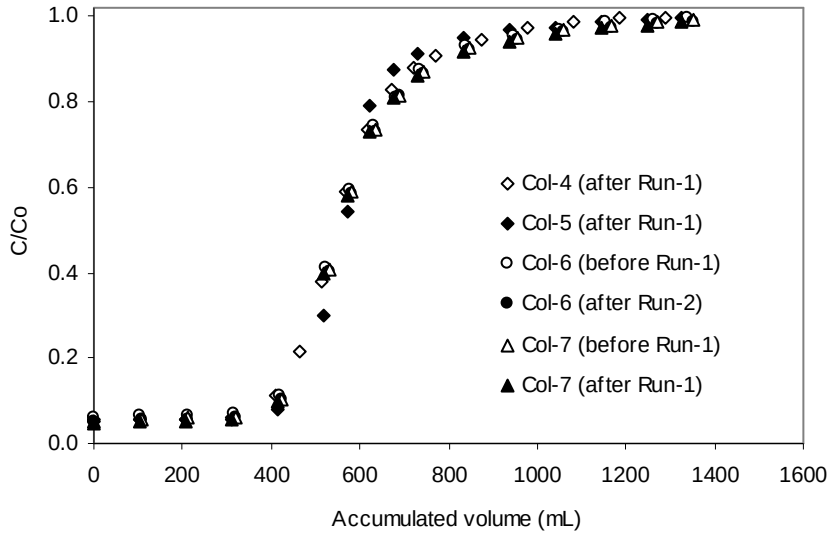

Figure 8.8 Chloride breakthrough curves for $KMnO_4$ pine column

The pore volume (PV) of all columns was determined from chloride tracer tests. The PV for each column is shown in Table 8.7.

Table 8.7 Column characteristics: pine particle size 4.75 mm, mass of pine 66 g, mass of glass beads 1665 g

Column and Run No.	Flow (mL min^{-1})	Pore volume (mL)	Porosity
Col-4 (After Run-1)	10	513	0.42
Col-5 (After Run-1)	5	531	0.43
Col-6 (Before Run-1)	5	526	0.43
Col-6 (After Run- 2)	5	518	0.41
Col-7 (Before Run-1)	5	525	0.43
Col-7 (After Run-1)	5	517	0.42

The $KMnO_4$ breakthrough curves were developed from the $KMnO_4$ consumption based on the influent quantity of $KMnO_4$ supplied to the columns and the quantity of $KMnO_4$

recovered from the effluent. The first goal was to determine the extent of pine reaction with permanganate particularly at different flow rates. Those flow rates were designed to simulate different kinetic conditions. The second goal was to investigate the reactivity.

8.4.1 $KMnO_4$ consumption with pine (effect of flow)

Two pine columns were flushed with $KMnO_4$ at concentration ~3.8 mM with flow rates of 5 and 10 mL min^{-1}. The $KMnO_4$ BTCs were measured at flow rate 5 and 10 mL min^{-1} under the Col-4 (Run-1) and Col-5 (Run-1) (Table 3.4). The flow was continued until the effluent concentration of $KMnO_4$ changed less than 2% of the previous effluent reading. The breakthrough curves for $KMnO_4$ at flow rate 5 and 10 mL min^{-1} are shown in Figure 8.9:

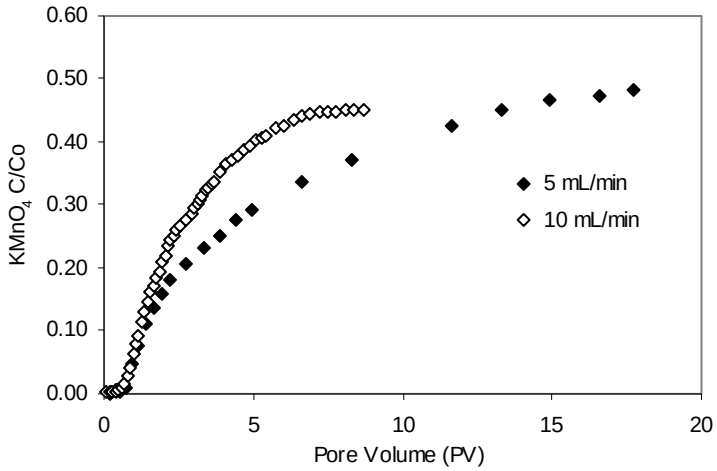

Figure 8.9 $KMnO_4$ consumptions by pine at different flow rate: Col-4 (Run-1) and Col-5 (Run-1), $KMnO_4$ ~3.8 mM, Pine 4.75 mm

Table 8.8 Column data and parameters obtained at different flow rates

Column No.	Flow mL min^{-1}	C/C_o = 0.01 Time (min)	C/C_o = 0.01 No. of PV	C/C_o = ~ 0.5 Time (min)	C/C_o = ~ 0.5 No. of PV	$KMnO_4$ Consumption as MnO_4^- (mg g^{-1})
Col-4 (Run-1)	10	30	0.58	445	8.7	5
Col-5 (Run-1)	5	80	0.74	1920	17.7	12.3

PV-pore volume

The point on the breakthrough curve (in case of $KMnO_4$ and pine reaction) at which the $KMnO_4$ concentration reaches to C/C_o = 0.01 and C/C_o = 0.5 (i.e. 50% of the influent concentration) were considered break point and the point of column exhaustion, respectively. After this point the effluent concentration changes slowly (less than 2% of the previous reading). While the exhaustion point for pine and 2,4-DCP was (C/C_o ~0.8). Therefore to run this experiment to exhaustion (i.e. C/C_o ~0.8) would require a very long time. The consumption of $KMnO_4$ onto pine was strongly influenced by flow rate. The data (Table 8.8) indicates that the performance of MnO_4^- pine column until the (C/C_o ~ 0.5) at flow rate 10 mL min^{-1} is lower than that at flow rate 5 mL min^{-1}. The effect of flow on the breakthrough curve is similar to that found for the sorption data (Figure 7.2). However, the sorption effluent data reached a relatively higher fraction of influent (~0.8) compared with the oxidation data (~0.5). This suggests that the impact of kinetics was found for pine oxidation compared to sorption at this pH and flow rate.

The delay in permanganate breakthrough (C/C_o ~0.5) with flow rate 5 mL min^{-1} compared to the flow rate 10 mL min^{-1} was due to the greater reaction time available with pine. Thus at flow rate 5 mL min^{-1} it requires more volume to fulfil its permanganate consumption requirements rather than less volume at flow rate 10 mL min^{-1}.

8.4.2 $KMnO_4$ consumption with pine/sorbed-2,4-DCP at flow 5 mL min^{-1}

One column (Col-5, Run-1) was flushed with $KMnO_4$ (~3.8 mM) at flow rate 5 mL min^{-1}. Another column (Col-6) was initially flushed with 2,4-DCP (~1.84 mM) and then flushed with $KMnO_4$ (Section 3.7.13) keeping the same flow rate to determine the oxidation behaviour of pine with sorbed 2,4-DCP by $KMnO_4$. The breakthrough curve for $KMnO_4$ and sorbed 2,4-DCP column at flow rate 5 mL min^{-1} is shown in Figure 8.10:

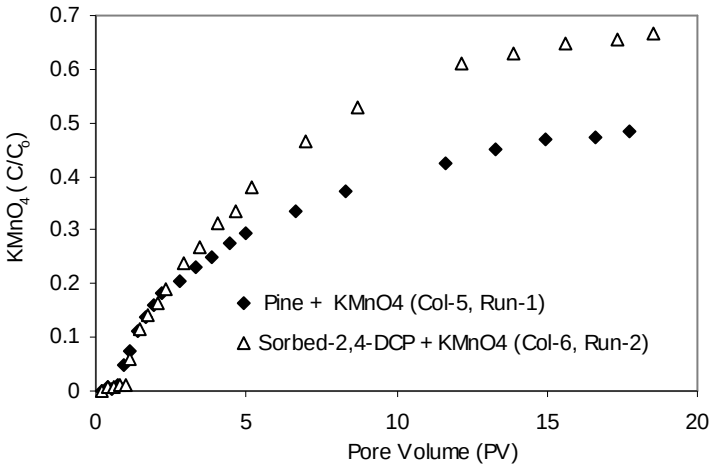

Figure 8.10 $KMnO_4$ consumption after 2,4-DCP sorption to pine: Col-5 (Run-1) and Col-6 (Run-2), 2,4-DCP ~1.84 mM, $KMnO_4$ ~3.8 mM, Pine 4.75 mm

Table 8.9 Column data and parameters obtained with pine/sorbed 2,4-DCP at flow 5 mL min^{-1}

	C/C_o = 0.01		C/C_o = ~0.5		C/C_o = ~0.7		$KMnO_4$ Consumption as MnO_4^- (mg g^{-1})
Column No.	Time (min)	No. of PV	Time (min)	No. of PV	Time (min)	No. of PV	
Col-5 (Run-1)	80	0.74	1920	17.7	--	--	12.3
Col-6 (Run-2)	86	0.83	900	8.7	1920	18.2	17.7

PV- pore volume

The point on the breakthrough curve (in case of $KMnO_4$ and sorbed 2,4-DCP with pine reaction) at which the $KMnO_4$ concentration reaches to C/C_o = 0.01 and C/C_o = ~0.7 (i.e. 70% of the influent concentration) were considered break point and the point of column exhaustion, respectively. After this point the effluent concentration changes slowly (less than 2% of the previous reading) while the exhaustion point for pine and $KMnO_4$ was (C/C_o ~0.5).

The results show (Table 8.9) exhaustion point 0.5 for pine and permanganate oxidation while exhaustion required ~ 0.7 for oxidation pine with sorbed 2,4-DCP within the same time frame (1920 min). This is due to the oxidation of permanganate with 2,4-DCP and pine where more permanganate (17.7 mg g^{-1}) is consumed compared with pine alone (12.3 mg g^{-1}). It indicates a greater capacity of reaction of permanganate with 2,4-DCP compared to pine which is consistent with our observations from the batch experiments initial kinetic results (for pine and $KMnO_4$ = 0.056 min^{-1}, sorbed 2,4-DCP with pine and $KMnO_4$ = 0.069 min^{-1}, Table 8.4).

The effluent concentration of permanganate reached only 50 and 67% of the inlet concentration for Col-5 (Run-1) and Col-6 (Run-2) respectively. The incomplete breakthrough (C/C_o < 100%) occurred with 18.2 pore volumes (PV) for Col-6 (Run-2) and 8.7 PV for Col-5 (Run-1). It indicates that a slow reaction was still occurring between the pine and sorbed 2,4-DCP at the end of each column experiments which is consistent with the batch test. The initial pH was stable (~5.6-5.8) while the effluent pH varied to a larger extent (5.9-7.05). The consumption of $KMnO_4$ by pine and 2,4-DCP sorbed pine were 12.3 mg g^{-1} and 17.7 mg g^{-1} , respectively at flow rate 5 mL min^{-1} (Table 8.9). Therefore, 2,4-DCP sorbed on pine has a higher rate of $KMnO_4$

consumption in the oxidation column compared to the column without 2,4-DCP. Further work into this apparent inhibition of oxidant consumption at neutral pH is needed.

The consumption of $KMnO_4$ by pine alone observed in the column study was approximately 0.86 and 0.35 times lower than the batch study for 5 mL min^{-1} and 10 mL min^{-1} respectively (Tables 8.3 and 8.8). This difference may be due to the pine and aqueous solution contact differences between column and batch study. This is consistent with the study found by Mumford et al. (2005). They also observed much lower $KMnO_4$ consumption (average 0.35 mg g^{-1}) in the column experiments compared to the batch experiments (>1.2 mg g^{-1}) using aquifer materials.

The removal of 2,4-DCP was determined from the stoichiometry relationship in equation 8.1. It was found that the consumption of $KMnO_4$ by pine was 12.3 mg g^{-1} (Col-5, Run-1) and pine with sorbed 2,4-DCP was 17.7 mg g^{-1} (Col-6, Run-2). For sorbed pine, 2,4-DCP loading was 17.5 mg g^{-1} (Col-6, Run-1). Using these data percentage removal of 2,4-DCP was found 11.6%. The lower percentage of removal may be due to 2,4-DCP desorbed within the $KMnO_4$ aqueous solution during flushing of $KMnO_4$ through the column. In addition, higher removal may not be possible at this flow rate due to relatively short contact time. At the end of each column experiment, the BTCs exhibited a long tail where the change of permanganate concentration was very slow, indicating a slow reaction.

8.4.3 Evidence of MnO_2

The oxidation of CP with permanganate will give manganese dioxide particles as described by equation 8.1. Evidence of particulates produced in the system was also found in the effluent sample analysis. The increase in absorbance at 418 nm suggests that the MnO_2 particulates and the brown colour in the effluent are due to increase on the amount MnO_2. Also, it was found that the absorbance at 418 nm in the reaction of pine with sorbed 2,4-DCP is higher than just pine (Figure 8.11).

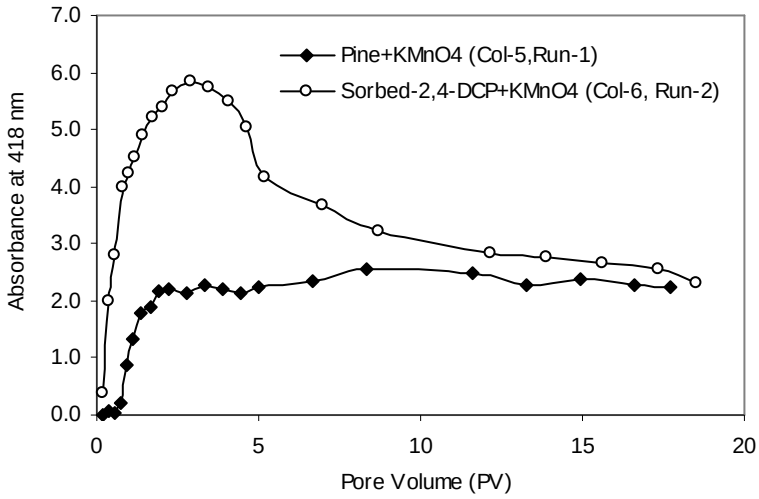

Figure 8.11 MnO_2 absorbance for effluent sample under the Conditions: Col-5 (Run-1) and Col-6 (Run-2)

The increasing MnO_2 absorbance for pine with sorbed 2,4-DCP was due to a greater consumption of $KMnO_4$ from greater oxidation. Other authors have also observed brown precipitates in the effluent of column studies during oxidation of PCE and TCE with permanganate (MacKinnon and Thomson, 2002; Schroth et al., 2001).

At the end of the experiment the Col-6 (Run-2) was flushed with distilled water and the pore volume determined. The porosity of the Col-6 (Run-2) was calculated and found to be 0.41 which is slightly lower than the previous porosity (0.43) of the Col-6 at flow rate 5 mL min^{-1}. However, the porosity was not significantly decreased after a tracer test in the Col-6. The difference of porosity is assumed to be due to the plugging of MnO_2 from the interaction of $KMnO_4$ with pine materials and the sorbed 2,4-DCP within the column. Therefore, the Col-6 (Run-2) may have some in-situ MnO_2.

The formation of MnO_2 resulting from the oxidation of $KMnO_4$ have been studied by many authors (Siegrist et al., 2002; Waldemer and Tratnyek, 2006). Siegrist et al., (2002) reported from their column experiment, permeability loss was possible during ISCO by $KMnO_4$ under conditions with very high MnO_2 production. Lowe et al. (2002) observed no loss of permeability where 250 mg L^{-1} was delivered during ISCO. In contrast, when flushed with high concentrations of MnO_4^- through a column there was a loss in permeability (Li and Schwartz, 2000; Reitsma and Marshall, 2000).

These studies used relatively course particles (4.75 mm) as well as high permeability sand (0.6 mm) and therefore the mass of precipitate was minor compared to the pore space and hence minimum permeability decline (clogging) was found. Also, this study use lower concentration (~4 mM $KMnO_4$) in all of the $KMnO_4$ column experiments, a decrease in porosity (2.3-4.7%) was observed by pre-oxidant and post-oxidant tracer test. This suggests that the decrease in porosity was due to the precipitation/clogging of MnO_2 on porous media (pine) was not significant.

Visual post-experimental inspection of pine material indicates that the colour of the pine material was changed to brownish black (Figures 8.12, 8.13). These brownish black coatings are believed to be MnO_2, which is the by product of $KMnO_4$ oxidation by both pine materials and 2,4-DCP. The presence of MnO_2 coatings on the pine material may restrict the ability of $KMnO_4$ to further oxidize on the surface or internal to the pine materials.

Figure 8.12 MnO_2 on pine

Figure 8.13 MnO_2 particles

8.4.4 Zeta potential

Qualitative information of colloid particle growth was obtained from a UV-visible spectrophotometer. To evaluate the stability of manganese colloid particle, zeta potential was measured for the effluent of column 5 after the interaction of MnO_4^- and a pine material which reflects the surface charge of the MnO_2 and indicates the surface charge of the colloids are negative. The higher the repulsive force of the colloidal particle, the more stable (i.e. particles tends to suspend), no matter whether the surface charge is positive or negative (Koohestanian et al., 2008). The zeta potential value ±33 to ±41 (moderate stability) shows repulsive forces of colloid particles (Figure 8.14) which indicates the presence of MnO_2.

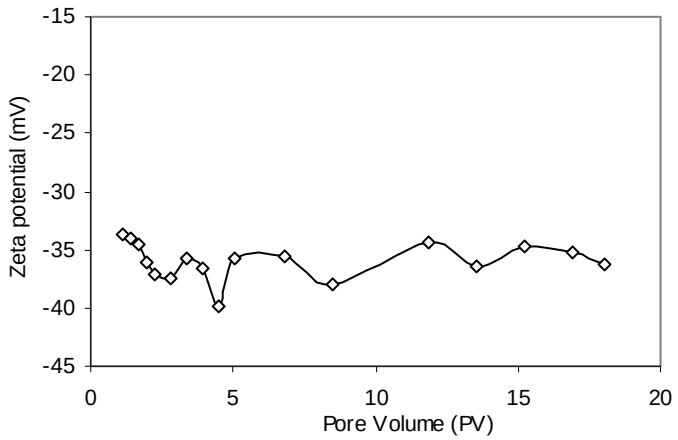

Figure 8.14 Zeta potential measurements of colloidal particles under the conditions: Col-5 (Run-1), $KMnO_4$ ~3.8 mM, Pine 4.75 mm, Flow 5 mL min^{-1}

8.4.5 pH change

It was found that the effluent pH increases (Figure 8.15) with time and has a similar trend to MnO_2 absorbance.

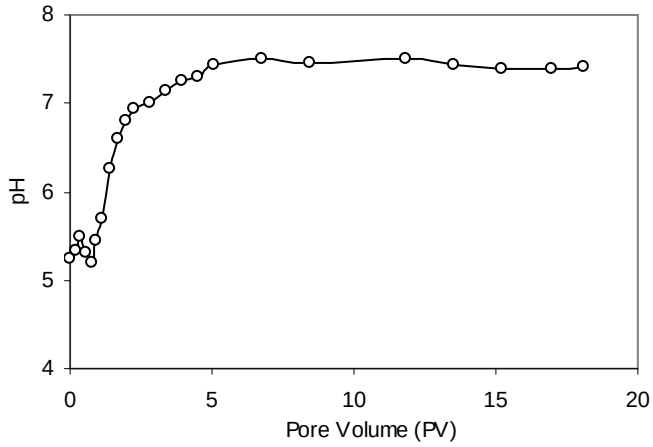

Figure 8.15 pH measurements for effluent sample under conditions: Col-5 (Run-1), $KMnO_4$ ~3.8 mM, Pine 4.75 mm, Flow 5 mL min^{-1}

The stoichiometric equation (8.1) shows that OH^- if generated from oxidation. Therefore, the relationship between pH change and increased MnO_2 generation is linked. Jiang et al. (2009) observed notable catalytic effect of MnO_2 colloids in the pH range 5-6 but negligible at pH 7-9 during oxidation of 2,4-DCP. Also, he mentioned that sorption of phenolic on to MnO_2 decreases with pH increase. Based on the pH analysis, decreases in porosity and the flow rate throughout the Col-6 (Run-2) was not significantly changed indicating the lower precipitation expected under the experimental condition of the Col-6 (Run-2).

8.4.6 Batch $KMnO_4$ consumption at pH ~2

A batch experiment was also conducted with $KMnO_4$ (~61 mM) mixed with 5 g pine. The disappearance of MnO_4^- from the aqueous phase indicates the significant reaction between pine and MnO_4^- at this pH compared to pH 6.15. It was observed that the consumption of $KMnO_4$ increased rapidly in the first stage and then slowly thereafter (Figure 8.16).

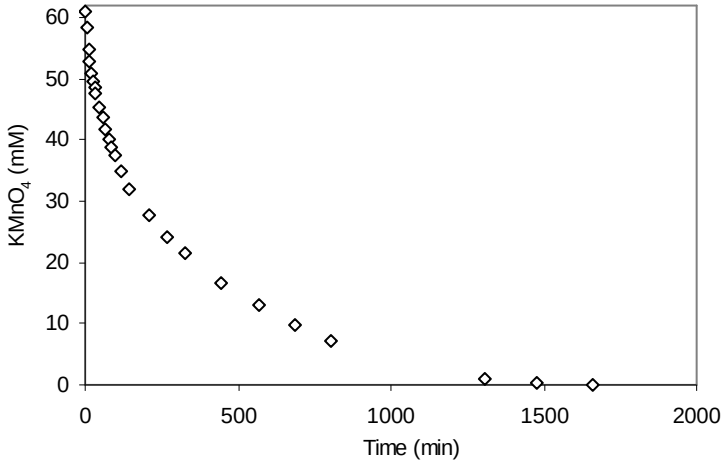

Figure 8.16 The kinetics of oxidation of $KMnO_4$ with pine:
Pine 4.75 mm, $KMnO_4$ (~61mM), pH ~2, 22 °C

The experiment was carried out at pH ~2 to avoid MnO_2 interference. The consumption of MnO_4^- after 160 min reaction using concentration (~61 mM) by 5 g pine was 180 mg g^{-1} which is much greater than at pH 6.15 (Table 8.3). The consumption of MnO_4^- at the end (1657 min) of the experiment was 364 mg g^{-1} and this data provide the maximum consumption of MnO_4^- by pine (4.75 mm).

8.4.7 Column $KMnO_4$ consumption at pH ~2

The column experiments were carried out by passing $KMnO_4$ solution with a flow rate 5 mL min^{-1} and pH~2 through the column (section 3.7.13). Col-7 (Run-1) was flushed with permanganate to observe the pine behaviour during MnO_4^- transport through the uncontaminated pine media. A tracer test was performed before the MnO_4^- flush and after the distilled water flush i.e. post-MnO_4^- tracer test. The detailed column characteristics and parameters are described in section 3.7.13.

The permanganate mass that was consumed in the column was calculated from the area above the breakthrough curve. Breakthrough curve data showed that for the col-7 (Run-1) significant MnO_4^- breakthrough (C/C_o > 97%) was observed (Figure 8.17).

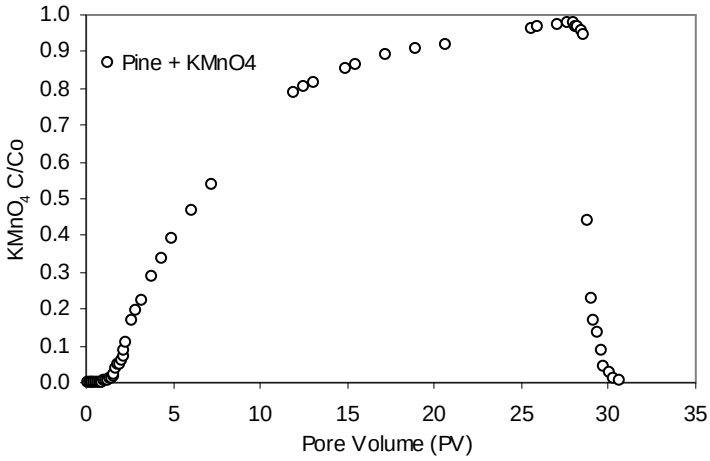

Figure 8.17 $KMnO_4$ consumption by pine: at pH ~2.
Col-7 (Run-1), $KMnO_4$ ~63 mM, Pine 4.75 mm

The appearance of permanganate as a sharp front suggests that breakthrough was possible with nearly complete consumption of MnO_4^- by pine. This can be used to

evaluate the progress of the oxidation reaction of pine and sorbed-2,4-DCP. The lower permanganate consumption by pine was found in the column experiments (~42 mg g^{-1}) compared to the batch experiments (364 mg g^{-1}) at pH 2. This may be due to differing solid liquid ratio, however this significant difference needs to be further investigated. The desorption cycle started immediately after the C/C_o of $KMnO_4$ reached more than 97%. The desorption curves of $KMnO_4$ from pine columns showed a rapid decrease of $KMnO_4$ (Figure 8.17).

8.5 Conclusion

The kinetic concept suggests that $KMnO_4$ consumption by pine material consists of a fast and slow reaction. The MnO_2 might play an important role to passivate the pine materials by making coatings on the surface. The consumption of $KMnO_4$ is important for pine material to fix the $KMnO_4$ delivery efficiency in a remedial scheme. The column experiments indicate that the oxidation of 2,4-DCP by $KMnO_4$ is a promising remediation technology. However, a lower concentration of $KMnO_4$ is useful to reduce the pore plugging which will improve the flushing efficiency. Therefore, the issue of flushing efficiency needs to be considered in the field scale design. Permanganate consumption can be used to evaluate the oxidation reaction of pine and it can be used to design the oxidation reaction of sorbed CP.The influence of different initial $KMnO_4$ concentrations during oxidation of pine and sorbed CP in pine to be further investigated. These analytical results also help determine the applicability of permanganate as regenerant. The feasibility of this technology under actual operating condition at a pilot scale may need to be investigated.

CHAPTER 9

Summary, conclusions and recommendations

9 Summary, conclusions and recommendations

Summary

In this study, investigations were undertaken into mechanisms which would occur in an oxidation-sorption barrier for treating chlorophenol (CP) contaminated water. The chosen oxidant was potassium permanganate ($KMnO_4$) while pine and hardwood were evaluated as sorbents. In conceptualising an oxidation-sorption barrier using permanganate and woody biomass the following potential mechanisms were identified;

- sorption of CP to pine
- oxidation of dissolved CP by dissolved $KMnO_4$
- oxidation of pine by dissolved $KMnO_4$
- oxidation of sorbed CP by dissolved $KMnO_4$
- oxidation of sorbed CP by MnO_2
- desorption of sorbed CP from pine

Within the research timeframe it was not possible to completely investigate all mechanisms with rigour although considerable insight has been gained into this very complex technology. This study involved the development of an analytical method as well as batch and column experiments into oxidation and sorption-desorption processes.

Analytical method development

A simple spectrophotometric method was further developed to quantify chlorophenol concentrations during the study. Analysis at pH 12 gave greater absorption and sensitivity for the method compared with pH 5.6 and in methanol. However existing

chemical methods to quench permanganate-chlorophenol oxidation reactions were not compatible with the spectroscopic method. Traditional quenching agents (peroxide, sodium thiosulfate, hydroxylamine hydrochloride) were found to create absorbance in the spectral range required for CP quantification. Sodium sulphite was found to be suitable. The calibration curves of the proposed method were linear in the concentration ranges 0.0034–0.52, 0.0062–0.62 and 0.0063–0.79 mM with detection limit of 0.0006–0.0008 mM for trichlorophenol, dichlorophenols and monochlorophenols, respectively at pH 12. This method development allowed the oxidation kinetics of six chlorophenols in aqueous solution with excess potassium permanganate to be evaluated.

Oxidation studies

Permanganate oxidation of dissolved trichlorophenol, dichlorophenols and monochlorophenols at neutral pH were evaluated in batch studies. It was found that the reaction is first-order individually with respect to both permanganate and all chlorophenols. The pseudo-first-order rate constant increased with increased initial permanganate dosage and fixed CP concentrations. However the pseudo-first-order rate had minimal change with fixed excess permanganate concentration and increased CP concentration. The reaction of CPs with permanganate was of second-order overall (0.86 to 19.0 M^{-1} s^{-1}) at an initial pH 7.0 and 22 °C with a reaction sequence of 2,4,6-TCP > 2-CP ~2,6-DCP > 2,4-DCP ~4-CP > 3-CP. The reaction rates of 4-CP with permanganate did not show any significant change over pH 5.5–8.5 and ionic strength ~0.02–0.2 M.

Permanganate oxidation of the pine sorbent as well as chlorophenol sorbed to the pine were undertaken both in batch and column experiments. Initial experiments were conducted in a neutral pH, poorly buffered system which was considered representative of many groundwaters. Batch results indicated that $KMnO_4$ consumption by pine and CP sorbed onto pine can be characterized more than one rate constant. Pine appears to compete with the sorbed CPs for $KMnO_4$.

The consumption of $KMnO_4$ by pine was slightly greater for the smaller particle size (16–18 mg g^{-1}) compared with the larger particle size (~14 mg g^{-1}). The results also show a greater MnO_4^- consumption (19–24) mg g^{-1}) when the pine has sorbed CP compared to pine alone (16–18 mg g^{-1}). There is an initial fast reaction (<4 min) which was first-order for both pine and CP sorbed pine. The early time first-order rate constant for $KMnO_4$ and pine were ~0.06 $min^{-1,}$ CP sorbed to pine 0.07–0.12 $min^{-1.}$ In comparison $KMnO_4$ oxidation of dissolved CPs was 0.39–1.48 min^{-1}. Due to faster reaction rates for the oxidation of CP, pine does not need to be consumed fully before CP oxidized. This suggests that the reaction between permanganate and cellulosic materials (lignin, hemicellulose and cellulose) will dominate only after the oxidation reaction with CP. It appears the more strongly sorbed compounds i.e. 2,4-DCP < 2-CP < 4-CP have slightly lower rates of oxidation. Spectral evidence suggests that the concentration of permanganate decreased during oxidation of pine and sorbed CP causing the occurrence of MnO_2. The results of this study also indicate that in-situ MnO_2 will not facilitate the oxidation of CP at these experimental conditions.

Column studies were carried out to investigate $KMnO_4$ oxidation of pine and 2,4-DCP sorbed onto pine at a neutral pH in un-buffered water under two different flow rates. It

was found that at a lower flow rate (5 mL min^{-1}) more $KMnO_4$ was consumed in the pine compared to a higher flow rate (10 mL min^{-1}). This was due to the lower residence time. Column study also indicated that more permanganate consumption (17.7 mg g^{-1}) by the oxidation reaction with sorbed 2,4-DCP rather than reaction with only pine (12.3 mg g^{-1}). It was observed that the effective porosity for column slightly decreased (0.43 to 0.41) due to the precipitation of MnO_2. A batch and column study was then undertaken at pH ~2 to avoid MnO_2 interferences. Under these conditions the batch results showed a significantly greater $KMnO_4$ consumption (364 mg g^{-1}) and the column had a normal breakthrough curve with a consumption of 42 mg g^{-1}.

Sorption studies

Sorption studies were undertaken on Granular Activated Carbon (GAC), filter coal (FC), pine and hardwood (HW). Both sorption capacities and sorption kinetics were investigated to identify a suitable sorbent for the barrier system. Sorption capacity data showed that GAC has a high sorption capacity (294–467 mg g^{-1}) compared to other sorbents (3.2–7.5 mg g^{-1}). However, wood and coal had a greater sorption capacity per unit surface area than GAC. The equilibrium data of pine, HW and FC were found to best fit to both Langmuir and Freundlich models while GAC was best described by Freundlich model. The sorption capacity for all sorbents was 2-chlorophenol (2-CP) < 4-chlorophenol (4-CP) < 2,4-dichlorophenol (2,4-DCP) which correlates well with solute hydrophobicity, although the relative differences were much less in coal than the other sorbents.

The rate of chlorophenol uptake onto pine and HW within 3 hours (50 %) is likewise identical to conventional GAC while FC had a significantly lower uptake (~10% of final uptake after 3 hours) due to intra-particle diffusion limitations. The rapid uptake on wood makes it a good sorbent like GAC. The data fitted a pseudo-second-order model. Determined pseudo-first-order uptake rates indicate that the sorption of chlorophenols on pine and HW is 0.21–0.27 h^{-1} and broadly comparable to that for conventional GAC (0.31–0.38 h^{-1}). Also, chlorophenol interactions with woody materials are similar to GAC through hydrogen bonding. It is possible to use wood (pine, HW) as an alternative low-cost sorbents for the treatment of chlorophenols contaminated water. Intra-particle diffusion studies showed that the sorption rates for the three sorbents (GAC, pine and HW) were not solely controlled by the diffusion step whereas intra-particle is the only rate limiting mechanism for sorption onto coal over a long contact time period. However, FC could be used for the long residence time within a groundwater barrier.

The influence of sorbent particle size on sorption kinetics of CP by different sorbents was evaluated. The range of particle sizes used in this study does not appear to have a significant affect on chlorophenol sorption. This was investigated and attributed to the elongate nature of the wood particles. From particle size experiments it appeared that the equilibrium sorption capacity of pine did not change with the particle size, but the rate of sorption for pine, GAC and FC were slightly decreased with increasing particle size. The results showed that pine, hardwood and filter coal can be used as sorbent materials for the removal of chlorophenol from water; however kinetic considerations may limit the application of filter coal**.**

Desorption experiments were conducted for pine and HW after equilibrium sorption. Desorption kinetics from pine and HW followed a biphasic pattern with a fast desorption phase in the first 6 hours and followed by slow phase. The results revealed that desorption of CP from pine and HW exhibited positive hysteresis.

In the column study, pine used as a reactive porous media for the removal of 2,4-DCP, sorption breakthrough curves were measured under different flow rates and with different sorbent particle sizes. It was found that the sorption capacity of 2,4-DCP (21 mg g^{-1}) on pine (1.18 mm) was higher than the equilibrium batch sorption studies. The breakthrough time and uptake capacity decreased as the flow rate increased whereas particle size did not significantly affect on sorption capacity. Several different analytical models (Thomas, Yan and Yoon-Nelson) were used to evaluate the breakthrough data. It was found that at the lower flow rates the models better approximated the measured sorbent uptake. This is likely to be due to the non-ideal conditions (ie non-equilibrium sorption which occurred in the columns.

Oxidation-sorption barrier quantification

Chlorophenols contaminated water was efficiently treated using pine as a sorption media in un-buffered neutral pH conditions. Oxidation processes were important in order to destroy the sorbed chlorophenol and consequently, will increase the barrier lifetime. However, in a sorption processes, at a certain stage sorption sites are filling up. Therefore, sorption-oxidation integrated processes are suggested in order to improve the removal.

To demonstrate contaminant treatment within the proposed sorption-oxidation barrier, the results from the sorption and oxidation studies have been integrated into calculations of groundwater flow within a barrier.

In the first stage of the barrier process, 2,4-DCP is sorbed by pine and in the second stage sorbed 2,4-DCP is subsequently oxidised by $KMnO_4$. Assume the contaminant concentration is 300 mg L^{-1} and the groundwater velocity is 0.5 m d^{-1} (typical of Botany aquifer). The residence time for a 1m thick pine barrier is 2 d ($Z=V\times t$, where Z= thickness of the barrier, V= velocity of groundwater and t is the residence time.).

To calculate the frequency of oxidising sorbed 2,4-DCP it is necessary to calculate whether sufficient 2,4-DCP can be sorbed to the pine during the groundwater resident time in the barrier. Using the measured pseudo-first-order rate constant ($k = 0.196\ h^{-1}$) for sorption of 2,4-DCP on 4.75 mm pine (Table 6.1), the residual 2,4-DCP at the downstream face of the barrier can be calculated as ~0.025 mg L^{-1} ($C_t = C_o \times e^{-kt}$). This indicates that a 1 m thick pine barrier has sufficient residence time to remove about 99 % of the influent 2,4-DCP.

It is also necessary to calculate the mass of 2,4-DCP removed by sorption in a 1 m^3 barrier. The 1 m^3 barrier contains 300 kg (0.3 g × 100 cm × 100 cm × 100 cm) of wood chips where density of wood is 0.3 g cc^{-1}. If it is assumed the porosity of 4.75 mm pine is 0.43 (Table 7.1), then a 1 m^3 barrier has a pore volume of 430 L (pore volume = $0.43\times 1\ m^3$). From batch experiments, the 2,4-DCP sorption capacity of 4.75 mm pine wood chips is 6.8 mg g^{-1} or 6.8 g kg^{-1} (Table 6.5). Therefore, 1 m^3 barrier can theoretically sorb 2040 g (300 kg × 6.8 g kg^{-1}) of 2, 4-DCP. One pore volume of a 1 m^3

barrier would sorb 129 g (0.3 g L^{-1} × 430 L) of 2,4-DCP from 0.3 g L^{-1} of 2,4-DCP contaminated water within 2 days (residence time). Therefore, ~16 pore volume (2040 g ÷ 129 g) would be required to sorb 2040 g of 2,4-DCP. Therefore a 1 m^3 barrier would be saturated in 32 days (16 × 2). This means the barrier can operate in sorption mode for 32 days before requiring oxidation to replenish the sorption sites.

To calculate the length of the oxidation phase of the barrier treatment requires calculations of the kinetics and efficiency of the oxidation process for 2,4-DCP sorbed onto pine. We can conservatively assume 50 % of 2,4-DCP can be remove from 1 m^3 barrier by oxidation. The measured rates from my study show approximately 76% can be removed (Table 8.3). To calculate the rate of this oxidation process requires the kinetic data for sorbed 2,4 DCP oxidation. The data available from the thesis is for first-order rate constants for pine (1.18 mm) and sorbed CP oxidation by $KMnO_4$ (~4 mM) is 0.008 min^{-1} over a 160 minute period (Table 8.4). This data is adequate for this calculation. The equation for mean residence time (t) for a first order batch reactor is $t=\ln(C_o-C_t)/k$ where C_o is the maximum sorbed mass (6.8 mg g^{-1}) and C_t is the final sorbed mass (1.6 mg g^{-1}, consistent with 76% removal) and k is the first order reaction rate (0.008 min^{-1}). The required residence time for this removal is 206 minutes.

Therefore a plausible operating cycle for the sorption-oxidation pine barrier for 300 mg L^{-1} 2,4-DCP would be 32 days of sorption followed by 3.4 hours of $KMnO_4$ injection followed by another cycle. This demonstrates an effective proof of concept using the results obtained from this research.

Conclusions

In summary, the following important conclusions can be drawn for the sorption and oxidation of chlorophenols:

- The proposed new analytical method for chlorophenol quantification applied here is simple. The study has found that permanganate oxidation of contaminants can be efficiently measured using spectrophotometric methods. This has particular benefit for rapid determination of oxidation reaction rates. Also proposed liquid-liquid extraction method followed by UV-visible absorption measurement may be useful in the chlorophenol contaminated area for on-site analysis.
- Oxidation kinetics indicated that CP can be rapidly degraded by permanganate. The oxidation of CP by $KMnO_4$ is second-order overall and first-order individually with respect to $KMnO_4$ and CP. The CP degradation rates can be accelerated by increasing oxidant concentration.
- The kinetic reaction model best describes the kinetic sorption data. The second-order equation gave the better correlation for kinetics sorption data. These fundamental will be useful for further applications in the treatment of field level or large scale chlorophenol contaminated water.
- The Freundlich model fits sorption equilibrium data better for all sorbents than the Langmuir model.
- Filter coal exhibited similar sorption patterns with respect to different chlorophenols while sorption capacity by other sobents increases with relative hydrophobicity.

- The degree of irreversibility of sorption on pine increases from 2-CP ~4-CP to 2,4-DCP.
- The equilibrium sorption capacity of pine did not change with the particle size, but rate of sorption for all sorbents were slightly decreased with increasing particle size. The poor correlation between particle size and surface area is due to the elongate nature of the particles.
- In the column study where pine used as a reactive porous media for the removal of 2,4-DCP were measured under different flow rate, particle size and $KMnO_4$. Higher removal were achieved at lower flow rate as there was more residence time whereas particle size and $KMnO_4$ modified pine did not significantly affect 2,4-DCP sorption capacity.
- The consumption of permanganate and oxidation of CP in a pine material can be described by more than one rate constant. In the initial 4 min reaction can be applied for first-order reaction. Batch and column study indicated that more permanganate consumed with the sorbed CP compared with using pine alone.
- The reaction between permanganate and cellulosic materials (lignin, hemicellulose and cellulose) will dominate only after the oxidation reaction with CP.
- It is needed to consider the pine oxidant demand (POD) for the implementation of proposed pine-permanganate reactive barrier system.
- The sorption and oxidation data describe the benefits of proposed combined sorption-oxidation for treatment of chlorophenol contaminant instead of single treatment process
- In a proposed sorption-oxidation barrier system $KMnO_4$ consumption will reduce and saturated pine can be regenerated and used for a longer time

- It was also found that the reaction of CP with in-situ MnO_2 has no significant effect at this experimental condition.

Recommendation/Further work

The research study has provided a solid foundation for understanding the mechanisms involved in an oxidative-sorption barrier which uses permanganate and pine. The use of batch and then column studies to focus on individual mechanisms which possibly has given insight. However there are a number of areas where further work into individual mechanisms as well as integrated processes and their prediction are needed.

Sorption processes

This study only looked at sorption of a single chlorophenol onto woody biomass. In reality there may be multiple chlorophenols present and the effect of competitive sorption would be important. An important aspect of having an MnO_2 impregnated sorbent in the barrier is the potential for heavy metal sorption. Further work is needed to better understand this mechanism of chlorophenol oxidation.

Oxidation processes

The oxidation processes occurring within an aqueous solution are relatively straightforward while those in a sorption barrier system are complex and require further work. In particular there were greater differences between the batch results and the column studies for oxidation compared with sorption. Further work needs to be done using columns with their higher solid to liquid ratio for oxidation. The effect of short residence/reaction times in these porous media systems needs to be better understood if

this technology is to be useful for a short residence time (ie horizontal biofiltration barriers) as well as longer residence times as vertical groundwater flow barriers. The development and utilisation of suitable porous media flow models that incorporate first and second-order oxidation kinetics as well as sorption are required. These were beyond the scope of this work. This would then allow the prediction of treatment effectiveness in an integrated oxidation-sorption barrier.

References

AFIA. (2010). Australian Fodder Industry Association Laboratory manual: Acid Detergent Fibre - Wet chemistry – (CSL Method ID: LMOP 2-1108), Acid Detergent Lignin - Wet chemistry; (CSL Lab Manual Operating Procedure 2-1111), Neutral Detergent Fibre - Wet chemistry (CSL Lab Manual Operating Procedure 2-1107).

Ahmaruzzaman, M. and Sharma, D. K. (2005). Adsorption of phenols from wastewater. Journal of Colloid and Interface Science, 287, pp. 14–24.

Ahmaruzzaman, M. (2008). Adsorption of phenolic compounds on low-cost adsorbents: A review. Advances in Colloid and Interface Science, 143, 48–67.

Ahmed, S., Rasul, M. G., Martens, W. N., Brown, R. and Hasib, M. A. (2011). Advances in heterogeneous photocatalytic degradation of phenols and dyes in waste water: A review. Water, Air, and Soil Pollution, 215, 3–29.

Aiken, G. R. and Kuniansk, E. L. (2002). Organic matter in ground water, US Geological Survey, Artificial Recharge Workshop Proceedings, Sacramento, California, April 2-4.

Aitken, M. D., Massey I. J., Chen, T. and Heck, P. E. (1994). Characterization of reaction products from the enzyme catalyzed oxidation of phenolic pollutants. Water Research, 28, 1879-1889.

Aksu, Z. and Yener, J. (2001). A comparative adsorption /biosorption study of mono-chlorinated phenols onto various sorbents. Waste Management, 21, 695–702.

Aksu, Z. and Gonen, F. (2004). Biosorption of phenol by immobilized activated sludge in a continuous packed bed: prediction of breakthrough curves. Process Biochemistry, 39, 599–613.

Al, T. A., Banks, V., Loomer, D., Parker, B. L. and Ulrich Mayer, K. (2006). Metal mobility during in situ chemical oxidation of TCE by $KMnO_4$. Journal of Contaminant Hydrology, 88, 137–152.

Andresen, J. M., Burgess, C. E., Pappano, P. J. and Schobert, H. H. (2004). New directions for non-fuel uses of anthracites. Fuel Processing Technology, 85, 1373–1392.

APHA/AWWA/WEF. (1998). Standard methods for the examination of water and wastewater. 20th edition. American Public Health Association/American Water Works Association/Water Environment Federation, Washington, DC.

ASTM. (1998). ASTM Standards: D422-63(1998) Standard Test Method for Particle Size Analysis of Soils. American Society for Testing Materials.

Avery, H. E. (1974). Basic Reaction Kinetics and Mechanisms. The Macmillan Press Ltd., London, pp 2–10.

Barrera-Garcia, V. D., Gougeon, R. D., Karbowiak, T., Voilley, A. and Chassagne, D. (2008). Role of wood macromolecules on selective sorption of phenolic compounds by wood. Journal of Agricultural and Food Chemistry, 56, 8498–8506.

Barry, D. A. and Parker, J. C. (1987). Approximations for solute transport through porous media with flow transverse to layering. Transport in Porous Media, 2**,** 65–82.

Bastos, P. M., Eriksson, J., Green, N. and Bergman, A. (2008). A standardized method for assessment of oxidative transformations of brominated phenols in water. Chemosphere, 70, 1196–1202.

Benerjee, J. and Sengupta, K. K. (1964). Studies of reaction kinetics of monohydric alcohols by acid permanganate. The Review of Physical Chemistry of Japan, 34, 81–87.

Bianchi-Mosquera, G. C., Allen-King, R. M. and Mackay, D. M. (1994). Enhanced degradation of dissolved benzene and toluene using a solid oxygen-releasing compound. Ground water Monitoring Remediation, Winter, 120–128.

Billo, E. J. (2007). Excel for Scientists and Engineers: Numerical Methods. Wiley-Blackwell.

Boekel, M. A. J. S. van. (2008). Kinetic modeling of reactions in foods. CRC Press, Boca Raton, New York.

Bohart, G. S. and Adams, E. Q. (1920). Behavior of charcoal towards chlorine. Journal of Chemical Society, 42, 523–529.

Bolster, C. H. and Hornberger, G. M. (2007). On the use of linearized Langmuir equations. Soil Science Society of American Journal, 71, 1796–1806.

Boluda, N., Cases, V., Leon, V. M., Gomis, V. and Prats, D. (2007). Reactive transport experiments of linear alkylbenzene sulfonate in laboratory soil columns. International Conference on Water Pollution in national porous media at different scales, assessment of fate, impact and indicators, Barcelona (Spain), April 11th–13th.

Borden, R. C., Goin, R. T. and Kao, C. M. (1997). Control of BTEX migration using a biologically enhanced permeable barrier. Ground water Monitoring Remediation, Winter, 70–80.

Bose, R. N., Keane, C., Xidis, A., Reed, J. W., Ruiming Li, Tu, H. and Halmet, P. L. (1991). Oxidation of ethylenediaminetetracetic acid by permanganate ion: a kinetic study. Inorganic Chemistry, 30, 2638-2642.

Boving, T. B. and Zhang, W. (2004). Removal of aqueous-phase polynuclear aromatic hydrocarbons using aspen wood fibers. Chemosphere, 54, 831–839.

Bowman, R. S., Haggerty, G. M., Huddleston, R. G., Neel, D. and Flynn, M. M. (1995). Sorption of nonpolar organic compounds, inorganic cations and inorganic oxyanions by surfactant-modified zeolites. (Sabatini, D. A., Knox, R. C. and Harwell, J. H., Eds.) Surfactant-Enhanced Remediation of Subsurface Contamination. ACS Symposium Series 594. American Chemical Society, Washington D. C. pp. 54–64.

Bras, I. P., Santos, L. and Alves, A. (1999). Organochlorine pesticides removal by pinus barks sorption. Environmental Science and Technology, 33, 631–634.

Bra´s, I., Lemos, L., Alves, A. and Pereira, M. F. R. (2005). Sorption of pentachlorophenol on pine bark. Chemosphere, 60, 1095–1102.

Brown, G. S., Barton, L. L. and Thomson, B. N. (2003). Permanganate oxidation of sorbed polycyclic aromatic hydrocarbon, Waste Management, 23, 737–740.

Brusseau, M. L. and Rao, P. S. C. (1989). Sorption nonideality during organic contaminant transport in porous media. Critical Reviews in Environmental Control, 19, 33–99.

Brusseau, M. L., Hu, Q. H. and Srivastava, R. (1997). Using flow interruption to identify factors causing nonideal contaminant transport. Journal of Contaminant Hydrology, 24, 205–219.

Burris, D. R. and Antworth, C. P. (1992). In situ modification of an aquifer material by a cationic surfactant to enhance retardation of organic contaminants. Journal of Contaminant Hydrology, 10, 325–337.

Butler, J. A.V. and Ockrent, C. (1929). Studies in electrocapillarity. Part III - The surface tensions of solutions containing two surface-active solutes. Journal of Physical Chemistry, 34, 2841–2859.

Calace, N., Nardi, E., Petronio, B. M. and Pietroletti, M. (2002). Adsorption of phenols by papermill sludges. Environmental Pollution, 118, 315-319.

Cao, H. and Suib, S. L. (1994). Highly efficient hetereogeneous photooxidation of 2-propanol to acetone with amorphous manganese oxide catalysis. Journal of American Chemical Society, 116, 5334-5342.

Casado, J., Lopez-Quintela, M. A. and Lorenzo-Barral, F. M. (1986). The initial rate method in chemical kinetics. Journal of Chemical Education, 63, 450–452.

Chai, X. S. and Zhu, J. Y. (1999). Rapid and direct kappa number determination using spectrophotometry. Institute of Paper Science and Technology Atlanta, Georgia, IPST Technical paper series number 802.

Chang, H. S., Korshin, G. V. and Ferguson, J. F. (2006). Examination of reaction mechanisms and reaction products for the oxidation of EDTA by permanganate at high pH values. Environmental Science and Technology, 40, 5089–5094.

Chen, G., Hoag, G. E., Chedda, P., Nadim, F., Woody, B. A. and Dobbs, G. M. (2001). The mechanism and applicability of in situ oxidation of trichloroethylene with Fenton's reagent. Journal of Hazardous Materials, B87, 171-186.

Chen, X., Xiao, B., Liu, J., Fang, T. and Xu, X. (2005). Kinetics of the oxidation of MCRR by potassium permanganate. Toxicon, 45 , 911–917.

Cho, H. J., Fiacco, R. J. and Daly, M. H. (2002). Soil vapours extraction and chemical oxidation to remediate chlorinated solvents in fractured crystalline bedrock: Pilot study results and lessons learned. Remediation, 12, 35-50.

Choi, H., Lim, H. N., Kim, J., Hwang, T. M. and Kang, J. W. (2002). Transport characteristics of gas phase ozone in unsaturated porous media for in-situ chemical oxidation. Journal of Contaminant Hydrology, 57, 81-98.

Choi, J. H., Kim, Y. H. and Choi, S. J. (2007). Reductive dechlorination and biodegradation of 2,4,6-trichlorophenol using sequential permeable reactive barriers: Laboratory studies. Chemosphere, 67, 1551–1557.

Choi, J. W., Chung, S. G., Cho, K.Y., Baek, K. Y., Hong, S. W., Kim, D. J. and Lee, S. H. (2012). Photocatalytic degradation of chlorophenol compounds using poly aromatic star copolymer. Water Air Soil Pollution, 223, 1437–1441.

Cline, S. R., West, O. R., Siegrist, R. L. and Holden, W. L. (1997). Performance of in-situ chemical oxidation field demonstrations at DOE sites, pp. 338-348. In- Situ Remediation of the Geo environment. Proceedings of the Conference held in

Minneapolis, MN, October 5-8, 1997. ASCE Geotechnical Special Publication vol. 71.

Colella, L. S., Armenante, P. M., Kafkewitz, D., Allen, S. J. and Balasundaram, V. (1998). Adsorption isotherms for chlorinated phenols on activated carbons. Journal of Chemical Engineering Data, 43, 573–579.

Connors, K. A. (1990). Chemical Kinetics. John Wiley and Sons.

Cortés-Martínez, R., Solache-Ríos, M., Martínez-Miranda, V. and Alfaro-Cuevas V, R. (2007). Sorption behaviour of 4-chlorophenol from aqueous solution by a surfactant-modified Mexican zeolitic rock in batch and fixed bed systems. Water, Air, and Soil Pollution, 183, 85–94.

Coughlin, R. W. and Ezra, F. S. (1968). Role of surface acidity in the adsorption of organic pollutants on the surface of carbon. Environmental Science and Technology, 2, 291–297.

Cox, L., Koskinen, W. C. and Yen, P. Y. (1997). Sorption-desorption of imidacloprid and its metabolites in soils. Journal of Agricultural and Food Chemistry, 45, 1468–1472.

Crimi, M. L. and Siegrist, R. L. (2004). Impact of reaction conditions on MnO_2 genesis during permanganate oxidation. Journal of Environmental Engineering, 130, 562– 567.

Czaplicka, M. (2004). Sources and transformations of chlorophenols in the natural environment. Science of the Total Environment, 322, 21-39.

Dabrowski, A., Podkoscielny, P., Hubicki, Z. and Barczak, M. (2005). Adsorption of phenolic compounds by activated carbon–a critical review. Chemosphere 58, 1049–1070.

Damm, J. H., Hardacre, C., Kalin, R. M. and Walsh, K. P. (2002). Kinetics of the oxidation of methyl tert-butyl ether (MTBE) by potassium permanganate. Water Research, 36, 3638–3646.

Deborde, M. and von Gunten, U. (2008). Reactions of chlorine with inorganic and organic compounds during water treatment-kinetics and mechanisms: a critical review. Water Research, 42, 13–51.

Devis, G. B., Bastow, T., Fisher, S. J., Franzmann, P. D., Zappia, L. R., Puhakka, J. A. and Trefry, M. G. (2008). Invesigation of the persistence and degradability of chlorophenol and chlorophenoxy acids in groundwater. Groundwater quality:

securing groundwater quality in urban and industrial environments (Proceedings of 6th international groundwater quality conference held in Fremantle, Western Australia, December 2007), IAHS Publications, 324, 311–318.

Devlin, J. F. and Barker, J. E. (1999). Field demonstration of permeable wall flushing for biostimulation of a shallow sandy aquifer. Ground Water Monitoring and Remediation, 19, 75–83.

Drescher, E., Gavaskar, A. R., Sass, B. M., Cumming, L. J. and Williamson, T. K. J. (1998). Batch and column testing to evaluate chemical oxidation of DNAPL source zones. In proceeding from the 1st international Conference on Remediation of Chlorinated and Recalcitrant Compounds, Battelle, Monterey, Calif.

Dubinin, M. M. (1967). Adsorption in micropores. Journal of Colloid Interface Science, 23, 487–499.

Ekpete, O. A., Horsfall, M. Jnr. and Tarawout, T. (2011). Evaluation of activated carbon from fluted pumpkin stem waste for phenol and chlorophenol adsorption in a fixed-bed micro-column. Journal of Applied Science Environmental Management, 15, 141–146.

Ermer, J. (2001). Validation in pharmaceutical analysis. Part I: An integrated approach. Journal of Pharmaceutical and Biomedical Analysis, 24, 755–767.

Esteves da Silva, J. C. G. and Marques, M. C. P. O. (2007). Pentachlorophenol association with fulvic acids from recycled wastes. Environmental Pollution, 146, 174-179.

Farrell, J., Kason, M., Melitas, N. and Li, T. (2000). Investigation of the longterm performance of zero-valent iron for reductive dechlorination of trichloroethylene. Environmental Science and Technology, 34, 514–521.

Freundlich, H. M. F. (1906). Uber die adsorption in lösungen. Z. Phys.Chem. 57, 385–470.

Furuya, E. G., Chang, H. T., Miura, Y. and Noll, K. E. (1997). A fundamental analysis of the isotherm for the adsorption of phenolic compounds on activated carbon. Separation and Purification Technology, 11, 69–78.

Gan, H., Nandi, S. P. and Walker Jr., P. L. (1972). Nature of the porosity in American coals. Fuel, 51, 272–277.

Garves, K. (1997). Degradation and oxidation of cellulose in acidic potassium permanganate solutions: Kinetics and product analyses. Holzforschung, 51, 526–530.

Gates, D. D. and Siegrist, R. L. (1995). In-situ chemical oxidation of trichloroethylene using hydrogen peroxide. Journal of Environmental Engineering, 121, 639-644.

Gates, D. D., Siegrist, R. L. and Cline, S. R. (1995). Chemical oxidation of contaminants in clay or sandy soil, pp. 528-588. In Innovative Technologies for Site Remediation and Hazardous Waste Management, Proceedings of the National Conference, Pittsburgh, July 23-26, ASCE, New York, NY.

Gates-Anderson, D. D., Siegrist, R. L. and Cline, S. R. (2001). Comparison of potassium permanganate and hydrogen peroxide as chemical oxidants for organically contaminated soils. Journal of Environmental Engineering, 127, 337–347.

Georgi, A., Schierz, A., Trommler, U., Horwitz, C. P., Collins, T. J. and Kopinke, F. D. (2007). Humic acid modified Fenton reagent for enhancement of the working pH range. Appled Catalysis B: Environmental, 72, 26–36.

Gerente, C., Lee, V. K. C., Cloirec, P. Le. and McKay, G. (2007). Application of chitosan for the removal of metals from wastewaters by adsorption-mechanisms and models review. Critical Review Environmental Science Technology, 37, 41–127.

Gimeno, O., Carbajo, M., Beltrain, F. J. and Rivas, F. J. (2005). Phenols and substituted phenols AOPs remediation. Journal of Hazardous Materials, B119, 99–108.

Gupta, M. D., Ghosh, R. and Palit, S. K. (1990). Studies on adsorption of aqueous phenol systems over NaX zeolite and the copper ion-exchanged modification. Journal of Surface Science and Technology, 6, 231–240.

Gupta, V. K., Srivastava, S. K. and Tyagi, R. (2000). Design parameters for the treatment of phenolic wastes by carbon columns (obtained from fertilizer waste material). Water Research, 34, 1543–1550.

Gupta, V. K., Ali, I. and Saint, V. K. (2004). Removal of chlorophenols from wastewater using red mud: An aluminium industry waste. Environmental Science and Technology, 38, 4012–4018.

Gurdal, G. and Yalcin, M. N. (2001). Pore volume and surface area of the carboniferous coals from the zonguldak basin (NW Turkey) and their variations with rank maceral composition. International Journal of Coal Geology, 48, 133–144.

Hamdaoui, O. and Naffrechoux, E. (2007). Modeling of adsorption isotherms of phenol and chlorophenols onto granular activated carbon: Part I. Two-parameter models and equations allowing determination of thermodynamic parameters. Journal of Hazardous Materials, 147, 381–394.

Han, J., Deming, R. L. and Tao, F. M. (2004). Theoretical study of molecular structures and properties of the complete series of chlorophenols. Journal of Physical Chemistry A, 108, 7736–7743.

Han, J., Deming, R. L. and Tao, F. M. (2005). Theoretical study of hydrogen-bonded complexes of chlorophenols with water or ammonia: Correlations and predictions of pK_a values. Journal of Physical Chemistry A, 109, 1159–1167.

Hartmann, H., Bohm, T., Daugbjerg Jensen, P., Temmerman, M., Rabier, F. and Golser, M. (2006). Methods for size classification of wood chips. Biomass and Bioenergy, 30, 944–953.

He, D., Guan, X. H., Ma, J., Yang, X. and Cui, C. W. (2010). Influence of humic acids of different origins on oxidation of phenol and chlorophenols by permanganate. Journal of Hazardous Materials, 182, 681–688.

Ho, Y. S. and McKay, G. (1999). Pseudo-second order model for sorption processes. Process Biochemistry, 34, 451–465.

Hood, E. D., Thomson, N. R., Grossi, D. and Farquhar, G. J. (2000). Experimental determination of the kinetic rate law for the oxidation of perchloroethylene by potassium permanganate. Chemosphere, 40, 1383–1388.

Howard, P. H. (1989). Handbook of environmental fate and exposure data for organic chemical. Vol. I, Large production and priority pollutants, Lewis Publishers, Chelsea, MI, USA.

Huang, K. C., Hoag, G. E., Chheda, P., Woody, B. A. and Dobbs, G. M. (1999). Kinetic study of oxidation of trichloroethylene by potassium permanganate. Environmental Engineering Science, 16, 265–274.

Huang, K. C., Hoag, G. E., Chheda, P., Woody, B. A. and Dobbs, G. M. (2001). Oxidation of chlorinated ethenes by potassium permanganate: a kinetics study. Journal of Hazardous Materials, 87, 155–169.

Huang, K. C., Hoag, G. E., Chheda, P., Woody, B. A. and Dobbs, G. M. (2002). Kinetics and mechanism of oxidation of tetrachloroethylene with permanganate. Chemosphere, 46, 815–825.

Huang, K. C., Couttenye, R. A. and Hoag, G. E. (2002a). Kinetics of heat-assisted persulfate oxidation of methyl tert-butyl ether (MTBE). Chemosphere, 49, 413-420.

Huang, L., Boving, T. B. and Xing, B. (2006). Sorption of PAHs by aspen wood fibers as affected by chemical alterations. Environmental Science and Technology, 40, 3279–3284.

Ishaq, M., Ahmad, I., Shakirullah, M., Rehman, H. U., Khan, M. A., Ahmad, I. and Rehman, I. U. (2007). Adsorption study of phenol on lakhra coal. Toxicological and Environmental Chemistry, 89, 1–6.

ITRC. (1999). Regulatory Guidance for Permeable Barrier Walls Designed to Remediate Chlorinated solvents, 2nd ed. PBW-1. Interstate Technology and Regulatory Council, Permeable Reactive Barriers Team, Washington, D.C.

ITRC. (2005). Technical and regulatory guidance for in situ chemical oxidation of contaminated soil and groundwater. 2nd ed. Interstate Technology and Regulatory Council, In Situ Chemical Oxidation Team, Washington, DC.

ITRC. (2011). Technical/ regulatory guidance. Permeable reactive barrier: technology update, Interstate Technology and Regulatory Council, PRB: Technology Update Team, Washington, DC.

Jadhav, D. N. and Vanjara, A. K. (2004). Removal of phenol from wastewater using sawdust, polymerized sawdust and sawdust carbon. Indian Journal of Chemical Technology, 11, 35–41.

Jain, S. and Jayaram, R. V. (2007). Adsorption of phenol and substituted chlorophenols from aqueous solution by activated carbon prepared from jackfruit (artocarpus heterophyllus) peel– kinetics and equilibrium studies. Separation Science and Technology, 42, 2019–2032.

Jarvinen, K. T., Melin, E. S. and Puhakka, J. A. (1994). High rate bioremediation of chlorophenol-contaminated groundwater at low temperatures. Environmental Science and Technology, 28, 2387–2392.

Jeen, S. W., Gillham, R. W. and Blowes, D. W. (2006). Effects of carbonate precipitate on long-term performance of granular iron for reductive dechlorination of TCE. Environmental Science and Technology, 40, 6432–6437.

Jiang, J., Pang, S. and Ma, J. (2009). Oxidation of triclosan by permanganate (Mn (VII)): Importance of ligands and in-situ formed manganese oxides. Environmental Science and Technology, 43, 8326–8331.

Jolly, G., Dupont, L., Aplincourt, M. and Lambert, J. (2006). Improved Cu and Zn sorption on oxidized wheat lignocellulose. Environmental Chemistry Letters, 4, 219–223.

Jones, A. P. and Watts, R. J. (1997). Dry phase dioxide-mediated photocatalysis: basis for in situ surface destruction of hazardous chemicals. Journal of Environmental Engineering, 123, 974–981.

Jones, C.W. (1999). Applications of hydrogen peroxide and derivatives. The Royal Society of Chemistry, UK.

Jung, M. W., Ahn, K. H., Lee, Y., Kim, K. P., Rhee, J. S., Park, J. T. and Paeng, K. J. (2001). Adsorption characteristics of phenol and chlorophenols on granular activated carbons (GAC). Microchemical Journal, 70, 123–131.

Kang, C., Wang, Y., Li, R., Du, Y., Li, J., Zhang, B., Zhou, L. and Du, Y. (2000). A modified spectrophotometric method for the determination of trace amounts of phenol in water. Microchemical Journal, 64, 161–171.

Kao, C. M. and Borden, R. C. (1997). Enhanced TEX biodegradation in nutrient briquete-peat barrier system. Journal of Environmental Engineering, 123, 18-24.

Kao, P. C., Tzeng, J. H. and Huang, T. L. (2000). Removal of chlorophenols from aqueous solution by fly ash. Journal of Hazardous Materials, 76, 237–249.

Kauffman, M. D., LaChance, J. C., Traviglia, A. M., Krivansky, M. E. and Leipert, M. W. (2002). In-situ chemical oxidation of CVOCs in fractured bedrock, 2C-40. In Proceedings of the 3rd International Conference on Remediation of Chlorinatedand Recalcitrant Compounds, Monterey, CA, May 20-23, CD-ROM. Battelle Press, Columbus OH.

Ko, D. C. K., Porter, J. F. and McKay, G. (2000). Optimised correlations for the fixed-bed adsorption of metal ions on bone char. Chemical Engineering Science, 55, 5819–5829.

Ko, S. O., Jun, S. Y., Lee, D. H., Park, J. and Shin, W. S. (2007). Effects of oxidative coupling of 4-chlorophenol with manganese dioxide on the phenanthrene sorption. Journal of Environmental Health Part A, 42, 257–263.

Koohestanian, A., Hosseini, M. and Abbasian, Z. (2008). The separation method for removing of colloidal particles from raw water. American-Eurasian Journal of Agricultural and Environmental Science, 4, 266–273.

Korshin, G. V., Chang, H. S., Frenkel, A. I. and Ferguson, J. E. (2007). Structural study of the incorporation of heavy metals into solid phase formed during the oxidation of EDTA by permanganate at high pH. Environmental Science and Technology, 41, 2560-2565.

Koumanova, B. Peeva, P. and Allen, S. J. (2003). Variation of intraparticle diffusion parameter during adsorption of p-chlorophenol onto activated carbon made from apricot stones. Journal of Chemical Technology and Biotechnology, 78, 582–587.

Langmuir, I. (1916). The constitution and fundamental properties of solids and liquids. Journal of American Chemical Society, 38, 2221–2295.

Langwaldt, J. H., Munster, U. and Puhakka, J. A. (2005). Characterisation and microbial utilization of dissolved organic carbon in groundwater contaminated with chlorophenols. Chemosphere, 59, 983–996.

Lee, D. G. and Brownridge, J. R. (1974). Oxidation of hydrocarbons. IV. Kinetics and mechanism of the oxidative cleavage of cinnamic acid by acidic permanganate. Journal of American Chemical Society, 96, 5517–5523.

Lee, D. G. and Sebastian, C. F. (1981). The oxidation of phenol and chlorophenols by alkaline permanganate. Canadian Journal of Chemistry, 59, 2776–2779.

Lee, D. G. and Perez-Benito, J. F. (1985). Oxidation of hydrocarbons. 14. Autocatalysis during the oxidation of 1-tetradecene by methyltributylammonium permanganate. Canadian Journal of Chemistry, 63, 1275–1279.

Lee, J. F., Crum, J. R. and Boyd, S. A. (1989). Enhanced retention of organic contaminants by soil exchanged with organic cations. Environmental Science and Technology, 23, 1365–1372.

Li, X. D. and Schwartz, F. W. (2000). Efficiency problems related to permanganate oxidation schemes. Chemical oxidation and reactive barriers, G.B.

Wickramanayake, A. R. Gavasker, and A.S.C. chen, eds. Battelle, Columbus, Ohio, 41–48.

Liang, C., Bruell, C. J., Marley, M. C. and Sperry, K. L. (2004). Persulfate oxidation for in- situ remediation of TCE. I. Activated by ferrous iron with and without a persulfate-thiosulfate redox couple. Chemosphere, 55, 1213–1223.

Lowe, K. S., Gardner, F. G. and Siegrist, R. L. (2002). Field evaluation of in situ chemical oxidation through vertical well to well recirculation of $NaMnO_4$. Ground Water Monitoring Remediation, Winter, 106–115.

Ma, K. C., Shiu, W. Y. and Mackay, D. (1993). Aqueous solubilities of chlorinated phenols at 25 ^{o}C. Journal of Chemical Engineering Data, 38, 364–366.

MacKay, A. A. and Gschwend, P. M. (2000). Sorption of monoaromatic hydrocarbons to wood. Environmental Science and Technology, 34, 839–845.

MacKinnon, L. K. and Thomson, N. R. (2002). Laboratory-scale in situ chemical oxidation of a perchloroethylene pool using permanganate. Journal of Contaminant Hydrology, 56, 49-74.

Mahajan, O. P., Moreno-Castilla, C. and Walker, Jr. P. L. (1980). Surface-treated activated carbon for removal of phenol from water. Separation Science and Technology, 15, 1733–1752.

Marley, M. C., Cookson, J. and Sperry, K. L. (2002). In Situ Chemical Oxidation (ISCO) – Short course. Workshop – 3rd international conference on remediation of chlorinated and recalcitrant compounds, May 24, Monterey, Ca.

Mata-Perez, F. and Perez-Benito, J. F. (1985). Identification of the product from the reduction of permanganate ion by trimethylamine in aqueous phosphate buffers. Canadian Journal of Chemistry, 63, 988–992.

Mattson, J. S., Mark, Jr. H. B., Malbin, M. D., Weber, Jr. W. J. and Crittenden, J. C. (1969). Surface chemistry of active carbon: Specific adsorption of phenols. Journal of Colloid Interface Science, 31, 116–130.

McKay, G., Blair, H. S. and Gardner, J. R. (1982). Adsorption of dyes on chitin. I: Equilibrium Studies. Journal of Applied Polymer Science, 27, 3043–3057.

McMurry, J. (2008). Organic Chemistry, Belment, CA: Thomson-Books/cole.

Molin, J., Vogan, J., Przepiora, A., Moreno, J. and Bellehumeur, T. (2009). Longevity of microscale ZVI and organic carbon in permeable reactive barrier and source

applications. Presented at Clemson University Technology Symposium, December.

Morrison, R. T. and Boyd, R. N. (1992). Organic Chemistry, Allyn and Bacon, Boston.

Mumford, K. G., Thomson, N. R. and Allen-King, R. M. (2005). Bench-scale investigation of permanganate natural oxidant demand kinetics. Environmental Science and Technology, 39, 2835–2840.

Nassar, M. M. and El-Geundi, M. S. (1991). Comparative cost of colour removal from textile effluents using natural adsorbents. Journal of Chemical Technology and Biotechnology, 50, 257–264.

Nelson, P. O. and Yang, M. (1995). Equilibrium adsorption of chlorophenols on granular activated carbon. Water Environmental Research, 67, 892–898.

Nenkova, S. and Radev, L. (2004). Adsorption of phenol from wastewaters over wood sawdust, barks and technical hydrolysis lignin. Jounal of University Chemical Technology and Metallurgy, Book 2, 39.

Neyens, E. and Baeyens, J. (2003). A review of classic Fenteon's peroxidation as an advanced oxidation technique. Journal of Hazardous Materials, B98, 33-50.

NPI (National Pollutant Inventory), Department of Sustainability, Environment, Water, Population and Communities, Canberra ACT 2601 Australia.

Oliviera, I. B., Demond, A. H. and Salehzadeh, A. (1996). Packing of sands for the production of homogeneous porous media. Soil Science Society of American Journal, 60, 49–53.

Papadopoulos, A. N., Hill, C. A. S. and Gkaraveli, A. (2003). Determination of surface area and pore volume of holocellulose and chemically modified wood flour using the nitrogen adsorption technique. Holz als Roh-und Werkstoff, 61, 453–456.

Pera-Titus, M., García-Molina, V., Baños, M. A., Giménez, J. and Esplugas, S. (2004). Degradation of chlorophenols by means of advanced oxidation processes: a general review. Applied Catalysis B: Environmental, 47, 219–256.

Pignatello, J. J., Oliveros, E., and MacKay, A. (2006). Advanced oxidation processes for organic contaminated destruction based on the Fenton reaction and related chemistry. Critical Reviews in Environmental Science and Technology, 36, 1–84.

Plambeck, J. A. (1996). Chemical Kinetics: Laws of Rates and Orders, Institute: Science, engineering and technology, URL: http://www.intute.ac.uk/references/sciences/plambeck/chem2/p02141.htm.

Polat, H., Molva, M. and Polat, M. (2006). Capacity and mechanism of phenol adsorption on lignite. International Journal of Mineral Processing, 79, 264–273.

Puhakka, J. A. (2010). Bioreactor treatment of contaminated groundwater. Institute of Water and Environmental Engineering, Tempere University of Technology, Tampere, Finland at http://www.nessling.fi/symposiot/Symposio2/puhakka.htm.

Rael, J., Shelton, S. and Dayaye, R. (1995). Permeable barriers to remove benzene: candidate media evaluation. Journal of Environmental Engineering, 121, 411–415.

Rayment, G. E. and Higginson, F. R. (1992). The Australian Laboratory Handbook of Soil and Water Chemical Methods, Inkata Press, Melbourne.

Reitsma, S. and Marshall, M. (2000). Experimental study of oxidation of pooled NAPL. Chemical oxidation and reactive barriers, G.B. Wickramanayake, A. R. Gavasker, and A. S. C. chen, eds. Battelle, Columbus, Ohio, 25–32.

Rodríguez-Cruz, M. S., Andrades M. S., Parada, M. A. and Sánchez-Martín, M. J. (2008). Effect of different wood pre-treatments on the sorption-desorption of linuron and metalaxyl by woods. Jounal of Agricultural and Food Chemistry, 56, 7339–7346.

Rowell, R. M. (2005). Handbook of wood chemistry and wood composites, CRC Press, 328.

Scherer, M. M., Richter, S., Valentine, R. L. and Alvarez, P. J. J. (2000). Chemistry and microbiology of permeable reactive barriers for in situ groundwater clean up. Crtical Reviews in Environmental Science and Technology, 30, 363–411.

Schnarr, M. J. and Farquhar, G. J. (1992). An in-situ oxidation technique to destroy residual DNAPL from soil. Proc.: Subsurface Restoration Conference, Third International Conference on Ground Water Quality. Dallas, Texas. June 21–24.

Schnarr, M., Truax, C., Farquhar, G., Hood, E., Gonullu, T. and Stickney, B. (1998). Laboratory and controlled field experiments using potassium permanganate to remediate trichloroethylene and perchloroethylene DNAPLs in porous media. Journal of Contaminant Hydrology, 29, 205–224.

Schroth, M. H., Oostrom, M., Wietsma, T. W. and Istok, J. D. (2001). In-situ oxidation of trichloroethene by permanganate: effects on porous medium hydraulic properties. Journal of Contaminant Hydrology, 29, 205–224.

Seelsaen, N., McLaughlan, R. G., Moore, S. and Stuetz, R. M. (2007). Influence of compost characteristics on heavy metal sorption from synthetic stormwater. Water Science Technology, 55, 219–226.

Seo, Y., Jang, A. and Bishop, P. L. (2007). Organic mulch biowall for PAH contaminated groundwater remediation. European Journal of Soil Biology, 43, 304–309.

SERDP (Strategic Environmental Research and Development Program). (2006). Reaction and transport processes controlling in -situ chemical oxidation of DNAPLs. SERDP Project CU-1290, Colorado.

Severtson, S. J. and Banerjee, S. (1996). Sorption of chlorophenols to wood pulp. Environmental Science and Technology, 30, 1961–1969.

Shukla, A., Zhang, Y. H., Dubey, P., Margrave, J. L. and Shukla, S. S. (2002). The role of sawdust in the removal of unwanted materials from water. Journal of Hazardous Materials B95, 137–152.

Siegrist, R. L., Urynowicz, M. A., West, O. R., Crimi, M. L. and Lowe, K. S. (2001). Principles and practices of in-situ chemical oxidation using permanganate. Batelle press, Columbus, Ohio.

Siegrist, R. L., Urynowicz, M. A., Crimi, M. L. and Lowe, K. S. (2002). Genesis and effects of particles produced during in situ chemical oxidation using permanganate. Journal of Environmental Engineering, 128, 1068–1076.

Simon, F. G. and Meggyes, T. (2000). Removal of organic and inorganic pollutants from groundwater using permeable reactive barriers. Land Contamination and Reclamation, 8, 103-116.

Smith, J. A., Jaffe, P. R. and Chiou, C. T. (1990). Effect of ten quaternary ammonium cations on tetrachloromrthane sorption to clay from water. Environmental Science and Technology, 24, 1167–1172.

Smith, J. A. and Jaffe, P. R. (1994). Adsorptive selectivity of organic-cation-modified bentonite for non-ionic organic contaminants. Water Air and Soil pollution, 72, 205–211.

Smith, J. A. and Galan, A. (1995). Sorption of non-ionic organic contaminants to single and dual organic carbon bentonites from water. Environmental Science and Technology, 29, 685–692.

Snoeyink, V. and Weber, Jr. W. (1967). The surface chemistry of active carbon: A discussion of structure and surface functional groups. Environmental Science and Technology, 1, 228–234.

Sorial, G. A., Suidan, M. T. and Vidic, R. D. (1993). Effect of GAC characteristics on adsorption of organic pollutants. Water Environment Research 65, 53–57.

Sternberg, S. P. K. (2004). Dispersion measurements in highly heterogeneous laboratory scale porous media. Transport in Porous Media, 54, 107-124.

Stewart, R. (1965). Oxidation in Organic Chemistry: Oxidation by Permanganate. NewYork, Academic Press Inc.

Stone, A. T. (1987). Reductive dissolution of manganese (III/IV) oxides by substituted phenols. Environmental Science and Technology, 21, 979–988.

Striegel, J. A., Sanders, D. A. and Veenstra, J. N. (2001). Treatment of contaminated groundwater using permeable reactive barriers. Environmental Geosciences, 8, 258–265.

Suthersan, S. S. (1999). Remediation Engineering: Design Concepts, CRC Lewis Publishers, New York.

Thomas, H. C. (1944). Heterogeneous ion exchange in a flowing system. Soil Science Society of American Journal, 66, 1664–1666.

Thomas, O. and Burgess, C. (2007). UV-visible spectrophotometry of water and waste water, Elsevier, Amsterdam, pp. 299–313.

Tong, G., Yokoyama, T., Matsumoto, Y. and Meshitsuka, G. (2000). Analysis of progress oxidation reaction during oxygen-alkali treatment of lignin I: method and its application to lignin oxidation. Journal of Wood Science, 46, 32–39.

Tseng, R. L., Wu, F. C. and Juang, R. S. (2003). Liquid-phase adsorption of dyes and phenols using pinewood-based activated carbons. Carbon, 41, 487–495.

Tutem, E., Apak, R. and Unal, C. F. (1998). Adsorptive removal of chlorophenols from from water by bituminous shale. Water Research, 32, 2315–2324.

Tyre, B., Watts, R. J. and Miller, G. C. (1991). Treatment of four biorefractory contaminants in soils using catalyzed hydrogen peroxide. Journal of Environmental Quality, 20, 832–838.

Ulrich, H. J. and Stone, A. T. (1989). Oxidation of chlorophenols adsorbed to manganese oxide surfaces. Environmental Science and Technology, 23, 421–428.

USDOE (U.S. Department of Energy). (1999). In-situ chemical oxidation using potassium permanganate, Office of Environmental Management, DOE/EM-0496, Washington, DC 20585.

USEPA. (1997). Permeable reactive subsurface barriers for the interception and remediation of chlorinated hydrocarbon and chromium (VI) plumes in groundwater. EPA/600/F-97/008. Washington, DC, Office of Research and Development, National Risk Management Research Laboratory.

USEPA. (1998). Field application of in situ remediation technologies: chemical oxidation, EPA 542-R-98-008, 31pp. September 1998, http://www.epa.gov.swertio/ download/remed/chemox.pdf

USEPA. (2000). Office of Solid Waste and Emergency Response (5102G), EPA 542-N-00-006, September.

USEPA. (2006). Engineering Issue: In-situ chemical oxidation. Office of Research and Development, Washington, DC. EPA/600/R-06/072.

Vella, P. A. and Munder, J. A. (1993). Toxic pollutant destruction. In: Emerging technologies in hazardous waste management III. Atlanta: American Chemical Society, 85–105.

Waldemer, R. H. and Tratnyek, P. G. (2006). Kinetics of contaminant degradation by permanganate. Environmental Science and Technology, 40, 1055–1061.

Waldemer, R. H., Tratnyek, P. G., Johnson, R. L. and Nurmi, J. T. (2007). Oxidation of chlorinated ethenes by heat-activated persulfate: Kinetics and products. Environmental Science and Technology, 41, 1010–1015.

Wagner, J., Chen, H., Brownawell, B. J. and Westall, J. C. (1994). Use of cationic surfactants to modify soil surfaces to promote sorption and retard migration of hydrophobic organic compounds. Environmental Science and Technology, 28, 231–237.

Walker, Jr. P. L. and Mahajan, O. P. (1993). Pore structure in coals. Energy and Fuels, 7, 559–560.

Watts, R. J., Udell, M. D., Rauch, P. A. and Leung, S. W. (1990). Treatment of contaminated soils using catalyzed hydrogen peroxide. Hazardous Waste and Hazardous Materials, 7, 335–345.

Weber, Jr., W. J. and Morris, J. C. (1963). Kinetics of adsorption on carbon from solution. Journal of the Sanitary Engineering Division. Proceedings of the American Society of Civil Engineers 89, 31–59.

Xiao, H., Xu, Y., Yu, M. and Zhang, Q. (2010). Enhanced mineralization of 2,4-dichlorophenol by ozone in the presence of trace permanganate: effect of pH. Environmental Technology, 31, 1295–1300.

Yan, G., Viraraghavan, T. and Chen, M. (2001). A new model for heavy metal removal in a biosorption column. Adsorption Science Technology, 19, 25–43.

Yan, Y. E. and Schwartz, F. W. (1999). Oxidative degradation and kinetics of chlorinated ethylenes by potassium permanganate. Journal of Contaminant Hydrology, 37, 343–365.

Yan, Y. E. and Schwartz, F. W. (2000). Kinetics and mechanisms for TCE oxidation by permanganate. Environmental Science and Technology, 34, 2535-2541.

Yang, J., Cao, L., Guo, R. and Jia, J. (2010). Permeable reactive barrier of surface hydrophobic granular activated carbon coupled with elemental iron for the removal of 2,4-dichlorophenol in water. Journal of Hazardous Materials, 184,782–787.

Ye, F. X. and Shen, D. S. (2004). Acclimation of anaerobic sludge degrading chlorophenols and the biodegradation kinetics during acclimation period. Chemosphere, 54, 1573-1580.

Yoon, Y. H. and Nelson, J. H. (1984). Application of gas adsorption kinetics. I. A theoretical model for respirator cartridge service time. American Industrial Hygiene Association Journal, 45, 509–16.

Zhai, X. H., Hua, I., Rao, P. S. C. and Lee, L. S. (2006). Cosolvent-enhanced chemical oxidation of perchloroethylene by potassium permanganate. Journal of Contaminant Hydrology, 82, 61–74.

Zhang, J., Li, G. B. and Ma, J. (2003). Effects of chlorine content and position of chlorinated phenols on their oxidation kinetics by potassium permanganate. Journal of Environmental Science, 15, 342–345.

Zhu, H. X. and Selim, H. M. (2000). Hysteretic behavior of metolachlor adsorption-desorption in soils. Soil Science, 165, 632–645.

Zogorski, J. S., Faust, S. D. and Haas, J. H. Jr. (1976). The kinetics of adsorption of phenols by granular activated carbon. Journal of Colloid Interface Science, 55, 329–341.

APPENDICES

Appendix A

The graph for concentration-time curve of 2-CP, 3-CP, 2,4-DCP, 2,6-DCP and 2,4,6-TCP (section 5.2).

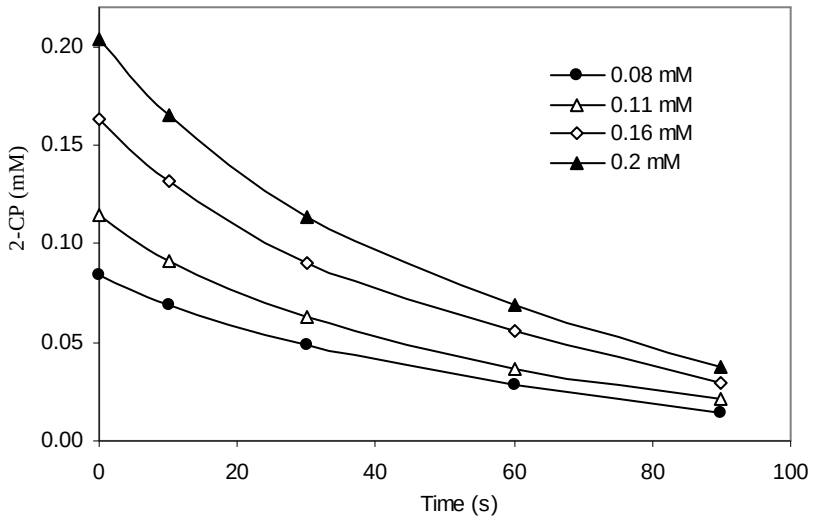

Figure A1 Degradation of 2-CP under various initial 2-CP concentration with fixed $KMnO_4$. $[2\text{-CP}]_o$ ~ (0.08–0.20) mM, $[KMnO_4]$ ~ 1.5 mM, I ~0.02 M, initial, pH 7.0 (22 ^oC)

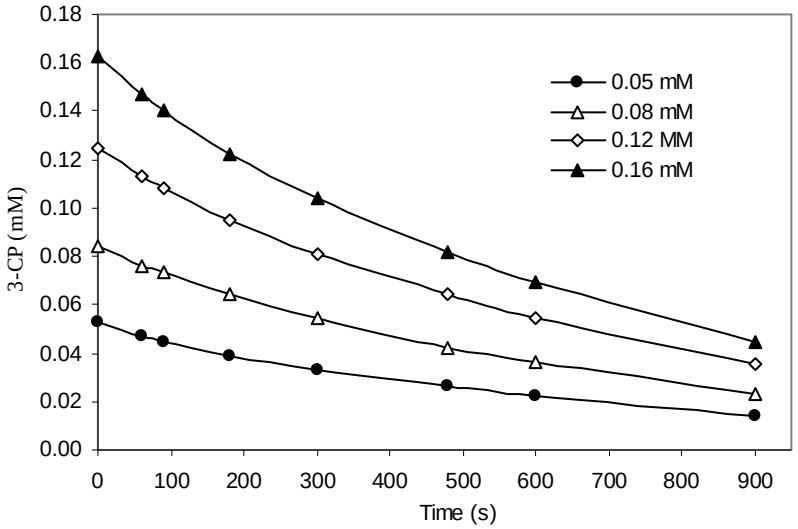

Figure A2 Degradation of 3-CP under various initial 3-CP concentration with fixed $KMnO_4$. $[3\text{-CP}]_o$ ~ (0.05–0.16) mM, $[KMnO_4]$ ~ 1.5 mM, I ~0.02 M, initial, pH 7.0 (22 ^0C)

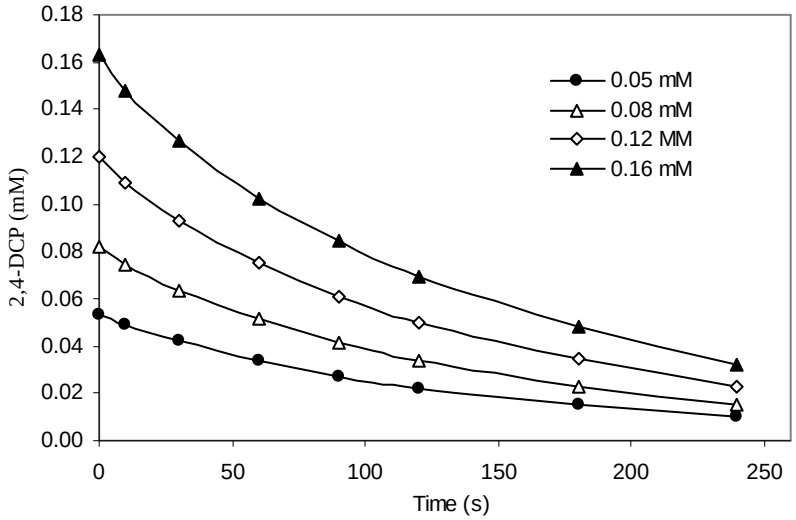

Figure A3 Degradation of 2,4-DCP under various initial 2,4-DCP concentration with fixed $KMnO_4$. $[2,4\text{-DCP}]_o$ ~ (0.05–0.16) mM, $[KMnO_4]$ ~ 1.5 mM, I ~0.02 M, initial, pH 7.0 (22 ^oC).

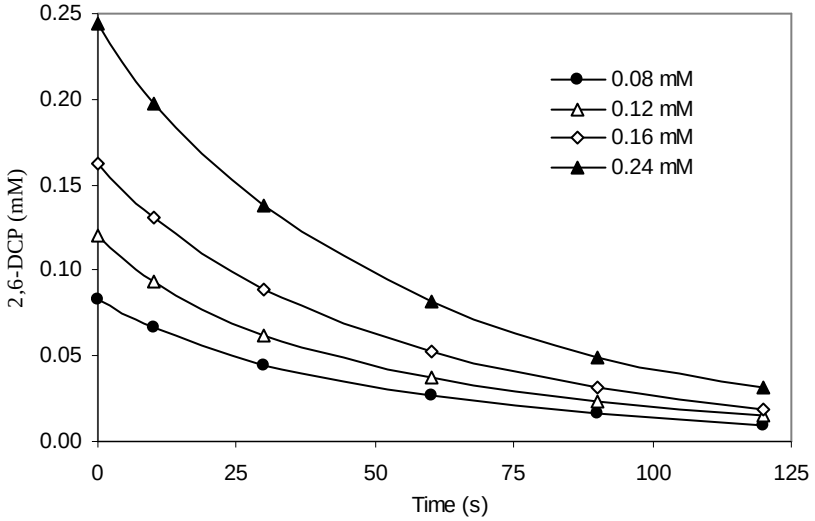

Figure A4 Degradation of 2,6-DCP under various initial 2,6-DCP Concentration with fixed $KMnO_4$. $[2,6\text{-DCP}]_o$ ~ (0.08–0.24) mM, $[KMnO_4]$ ~ 1.5 mM, I ~0.02 M, initial, pH 7.0 (22 ^oC)

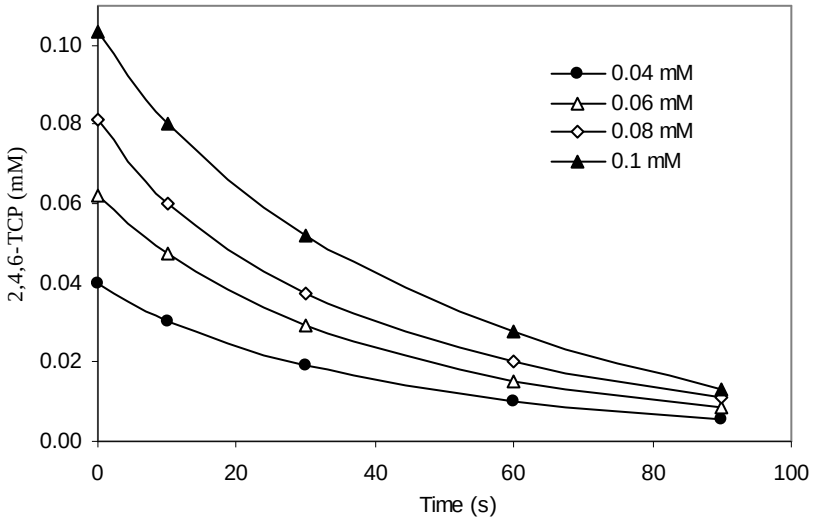

Figure A5 Degradation of 2,4,6-TCP under various initial 2,4,6-TCP Concentration with fixed $KMnO_4$. $[2,4,6\text{-TCP}]_o$ ~ (0.04–0.10) mM, $[KMnO_4]$ ~ 1.5 mM, I ~0.02 M, initial, pH 7.0 (22 ^oC)

The plot of pseudo-first-order reaction rate under different excess initial permanganate concentration for 2-CP, 3-CP, 2,4-DCP, 2,6-DCP and 2,4,6-TCP (section 5.2).

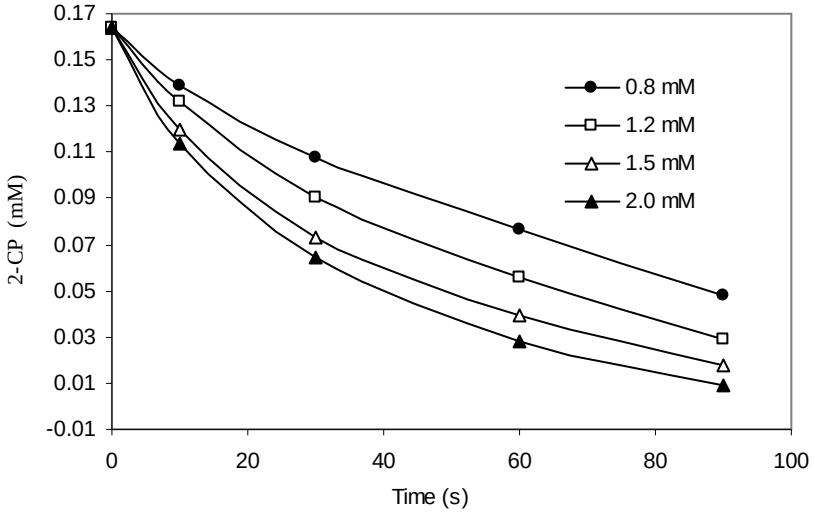

Figure A6 Degradation of 2-CP under various concentration of $KMnO_4$. $[2\text{-CP}]_o$ ~ 0.16 mM, $[KMnO_4]$ ~(0.8–2.0 mM), I ~0.02 M, Initial pH 7.0 (22 ^oC)

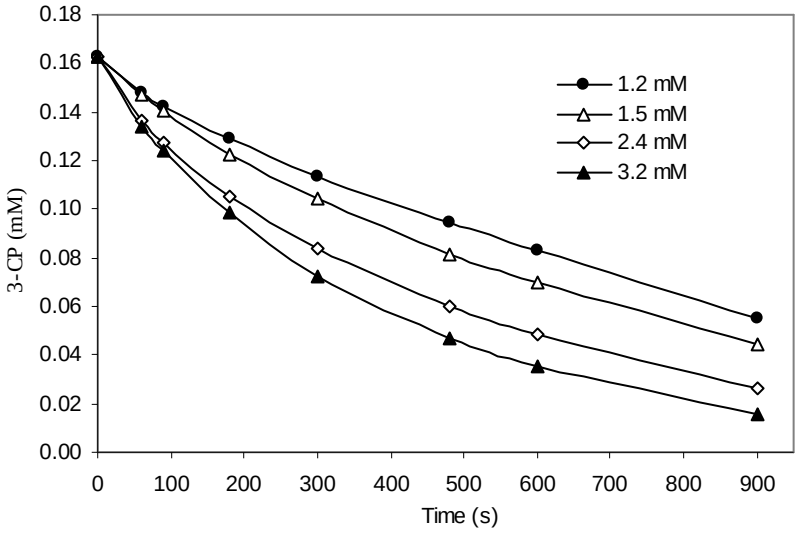

Figure A7 Degradation of 3-CP under various concentration of $KMnO_4$. $[3\text{-CP}]_o$ ~ 0.16 mM, $[KMnO_4]$ ~(1.2–3.2 mM), I ~0.02 M, Initial pH 7.0 (22 ^oC)

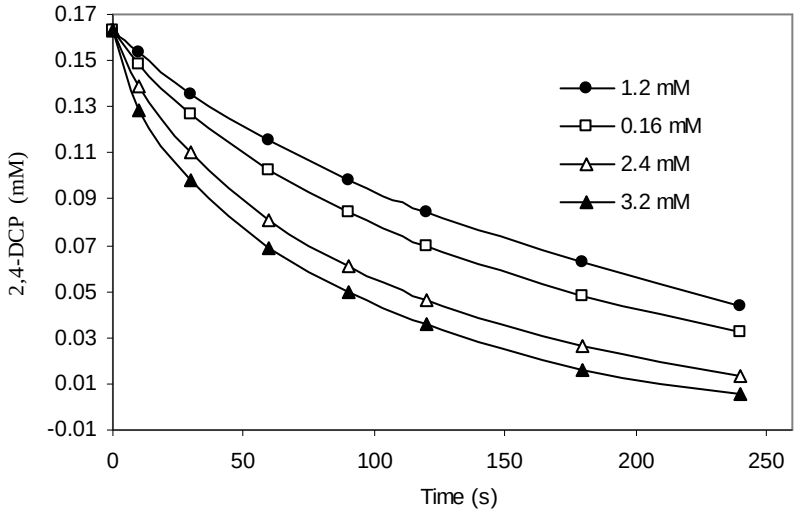

Figure A8 Degradation of 2,4-DCP under various concentration of $KMnO_4$. $[2,4\text{-DCP}]_o$ ~ 0.16 mM, $[KMnO_4]$ ~(1.2–3.2 mM), I ~ 0.02 M, Initial pH 7.0 (22 ^oC)

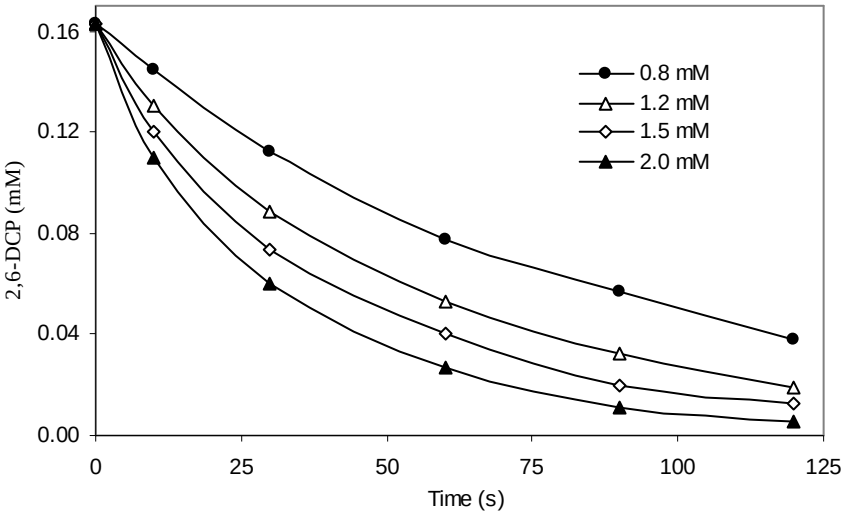

Figure A9 Degradation of 2,6-DCP under various concentration of $KMnO_4$. $[2,6\text{-DCP}]_o$ ~ 0.16 mM, $[KMnO_4]$ ~(0.8–2.0 mM), I ~ 0.02 M, Initial pH 7.0 (22 ^oC)

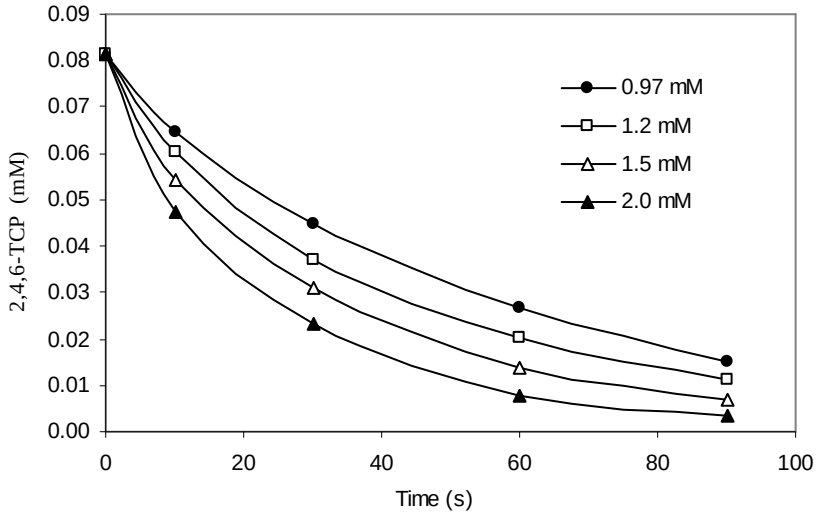

Figure A10 Degradation of 2,4,6-TCP under various concentration of $KMnO_4$. $[2,4,6\text{-TCP}]_o$ ~ 0.16 mM, $[KMnO_4]$ ~(0.97–2.0 mM), I ~ 0.02 M, Initial pH 7.0 (22 ^oC)

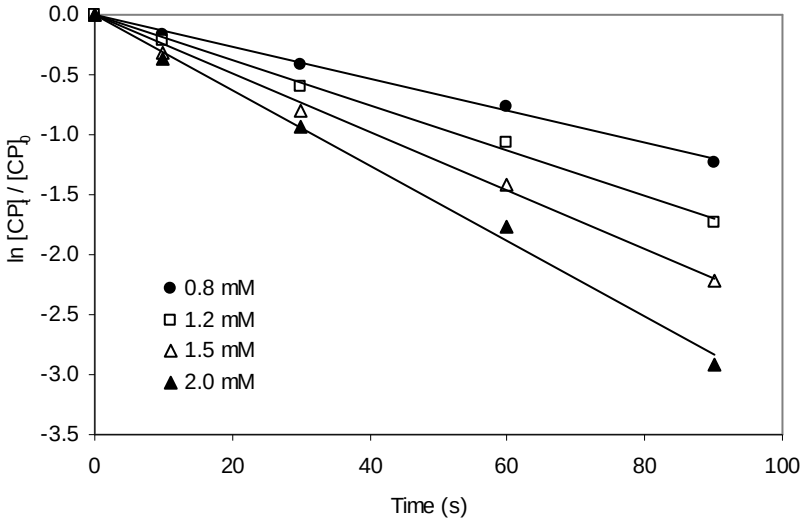

Figure A11 Oxidation fit curves of 2-CP at various concentration of $KMnO_4$. $[2\text{-CP}]_o$ ~0.16 mM, $[KMnO_4]$ ~ (0.8–2.0 mM), I ~0.02 M, Initial pH 7.0 (22 ^oC)

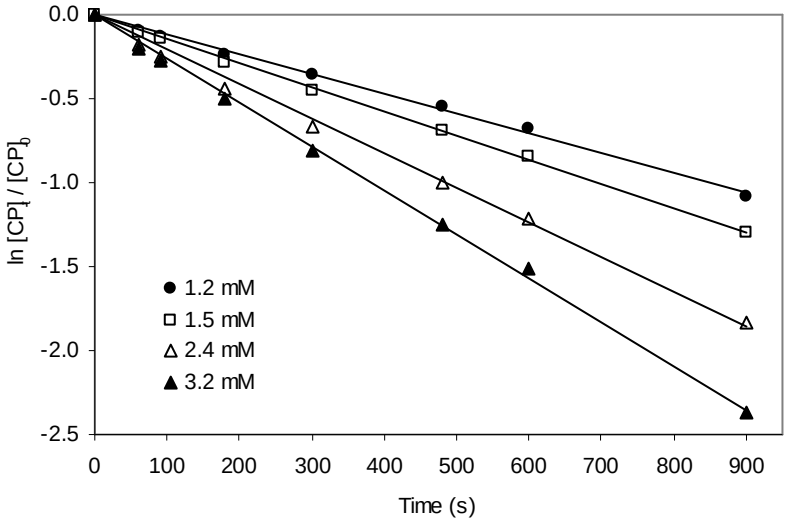

Figure A12 Oxidation fit curves of 3-CP at various concentration of $KMnO_4$. $[3\text{-CP}]_o$ ~0.16 mM, $[KMnO_4]$ ~ (1.2–3.2 mM), I ~0.02 M, Initial pH 7.0 (22 ^oC)

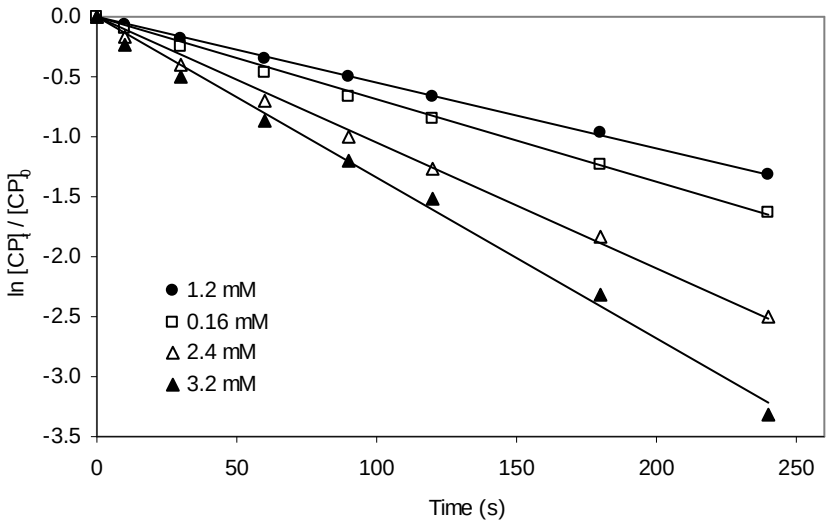

Figure A13 Oxidation fit curves of 2,4-DCP at various concentration of $KMnO_4$. $[2,4\text{-DCP}]_o$ ~0.16 mM, $[KMnO_4]$ ~ (1.2–3.2 mM), I ~0.02 M, Initial pH 7.0 (22 ^oC)

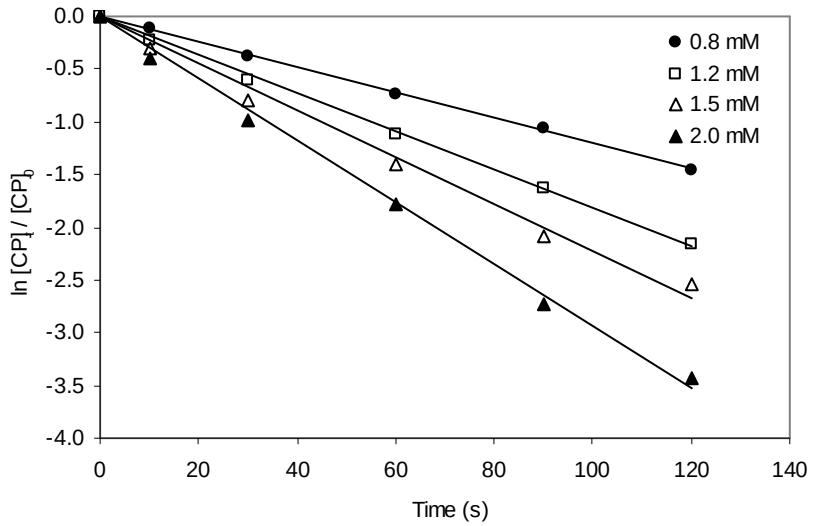

Figure A14 Oxidation fit curves of 2,6-DCP at various concentration of $KMnO_4$. $[2,6\text{-DCP}]_o$ ~0.16 mM, $[KMnO_4]$ ~ (0.8–2.0 mM), I ~0.02 M, Initial pH 7.0 (22 ^oC)

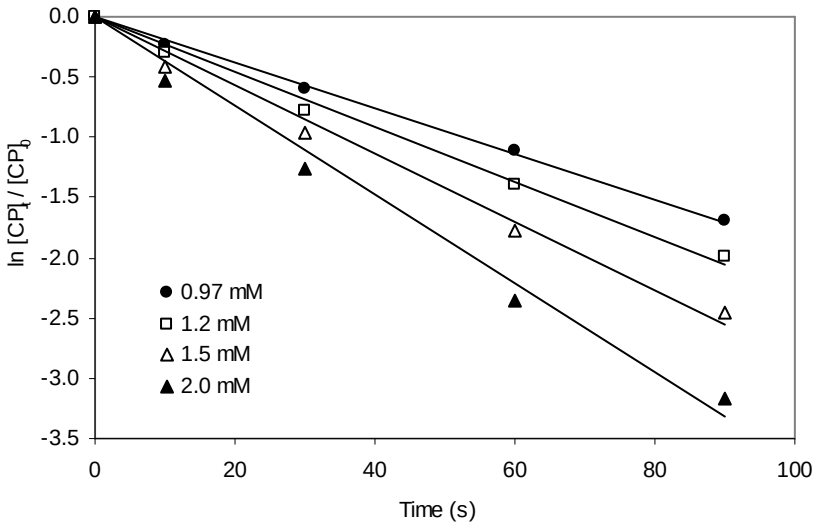

Figure A15 Oxidation fit curves of 2,4,6-TCP at various concentration of $KMnO_4$. $[2,4,6\text{-TCP}]_o$ ~0.16 mM, $[KMnO_4]$ ~(0.97–2.0 mM), I ~0.02 M, Initial pH 7.0 (22 ^oC)

The plot of pseudo-first-order reaction rate at various initial CP concentrations with fixed excess permanganate for 2-CP, 3-CP, 2,4-DCP, 2,6-DCP and 2,4,6-TCP (section 5.2).

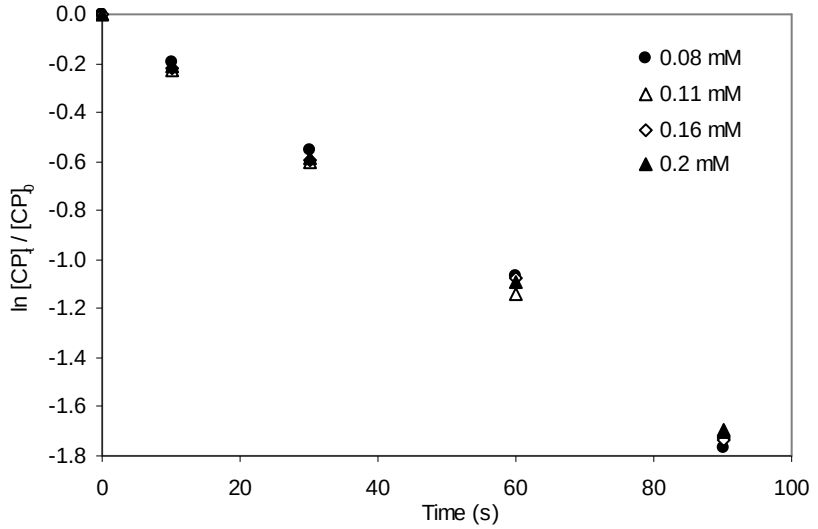

Figure A16 Oxidation fit curves of 2-CP at various initial 2-CP concentration with fixed $KMnO_4$. $[2\text{-CP}]_o$ ~ (0.08 – 0.20) mM, $[KMnO_4]$ ~ 1.5 mM, I ~ 0.02 M, Initial pH 7.0 (22 ^oC)

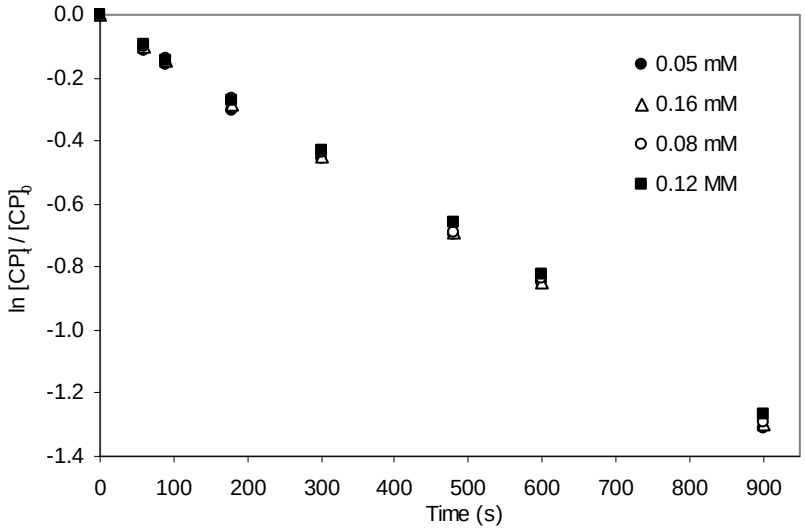

Figure A17 Oxidation fit curves of 3-CP at various initial 3-CP concentration with fixed $KMnO_4$. $[3\text{-CP}]_o$ ~ (0.05 – 0.12) mM, $[KMnO_4]$ ~ 1.5 mM, I ~ 0.02 M, Initial pH 7.0 (22 ^oC)

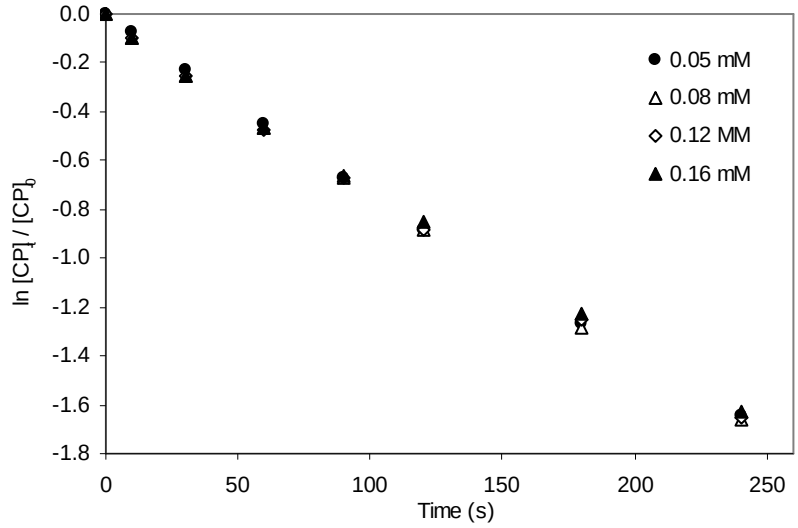

Figure A18 Oxidation fit curves of 2,4-DCP at various initial 2,4-DCP concentration with fixed $KMnO_4$. $[2,4\text{-DCP}]_o$ ~ (0.05 – 0.16) mM,$[KMnO_4]$ ~ 1.5 mM, I ~ 0.02 M, Initial pH 7.0 (22 ^oC)

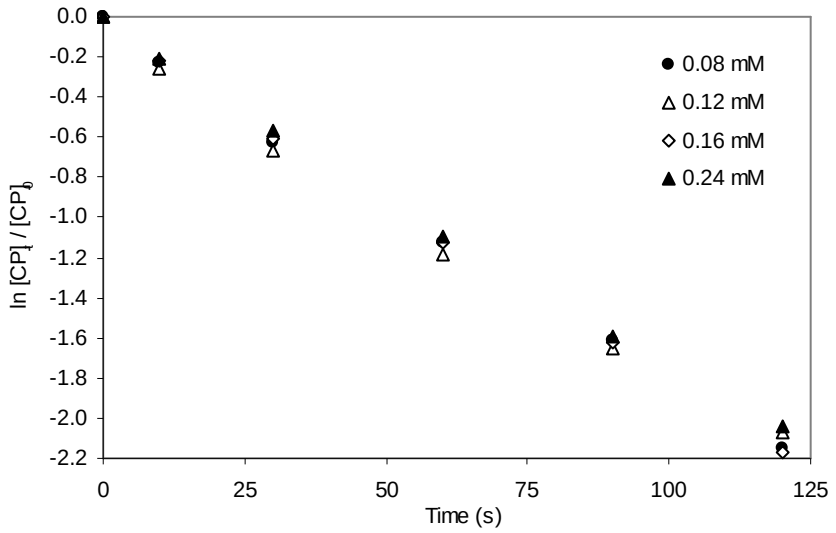

Figure A19 Oxidation fit curves of 2,6-DCP at various initial 2,6-DCP concentration with fixed $KMnO_4$. $[2,6\text{-DCP}]_o$ ~ (0.08–0.24) mM, $[KMnO_4]$ ~ 1.5 mM, I ~ 0.02 M, Initial pH 7.0 (22 ^oC)

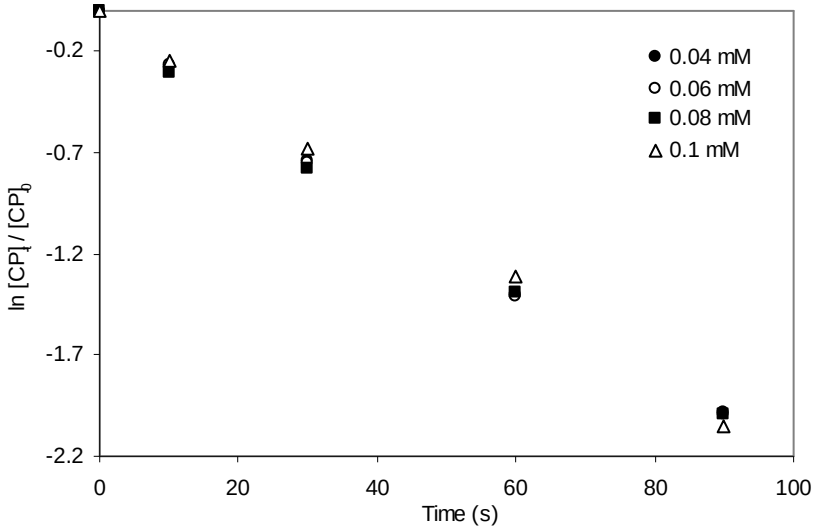

Figure A20 Oxidation fit curves of 2,4,6-TCP at various initial 2,4,6-TCP concentration with fixed $KMnO_4$. $[2,4,6\text{-TCP}]_o$ ~ (0.04 – 0.10) mM, $[KMnO_4]$ ~ 1.5 mM, I ~ 0.02 M, Initial pH 7.0 (22 ^oC)

Appendix B

Reproducibility of measurements

Four identical analytical measurements using UV-visible spectrophotometer for a sample 2,4-DCP solution during sorption experiments on pine, HW, GAC and FC were carried out. Initial concentration was ~200 mg L^{-1} for all cases and 1 mL of solution was diluted to 4 mL with Milli-Q water. The standard deviation and errors are given in Table B1.

Table B1 Reproducibility for analytical measurements

Sorbents	Absorbance at 284 nm	Average	Standard deviation	Error %
Pine	0.2580 0.2467 0.2520 0.2450	0.2505	0.005743	2.2
HW	0.1835 0.1892 0.1895 0.1891	0.1878	0.002888	1.5
GAC	0.2370 0.2410 0.2210 0.2250	0.2310	0.009522	4.1
FC	0.1235 0.1229 0.1265 0.1270	0.1250	0.002074	1.7

From repeated analytical measurements and their relative standard deviations it can be concluded that the errors from analytical methods is less than 5%. The errors were observed from the analytical methods such as transferring of solution using pipette and weighing of sorbents.

Blank test

Blank test results for 2-CP, 4-CP and 2,4-DCP were carried out at different time are shown in Table B2. Initial concentration was ~ 300 mg L^{-1} and samples are diluted from 1 mL to 4 mL with Milli-Q water. Control experiment without the sorbents in the glass vials showed that there was not significant loss of chlorophenols during the sorption experiments. It indicated that disappearance of the chlorophenol compound in liquid was due to sorption. The influence of volatilization and biodegradation may be neglected. However, to verify this, calculated values for the fraction of chlorophenol in the headspace for these experiments was found to be less than 0.115% based on published Henry's constants.

Table B2 Blank test results

Time h	2-CP at 274 nm	4-CP at 280 nm	2,4-DCP at 284 nm
0	1.066	0.878	0.974
3	1.067	0.878	0.975
6	1.067	0.879	0.976
20	1.068	0.879	0.976
48	1.066	0.877	0.975
72	1.068	0.878	0.975
120	1.075	0.878	0.973
168	1.067	0.881	0.976
216	1.071	0.88	0.975
264	1.072	0.878	0.974

Background correction for pine and HW leaching

The UV-visible absorbance was corrected for background sorption by wood matrix. The corrected absorbance was used to determine the concentration of chlorophenols in solution. The sample background absorbance is shown in Table B3:

Table B3 Wood background leaching absorbance after 3 days

Sorbent	Wave length (nm)	Abs 1	Abs 2	Abs 3	Abs 4	Abs 5	Abs 6	Std. Dev.	Error %
Pine 1.5g	274	0.0977	0.1033	0.0964	0.1027	0.0973	0.0992	0.0029	2.9
	280	0.0978	0.1024	0.0965	0.1016	0.0972	0.102	0.0027	2.7
	284	0.0942	0.0983	0.0927	0.0975	0.0949	0.0977	0.0023	2.3
Pine 2g	274	0.104	0.1092	0.1029	0.1092	0.1038	0.1035	0.0029	2.8
	280	0.104	0.1085	0.1027	0.1087	0.1039	0.1043	0.0026	2.4
	284	0.1001	0.1045	0.0987	0.1045	0.0984	0.1023	0.0028	2.7
HW 1.5g	274	0.1323	0.1254	0.1302	0.1255	0.1268	0.1308	0.0030	2.3
	280	0.1254	0.1196	0.1235	0.1197	0.1238	0.1209	0.0024	2.0
	284	0.1195	0.1143	0.1177	0.1143	0.1146	0.1171	0.0022	1.9
HW 2g	274	0.1585	0.1603	0.1584	0.1559	0.1616	0.161	0.0021	1.3
	280	0.1504	0.1531	0.1499	0.1517	0.1545	0.1507	0.0018	1.2
	284	0.1427	0.145	0.1461	0.1446	0.1438	0.1477	0.0018	1.2

Appendix C

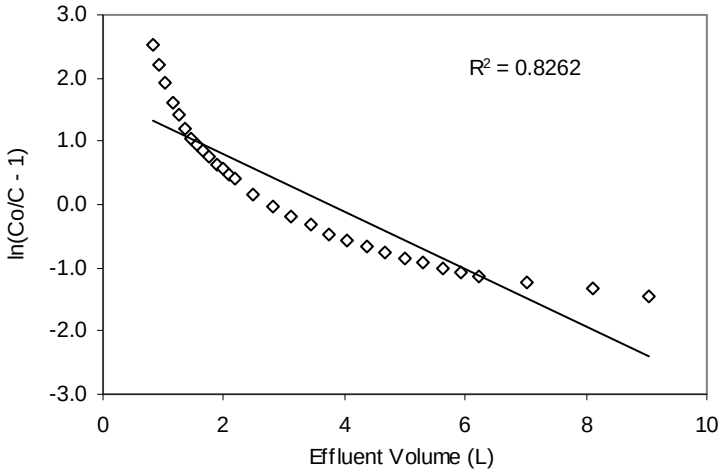

Figure C 1. Linearity of Thomas equation under the experimental condition Col-1 (Run-1)

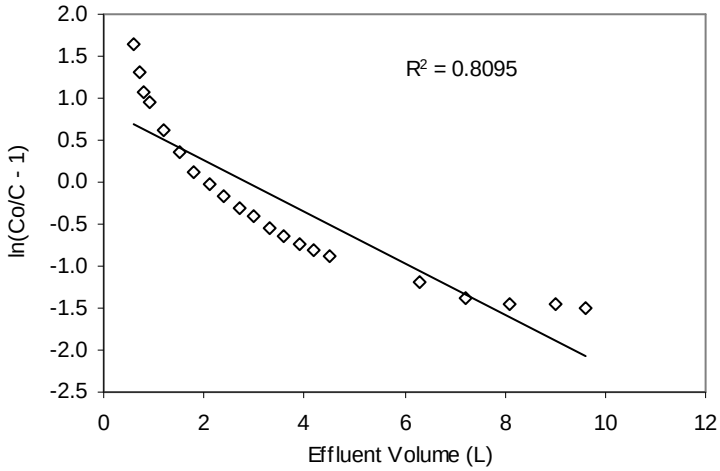

Figure C 2. Linearity of Thomas equation under the experimental condition Col-2 (Run-1)

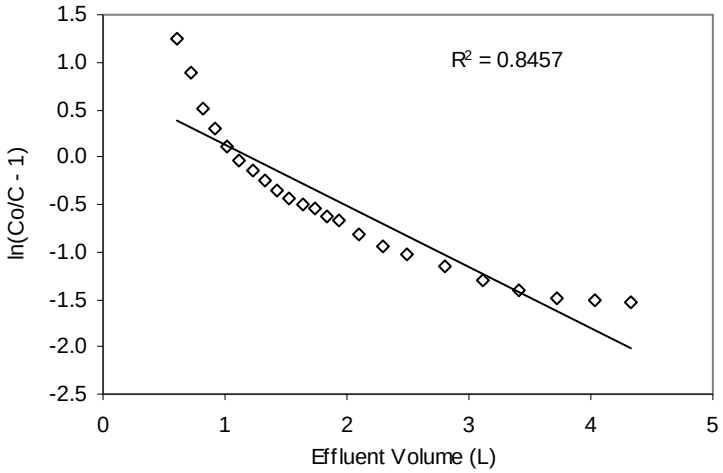

Figure C 3. Linearity of Thomas equation under the experimental condition Col-3 (Run-1)

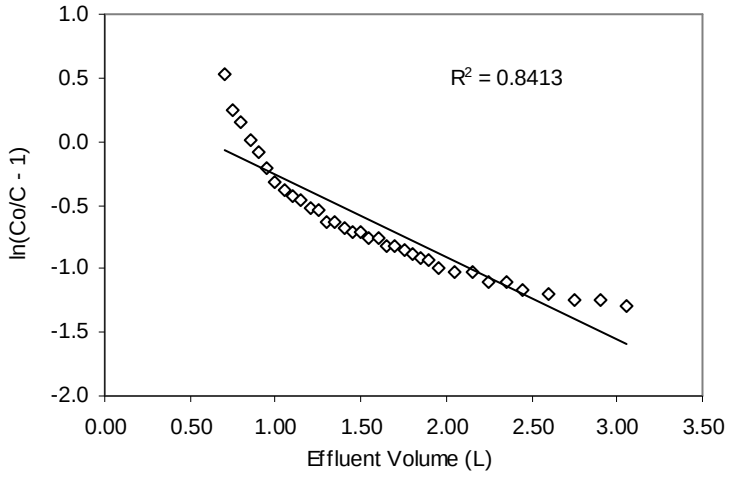

Figure C 4. Linearity of Thomas equation under the experimental condition Col-4 (Run-2)

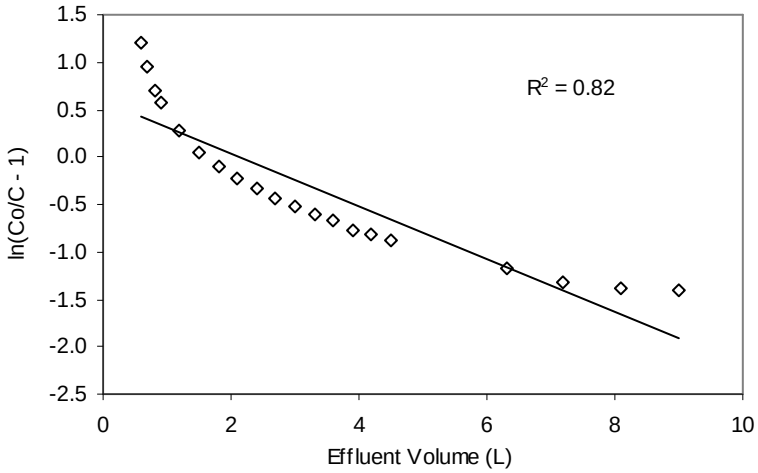

Figure C 5. Linearity of Thomas equation under the experimental condition Col-5 (Run-2)

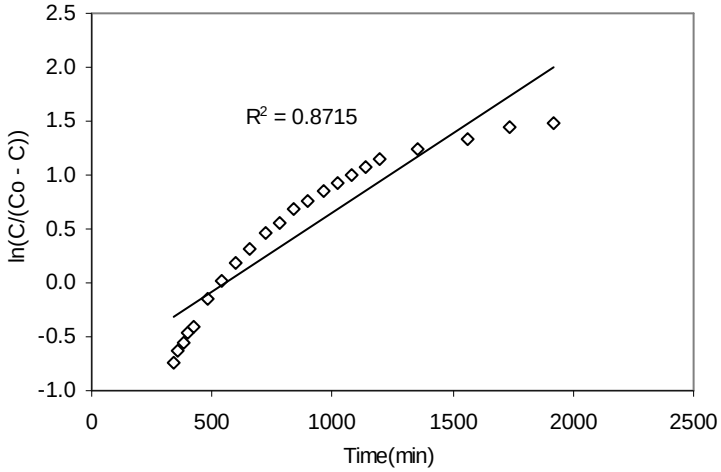

Figure C 6. Linearity of Yoon-Nelson equation under the experimental condition Col-1 (Run-1)

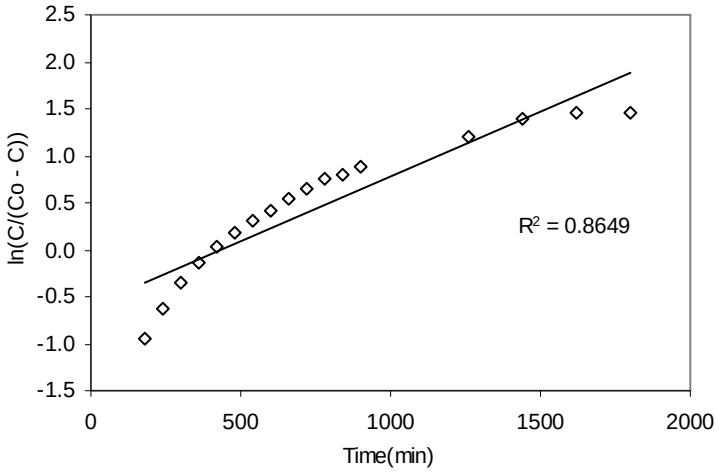

Figure C 7. Linearity of Yoon-Nelson equation under the experimental condition Col-2 (Run-1)

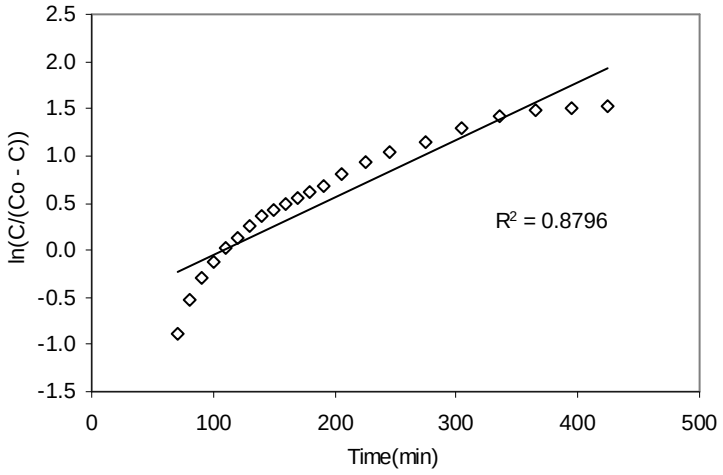

Figure C 8. Linearity of Yoon-Nelson equation under the experimental condition Col-3 (Run-1)

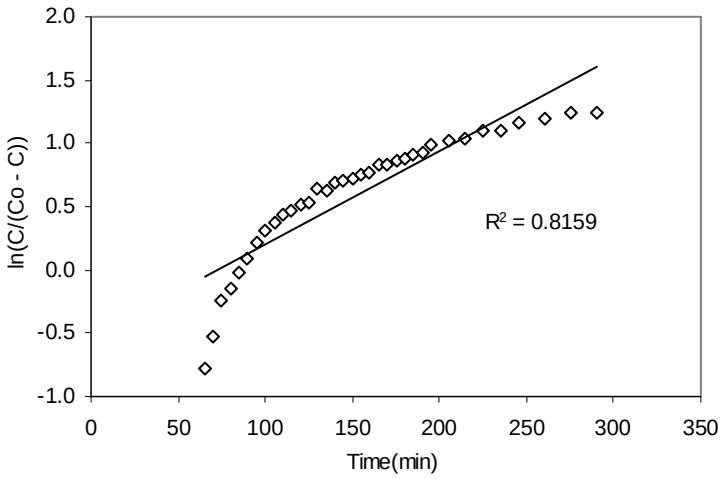

Figure C 9. Linearity of Yoon-Nelson equation under the experimental condition Col-4 (Run-2)

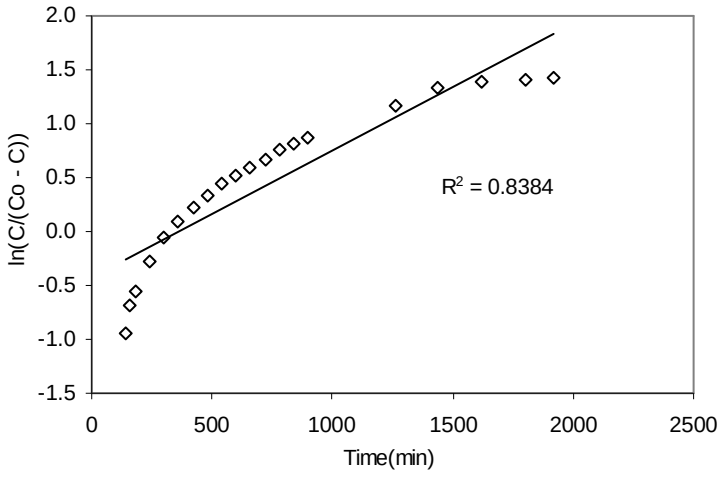

Figure C 10. Linearity of Yoon-Nelson equation under the experimental condition Col-5 (Run-2)

Appendix D

Publications: